CPAS

مركز الدراسات التخطيطية والمعمارية

CENTER OF PLANNING AND ARCHITECTURAL STUDIES

Applied Geotechnical Engineering: Foundation on Difficult Soils and Ground Modifications

By

Dr. Ahmed Mosalem Sameh, P.Eng

Assistant Prof. Of Geotechnical Engineering,

Helwan University

March 2000

14. EL Sobky St., M. EL-Bakry
Heliopolis - Cairo - Egypt .
P.O. Box : 6 Saray El Kobba - P.C. 11712
Tel. : (202) 4190843 / 744 / 271 Fax : (202) 2919341
E-mail : Srpah @ idsc. gov.eg

١٤ شارع السبكى / منشية البكرى
خلف نادى هليوبوليس - مصر الجديدة - القاهرة
ص . ب : ٦ سراى القبة - رمز بريدى ١١٧١٢
ت : ٨٤٣ / ٧٤١ / ٤١٩٠٢٧١ (٢٠٢) فاكس : ٢٩١٩٣٤١ (٢٠٢)

بسم الله الرحمن الرحيم

Table of Contents

1. Geotechnical Properties of Soils

1.1. Introduction

1.2. Grain Size and Classification Systems.

→ Important Diameters

- ** D_{10} **
- D_{30}
- D_{60}

→ $K = \frac{(D_{10})^2}{100} = \dots$ m/sec. (in mm)

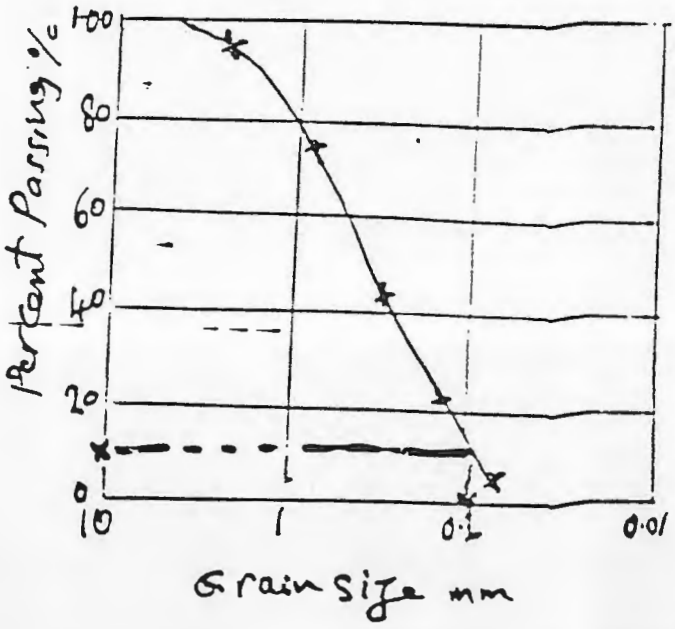

→ Classification Systems

- * AASHTO
- * Unified System
- * MIT System
- ----
- ----

Cohesive Soil ← ---???--- → Cohesionless Soils

Clay	Silt			Sand				Gravel
				F	M	C		
0.002	0.006	0.02	0.06	0.2	0.6	2.0		

hydrometer test. → Mechanical sieve analysis

1.3 Weight-Volume Relationships

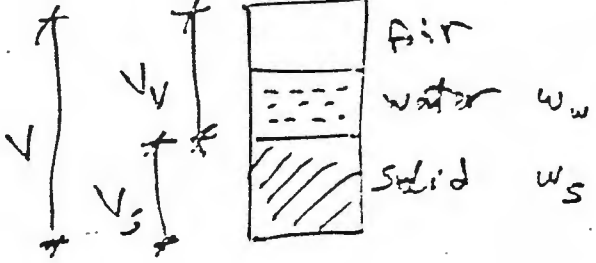

- Void Ratio $e = V_v / V_s$

- Dry unit weight γ_d

$$\gamma_d = \frac{W_s}{V} = \frac{G_s}{1+e}\gamma_w$$

- Specific Gravity

$G_s \simeq 2.66$ for sand, silt and inorganic clay.

1.4 Relative Density – Compaction of sand

* Relative Density & Compactness of Sand.

$$D_r = \frac{e_{max} - e}{e_{max} - e_{min}}$$

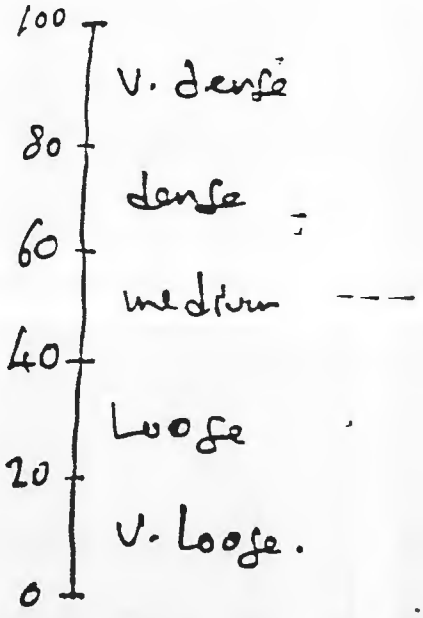

* → Compaction Control of Granular soils (sands).

→ Relative Compaction R.C.

→ Is relative compaction is an adequate parameters for Comp. Control ?

→ Relative Compaction ↔ D_r ??

1.5 Atterberg Limits

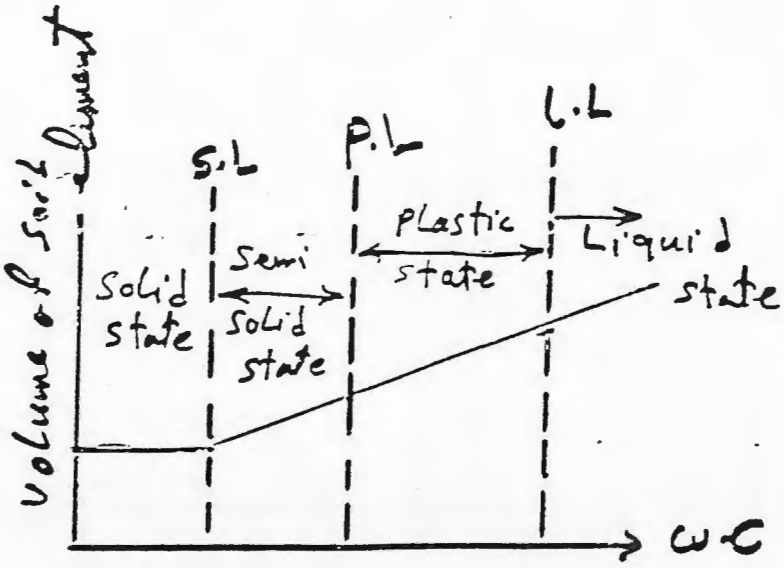

$$L.I. = \frac{w.c - PL}{LL - PL}$$

$$P.I = L.L - P.L.$$

Clay minerals →
- Kaolinite: 25 P.L 35 L.L 100
- Illite: 30 P.L. 60 L.L 100
- Montmorillonite: 50 P.L 100 L.L. 800

★ L.L. & P.I Usage for identification of Swelling Potential

L.L.	P. I.	Potential Swell Classification
<50	<25	Low
50-60	25-35	Marginal
>60	>35	High

→ absorbtion of swelling of expansive soils.

e – Log p' relationship

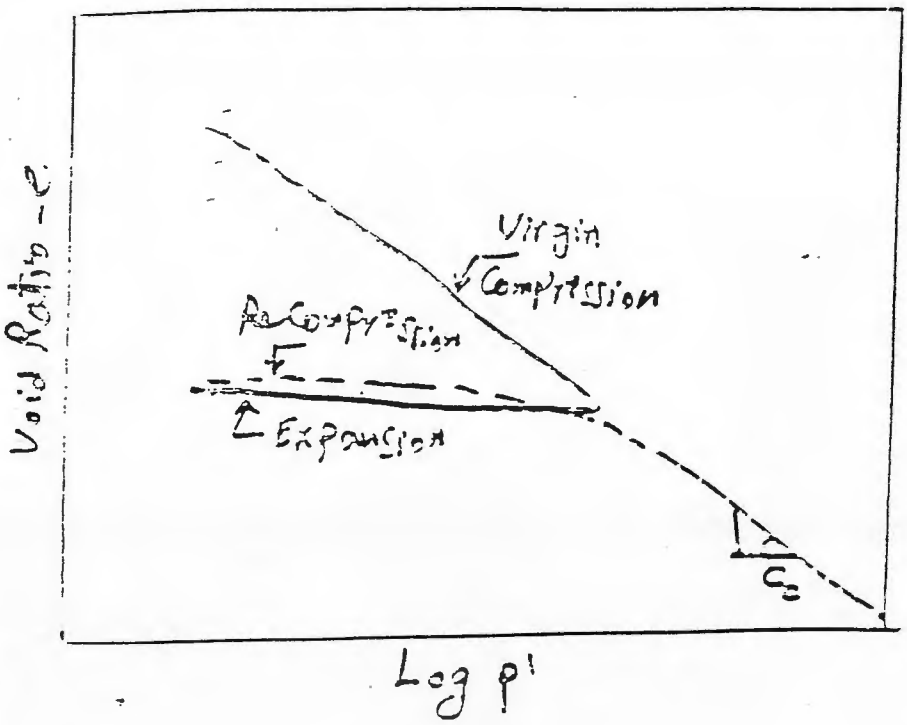

C_c Compression index

Coefficient of Volume Compressibility m_v

$$m_v = \frac{\Delta h / h}{\Delta p'}$$

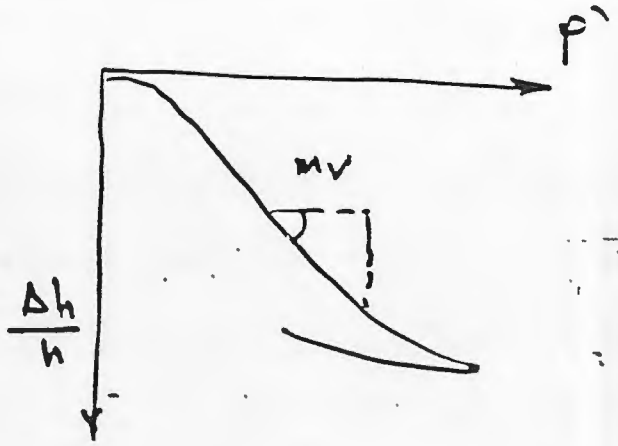

$$C_c = 0.009\,(L.L - 10)$$

Pre-Consolidation Stress

$\sigma_o' \leq \sigma_c'$ N.C. clay

$\sigma_o' > \sigma_c'$ O.C. clay

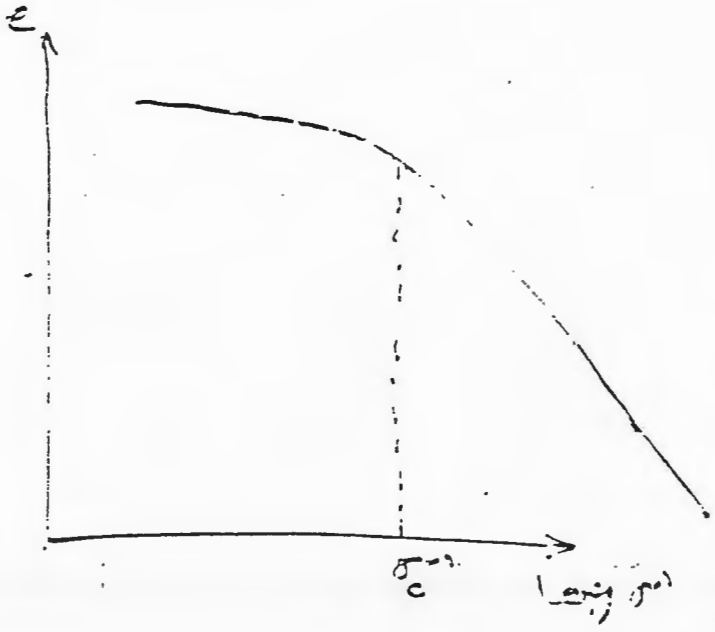

Settlement Calculation

$$\boxed{S_{max} = m_v \cdot \Delta\sigma' \cdot H_c}$$ for N.C. & O.C. clay.

$$S_{max} = \frac{C_c}{1+e_o} H_c \log \frac{\sigma_o + \Delta\sigma}{\sigma_o}$$ for N.C. clay.

Degree of Consolidation U

$$U = \frac{S_t}{S_{max}}$$

U vs. t ???

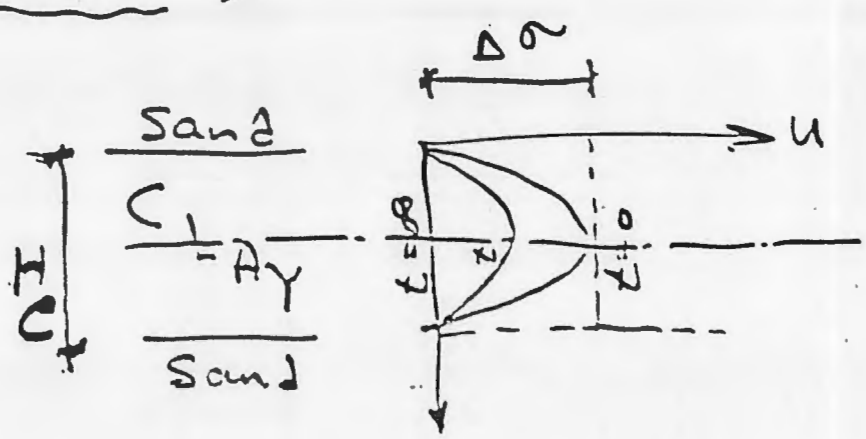

$$T_v = \frac{C_v \cdot t}{H}$$

H Drainage path

C_v Coefficient of Consolidation

$$C_v = \frac{K}{m_v \cdot \gamma_w}$$

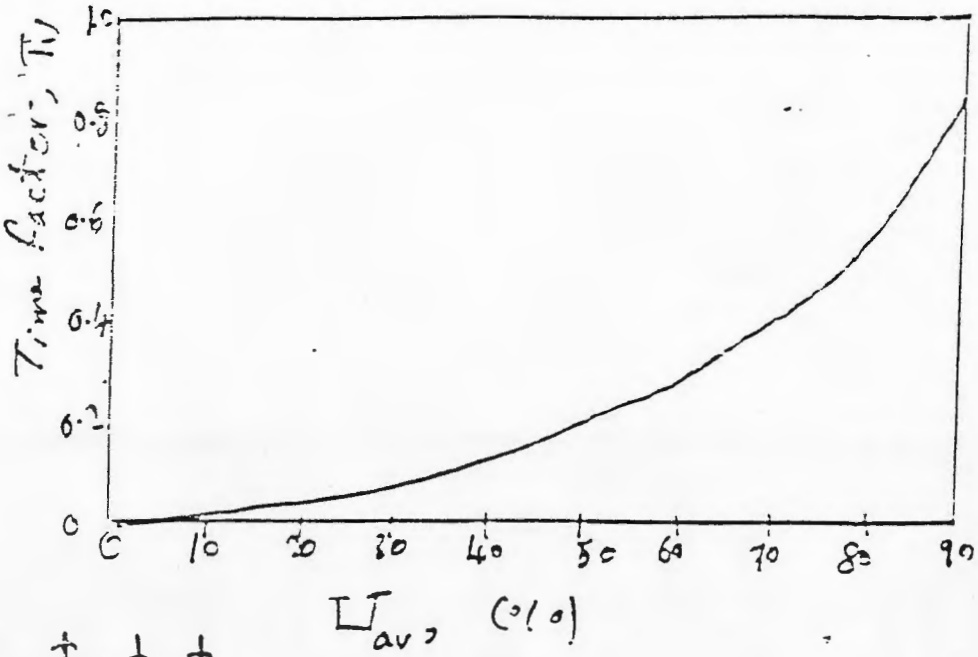

* Get C_v from Odometer test, or

L.L. versus C_v (approximately) Fig. 1.23 Page 46

* Mohr-Coulom Law

$$S' = C + \sigma \tan\phi$$

C, ϕ shear strength parameters

* Get C, ϕ ???

C, ϕ →
- Direct shear test
- Triaxial test
- Field tests.

} Lab tests mostly Used.

Direct shear test for sandy soils

Triaxial test for sand & clay.

* * * * * * * *

*** Drainage Conditions ***

* * * * * * * *

Types of Triaxial tests w.r.t drainage Conditions

	UU	CU	CD
Sand	research (rare)	research	✓✓ ϕ'
clay	✓✓ clay (saturated) $C_u = \frac{q_u}{2} = ✓✓$	✓✓ clay → N.C. $\phi_{cu} = ✓✓$; O.C. $C_{cu} = ✓✓$	✓✓ clay → N.C. $\phi' = ✓✓$, $C = 0$; O.C. C', ϕ'

Types of Analysis in Geotechnical Engineering

	Short term Analysis	Long term Analysis
Sand	ϕ' ≡ ≡ ≡	ϕ'
Clay	$q_u = (C_u) * 2$	C', ϕ'

ϕ' for clay (N.C. clay) vs. P.I. Fig. 1.29 (Page 55)

ϕ' for clay $20 \rightarrow 31^\circ$

ϕ'_{cs} for clay $15 \rightarrow 25^\circ$

Unconfined test of Clay $q_u = 2C_u$

$C_u = q_u/2$

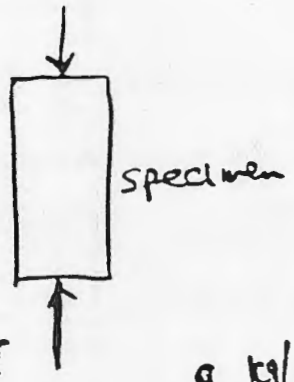

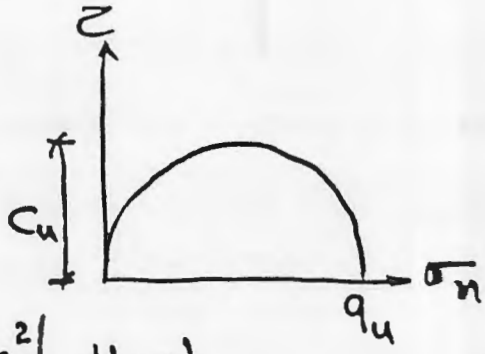

* C_v Vs. L.I
Fig. 1.31
Page 57

SPT	q_u kg/cm²	
		Hard
30	4.0	
		v. stiff
20	2.0	
		Stiff
10	1.0	
		Medium
5	0.5	
		Soft
2	0.25	
		V. Soft

S.P.T : Dr : ϕ for Sandy Soils

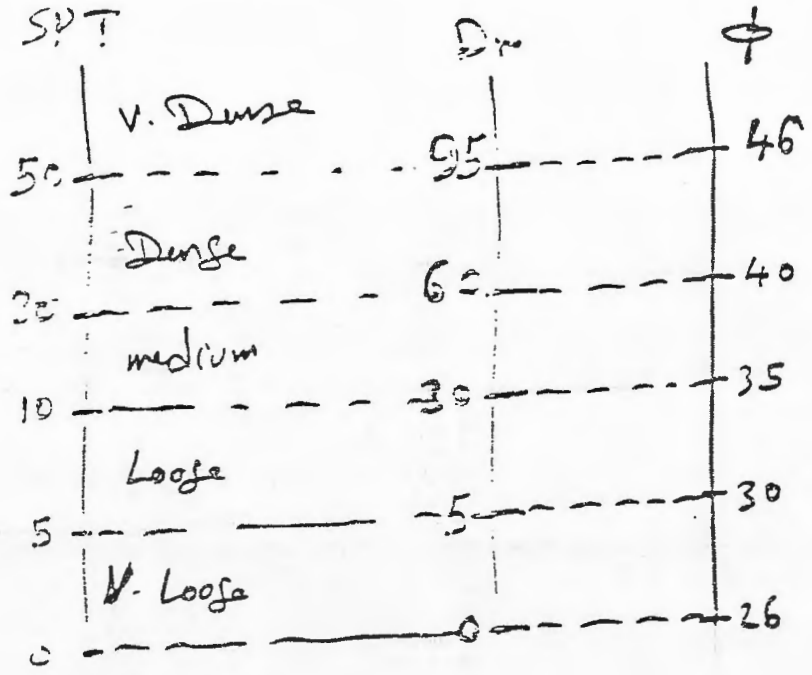

Sensitivity (S_t)

→ If the clay structure is disturbed, the soil becomes remoulded and its engineering properties changes considerably.

→ S_t indicates weakening of clay due to remoulding

$$S_t = \frac{(q_u)_u}{(q_u)_r}$$

← unconfined comp. strength of undist. clay

← unconfined comp. strength of remoulded clay.

	S_t	
Unstable and turns into slurry when remoulded		Quick
	16	
		Extra sensitive
	8	
Large reduction in strength due to remoulding		Sensitive
	4	
most clays		Moderately sensitive
	2	
		Little sensitive
	1	
		Insensitive

2. Expansive Soil

2.1 → Definition.

2.2 → Laboratory Measurement of Swell

(1) Oedometer test → unrestrained swell test. (To get swelling percent)
→ Swelling pressure test. (to get swelling pressure)

(2) Free swell test (very simple test).

Odometer Tests

→ Unrestrained swell test

هو النسبة المئوية الانتفاش لعينة بحالتها الطبيعية عند غمرها بالماء تحت ضغط راسي = ١ كجم/م٢.

→ Swelling Pressure test.

هو الضغط الراسي اللازم لعينة لكي يبقى ارتفاعها دون زيادة بعد إضافة الماء لها.

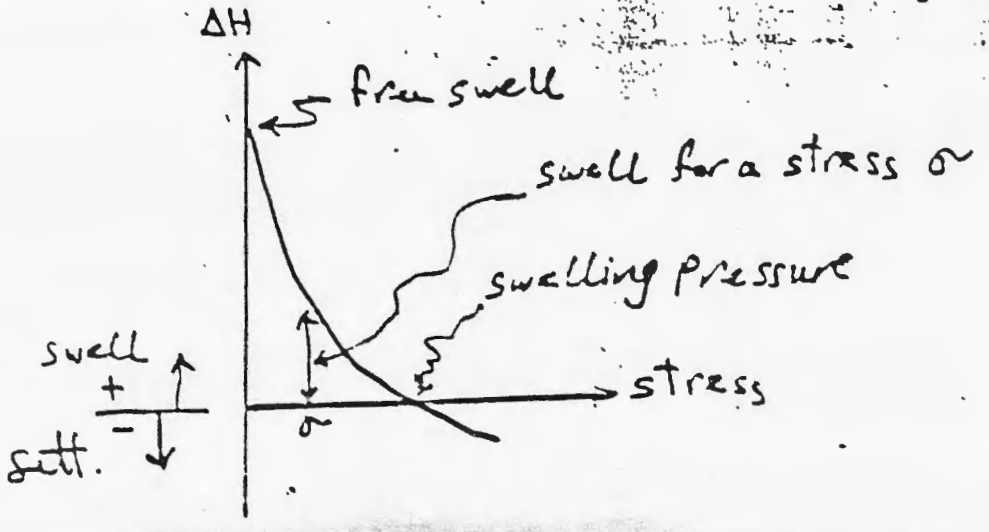

Free Swell Test

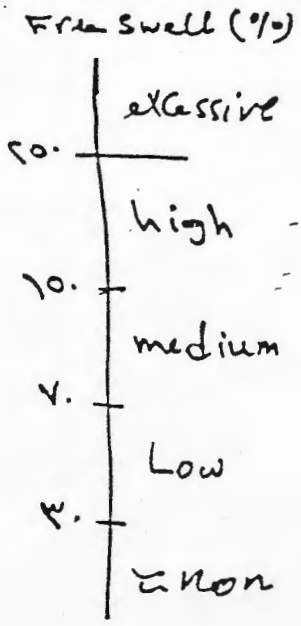

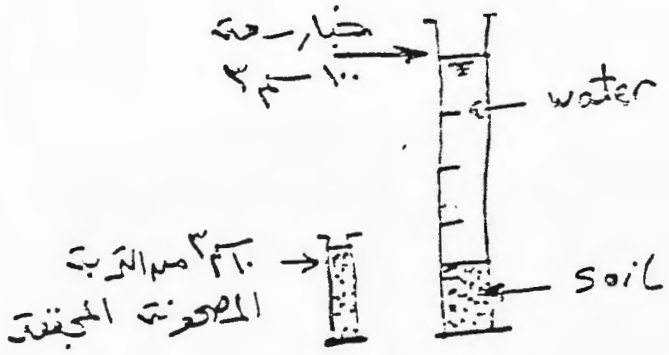

2.3 Classification of Expansive Soil

According to O'Neill & Poormoayed (1980)
& U.S Army Waterways (1977)

L.L	P.I.	Potential Swell Classification
<50	<25	Low
50-60	25-35	Marginal
>60	>35	High

مثال ٣ أساليب حماية المنشآت

١ ← استبدال التربة القابلة للانتفاش بسمك يتراوح بين ½ إلى ½٢ أسفل الأساسات وذلك حسب درجة قابلية التربة للانتفاش.

٢ ← تغيير طبيعة التربة عن طريق ادخال حواجز للحد من تغلغل الماء أو التثبيت الكيميائي.

٣ ← تقوية المنشأ لمقاومة الإجهادات المصاحبة للانتفاش. أو جعل المنشأ بنظام مرن بحيث لا تؤدي حركة التربة الى الانهيار بتركيبه أو وظائفه.

أسلوب استبدال التربة بتربة أخرى

← المعادي الجديدة - سمك الطفلة ١٥م - نسبة الانتفاش الحر ٢٦٠٪ - المبنى ٦ طوابق سمك الاحلال ١٫٥م - الاحلال رمل وزلط.

← العاشر من رمضان - سمك الطفلة ٢م - نسبة الانتفاش الحر ٢٥٠٪ - ارضيات فرسانية - سمك الاحلال ½م من الرمل المتدرج.

← الطين الرقاقي (مدينة نصر - الاسماعيلية - الواحات الخارجة والداخلة) أصبح قابليته لامتصاص الماء في الاتجاه الأفقي عالية جداً لاحتوائه على نسبة من الطمي والرمل الناعم. بالرغم من ان نسبة الانتفاش الحر من ٩٠ - ١١٠٪ الا انه انتفاخ عالي جداً وتأثيرها على المباني خطير نظراً لامكانية تغلغل المياه.

← ترسيبات النيل الطينية التي تعرضت للجفاف لانخفاض منسوب المياه الجوفية وانتهاء استخدامها للزراعة لفترة طويلة لها خاصية الانتفاش وتصل انتفاش صخري المتوسط ١١٠٪.

أسلوب تغيير طبيعة التربة

← إضافة رمل التربة لكثافته أقل ومحتوى مائي أكبر بـ ٣-٤٪ من أوزان محتوى مائي (O.M.C) يقلل بدرجة كبيرة من الخواص الانتفاشية للتربة.

← تنفيذ حواجز لتحد من انتشار الرطوبة (بعمق حوالي ١,٥ م حول الأساسات) في التربة. هذا الأسلوب ذو تكلفة اقتصادية عالية.

← * استعمال الجير (lime stabilization) وذلك بإضافة بين ٥-٣٪ إلى التربة والرمل وذلك لعمق من ١-١,٥ م يقلل بدرجة ملحوظة من الانتفاش.

تحدث تفاعلات كيميائية تغير من تركيب بللورات الطين وتعطيه مقاومة عالية بالإضافة إلى تقليل الـ L.L، P.I والخواص الانتفاشية.

* إنشاء أعمدة جير (lime columns) لعمق من ٤-٦ م

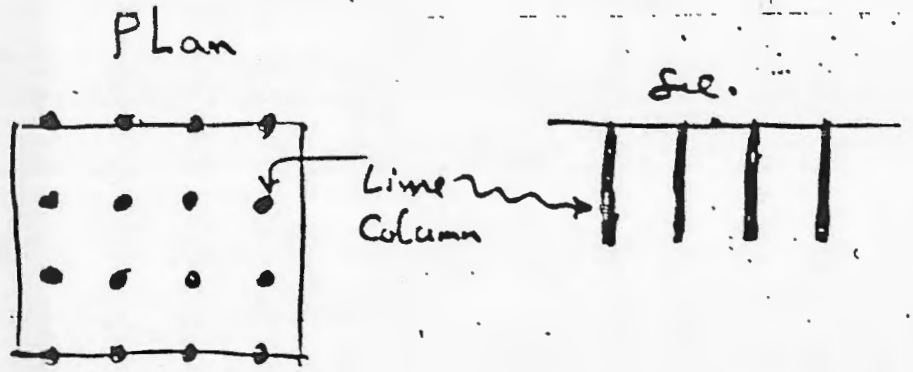

أسلوب تقوية المنشآت

- Box raft slab
- Waffle slab
- belled piers with a suspended floor slabs.

3. Collapsing Soil

3.1 Definition & Identification.

3.2 Site Investigation & Sampling

3.3 Laboratory testing of Collapsing Soil.

3.4 Field testing of Collapsing soil.

3.5 Treatment of Collapsing soil & Foundation Construction.

4 Dewatering Works

4.1. Purposes.

4.2 Dewatering Systems

4.2.1 Sumps & Ditches.

4.2.2 Wellpoints System

4.2.3 Deep wells system

4.2.4 Hydraulics of Slots & Wells

4.3 Project Conditions – Dewatering System – Cost.

4.4 Wells Construction, Development & Working Conditions.

4.5 Filter Design and Recommendations.

4.6 Case histories & General Discussions.

4.2.1 Sumps & Ditches

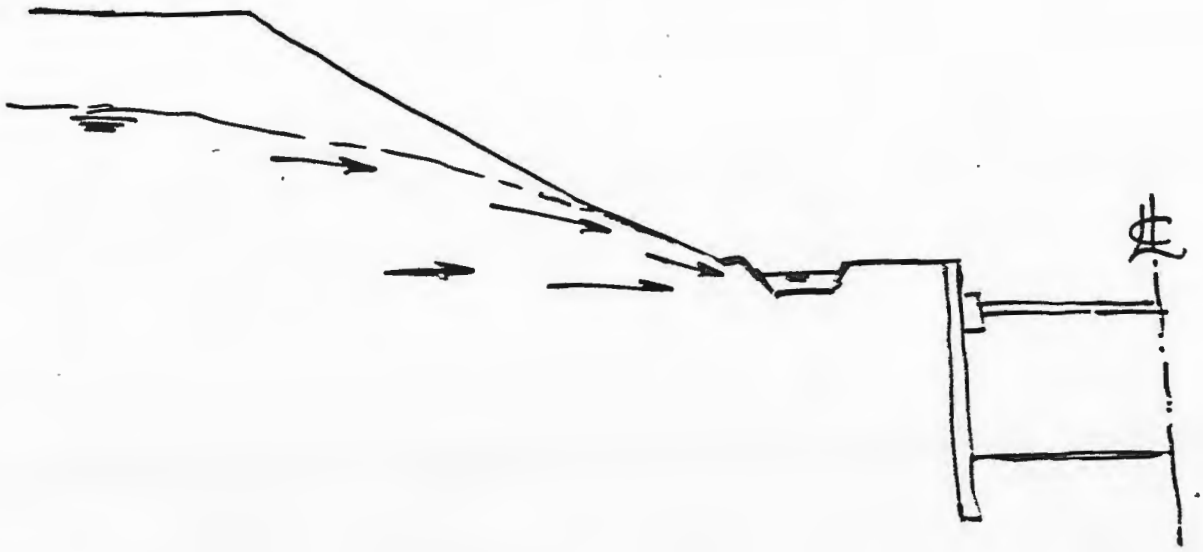

4.2.2 Wellpoint System.

Wellpoints System

Progressive System

Ring System

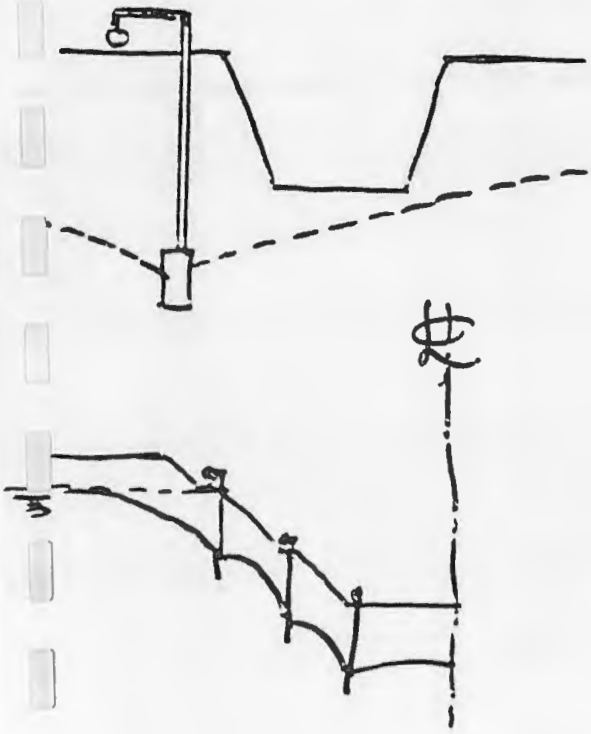

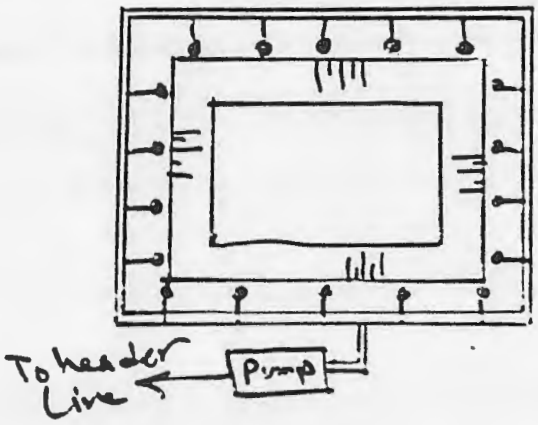

3.2.3 Deepwell System

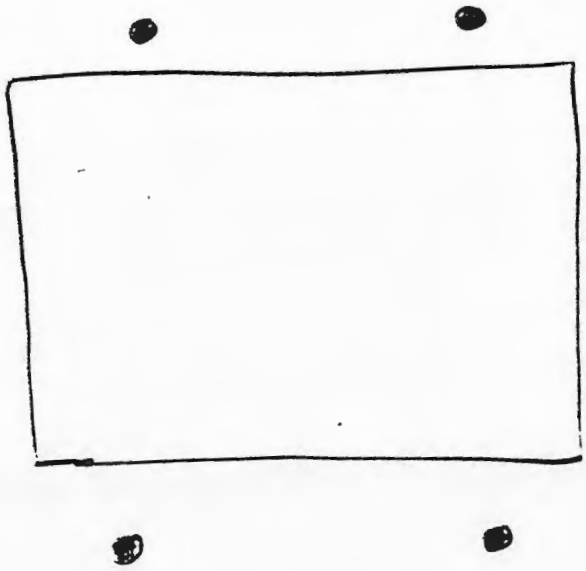

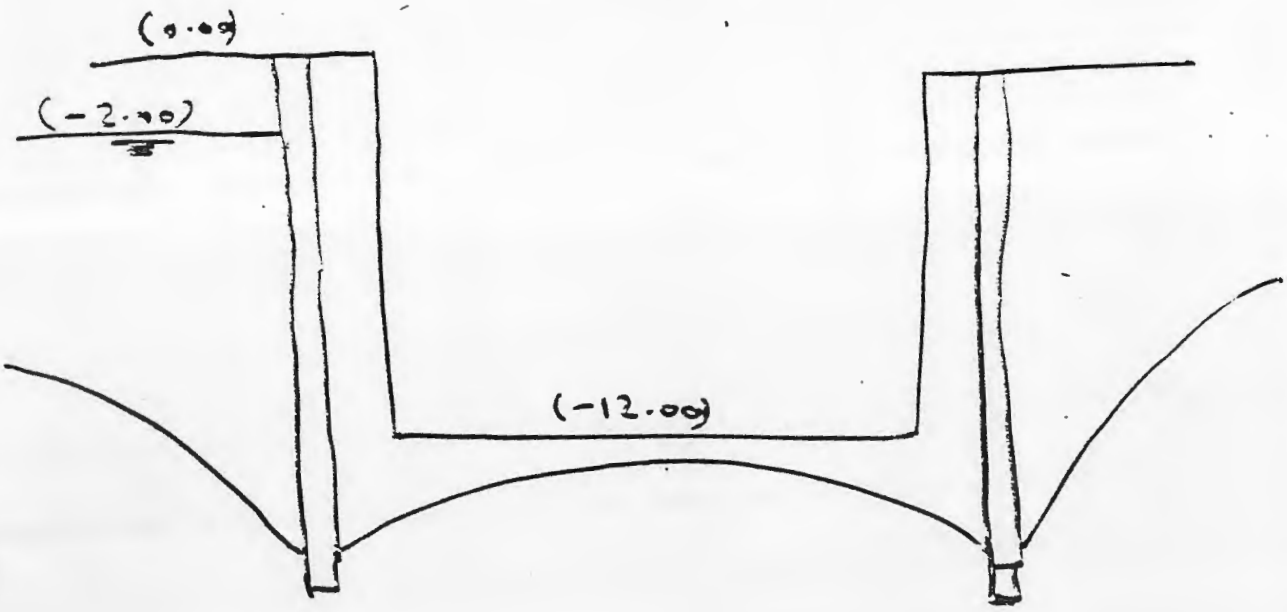

5 Ground Modification.

5.1. Introduction

5.2 Objectives

5.3 Choice of an improvement technique

1- Type & degree of improvement required

2- Type of soil, geological structure, seepage Conditio

3- Cost.

4- Availability of equipement and materials.

5- possible damage to adjacent structures.

6- Construction time available

7- Durability of the material involved (as related to the expected life of structure).

8- Side effects of any chemical additives.

5.4 Ground Modification techniques

5. Ground Improvement

- Mechanical Methods
  - Shallow Surface Compaction
  - Deep Compaction Techniques
    - Vibro replacement (Stone-Columns)
    - Vibro Compaction
      Dynamic Compaction
- Hydraulic Methods
  - Pre compression
  - Sand Drains
- Chemical modification- (stabilization by admixtures)
  - Lime Stabilization
  - Cement Stabilization
  - Fly As stabil
  - modification at depth by Grouting
- Modification by Inclusions (Soil. Reinforcement)

5.4.1 Dynamic Compaction

→ It is generally used for granular soil deposits. The process simply involves dropping a heavy weight repeatedly on the ground at regular intervals.

weigh of hammer varies from 8 → 35 ton

height of drops 7.0 → 30 m

→ The stress wave generated by the hammer drops help in the densification. In general, the degree of compaction achieved depends on

(1) The weight of the hammer

(2) Height of hammer drop.

(3) Spacing of the locations at which the hammer is dropped.

→ Significant depth of influence is ≈

$$D \approx \frac{1}{2}\sqrt{\frac{W}{h}\,h} = \cdots\ m \qquad \text{(Leonards 1980)}$$

وزن المطرقة بالطن ← $\frac{W}{h}$ ، h ← مسافة السقوط بالمتر

4.2 Vibro-Compaction

→ Construction methods

→ • First introduced in 1936
- Can be used for depths up to 35 m
- Diameter of influence of vibration ranges from 2 to 5 m
- Can be used even when G.W. exists and Compaction is achieved above and below water table.
- Spacing between probes is generally between 1.5 to 4.0 m.

→ most successful for Loose sandy soils (SPT from 5 to 10) near surface. (Not applicable for clays).

→ The back fill material used can be classified according to its suitability number S_N

$$S_N = 1.7\sqrt{\frac{1}{(D_{10})^2} + \frac{1}{(D_{20})^2} + \frac{3}{(D_{50})^2}}$$

S_N	
	unsuitable
50	
	Poor
30	
	Fair
20	
	Good
10	
	Excellent

→ Depending on the spacing between probes, relative densities of up to 85% can be achieved.

→ Grid of Vibro Centers

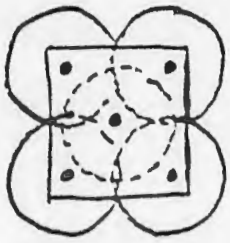

below raft Foundation

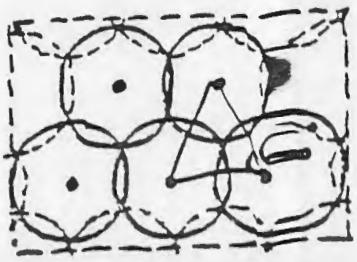

5.4.3 Vibro-replacement (Stone Columns)

* Used for silt & clayey formations (soft to medium clay).

* Can be arranged to suit varying conditions of Loads.

* Used to enhance bearing capacity & settlement characteristics.

* Spacing varies from 1.5 to 3.0 m

* A maximum depth up to 30 m can be reached by assistance of a strong water flow. They are most effective to a depth of 6-10 m.

* Diameters up to 1.3 m can be achieved.

→ Foundation of a single footing

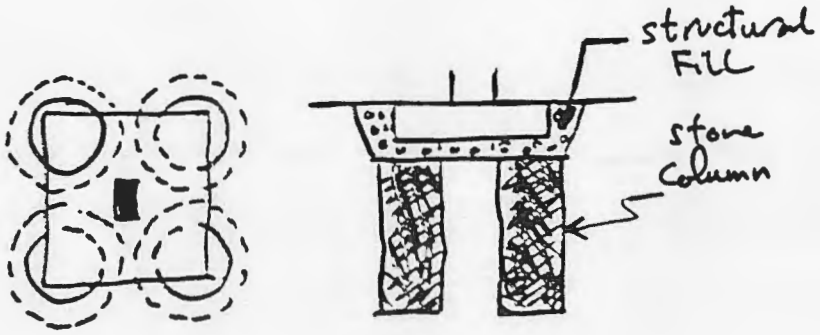

weight of air, W_a, in the soil mass is assumed to be negligible.

$$\text{Dry unit weight} = \gamma_d = \frac{W_s}{V} \tag{1.10}$$

When a soil mass is completely saturated (that is, all the void volume is occupied water), the moist unit weight of a soil [Eq. (1.9)] becomes equal to the *saturated unit ght* (γ_{sat}). So $\gamma = \gamma_{sat}$ if $V_v = V_w$.

More useful relations can now be developed by considering a representative soil ecimen in which the volume of soil solids is equal to *unity*, as shown in Figure 1.3b. te that if $V_s = 1$, from Eq. (1.4), $V_v = e$ and the weight of the soil solids is

$$W_w = G_s \gamma_w$$

ere G_s = specific gravity of soil solids
γ_w = unit weight of water (9.81 kN/m³, or 62.4 lb/ft³)

o, from Eq. (1.8), the weight of water $W_w = wW_s$. Thus, for the soil specimen under sideration, $W_w = wW_s = wG_s\gamma_w$. Now, for the general relation for moist unit weight en in Eq. (1.9),

$$\boxed{\gamma = \frac{W}{V} = \frac{W_s + W_w}{V_s + V_v} = \frac{G_s\gamma_w(1 + w)}{1 + e}} \tag{1.11}$$

nilarly, the dry unit weight [Eq. (1.10)] is

$$\boxed{\gamma_d = \frac{W_s}{V} = \frac{W_s}{V_s + V_v} = \frac{G_s\gamma_w}{1 + e}} \tag{1.12}$$

om Eqs. (1.11) and (1.12), note that

$$\gamma_d = \frac{\gamma}{1 + w} \tag{1.13}$$

a soil specimen is completely saturated as shown in Figure 1.3c,

$$V_v = e$$

lso, for this case

$$V_v = \frac{W_w}{\gamma_w} = \frac{wG_s\gamma_w}{\gamma_w} = wG_s$$

hus

$$e = wG_s \quad \text{(for saturated soil } \textit{only}\text{)} \tag{1.14}$$

The saturated unit weight of soil becomes

$$\boxed{\gamma_{sat} = \frac{W_s + W_w}{V_s + V_v} = \frac{G_s\gamma_w + e\gamma_w}{1 + e}} \tag{1.}$$

Relationships similar to Eqs. (1.11), (1.12), and (1.15) in terms of porosity can also obtained by considering a representative soil specimen with a unit volume. The relationships are

$$\gamma = G_s\gamma_w(1 - n)(1 + w) \tag{1.}$$

$$\gamma_d = (1 - n)G_s\gamma_w \tag{1.}$$

$$\gamma_{sat} = [(1 - n)G_s + n]\gamma_w \tag{1.}$$

1.5 REPRESENTATIVE VALUES OF G_s, e, AND γ_d FOR NATURAL SOILS

Except for peat and highly organic soils, the general range of the values of speci gravity of soil solids (G_s) found in nature is rather small. Table 1.3 gives some represe tative values. For practical purposes, a reasonable value can be assumed in lieu running a test.

▼ **TABLE 1.3** Specific Gravities of Some Soils

Soil type	G_s
Quartz sand	2.64–2.66
Silt	2.67–2.73
Clay	2.70–2.9
Chalk	2.60–2.75
Loess	2.65–2.73
Peat	1.30–1.9

Table 1.4 presents some representative values for the void ratio, dry uni weight, and moisture content (in a saturated state) of some naturally occurring soils Note that in most cohesionless soils the void ratio varies from about 0.4 to 0.8 The dry unit weights in these soils generally fall within a range of about 90–120 lb/ft³ (14–19 kN/m³).

▼ **TABLE 1.4** Typical Void Ratio, Moisture Content, and Dry Unit Weight for Some Soils

Type of soil	Void ratio	Natural moisture content in saturated condition (%)	Dry unit weight, γ_d (lb/ft³)	Dry unit weight, γ_d (kN/m³)
Loose uniform sand	0.8	30	92	14.5
Dense uniform sand	0.45	16	115	18
Loose angular-grained silty sand	0.65	25	102	16
Dense angular grained silty sand	0.4	15	120	19
Stiff clay	0.6	21	108	17
Soft clay	0.9–1.4	30–50	73–92	11.5–14.5
Loess	0.9	25	86	13.5
Soft organic clay	2.5–3.2	90–120	38–51	6–8
Glacial till	0.3	10	134	21

1.6 RELATIVE DENSITY

In *granular soils*, the degree of compaction in the field can be measured according to *relative density*, D_r, which is defined as

$$D_r(\%) = \frac{e_{max} - e}{e_{max} - e_{min}} \times 100 \tag{1.19}$$

where e_{max} = void ratio of the soil in the loosest state
e_{min} = void ratio in the densest state
e = *in situ* void ratio

The values of e_{max} are determined in the laboratory in accordance with the test procedures outlined in the American Society for Testing and Materials, *ASTM Standards* (1992, Test Designation D-4254).

The relative density can also be expressed in terms of dry unit weight, or

$$D_r(\%) = \left\{\frac{\gamma_d - \gamma_{d(min)}}{\gamma_{d(max)} - \gamma_{d(min)}}\right\} \frac{\gamma_{d(max)}}{\gamma_d} \times 100 \tag{1.20}$$

where γ_d = *in situ* dry unit weight
$\gamma_{d(max)}$ = dry unit weight in the *densest* state—that is, when the void ratio is e_{min}
$\gamma_{d(min)}$ = dry unit weight in the *loosest* state—that is, when the void ratio is e_{max}

The denseness of a granular soil is sometimes related to its relative density. Table 1.5 gives a general correlation of the denseness and D_r. For naturally occurring sands, the magnitudes of e_{max} and e_{min} [Eq. (1.19)] may vary widely. The main reasons

▼ **TABLE 1.5** Denseness of a Granular Soil

Relative density, D_r (%)	Description
0–20	Very loose
20–40	Loose
40–60	Medium
60–80	Dense
80–100	Very dense

for such wide variations are the uniformity coefficient, C_u, and the roundness of particles, R. The uniformity coefficient is defined in Eq. (1.1). *Roundness* is defined as

$$R = \frac{\text{minimum radius of the particle edges}}{\text{inscribed radius of the entire particle}} \tag{1.}$$

Measuring R is difficult, but it can be estimated. Figure 1.4 shows the gene range of the magnitude of R with particle roundness. Figure 1.5 shows the variation e_{max} and e_{min} with the uniformity coefficient for various values of particle roundn (Youd, 1973). This range is applicable to clean sand with normal to moderately skew particle-size distribution.

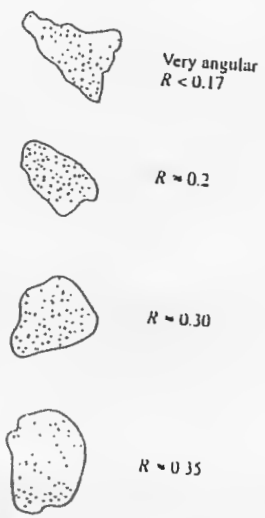

▼ **FIGURE 1.4** General range of the magnitude of R

$R \approx 0.49$

Well rounded
$R \approx 0.70$

FIGURE 1.4 (continued)

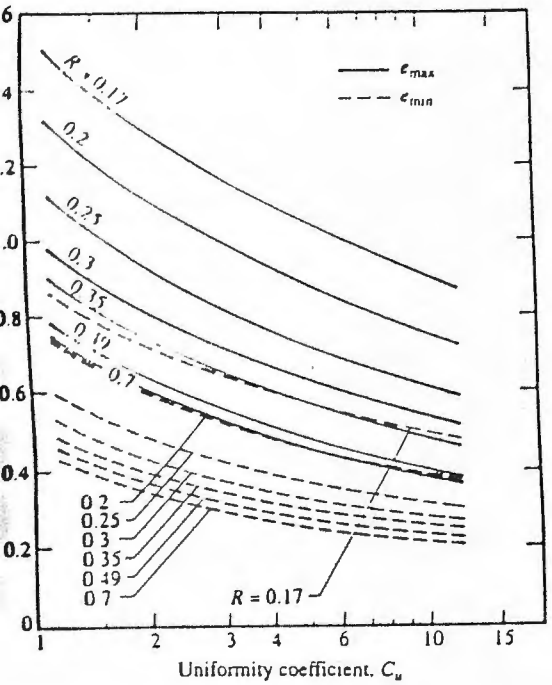

FIGURE 1.5 Approximate variation of e_{max} and e_{min} with uniformity coefficient (based on Youd, 1973)

EXAMPLE 1.1

a soil with void ratio = 0.81, moisture content = 21%, and $G_s = 2.68$, calculate the

a. Porosity
b. Degree of saturation
c. Moist unit weight in lb/ft³
d. Dry unit weight in lb/ft³

Solution

Part a: Porosity

From Eq. (1.6)

$$n = \frac{e}{1+e} = \frac{0.81}{1+0.81} = 0.448$$

Part b: Degree of Saturation

From Eqs. (1.7) and (1.14)

$$S = \frac{V_w}{V_v} = \frac{wG_s}{e} = \frac{(0.21)(2.68)}{0.81} = 0.695 = 69.5\%$$

Part c: Moist Unit Weight

From Eq. (1.11)

$$\gamma = \frac{G_s\gamma_w(1+w)}{1+e} = \frac{(2.68)(62.4)(1+0.21)}{1+0.81} = 111.8 \text{ lb/ft}^3$$

Part d: Dry Unit Weight

From Eq. (1.13)

$$\gamma_d = \frac{G_s\gamma_w}{1+e} = \frac{(2.68)(62.4)}{1+0.81} = 92.4 \text{ lb/ft}^3 \quad ▼$$

▼ EXAMPLE 1.2

A representative soil specimen collected in the field weighs 1.8 kN and has a volume of 0.1 m³. The moisture content as determined in the laboratory is 12.6%. For $G_s = 2.71$, determine the

a. Moist unit weight
b. Dry unit weight
c. Void ratio
d. Porosity
e. Degree of saturation

Solution

Part a: Moist Unit Weight

From Eq. (1.9)

$$\gamma = \frac{W}{V} = \frac{1.8 \text{ kN}}{0.1 \text{ m}^3} = 18 \text{ kN/m}^3$$

Part b: Dry Unit Weight

From Eq. (1.13)

$$\gamma_d = \frac{\gamma}{1+w} = \frac{18}{1+\frac{12.6}{100}} = 15.99 \text{ kN/m}^3$$

Part c: Void Ratio

From Eq. (1.12)

$$\gamma_d = \frac{G_s \gamma_w}{1+e}$$

or

$$e = \frac{G_s \gamma_w}{\gamma_d} - 1 = \frac{(2.71)(9.81)}{15.99} - 1 = 0.66$$

Part d: Porosity

From Eq. (1.6)

$$n = \frac{e}{1+e} = \frac{0.66}{1+0.66} = 0.398$$

Part e: Degree of Saturation

Refer to Figure 1.3b:

$$S = \frac{V_w}{V_v} = \frac{wG_s}{e} = \frac{(0.126)(2.71)}{0.66} \times 100 = \mathbf{51.7\%} \quad \blacktriangledown$$

▼ EXAMPLE 1.3

For a granular soil having $\gamma = 108$ lb/ft³, $D_r = 82\%$, $w = 8\%$, and $G_s = 2.65$, if $e_{min} = 0.44$, what would be e_{max}? What would be the dry unit weight in the loosest state?

Solution From Eq. (1.13)

$$\gamma_d = \frac{\gamma}{1+w} = \frac{108}{1+0.08} = 100 \text{ lb/ft}^3$$

From Eq. (1.12)

$$\gamma_d = \frac{G_s \gamma_w}{1+e}$$

$$100 = \frac{(2.65)(62.4)}{1+e}$$

$$e = 0.654$$

From Eq. (1.19)

$$D_r = \frac{e_{max} - e}{e_{max} - e_{min}}$$

$$0.82 = \frac{e_{max} - 0.654}{e_{max} - 0.44}$$

$$e_{max} = \mathbf{1.63}$$

$$\gamma_{d(min)} = \frac{G_s \gamma_w}{1+e_{max}} = \frac{(2.65)(62.4)}{1+1.63} = 62.9 \text{ lb/ft}^3 \quad \blacktriangledown$$

1.7 ATTERBERG LIMITS

When a clayey soil is mixed with an excessive amount of water, it may flow like a *semiliquid*. If the soil is gradually dried, it will lose moisture. Depending on its moisture content, it will behave like a *plastic*, *semisolid*, or *solid* material. The moisture content, in percent, at which the soil changes from a liquid to a plastic state is defined as the *liquid limit* (*LL*). Similarly, the moisture contents, in percent, at which the soil changes from a plastic to a semisolid state and from a semisolid to a solid state are defined as the *plastic limit* (*PL*) and the *shrinkage limit* (*SL*), respectively. These limits are referred to as *Atterberg limits* (Figure 1.6).

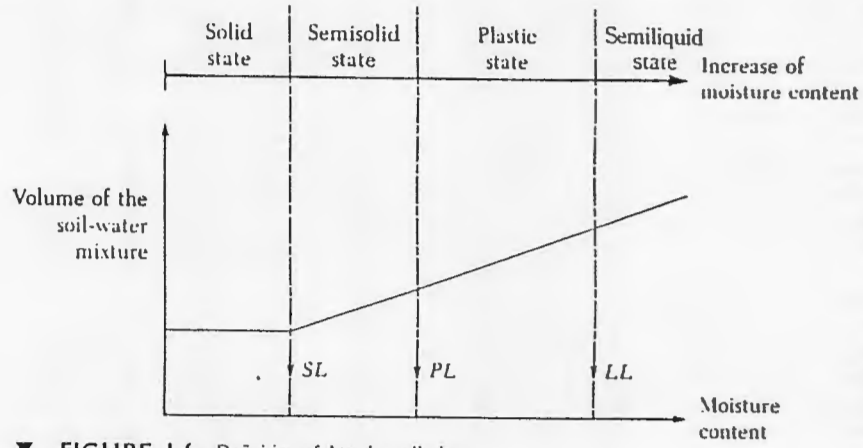

▼ **FIGURE 1.6** Definition of Atterberg limits

- ▶ The liquid limit of a soil is determined by Casagrande's liquid device (ASTM Test Designation D-4318) and is defined as the moisture content at which a groove closure of $\frac{1}{2}$ in. (12.7 mm) occurs at 25 blows.
- ▶ The *plastic limit* is defined as the moisture content at which the soil crumbles when rolled into a thread of $\frac{1}{8}$ in. (3.18 mm) in diameter (ASTM Test Designation D-4318).

▶ The *shrinkage limit* is defined as the moisture content at which the soil does not undergo further volume change with loss of moisture (ASTM Test Designation D-427). Figure 1.6 shows this limit.

The difference between the liquid limit and the plastic limit of a soil is defined as *plasticity index* (*PI*), or

$$PI = LL - PL \tag{1.22}$$

Table 1.6 gives some representative values of liquid limit and plastic limit several clay minerals and soils. However, Atterberg limits for various soils will considerably, depending on the soil's origin and the nature and amount of clay erals in it.

TABLE 1.6 Typical Liquid and Plastic Limits for Some Clay Minerals and Soils

Description	Liquid limit	Plastic limit
olinite	35–100	25–35
e	50–100	30–60
ntmorillonite	100–800	50–100
ston Blue clay	40	20
icago clay	60	20
uisiana clay	75	25
ndon clay	66	27
mbridge clay	39	21
ontana clay	52	18
ississippi Gumbo	95	32
essial soils in north and northwest China	25–35	15–20

SSIFICATION SYSTEMS

classification divides soils into groups and subgroups based on common engineer- properties such as *grain-size distribution, liquid limit,* and *plastic limit.* The two or classification systems presently in use are (1) the *AASHTO* (*American Associ- n of State Highway and Transportation Officials*) *System* and (2) the *Unified Soil sification System* (also *ASTM*). The AASHTO classification system is used mainly classification of highway subgrades. It is not used in foundation construction.

ASHTO System

AASHTO Soil Classification System was originally proposed by the Highway earch Board's Committee on Classification of Materials for Subgrades and Granular e Roads (1945). According to the present form of this system, soils can be classified according to eight major groups, A-1 through A-8, based on their grain-size distribution, liquid limit, and plasticity indices. Soils listed in groups A-1, A-2, and A-3 are coarse grained materials, and those in groups A-4, A-5, A-6, and A-7 are fine-grained materials. Peat, muck, and other highly organic soils are classified under A-8. They are identified by visual inspection.

The AASHTO classification system (for soils A-1 through A-7) is presented in Table 1.7. Note that group A-7 includes two types of soil. For the A-7-5 type, the

TABLE 1.7 AASHTO Soil Classification System

General classification	Granular materials (35% or less of total sample passing no. 200 sieve)						
	A-1			A-2			
Group classification	A-1-a	A-1-b	A-3	A-2-4	A-2-5	A-2-6	A-2-7
Sieve analysis (% passing)							
No. 10 sieve	50 max						
No. 40 sieve	30 max	50 max	51 min				
No. 200 sieve	15 max	25 max	10 max	35 max	35 max	35 max	35 max
For fraction passing No. 40 sieve							
Liquid limit (*LL*)				40 max	41 min	40 max	41 min
Plasticity index (*PI*)	6 max		Nonplastic	10 max	10 max	11 min	11 min
Usual type of material	Stone fragments, gravel, and sand		Fine sand	Silty or clayey gravel and sand			
Subgrade rating	Excellent to good						

General classification	Silt-clay materials (More than 35% of total sample passing no. 200 sieve)			
Group classification	A-4	A-5	A-6	A-7 A-7-5[a] A-7-6[b]
Sieve analysis (% passing)				
No. 10 sieve				
No. 40 sieve				
No. 200 sieve	36 min	36 min	36 min	36 min
For fraction passing No. 40 sieve				
Liquid limit (*LL*)	40 max	41 min	40 max	41 min
Plasticity index (*PI*)	10 max	10 max	11 min	11 min
Usual types of material	Mostly silty soils		Mostly clayey soils	
Subgrade rating	Fair to poor			

[a] If $PI \le LL - 30$, it is A-7-5
[b] If $PI > LL - 30$, it is A-7-6

plasticity index of the soil is less than or equal to the liquid limit minus 30. For the A-7-6 type, the plasticity index is greater than the liquid limit minus 30.

For qualitative evaluation of the desirability of a soil as a highway subgrade material, a number referred to as the *group index* has also been developed. The higher the value of the group index for a given soil, the weaker will be the soil's performance as a subgrade. A group index of 20 or more indicates a very poor subgrade material. The formula for group index, GI, is

$$GI = (F_{200} - 35)[0.2 + 0.005(LL - 40)] + 0.01(F_{200} - 15)(PI - 10) \quad (1.23)$$

where F_{200} = percent passing no. 200 sieve, expressed as a whole number
LL = liquid limit
PI = plasticity index

When calculating the group index for a soil belonging to groups A-2-6 or A-2-7, use only the partial group index equation relating to the plasticity index:

$$GI = 0.01(F_{200} - 15)(PI - 10) \quad (1.24)$$

The group index is rounded to the nearest whole number and written next to the soil group in parentheses; for example,

A = 4 (5)

Group index

Soil group

Unified System

The Unified Soil Classification System was originally proposed by A. Casagrande in 1942 and was later revised and adopted by the United States Bureau of Reclamation and the Corps of Engineers. This system is presently used in practically all geotechnical work.

In the Unified System, the following symbols are used for identification.

Symbol	G	S	M	C	O	Pt	H	L	W	P
Description	Gravel	Sand	Silt	Clay	Organic silts and clay	Peat and highly organic soils	High plasticity	Low plasticity	Well graded	Poorly graded

Table 1.8 and the plasticity chart (Figure 1.7 on page 23) show the procedure for determining the group symbols for various types of soil. When classifying a soil be sure to provide the group name that generally describes the soil, along with the group symbol. Tables 1.9, 1.10, and 1.11, respectively, give the criteria for obtaining the group names for coarse grained soil, inorganic fine grained soil, and organic fine grained soil. These tables are based on ASTM Designation D 2487.

TABLE 1.8 Group Symbols for Soil According to the Unified Classification System

Major divisions	Criteria	Group symbol
Coarse-grained soil $R_{200} > 50$	$F_{200} < 5$, $C_u \geq 4$, $1 \leq C_z \leq 3$	GW
	$F_{200} < 5$, $C_u < 4$, and/or C_z not between 1 and 3	GP
Gravelly soil $R_4 > 0.5R_{200}$	$F_{200} > 12$, $PI < 4$, or Atterberg limits plot below A line (Figure 1.7)	GM
	$F_{200} > 12$, $PI > 7$, and Atterberg limits plot on or above A line (Figure 1.7)	GC
	$F_{200} > 12$, $LL < 50$, $4 \leq PI \leq 7$, and Atterberg limits plot on or above A line	GC-GM*
	$5 \leq F_{200} \leq 12$; meets the gradation criteria of GW and the plasticity criteria of GM	GW-GM*
	$5 \leq F_{200} \leq 12$; meets the gradation criteria of GW and the plasticity criteria of GC	GW-GC*
	$5 \leq F_{200} \leq 12$; meets the gradation criteria of GP and the plasticity criteria of GM	GP-GM*
	$5 \leq F_{200} \leq 12$; meets the gradation criteria of GP and the plasticity criteria of GC	GP-GC*
Sandy soil $R_4 \leq 0.5R_{200}$	$F_{200} < 5$, $C_u \geq 6$, $1 \leq C_z \leq 3$	SW
	$F_{200} < 5$, $C_u < 6$, and/or C_z not between 1 and 3	SP
	$F_{200} > 12$, $PI < 4$, or Atterberg limits plot below A line (Figure 1.7)	SM
	$F_{200} > 12$, $PI > 7$, and Atterberg limits plot on or above A line (Figure 1.7)	SC
	$F_{200} > 12$, $LL > 50$, $4 \leq PI \leq 7$, and Atterberg limits plot on or above A line (Figure 1.7)	SC-SM*
	$5 \leq F_{200} \leq 12$; meets the gradation criteria of SW and the plasticity criteria of SM	SW-SM*
	$5 \leq F_{200} \leq 12$; meets the gradation criteria of SW and the plasticity criteria of SC	SW-SC*
	$5 \leq F_{200} \leq 12$; meets the gradation criteria of SP and the plasticity criteria of SM	SP-SM*
	$5 \leq F_{200} \leq 12$; meets the gradation criteria of SP and the plasticity criteria of SC	SP-SC*
Fine-grained soil (inorganic), $R_{200} \leq 50$	$PI < 4$, or Atterberg limits plot below A line (Figure 1.7)	ML
Silty and clayey soil $LL < 50$	$PI > 7$, and Atterberg limits plot on or above A line (Figure 1.7)	CL
	$4 \leq PI \leq 7$, and Atterberg limits plot above A line (Figure 1.7)	CL-ML*
	Atterberg limits plot below A line (Figure 1.7)	MH
Silty and clayey soil $LL \geq 50$	Atterberg limits plot on or above A line (Figure 1.7)	CH
Fine-grained soil (organic)		
Organic silt and clay $LL < 50$	$\frac{LL_{\text{not oven dry}}}{LL_{\text{oven dry}}} < 0.75$	OL
Organic silt and clay $LL \geq 50$	$\frac{LL_{\text{not oven dry}}}{LL_{\text{oven dry}}} < 0.75$	OH

Note: F_{200} = percent finer than no. 200 sieve; R_{200} = percent retained on no. 200 sieve; R_4 = percent retained on no. 4 sieve; C_u = uniformity coefficient; C_z = coefficient of gradation; LL = liquid limit; PI = plasticity index; Atterberg limits based on minus no. 40 fraction

* Borderline case; dual classification

▼ **TABLE 1.9** Group Names for Coarse-Grained Soils (Based on ASTM D-2487)

Group symbol	Criteria: Gravel fraction (%)	Criteria: Sand fraction (%)	Group name
GW		<15	Well graded gravel
		≥15	Well-graded gravel with sand
GP		<15	Poorly graded gravel
		≥15	Poorly graded gravel with sand
GM		<15	Silty gravel
		≥15	Silty gravel with sand
GC		<15	Clayey gravel
		≥15	Clayey gravel with sand
GC-GM		<15	Silty clayey gravel
		≥15	Silty clayey gravel with sand
GW-GM		<15	Well-graded gravel with silt
		≥15	Well-graded gravel with silt and sand
GW-GC		<15	Well graded gravel with clay
		≥15	Well graded gravel with clay and sand
GP-GM		<15	Poorly graded gravel with silt
		≥15	Poorly graded gravel with silt and sand
GP-GC		<15	Poorly graded gravel with clay
		≥15	Poorly graded gravel with clay and sand
SW	<15		Well graded sand
	≥15		Well graded sand with gravel
SP	<15		Poorly graded sand
	≥15		Poorly graded sand with gravel
SM	<15		Silty sand
	≥15		Silty sand with gravel
SC	<15		Clayey sand
	≥15		Clayey sand with gravel
SM-SC	<15		Silty clayey sand
	≥15		Silty clayey sand with gravel
SW-SM	<15		Well-graded sand with silt
	≥15		Well graded sand with silt and gravel
SW-SC	<15		Well-graded sand with clay
	≥15		Well-graded sand with clay and gravel
SP-SM	<15		Poorly graded sand with silt
	≥15		Poorly graded sand with silt and gravel
SP-SC	<15		Poorly graded sand with clay
	≥15		Poorly graded sand with clay and gravel

Note: Sand fraction = percent of soil passing no. 4 sieve but retained on no. 200 sieve = $R_{100} - R_4$; gravel fraction = percent of soil passing 3-in. sieve but retained on no. 4 sieve = R_4

▼ **TABLE 1.10** Group Names for Inorganic Fine-Grained Soils (Based on ASTM D-2487)

Group symbol	Criteria: R_{200}	Criteria: Sand fraction: Gravel fraction	Criteria: Sand fraction: Gravel fraction	Criteria: Sand fraction: Sand fraction	Group name
CL	<15				Lean clay
	15 to 29	≥1			Lean clay with sand
		<1			Lean clay with gravel
	≥30	≥1	<15		Sandy lean clay
		≥1	≥15		Sandy lean clay with gravel
		<1		<15	Gravelly lean clay
		<1		≥15	Gravelly lean clay with sand
ML	<15				Silt
	15 to 29	≥1			Silt with sand
		<1			Silt with gravel
	≥30	≥1	<15		Sandy silt
		≥1	≥15		Sandy silt with gravel
		<1		<15	Gravelly silt
		<1		≥15	Gravelly silt with sand
CL-ML	<15				Silty clay
	15 to 29	≥1			Silty clay with sand
		<1			Silty clay with gravel
	≥30	≥1	<15		Sandy silty clay
		≥1	≥15		Sandy silty clay with gravel
		<1		<15	Gravelly silty clay
		<1		≥15	Gravelly silty clay with sand
CH	<15				Fat clay
	15 to 29	≥1			Fat clay with sand
		<1			Fat clay with gravel
	≥30	≥1	<15		Sandy fat clay
		≥1	≥15		Sandy fat clay with gravel
		<1		<15	Gravelly fat clay
		<1		≥15	Gravelly fat clay with sand
MH	<15				Elastic silt
	15 to 29	≥1			Elastic silt with sand
		<1			Elastic silt with gravel
	≥30	≥1	<15		Sandy elastic silt
		≥1	≥15		Sandy elastic silt with gravel
		<1		<15	Gravelly elastic silt
		<1		≥15	Gravelly elastic silt with sand

Note: R_{200} = percent of soil retained on no. 200 sieve; sand fraction = percent of soil passing no. 4 sieve but retained on no. 200 sieve = $R_{100} - R_4$; gravel fraction = percent of soil passing 3-in. sieve but retained on no. 4 sieve = R_4

▼ **TABLE 1.11** Group Names for Organic Fine-Grained Soils (Based on ASTM D-2487)

Group symbol	Criteria: Plasticity	R_{200}	Sand fraction / Gravel fraction	Gravel fraction	Sand fraction	Group name
OL	$PI \geq 4$, and	< 15				Organic clay
	Atterberg	15 to 29	≥ 1			Organic clay with sand
	limits on		< 1			Organic clay with gravel
	or above	≥ 30	≥ 1	< 15		Sandy organic clay
	A line		≥ 1	≥ 15		Sandy organic clay with gravel
			< 1		< 15	Gravelly organic clay
			< 1		≥ 15	Gravelly organic clay with sand
	$PI < 4$, and	< 15				Organic silt
	Atterberg	15 to 29	≥ 1			Organic silt with sand
	limits plot		< 1			Organic silt with gravel
	below *A* line	≥ 30	≥ 1	< 15		Sandy organic silt
			≥ 1	≥ 15		Sandy organic silt with gravel
			< 1		< 15	Gravelly organic silt
			< 1		≥ 15	Gravelly organic silt with sand
OH	Atterberg	< 15				Organic clay
	limits plot	15 to 29	≥ 1			Organic clay with sand
	on or above		< 1			Organic clay with gravel
	A line	≥ 30	≥ 1	< 15		Sandy organic clay
			≥ 1	≥ 15		Sandy organic clay with gravel
			< 1		< 15	Gravelly organic clay
			< 1		≥ 15	Gravelly organic clay with sand
	Atterberg	< 15				Organic silt
	limits plot	15 to 29	≥ 1			Organic silt with sand
	below *A* line		< 1			Organic silt with gravel
		≥ 30	≥ 1	< 15		Sandy organic silt
			≥ 1	≥ 15		Sandy organic silt with gravel
			< 1		< 15	Gravelly organic silt
			< 1		≥ 15	Gravelly organic silt with sand

Note: R_{200} = percent of soil retained on no. 200 sieve; sand fraction = percent of soil passing no. 4 sieve but retained on no. 200 sieve = $R_{200} - R_4$; gravel fraction = percent of soil passing 3 in. sieve but retained on no. 4 sieve = R_4

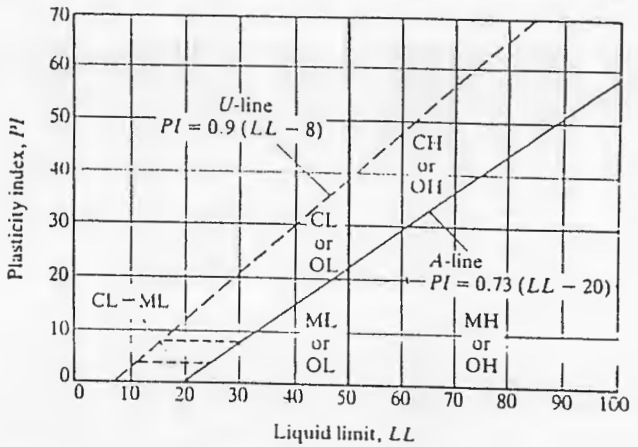

▼ **FIGURE 1.7** Plasticity chart

▼ **EXAMPLE 1.4**

Classify the following soil by the AASHTO classification system:

Percent passing no. 4 sieve = 82

Percent passing no. 10 sieve = 71

Percent passing no. 40 sieve = 64

Percent passing no. 200 sieve = 41

Liquid limit = 31

Plasticity index = 12

Solution Refer to Table 1.7. More than 35% passes through a no. 200 sieve, so it is a silt-clay material. It could be A-4, A-5, A-6, or A-7. Because $LL = 31$ (that is, less than 40) and $PI = 12$ (that is, greater than 11), this soil falls in group A-6. From Eq. (1.23)

$$GI = (F_{200} - 35)[0.02 + 0.005(LL - 40)] + 0.01(F_{200} - 15)(PI - 10)$$

So

$$GI = (41 - 35)[0.02 + 0.005(31 - 40)] + 0.01(41 - 15)(12 - 10)$$
$$= 0.37 \approx 0$$

Thus the soil is **A-6(0)**. ▼

▼ **EXAMPLE 1.5**

Classify the following soil by the AASHTO classification system.

Percent passing no. 4 sieve = 92

Percent passing no. 10 sieve = 87

Percent passing no. 40 sieve = 65

Percent passing no. 200 sieve = 30

Liquid limit = 22

Plasticity index = 8

Solution Table 1.7 shows that it is a granular material because less than 35% is passing a no. 200 sieve. With $LL = 22$ (that is, less than 40) and $PI = 8$ (that is, less than 10), the soil falls in group A-2-4. From Eq. (1.24)

$$GI = 0.01(F_{200} - 15)(PI - 10) = 0.01(30 - 15)(8 - 10)$$
$$= -0.3 \approx 0$$

The soil is **A-2-4(0).** ▼

▼ **EXAMPLE 1.6**

Classify the soil described in Example 1.5 according to the Unified Soil Classification System.

Solution For $F_{200} = 30$,

$$R_{200} = 100 - F_{200} = 100 - 30 = 70$$

As $R_{200} > 50$, it is a coarse-grained soil.

$$R_4 = 100 - \text{percent passing no. 4 sieve}$$
$$= 100 - 92 = 8$$

As $R_4 = 8 < 0.5R_{200} = 35$, it is a sandy soil. Now, refer to Table 1.8. Because F_{200} is greater than 12, the group symbol would be SM or SC. As the PI is greater than 7 and the Atterberg limits plot above the A line in Figure 1.7, it is SC.

For the group name, refer to Table 1.9. The gravel fraction is less than 15%, so the group name is **clayey sand.** ▼

1.9 PERMEABILITY OF SOIL

The void spaces or pores between soil grains allow water to flow through them. In soil mechanics and foundation engineering, you must know how much water is flowing through a soil in unit time. This knowledge is required to design earth dams, determine the quantity of seepage under hydraulic structures, and dewater before and during the construction of foundations. Darcy (1856) proposed the following equation (Figure 1.8) for calculating the velocity of flow of water through a soil.

$$\boxed{v = ki} \tag{1.25}$$

where v = Darcy velocity (unit: cm/sec)
k = coefficient of permeability of soil (unit: cm/sec)
i = hydraulic gradient

The hydraulic gradient, i, is defined as

$$i = \frac{\Delta h}{L} \tag{1.26}$$

where Δh = piezometric head difference between the sections at AA and BB
L = distance between the sections at AA and BB

(*Note:* Sections AA and BB are perpendicular to the direction of flow.)

Darcy's law [Eq. (1.25)] is valid for a wide range of soil types. However, with materials like clean gravel and open-graded rockfills, Darcy's law breaks down because of the turbulent nature of flow through them.

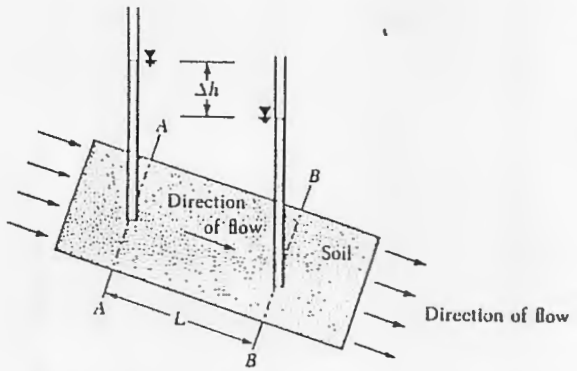

▼ **FIGURE 1.8** Definition of Darcy's law

The value of the coefficient of permeability of soils varies greatly. In the laboratory, it can be determined by means of *constant head* or *falling head* permeability tests. The constant head test is more suitable for granular soils. Table 1.12 provides the general range for the values of k for various soils. In granular soils, the value primarily

▼ **TABLE 1.12** Range of the Coefficient of Permeability for Various Soils

Type of soil	Coefficient of permeability, k (cm/sec)
Medium to coarse gravel	Greater than 10^{-1}
Coarse to fine sand	10^{-1} to 10^{-3}
Fine sand, silty sand	10^{-3} to 10^{-5}
Silt, clayey silt, silty clay	10^{-4} to 10^{-6}
Clays	10^{-7} or less

depends on the void ratio. In the past, several equations have been proposed to relate the value of k with the void ratio in the granular soil:

$$\frac{k_1}{k_2} = \frac{e_1^2}{e_2^2} \tag{1.27}$$

$$\frac{k_1}{k_2} = \frac{\left(\dfrac{e_1^2}{1+e_1}\right)}{\left(\dfrac{e_2^2}{1+e_2}\right)} \tag{1.28}$$

$$\frac{k_1}{k_2} = \frac{\left(\dfrac{e_1^3}{1+e_1}\right)}{\left(\dfrac{e_2^3}{1+e_2}\right)} \tag{1.29}$$

where k_1 and k_2 are the coefficients of permeability of a given soil at void ratios e_1 and e_2, respectively

Hazen (1930) proposed an equation for the coefficient of permeability of fairly uniform sand as

$$k = AD_{10}^2 \tag{1.30}$$

where k is in mm/sec
A = a constant that varies between 10 and 15
D_{10} = effective soil size, in mm

For clayey soils in the field, a practical relationship for estimating the coefficient of permeability (Tavenas et al., 1983) is

$$\log k = \log k_0 - \frac{e_0 - e}{C_k} \tag{1.31}$$

where k = coefficient of permeability at a void ratio e
k_0 = *in situ* coefficient of permeability at a void ratio e_0
C_k = permeability change index $\approx 0.5e_0$

For clayey soils, the coefficient of permeability for flow in the vertical and horizontal directions may vary substantially. The coefficient of permeability for flow in the vertical direction (k_v) for *in situ* soils can be estimated from Figure 1.9. For marine and other massive clay deposits

$$\frac{k_h}{k_v} < 1.5 \tag{1.32}$$

where k_h = coefficient of permeability for flow in the horizontal direction

For varved clays, the ratio of k_h/k_v may exceed 10.

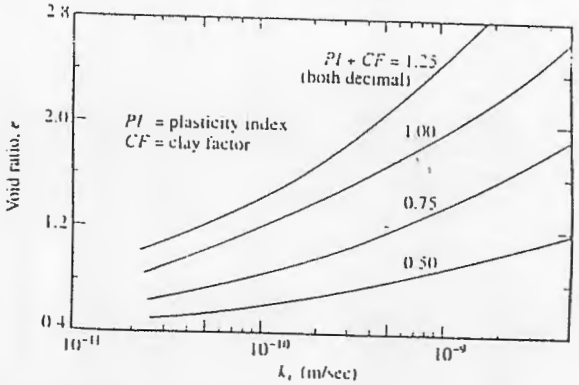

▼ **FIGURE 1.9** Variation of *in situ* k_v for clay soils (after Tavenas et al., 1983)

▼ **EXAMPLE 1.7**

The coefficient of permeability of a fine sand is 0.012 cm/sec at a void ratio of 0.57. Estimate the permeability coefficient of the sand at a void ratio of 0.72. Use Eqs. (1.27) and (1.29).

Solution From Eq. (1.27)

$$\frac{k_1}{k_2} = \frac{e_1^2}{e_2^2}$$

For $k_1 = 0.012$ cm/sec, $e_1 = 0.57$, and $e_2 = 0.72$

$$\frac{0.012}{k_2} = \frac{(0.57)^2}{(0.72)^2}$$

$$k_2 = 0.019 \text{ cm/sec}$$

From Eq. (1.29)

$$\frac{k_1}{k_2} = \frac{\dfrac{e_1^3}{1+e_1}}{\dfrac{e_2^3}{1+e_2}}$$

$$\frac{0.012}{k_2} = \frac{\dfrac{(0.57)^3}{1+0.57}}{\dfrac{(0.76)^3}{1+0.72}} = 0.544$$

$$k_2 = 0.022 \text{ cm/sec}$$ ▼

1.10 STEADY STATE SEEPAGE

For most cases of seepage under hydraulic structures, the flow path changes direction and is not uniform over the entire area. In such cases, one of the ways of determining the rate of seepage is by a graphical construction referred to as *flow net*. The flow net is based on Laplace's theory of continuity. According to this theory, for a steady flow condition, the flow at any point A (Figure 1.10) can be represented by the equation

$$k_x \frac{\partial^2 h}{\partial x^2} + k_y \frac{\partial^2 h}{\partial y^2} + k_z \frac{\partial^2 h}{\partial z^2} = 0 \qquad (1.33)$$

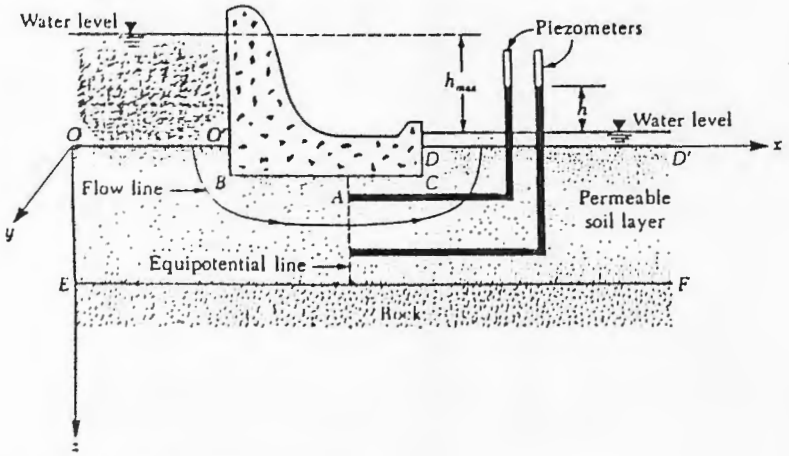

▼ FIGURE 1.10 Steady state seepage

where k_x, k_y, k_z = coefficient of permeability of the soil in x, y, and z directions, res tively

h = hydraulic head at point A (that is, the head of water that a piez eter placed at A would show with the *datum* as the *downstr water level* as shown in Figure 1.10)

For a two-dimensional flow condition as shown in Figure 1.10

$$\frac{\partial^2 h}{\partial^2 y} = 0$$

So Eq. (1.33) takes the form

$$k_x \frac{\partial^2 h}{\partial x^2} + k_z \frac{\partial^2 h}{\partial z^2} = 0 \qquad (1$$

If the soil is isotropic with respect to permeability, $k_x = k_z = k$, and

$$\boxed{\frac{\partial^2 h}{\partial x^2} + \frac{\partial^2 h}{\partial z^2} = 0} \qquad ($$

Equation (1.35), which is referred to as Laplace's equation and is valid for confined f represents two orthogonal sets of curves that are known as *flow lines* and *equipote lines*. A flow net is a combination of numerous equipotential lines and flow lines. A line is a path that a water particle would follow in traveling from the upstream sic the downstream side. An equipotential line is a line along which water in piezome would rise to the same elevation (see Figure 1.10).

In drawing a flow net, you need to establish the *boundary conditions*. example, in Figure 1.10 the ground surfaces on the upstream (OO') and downstr (DD') sides are equipotential lines. The base of the dam below the ground surf $O'BCD$, is a flow line. The top of the rock surface, EF, is also a flow line. Once boundary conditions are established, a number of flow lines and equipotential lines drawn by trial and error so that all the flow elements in the net have the same lengtl width ratio (L/B). In most cases, the L/B ratio is kept as 1—that is, the flow eleme are drawn as curvilinear "squares." This method is illustrated by the flow net shown Figure 1.11. Note that all flow lines must intersect all equipotential lines at *right angl*

Once the flow net is drawn, the seepage in unit time per unit length of the st ture can be calculated as

$$q = kh_{max} \frac{N_f}{N_d} n \qquad (1$$

where N_f = number of flow channels

N_d = number of drops

n = width to-length ratio of the flow elements in the flow net (B/L)

h_{max} = difference in water level between the upstream and downstream sides

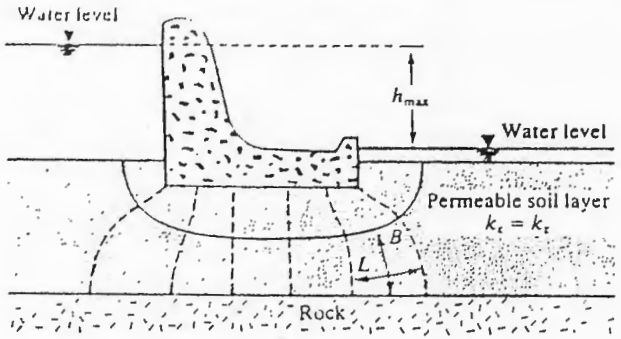

▼ **FIGURE 1.11** Flow net

The space between two consecutive flow lines is defined as a *flow channel*, and the space between two consecutive equipotential lines is called a *drop*. In Figure 1.11, $N_f = 2$, $N_d = 7$, and $n = 1$. When square elements are drawn in a flow net,

$$q = kh_{max}\frac{N_f}{N_d} \tag{1.37}$$

1.11 FILTER DESIGN CRITERIA

In the design of earth structures the engineer often encounters problems caused by the flow of water, such as soil erosion, which may result in structural instability. Erosion is generally prevented by building soil zones that are referred to as *filters* (see Figure 1.12). Two main factors influence the choice of filter material: The grain-size distribution of the filter materials should be such that (a) the soil to be protected is not washed into the filter and (b) excessive hydrostatic pressure head is not created in the soil that has a lower coefficient of permeability.

The preceding conditions can be satisfied if the following requirements are met (Terzaghi and Peck, 1967):

$$\frac{D_{15(F)}}{D_{85(B)}} < 5 \quad \text{[to satisfy condition (a)]} \tag{1.38}$$

$$\frac{D_{15(F)}}{D_{15(B)}} > 4 \quad \text{[to satisfy condition (b)]} \tag{1.39}$$

In these relations, the subscripts F and B refer to the *filter* and the *base* material (that is, the soil to be protected). Also D_{15} and D_{85} refer to the diameters through which 15% and 85% of the soil (filter or base, as the case may be) will pass.

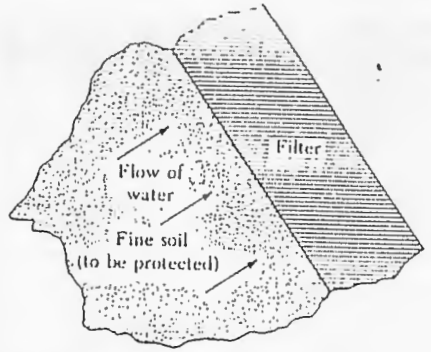

▼ **FIGURE 1.12** Filter design

The U.S. Department of the Navy (1971) provides some additional requirem for filter design to satisfy condition (a):

$$\frac{D_{50(F)}}{D_{50(B)}} < 25 \quad (1$$

$$\frac{D_{15(F)}}{D_{15(B)}} < 20 \quad (1$$

Currently, geotextiles are also used as filter materials (see Chapter 11).

1.12 EFFECTIVE STRESS CONCEPT

Consider the vertical stress at a point A located at a depth $h_1 + h_2$ below the gro surface, as shown in Figure 1.13a. The total vertical stress, σ, at A is

$$\sigma = h_1\gamma + h_2\gamma_{sat} \quad (1$$

where γ and γ_{sat} are unit weights of soil above and below the water table, respectivel

The total stress is carried partially by the *pore water* in the void spaces partially by the *soil solids* at their points of contact. For example, consider a wavy pl AB drawn through point A (see Figure 1.13a) that passes through the points of cont of soil grains. The plan of this section is shown in Figure 1.13b. The small dots Figure 1.13b represent the areas in which there is solid-to-solid contact. If the sum these areas equals A', the area filled by water equals $XY - A$. The force carried by pore water over the area shown in Figure 1.13b then is

$$F_w = (XY - A')u \quad (1.$$

where u = pore water pressure = $\gamma_w h_2$ (1.

Now let $F_1, F_2, \ldots$ be the forces of the contact points of the soil solids as shown Figure 1.13a. The sum of the vertical components of these forces over a horizontal a

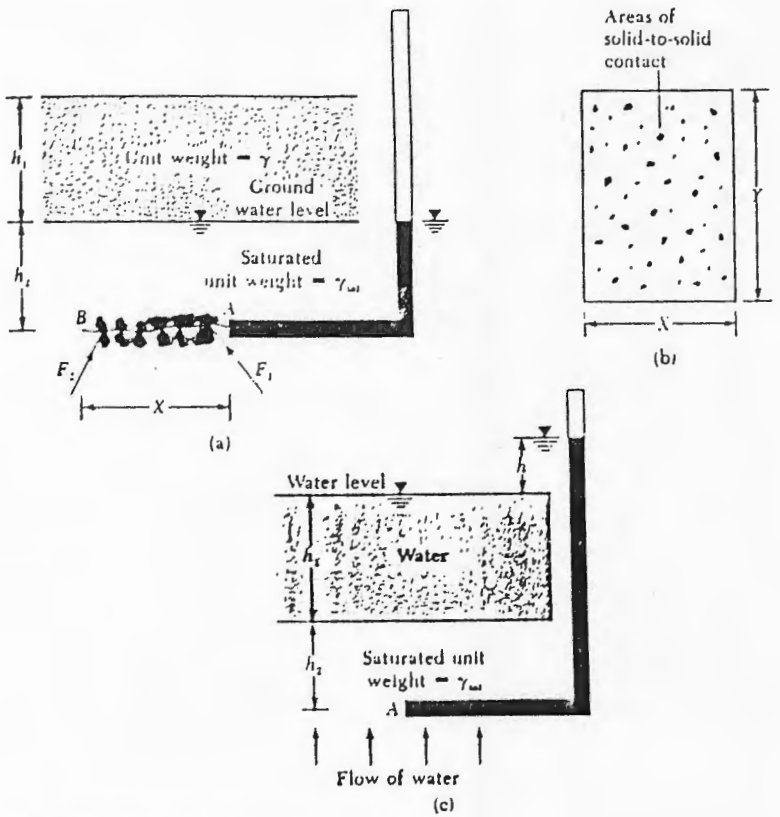

▼ **FIGURE 1.13** Effective stress calculation

XY is

$$F_s = \Sigma F_{1(v)} + F_{2(v)} + \cdots \tag{1.45}$$

where $F_{1(v)}, F_{2(v)}, \ldots$ are vertical components of forces $F_1, F_2, \ldots$, respectively

Based on the principles of statics

$$(\sigma)XY = F_w + F_s$$

or

$$(\sigma)XY = (XY - A')u + F_s$$

So

$$\sigma = (1 - a)u + \sigma' \tag{1.46}$$

where $a = A'/XY$ = fraction of the unit cross-sectional area occupied by solid-to-solid contact

$\sigma' = F_s/(XY)$ = vertical component of forces at solid-to-solid contact points over a unit cross-sectional area

The term σ' in Eq. (1.46) is generally referred to as the *vertical effective stress*. Also, the quantity a in Eq. (1.46) is very small. Thus

$$\boxed{\sigma = u + \sigma'} \tag{1.4}$$

Note that the effective stress is a *derived* quantity. Also, because the effective stress σ' is related to the contact between the soil solids, changes in effective stress will induce volume changes. It is also responsible for producing *frictional resistance* in soils and rocks. For dry soils, $u = 0$; hence $\sigma = \sigma'$.

For the problem under consideration in Figure 1.13a, $u = h_2\gamma_w$ (γ_w = unit weight of water). Thus the effective stress at point A is

$$\sigma' = \sigma - u = (h_1\gamma + h_2\gamma_{sat}) - h_2\gamma_w$$
$$= h_1\gamma + h_2(\gamma_{sat} - \gamma_w) = h_1\gamma + h_2\gamma' \tag{1.}$$

where γ' = effective or the submerged unit weight of soil
$= \gamma_{sat} - \gamma_w$

From Eq. (1.15)

$$\gamma_{sat} = \frac{G_s\gamma_w + e\gamma_w}{1 + e}$$

So

$$\gamma' = \gamma_{sat} - \gamma_w = \frac{G_s\gamma_w + e\gamma_w}{1 + e} - \gamma_w = \frac{\gamma_w(G_s - 1)}{1 + e} \tag{1.}$$

For the problem in Figure 1.13a and 1.13b, there was *no seepage of water* in the soil. Figure 1.13c shows a simple condition in a soil profile where there is upward seepage. For this case, at point A

$$\sigma = h_1\gamma_w + h_2\gamma_{sat}$$
$$u = (h_1 + h_2 + h)\gamma_w$$

Thus from Eq. (1.47)

$$\sigma' = \sigma - u = (h_1\gamma_w + h_2\gamma_{sat}) - (h_1 + h_2 + h)\gamma_w$$
$$= h_2(\gamma_{sat} - \gamma_w) - h\gamma_w = h_2\gamma' - h\gamma_w$$

or

$$\sigma' = h_2\left(\gamma' - \frac{h}{h_2}\gamma_w\right) = h_2(\gamma' - i\gamma_w) \tag{1.50}$$

Note in Eq. (1.50) that h/h_2 is the hydraulic gradient, i. If the hydraulic gradient is very high, so that $\gamma' - \gamma_w$ becomes zero, *the effective stress will become zero*. In other words, there is no contact stress between the soil particles, and the soil structure will break up. This situation is referred to as the *quick condition*, or *failure by heave*. So, for heave,

$$\boxed{i = i_{cr} = \frac{\gamma'}{\gamma_w} = \frac{G_s - 1}{1 + e}} \tag{1.51}$$

where i_{cr} = critical hydraulic gradient.

For most sandy soils, i_{cr} ranges from 0.9 to 1.1, with an average of about 1.

▼ EXAMPLE 1.8

For the soil profile shown in Figure 1.14, determine the total vertical stress, pore water pressure, and effective vertical stress at A, B, and C.

Solution At A:

$$\sigma = 0$$

$$u = 0$$

$$\sigma' = 0$$

At B:

$$\sigma = (\gamma_d)(10) = (110)(10) = 1100 \text{ lb/ft}^2$$

$$u = 0$$

$$\sigma' = 1100 - 0 = 1100 \text{ lb/ft}^2$$

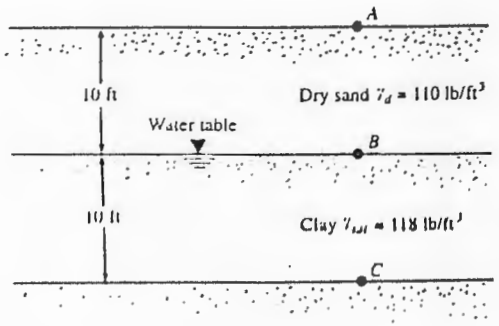

▼ FIGURE 1.14

At C:

$$\sigma = (\gamma_d)(10) + (\gamma_{sat})(10) = (110)(10) + (118)(10) = 2280 \text{ lb/ft}^2$$

$$u = (\gamma_w)(10) = (62.4)(10) = 624 \text{ lb/ft}^2$$

$$\sigma' = \sigma - u = 2280 - 624 = 1656 \text{ lb/ft}^2$$ ▼

1.13 CAPILLARY RISE IN SOIL

When a capillary tube is placed in water, the water level in the tube rises (Figure 1.1 This rise is caused by the *surface tension* effect. According to Figure 1.15a, the pres at any point A in the capillary tube (with respect to the atmospheric pressure) ca expressed as

$$u = -\gamma_w z' \qquad (\text{for } z' = 0 \text{ to } h_c)$$

and

$$u = 0 \qquad (\text{for } z' \geq h_c)$$

In a given soil mass, the interconnected void spaces can behave like a numb capillary tubes with varying diameters. The surface tension force may cause wat the soil to rise above the water table, as shown in Figure 1.15b. The height of capillary rise will depend on the diameter of the capillary tubes. The capillary rise *decrease* with the increase of the tube diameter. Because the capillary tubes in soil variable diameters, the height of capillary rise will be nonuniform. The pore w pressure at any point in the zone of capillary rise in soil can be approximated as

$$u = -S\gamma_w z' \tag{1}$$

where S = degree of saturation of soil [Eq. (1.7)]
z' = distance measured above the water table

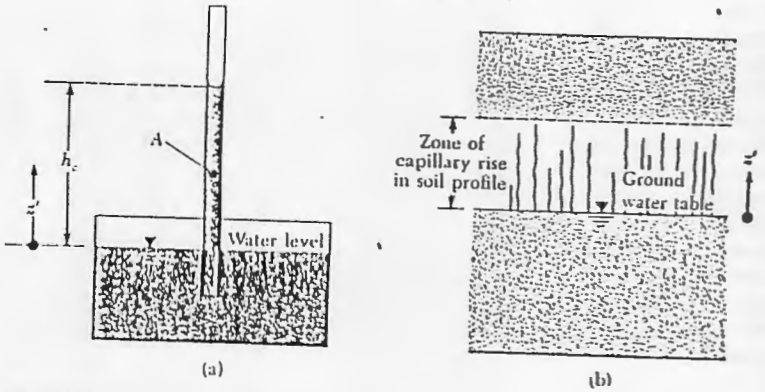

▼ FIGURE 1.15 Capillary rise

1.14 CONSOLIDATION

In the field when the stress on a saturated clay layer is increased—for example by the construction of a foundation—the pore water pressure in the clay will increase. Because the coefficients of permeability of clays are very small, some time will be required for the excess pore water pressure to dissipate and the stress increase to be transferred to the soil skeleton gradually. According to Figure 1.16, if Δp is a surcharge at the ground surface over a very large area, the increase of total stress, $\Delta\sigma$, at any depth of the clay layer will be equal to Δp, or

$$\Delta\sigma = \Delta p$$

However, at time $t = 0$ (i.e., immediately after the stress application), the excess pore water pressure at any depth, Δu, will equal Δp, or

$$\Delta u = \Delta h_i \gamma_w = \Delta p \qquad \text{(at time } t = 0\text{)}$$

Hence the increase of effective stress at time $t = 0$ will be

$$\Delta\sigma' = \Delta\sigma - \Delta u = 0$$

Theoretically, at time $t = \infty$, when all the excess pore water pressure in the clay layer has dissipated as a result of drainage into the sand layers,

$$\Delta u = 0 \qquad \text{(at time } t = \infty\text{)}$$

Then the increase of effective stress in the clay layer is

$$\Delta\sigma' = \Delta\sigma - \Delta u = \Delta p - 0 = \Delta p$$

This gradual increase in the effective stress in the clay layer will cause settlement over a period of time and is referred to as *consolidation*.

Laboratory tests on undisturbed saturated clay specimens can be conducted (ASTM Test Designation D-2435) to determine the consolidation settlement caused by

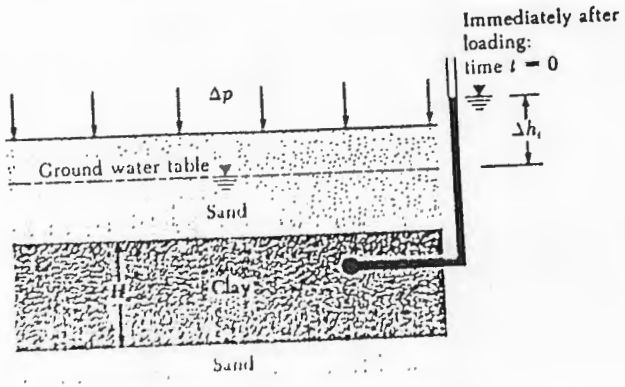

▼ **FIGURE 1.16** Principles of consolidation

various incremental loadings. The test specimens are usually 2.5 in. (63.5 mm) in diameter and 1 in. (25.4 mm) in height. Specimens are placed inside a ring, with one porous stone at the top and one at the bottom of the specimen. Figure 1.17a. Load on the specimen is then applied so that the total stress is equal to p. Settlement readings for the specimen are taken for 24 hours. After that, the load on the specimen is doubled and settlement readings are taken. At all times during the test the specimen is kept under water. This procedure is continued until the desired limit of stress on the clay specimen is reached.

Based on the laboratory tests, a graph can be plotted showing the variation of the void ratio e at the *end* of consolidation against the corresponding stress p (semilogarithmic graph: e on the arithmetic scale and p on the log scale). The nature of variation of e against log p for a clay specimen is shown in Figure 1.17b. After the

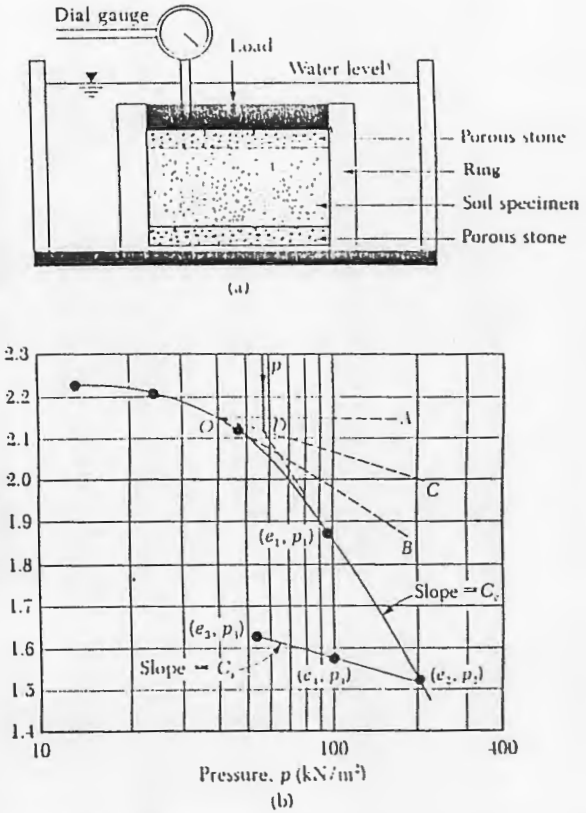

▼ **FIGURE 1.17** (a) Schematic diagram of consolidation test arrangement; (b) e–log p curve for a soft clay from East St. Louis, Illinois

desired consolidation pressure has been reached, the specimen can be gradually unloaded, which will result in the swelling of the specimen. Figure 1.17b also shows the variation of the void ratio during the unloading period.

From the e–log p curve shown in Figure 1.17b, three parameters necessary for calculating settlement in the field can be determined.

1. The *preconsolidation pressure*, p_c, is the *maximum past effective overburden pressure* to which the soil specimen has been subjected. It can be determined by using a simple graphical procedure as proposed by Casagrande (1936). This procedure for determining the preconsolidation pressure, with reference to Figure 1.17b, involves five steps:
   a. Determine the point O on the e–log p curve that has the sharpest curvature (that is, the smallest radius of curvature).
   b. Draw a horizontal line OA.
   c. Draw a line OB that is tangent to the e–log p curve at O.
   d. Draw a line OC that bisects the angle AOB.
   e. Produce the straight line portion of the e–log p curve backward to intersect OC. This is point D. The pressure that corresponds to point p is the preconsolidation pressure, p_c.

Natural soil deposits can be *normally consolidated* or *overconsolidated* (or *preconsolidated*). If the present effective overburden pressure $p = p_o$ is equal to the preconsolidated pressure p_c, the soil is *normally consolidated*. However, if $p_o < p_c$, the soil is *overconsolidated*.

Preconsolidation pressure (p_c) has been correlated with the index parameters by several investigators. Stas and Kulhawy (1984) suggested that

$$\frac{p_c}{\sigma_a} = 10^{(1.11 - 1.62LI)} \tag{1.53a}$$

where σ_a = atmospheric stress in derived unit
LI = liquidity index

The liquidity index of a soil is defined as

$$LI = \frac{w - PL}{LL - PL} \tag{1.53b}$$

where w = *in situ* moisture content
LL = liquid limit
PL = plastic limit

The U.S. Department of the Navy (1982) also provided generalized relationships between p_c, LI, and the sensitivity of clayey soils (S_t). This relationship was also recommended by Kulhawy and Mayne (1990). The definition of sensitivity is given in Section 1.17. Figure 1.18 shows the relationship.

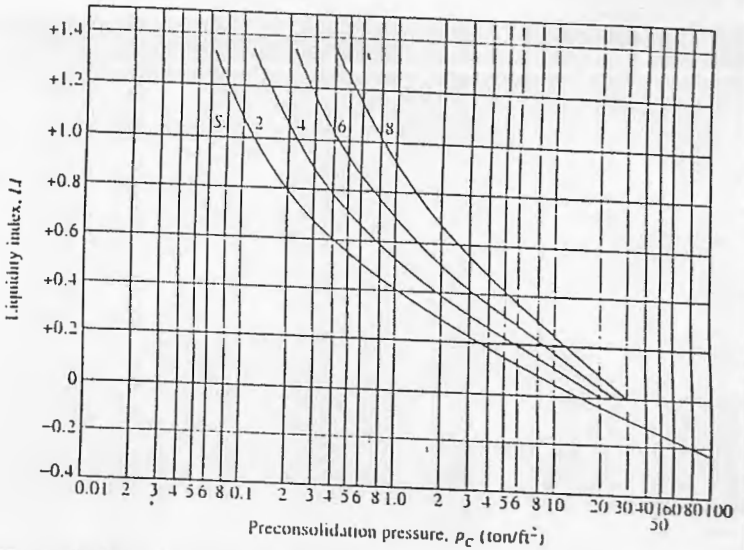

▼ **FIGURE 1.18** Variation of p_c with LI (after U.S. Department of the Navy, 1982)

2. The *compression index*, C_c, is the slope of the straight-line portion (latte of the loading curve), or

$$C_c = \frac{e_1 - e_2}{\log p_2 - \log p_1} = \frac{e_1 - e_2}{\log\left(\frac{p_2}{p_1}\right)}$$

where e_1 and e_2 are the void ratios at the end of consolidation under str p_1 and p_2, respectively

The *compression index*, as determined from the laboratory e–l curve, will be somewhat different from that encountered in the field. primary reason is that the soil remolds to some degree during the field e ration. The nature of variation of the e–log p curve in the field for a norm consolidated clay is shown in Figure 1.19. It is generally referred to as *virgin compression curve*. The virgin curve approximately intersects the la atory curve at a void ratio of $0.42e_o$ (Terzaghi and Peck, 1967). Note that the void ratio of the clay in the field. Knowing the values of e_o and p_c, can easily construct the virgin curve and calculate the compression inde the virgin curve by using Eq. (1.54).

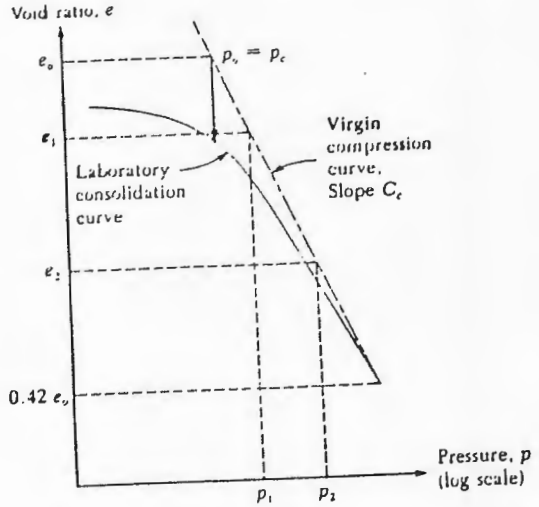

▼ **FIGURE 1.19** Construction of virgin compression curve for normally consolidated clay

The value of C_c can vary widely depending on the soil. Skempton (1944) has given an empirical correlation for the compression index in which

$$C_c = 0.009(LL - 10) \tag{1.55}$$

where LL = liquid limit

Besides Skempton, other investigators have proposed correlations for the compression index. Some of these correlations are summarized in Table 1.13.

3. The *swelling index*, C_s, is the slope of the unloading portion of the e–log p curve. In Figure 1.17b, it can be defined as

$$C_s = \frac{e_3 - e_4}{\log\left(\frac{p_4}{p_3}\right)} \tag{1.56}$$

In most cases the value of the swelling index (C_s) is $\frac{1}{4}$ to $\frac{1}{3}$ of the compression index. Following are some representative values of C_s/C_c for natural soil deposits.

Description of soil	C_s/C_c
Boston Blue clay	0.24–0.33
Chicago clay	0.15–0.3
New Orleans clay	0.15–0.28
St. Lawrence clay	0.05–0.1

▼ **TABLE 1.13** Correlations for Compression Index

References	Correlation
Azzouz, Krizek, and Corotis (1976)	$C_c = 0.01w_n$ (Chicago clay) $C_c = 0.208e_o + 0.0083$ (Chicago clay) $C_c = 0.0115w_n$ (organic soils, peat) $C_c = 0.0046(LL - 9)$ (Brazilian clay)
Rendon-Herrero (1980)	$C_c = 0.141G_s^{1.2}\left(\frac{1+e_o}{G_s}\right)^{2.18}$
Nagaraj and Murty (1985)	$C_c = 0.2343\left(\frac{LL}{100}\right)G_s$
Wroth and Wood (1978)	$C_c = 0.5G_s\left(\frac{PI}{100}\right)$
Leroueil, Tavenas, and LeBihan (1983)	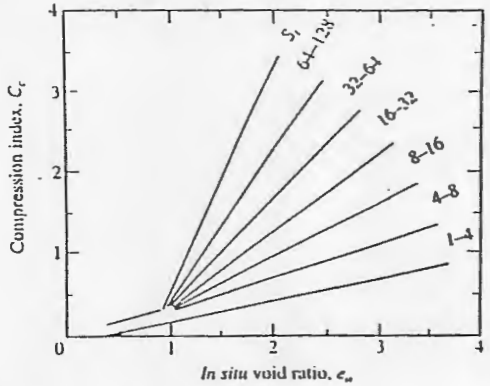

Note: G_s = specific gravity of soil solids
LL = liquid limit
PI = plasticity index
S_t = sensitivity
w_n = natural moisture content

The swelling index determination is important in the estimation of consolidation settlement of *overconsolidated clays*. In the field, depending on the pressure increase, an overconsolidated clay will follow and e–log p path abc, as shown in Figure 1.20. Note that point a, with coordinates of p_o and e_o, corresponds to the field conditions before any pressure increase. Point b corresponds to the preconsolidation pressure (p_c) of the clay. Line ab is approximately parallel to the laboratory unloading curve cd (Schmertmann, 1953). Hence, if you know e_o, p_o, p_c, C_c, and C_s, you can easily construct the field consolidation curve.

Nagaraj and Murthy (1985) expressed the swelling index as

$$C_s = 0.0463\left(\frac{LL}{100}\right)G_s \tag{1.57}$$

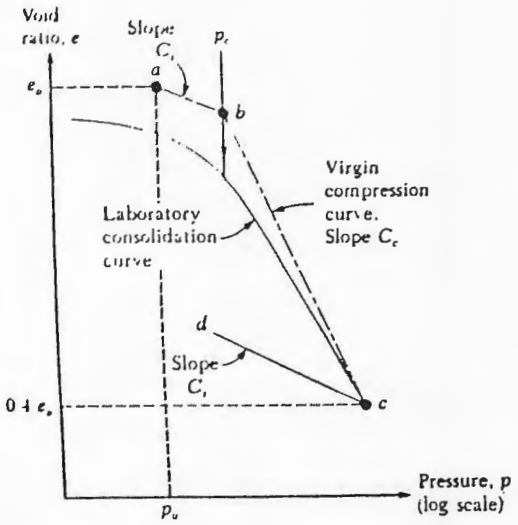

▼ **FIGURE 1.20** Construction of field consolidation curve for overconsolidated clay

Calculation of Settlement

The one-dimensional consolidation settlement (caused by an additional load) of a clay layer (Figure 1.21a) having a thickness H_c may be calculated as

$$\boxed{S = \frac{\Delta e}{1 + e_o} H_c} \tag{1.58}$$

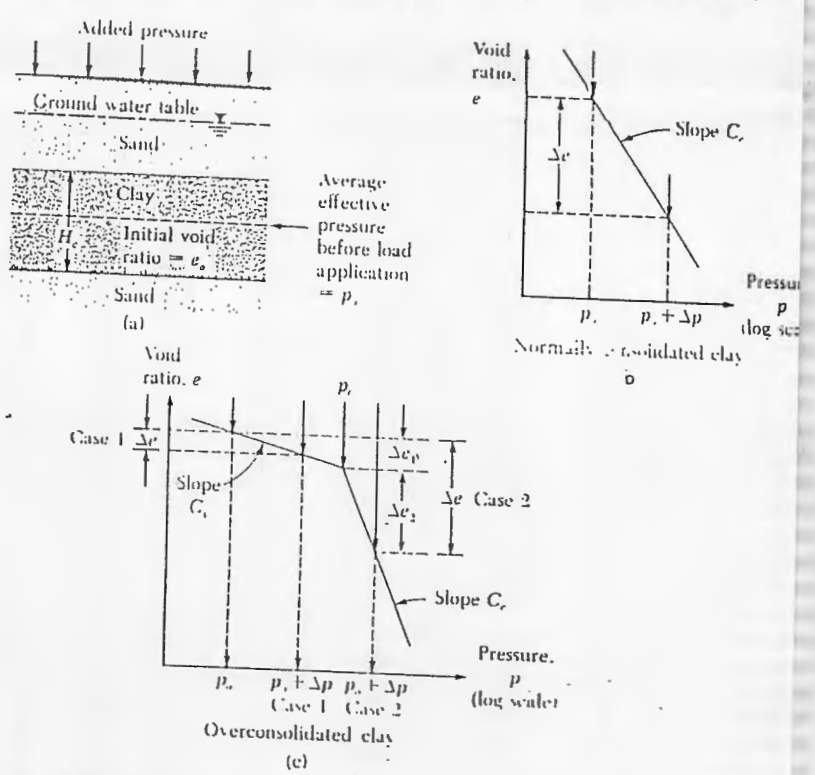

▼ **FIGURE 1.21** One dimensional settlement calculation: (b) is for Eq. (1.59); (c) is for Eqs. (1.62) and (1.64)

where S = settlement
Δe = total change of void ratio caused by the additional load application
e_o = the void ratio of the clay before the application of load

Note that

$$\frac{\Delta e}{1 + e_o} = \varepsilon_v = \text{vertical strain}$$

For normally consolidated clay, the field e–log p curve will be like the one shown in Figure 1.21b. If p_o = initial average effective overburden pressure on the clay layer and Δp = average pressure increase on the clay layer caused by the added load, the change of void ratio caused by the load increase is

$$\Delta e = C_c \log \frac{p_o + \Delta p}{p_o} \tag{1.59}$$

Now, combining Eqs. (1.58) and (1.59) yields

$$\boxed{S = \frac{C_c H_c}{1 + e_o} \log \frac{p_o + \Delta p}{p_o}} \tag{1.60}$$

For overconsolidated clay, the field e–log p curve will be like the one shown in Figure 1.21c. In this case, depending on the value of Δp, two conditions may arise. First, if $p_o + \Delta p < p_c$,

$$\Delta e = C_s \log \frac{p_o + \Delta p}{p_o} \tag{1.61}$$

Combining Eqs. (1.58) and (1.61) gives

$$\boxed{S = \frac{H_c C_s}{1 + e_o} \log \frac{p_o + \Delta p}{p_o}} \tag{1.62}$$

Second, if $p_o < p_c < p_o + \Delta p$

$$\Delta e = \Delta e_1 + \Delta e_2 = C_s \log \frac{p_c}{p_o} + C_c \log \frac{p_o + \Delta p}{p_o} \tag{1.63}$$

Now, combining Eqs. (1.58) and (1.63) yields

$$\boxed{S = \frac{C_s H_c}{1 + e_o} \log \frac{p_c}{p_o} + \frac{C_c H_c}{1 + e_o} \log \frac{p_o + \Delta p}{p_c}} \tag{1.64}$$

Average Degree of Consolidation

Earlier in this section (see Figure 1.16) we showed that consolidation is the result of gradual dissipation of the excess pore water pressure from a clay layer. Pore water pressure dissipation, in turn, increases the effective stress, which induces settlement. Hence, to estimate the degree of consolidation of a clay layer at some time t after the load application, you need to know the rate of dissipation of the excess pore water pressure.

Figure 1.22a shows a clay layer of thickness H_c that has highly permeable sand layers at its top and bottom. Here, the excess pore water pressure at any point A at any time t after the load application is $\Delta u = (\Delta h)\gamma_w$. For a vertical drainage condition (that is, in the direction of z only) from the clay layer, Terzaghi derived the following differential equation:

$$\frac{\partial(\Delta u)}{\partial t} = C_v \frac{\partial^2(\Delta u)}{\partial z^2} \tag{1.65}$$

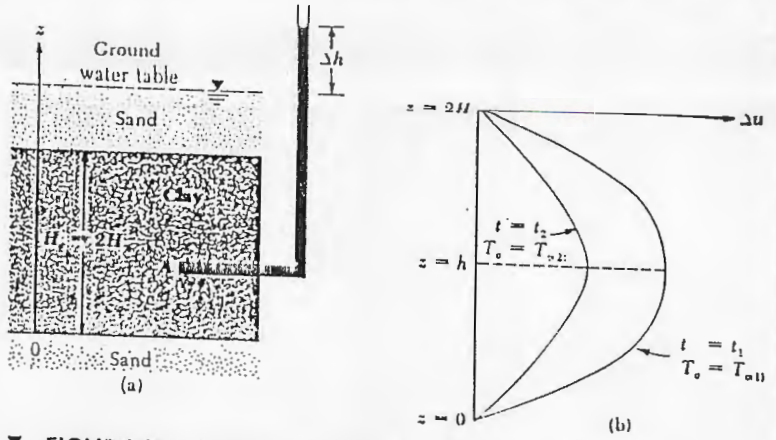

▼ **FIGURE 1.22** (a) Derivation of Eq. (1.67); (b) nature of variation of Δu with time

where C_v = coefficient of consolidation

$$\boxed{C_v = \frac{k}{m_v \gamma_w} = \frac{k}{\dfrac{\Delta e}{\Delta p(1 + e_{av})}\gamma_w}} \tag{1.}$$

where k = coefficient of permeability of the clay
Δe = total change of void ratio caused by a stress increase of Δp
e_{av} = average void ratio during consolidation
m_v = volume coefficient of compressibility = $\Delta e/[\Delta p(1 + e_{av})]$

Equation (1.65) can be solved to obtain Δu as a function of time t with the followi boundary conditions.

1. Because highly permeable sand layers are located at $z = 0$ and $z = H_c$, t excess pore water pressure developed in the clay at those points will be imm diately dissipated. Hence

   $\Delta u = 0$ at $z = 0$

   $\Delta u = 0$ at $z = H_c = 2H$

   where H = length of maximum drainage path (due to two-way drainag condition—that is, at the top and bottom of the clay)

2. At time $t = 0$

   $\Delta u = \Delta u_o$ = initial excess pore water pressure after the load application

With the preceding boundary conditions, Eq. (1.65) yields

$$\Delta u = \sum_{m=0}^{m=\infty} \left[\frac{2(\Delta u_o)}{M} \sin\left(\frac{Mz}{H}\right) \right] e^{-M^2 T_v} \tag{1.67}$$

where $M = [(2m+1)\pi]/2$

m = an integer = 1, 2, ...

T_v = nondimensional time factor = $(C_v t)/H^2$ (1.68)

Determining the field value of C_v is difficult. Figure 1.23 provides a first-order determination of C_v using the liquid limit (U.S. Department of the Navy, 1971). The value of Δu for various depths (that is, $z = 0$ to $z = 2H$) at any given time t (thus T_v) can be calculated from Eq. (1.67). The nature of this variation of Δu is shown in Figure 1.22b.

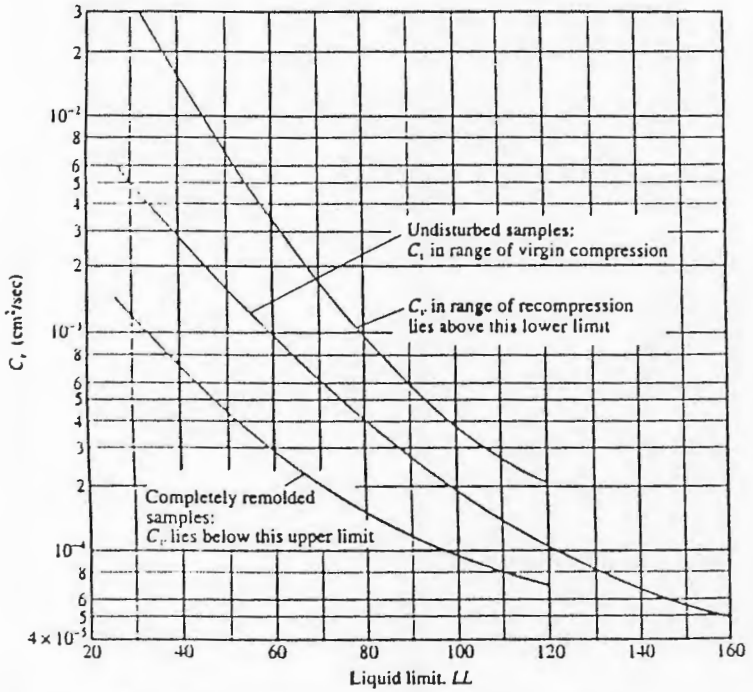

▼ **FIGURE 1.23** Range of C_v (after U.S. Department of the Navy, 1971)

The *average degree of consolidation* of clay layer can be defined as

$$\boxed{U = \frac{S_t}{S_{max}}} \tag{1.69}$$

where U = average degree of consolidation

S_t = settlement of a clay layer at time t after the load application

S_{max} = maximum consolidation settlement that the clay will undergo under a given loading

If the initial pore water pressure (Δu_o) distribution is constant with depth shown in Figure 1.24a, the average degree of consolidation can also be expressed as

$$U = \frac{S_t}{S_{max}} = \frac{\int_0^{2H} (\Delta u_0)dz - \int_0^{2H} (\Delta u)dz}{\int_0^{2H} (\Delta u_0)dz}$$

or

$$U = \frac{(\Delta u_0)2H - \int_0^{2H} (\Delta u)dz}{(\Delta u_o)2H} = 1 - \frac{\int_0^{2H} (\Delta u)dz}{2H(\Delta u_o)}$$

Now, combining Eqs. (1.67) and (1.71), we obtain

$$U = \frac{S_t}{S_{max}} = 1 - \sum_{m=0}^{m=\infty} \left(\frac{2}{M^2}\right) e^{-M^2 T_v}$$

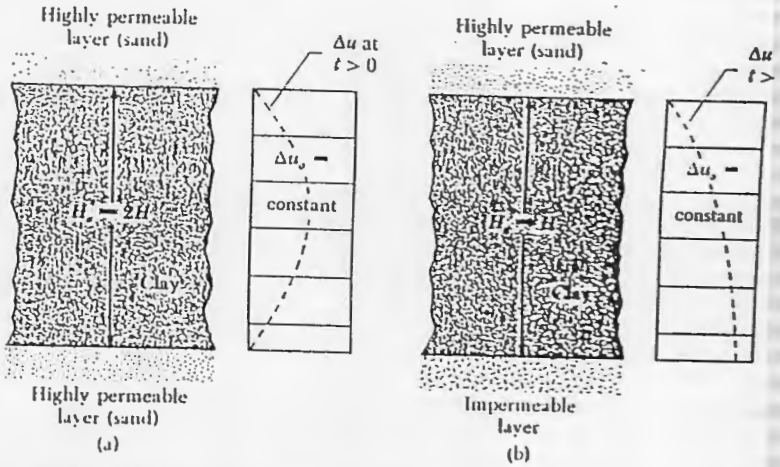

▼ **FIGURE 1.24** Drainage condition for consolidation: (a) two-way drainage; (b) one-way drainag

The variation of U with T_v can be calculated from Eq. (1.72) and is plotted Figure 1.25. Note that Eq. (1.72) and thus Figure 1.25 are also valid when an impen

able layer is located at the bottom of the clay layer (Figure 1.24b). In that case, excess pore water pressure dissipation can take place in one direction only. The length of the *maximum drainage path* then is equal to $H = H_c$.

The variation of T_v with U shown in Figure 1.25 can also be approximated by

$$T_v = \frac{\pi}{4}\left(\frac{U\%}{100}\right)^2 \qquad (\text{for } U = 0\text{–}60\%) \tag{1.73}$$

and

$$T_v = 1.781 - 0.933 \log (100 - U\%) \qquad (\text{for } U > 60\%) \tag{1.74}$$

Sivaram and Swamee (1977) have also developed an empirical relationship between T_v and U that is valid for U varying from 0 to 100%. It is of the form

$$\boxed{T_v = \frac{\left(\frac{\pi}{4}\right)\left(\frac{U\%}{100}\right)^2}{\left[1 - \left(\frac{U\%}{100}\right)^{5.6}\right]^{0.357}}} \tag{1.75}$$

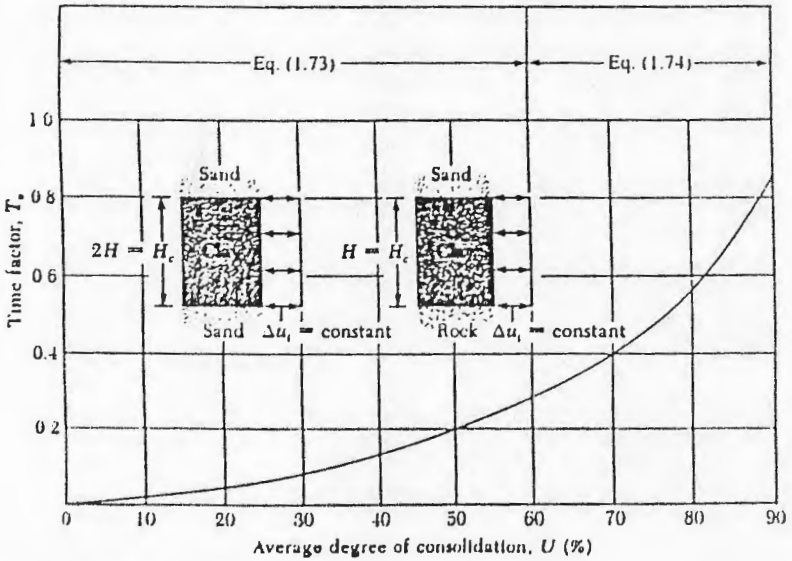

▼ **FIGURE 1.25** Plot of time factor against average degree of consolidation (Δu_i = constant)

▼ **EXAMPLE 1.9**

A laboratory consolidation test on a normally consolidated clay showed the follo

Load, p (kN/m²)	Void ratio at the end of consolidation, e
140	0.92
212	0.86

The specimen tested was 25.4 mm in thickness and drained on both sides. T required for the specimen to reach 50% consolidation was 4.5 min.

A similar clay layer in the field, 2.8 m thick and drained on both sides, jected to similar average pressure increase (that is, p_o = 140 kN·m² and $p_o + \Delta$ kN/m²). Determine the

a. Expected maximum consolidation settlement in the field
b. Length of time required for the total settlement in the field to reach 40

Solution

Part a

For normally consolidated clay [Eq. (1.54)]

$$C_c = \frac{e_1 - e_2}{\log\left(\frac{p_2}{p_1}\right)} = \frac{0.92 - 0.86}{\log\left(\frac{212}{140}\right)} = 0.333$$

From Eq. (1.60)

$$S = \frac{C_c H_c}{1 + e_o}\log\frac{p_o + \Delta p}{p_o} = \frac{(0.333)(2.8)}{1 + 0.92}\log\frac{212}{140} = 0.0875 \text{ m} = \mathbf{87.5 \text{ mm}}$$

Part b

From Eq. (1.69) the average degree of consolidation is

$$U = \frac{S_t}{S_{max}} = \frac{40}{87.5}(100) = 45.7\%$$

The coefficient of consolidation, C_v, can be calculated from the laboratory From Eq. (1.68)

$$T_v = \frac{C_v t}{H^2}$$

For 50% consolidation (Figure 1.25), $T_v = 0.197$, $t = 4.5$ min, and $H = H_c/2 = 12.7$ mm. So

$$C_v = T_{50}\frac{H^2}{t} = \frac{(0.197)(12.7)^2}{4.5} = 7.061 \text{ mm}^2/\text{min}$$

Again, for field consolidation, $U = 45.7\%$. From Eq. (1.73)

$$T_v = \frac{\pi}{4}\left(\frac{U\%}{100}\right)^2 = \frac{\pi}{4}\left(\frac{47.5}{100}\right)^2 = 0.177$$

But

$$T_v = \frac{C_v t}{H^2}$$

or

$$t = \frac{T_v H^2}{C_v} = \frac{0.177\left(\frac{2.8 \times 1000}{2}\right)^2}{7.061} = 49132 \text{ min} = 34.1 \text{ days}$$ ▼

1.15 SHEAR STRENGTH

The shear strength, s, of a soil, in terms of effective stress, is

$$\boxed{s = c + \sigma' \tan\phi} \tag{1.76}$$

where σ' = effective normal stress on plane of shearing
c = cohesion, or apparent cohesion
ϕ = angle of friction

Equation (1.76) is referred to as the *Mohr–Coulomb failure criteria*. The value of c for sands and normally consolidated clays is equal to zero. For overconsolidated clays, $c > 0$.

For most day-to-day work, the shear strength parameters of a soil (that is, c and ϕ) are determined by two standard laboratory tests. They are (a) the *direct shear test* and (b) the *triaxial test*.

Direct Shear Test

Dry sand can be conveniently tested by direct shear tests. The sand is placed in a shear box that is split into two halves (Figure 1.26a). A normal load is first applied to the

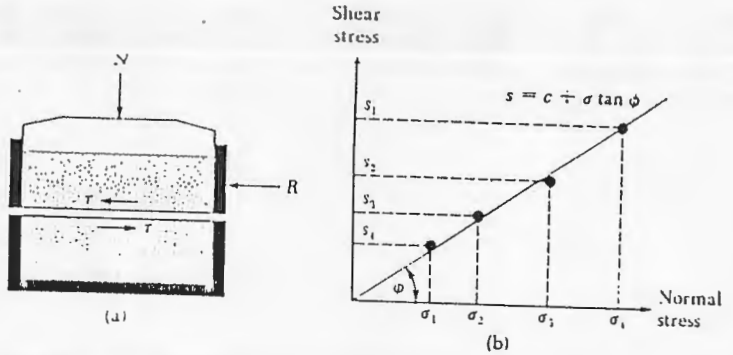

▼ **FIGURE 1.26** Direct shear test in sand: (a) schematic diagram of test equipment; (b) plot of te results to obtain the friction angle, ϕ

specimen. Then a shear force is applied to the two halves of the shear box to ca failure in the sand. The normal and shear stresses at failure are

$$\sigma' = \frac{N}{A}$$

$$s = \frac{R}{A}$$

where A = area of the failure plane in soil—that is, the area of cross section of shear box

Several tests of this type can be conducted by varying the normal load. The angle friction of the sand can be determined by plotting a graph of s against σ', as shown Figure 1.26b, or

$$\boxed{\phi = \tan^{-1}\left(\frac{s}{\sigma'}\right)} \tag{1.}$$

For sands the angle of friction usually ranges from 26° to 45°, increasing with t relative density of compaction. The approximate range of the relative density of co paction and the corresponding range of the angle of friction for various coarse-grain soils is shown in Figure 1.27.

Triaxial Tests

Triaxial compression tests can be conducted on sands and clays. Figure 1.28a shows schematic diagram of the triaxial test arrangement. Essentially, it consists of placing soil specimen confined by a rubber membrane in a lucite chamber. An all-around confi ing pressure (σ_3) is applied to the specimen by means of the chamber fluid (general

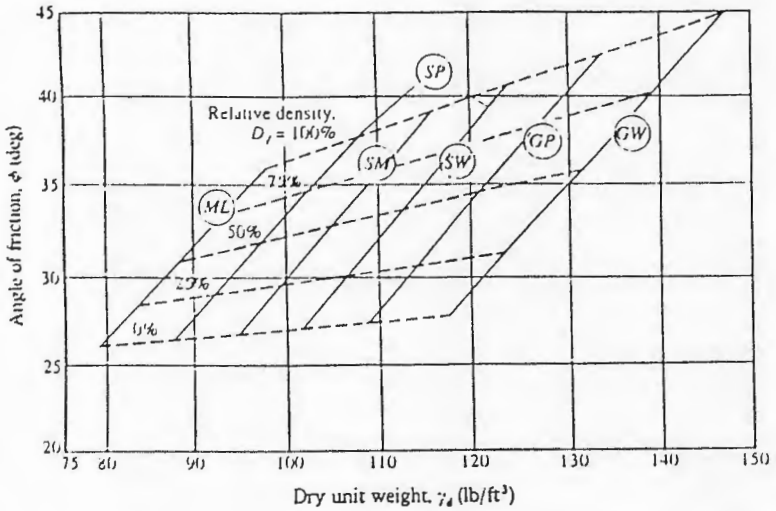

▼ **FIGURE 1.27** Range of relative density of compaction and corresponding range of angle of friction for coarse grained soil (after U.S. Department of the Navy, 1971)

water or glycerin). An added stress ($\Delta\sigma$) can also be applied to the specimen in the axial direction to cause failure ($\Delta\sigma = \Delta\sigma_f$ at failure). Drainage from the specimen can be allowed or stopped, depending on the test condition. For clays, three main types of tests can be conducted with triaxial equipment:

1. Consolidated-drained test (CD test)
2. Consolidated-undrained test (CU test)
3. Unconsolidated undrained test (UU test)

Table 1.14 summarizes these three tests.

For *consolidated-drained tests*, at failure,

Major principal effective stress $= \sigma_3 + \Delta\sigma_f = \sigma_1 = \sigma'_1$

Minor principal effective stress $= \sigma_3 = \sigma'_3$

Changing σ_3 allows several tests of this type to be conducted on various clay specimens. The shear strength parameters (c and ϕ) can now be determined by plotting Mohr's circle at failure, as shown in Figure 1.28b, and drawing a common tangent to the Mohr's circles. This is the *Mohr-Coulomb failure envelope*. (*Note:* For normally consolidated clay, $c \approx 0$.) At failure

$$\boxed{\sigma'_1 = \sigma'_3 \tan^2\left(45 + \frac{\phi}{2}\right) + 2c \tan\left(45 + \frac{\phi}{2}\right)} \tag{1.78}$$

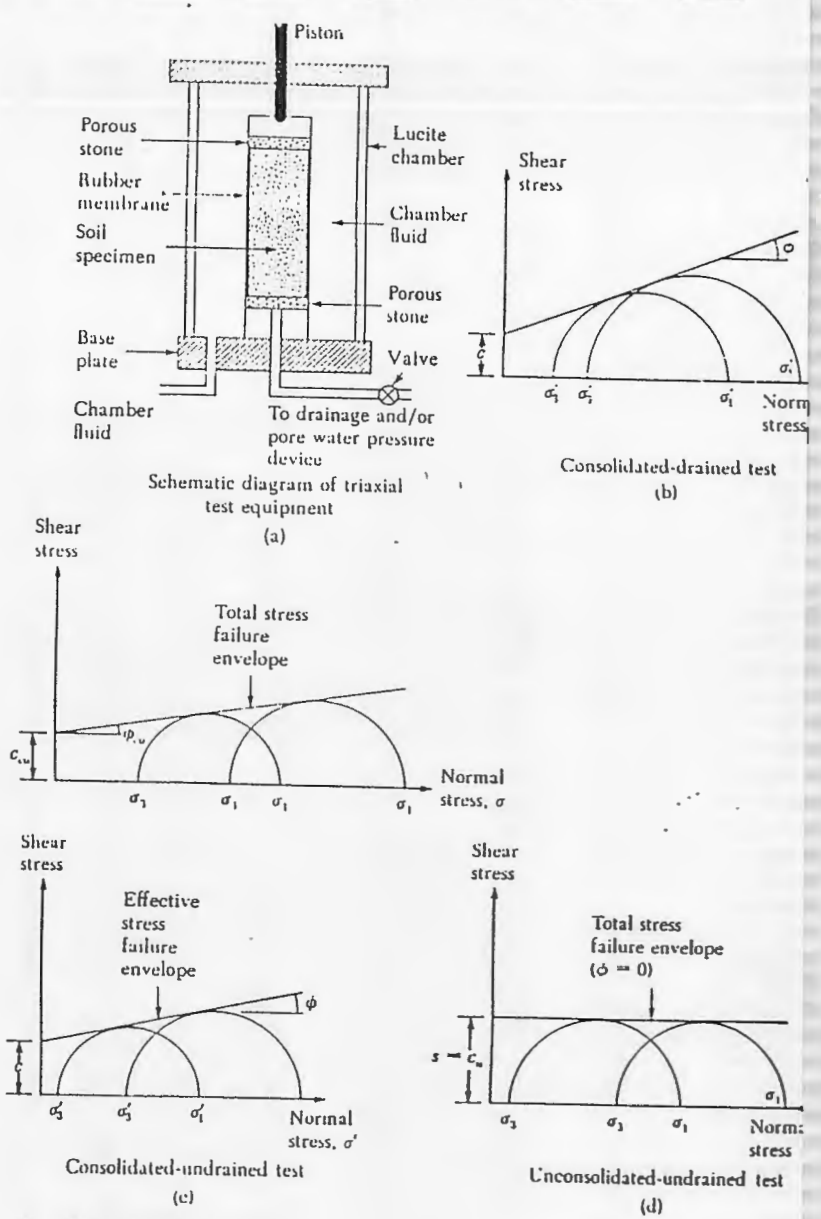

▼ **FIGURE 1.28** Triaxial test

▼ **TABLE 1.14** Summary of Triaxial Tests on Saturated Clays

Test type	Step 1	Step 2
Consolidated-drained	Apply chamber pressure, σ_3. Allow complete drainage, so pore water pressure ($u = u_a$) developed is zero.	Apply axial stress, $\Delta\sigma$, slowly. Allow drainage, so pore water pressure ($u = u_a$) developed through application of $\Delta\sigma$ is zero. At failure, $\Delta\sigma = \Delta\sigma_f$; total pore water pressure $u_f = u_a + u_d = 0$.
Consolidated-undrained	Apply chamber pressure, σ_3. Allow complete drainage, so pore water pressure ($u = u_a$) developed is zero	Apply axial stress, $\Delta\sigma$. Do not allow drainage ($u = u_d \neq 0$). At failure, $\Delta\sigma = \Delta_f$; pore water pressure $u = u_f = u_a + u_d = 0 + u_{d(f)}$.
Unconsolidated-undrained	Apply chamber pressure, σ_3. Do not allow drainage, so pore water pressure ($u = u_a$) developed through application of σ_3 is not zero.	Apply axial stress, $\Delta\sigma$. Do not allow drainage ($u = u_d \neq 0$). At failure $\Delta\sigma = \Delta\sigma_f$; pore water pressure $u = u_f = u_a + u_{d(f)}$.

For *consolidated undrained* tests, at failure,

$$\text{Major principal total stress} = \sigma_3 + \Delta\sigma_f = \sigma_1$$

$$\text{Minor principal total stress} = \sigma_3$$

$$\text{Major principal effective stress} = (\sigma_3 + \Delta\sigma_f) - u_f = \sigma'_1$$

$$\text{Minor principal effective stress} = \sigma_3 - u_f = \sigma'_3$$

Changing σ_3 permits multiple tests of this type to be conducted on several soil specimens. The total stress Mohr's circles at failure can now be plotted, as shown in Figure 1.28c, and then a common tangent can be drawn to define the *failure envelope*. This *total stress failure envelope* is defined by the equation

$$s = c_{cu} + \sigma \tan \phi_{cu} \tag{1.79}$$

where c_{cu} and ϕ_{cu} are the ***consolidated-undrained cohesion*** and ***angle of friction***, respectively (*note:* $c_{cu} \approx 0$ for normally consolidated clays)

Similarly, effective stress Mohr's circles at failure can be drawn to determine the *effective stress failure envelopes* (Figure 1.28c). They follow the relation expressed in Eq. (1.76).

Kenney (1959) has given a correlation between the friction angle, ϕ, and the plasticity index, *PI*, of normally consolidated clays based on the observations of more than 60

soils. This correlation is shown in Figure 1.29. Based on the average plot, the value generally decreases from about 37–38° with a plasticity index of about 10, to abou with a plasticity index of about 100. The consolidated undrained friction angle (ϕ_c normally consolidated saturated clays generally ranges from 5° to 20°.

For *unconsolidated-undrained* triaxial tests

$$\text{Major principal total stress} = \sigma_3 + \Delta\sigma_f = \sigma_1$$

$$\text{Minor principal total stress} = \sigma_3$$

The total stress Mohr's circle at failure can now be drawn, as shown in ure 1.28d. For saturated clays, the value of $\sigma_1 - \sigma_3 = \Delta\sigma_f$ is a constant, irrespecti the chamber confining pressure, σ_3 (also shown in Figure 1.28d). The tange these Mohr's circles will be a horizontal line, called the $\phi = 0$ condition. The stress for this condition is

$$\boxed{s = c_u = \frac{\Delta\sigma_f}{2}}$$

where c_u = undrained cohesion (or undrained shear strength)

The pore pressure developed in the soil specimen during the unconsolid undrained triaxial test is

$$u = u_a + u_d$$

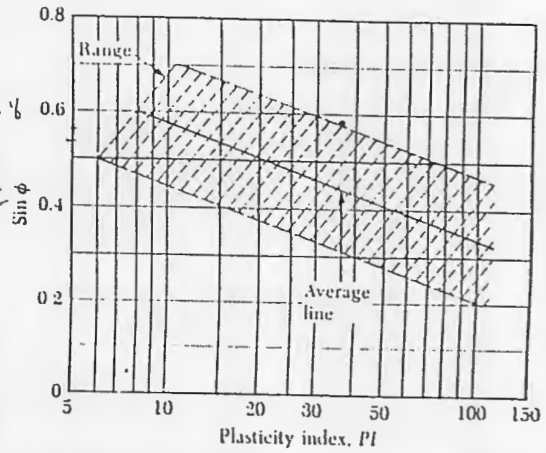

▼ **FIGURE 1.29** Variation of sin ϕ with the plasticity index of several clays (redrawn after Kenne 1959)

The pore pressure u_a is the contribution of the hydrostatic chamber pressure, σ_3. Hence

$$u_a = B\sigma_3 \tag{1.82}$$

where B = Skempton's pore pressure parameter

Similarly, the pore pressure u_d is the result of added axial stress, $\Delta\sigma$, so

$$u_d = A\ \Delta\sigma \tag{1.83}$$

where A = Skempton's pore pressure parameter

However

$$\Delta\sigma = \sigma_1 - \sigma_3 \tag{1.84}$$

Combining Eqs. (1.81), (1.82), (1.83), and (1.84) gives

$$u = u_a + u_d = B\sigma_3 + A(\sigma_1 - \sigma_3) \tag{1.85}$$

The pore water pressure parameter B in soft saturated soils is 1, so

$$\boxed{u = \sigma_3 + A(\sigma_1 - \sigma_3)} \tag{1.86}$$

The value of the pore water pressure parameter A at failure will vary with the type of soil. Following is a general range of the values of A at failure for various types of clayey soil encountered in nature.

Type of soil	A at failure
Sandy clays	0.5–0.7
Normally consolidated clays	0.5–1
Overconsolidated clays	−0.5–0

Figure 1.30 shows a photograph of laboratory triaxial equipment.

Figure 1.31 shows the range of variation between c_u/σ_a (σ_a = atmospheric stress) and liquidity index for undisturbed clayey soils of low sensitivity. The definition of liquidity index is given in Eq. (1.53a).

1.16 UNCONFINED COMPRESSION TEST

The *unconfined compression test* (Figure 1.32a) is a special type of unconsolidated-undrained triaxial test in which the confining pressure $\sigma_3 = 0$, as shown in Figure 1.32b. In this test an axial stress, $\Delta\sigma$, is applied to the specimen to cause failure

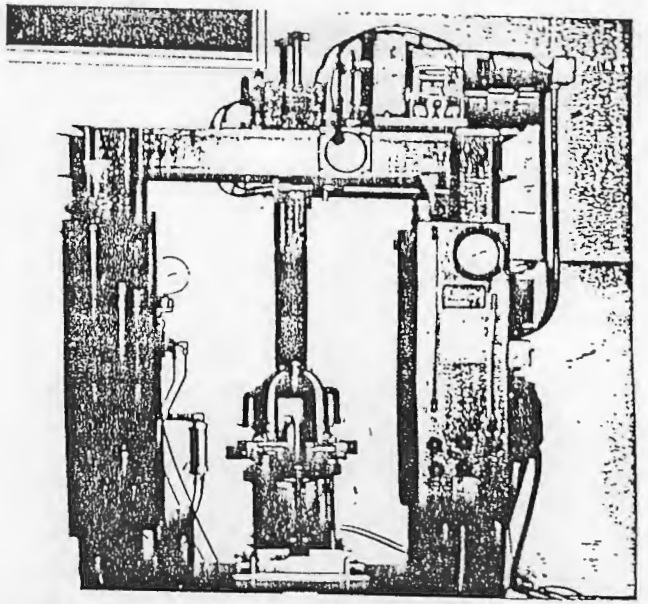

▼ FIGURE 1.30 Triaxial test equipment

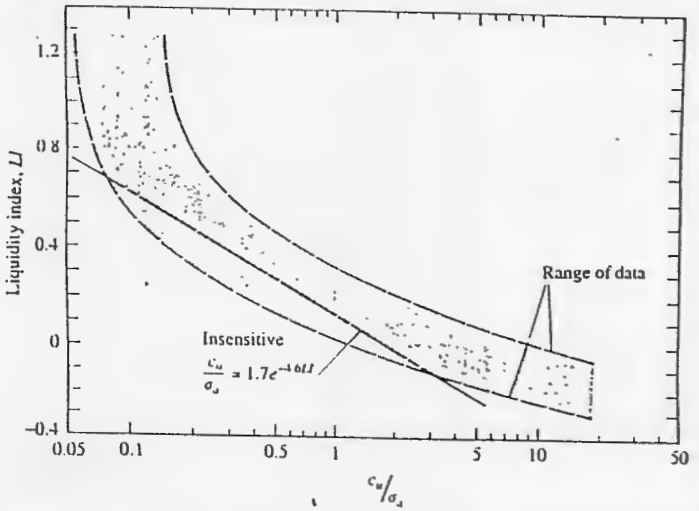

▼ FIGURE 1.31 Variation of c_u/σ_a with liquidity index (based on Wood, 1983; Kulhawy and M 1990)

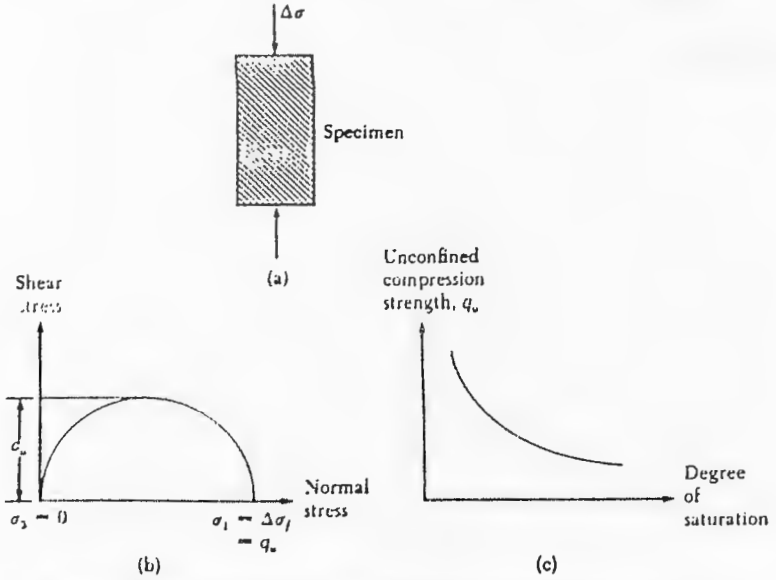

▼ **FIGURE 1.32** Unconfined compression test: (a) soil specimen; (b) Mohr's circle for the test; (c) variation of q_u with the degree of saturation

is, $\Delta\sigma = \Delta\sigma_f$). The corresponding Mohr's circle is shown in Figure 1.32b. Note that, for this case,

Major principal total stress $= \Delta\sigma_f = q_u$

Minor principal total stress $= 0$

The axial stress at failure, $\Delta\sigma_f = q_u$, is generally referred to as the *unconfined compression strength*. The shear strength of saturated clays under this condition ($\phi = 0$), from Eq. (1.76), is

$$\boxed{s = c_u = \frac{q_u}{2}} \tag{1.87}$$

The unconfined compression strength can be used as an indicator for the consistency of clays.

Unconfined compression tests are sometimes conducted on unsaturated soils. With the void ratio of a soil specimen remaining constant, the unconfined compression strength rapidly decreases with the degree of saturation (Figure 1.32c).

Figure 1.33 shows an unconfined compression test in progress.

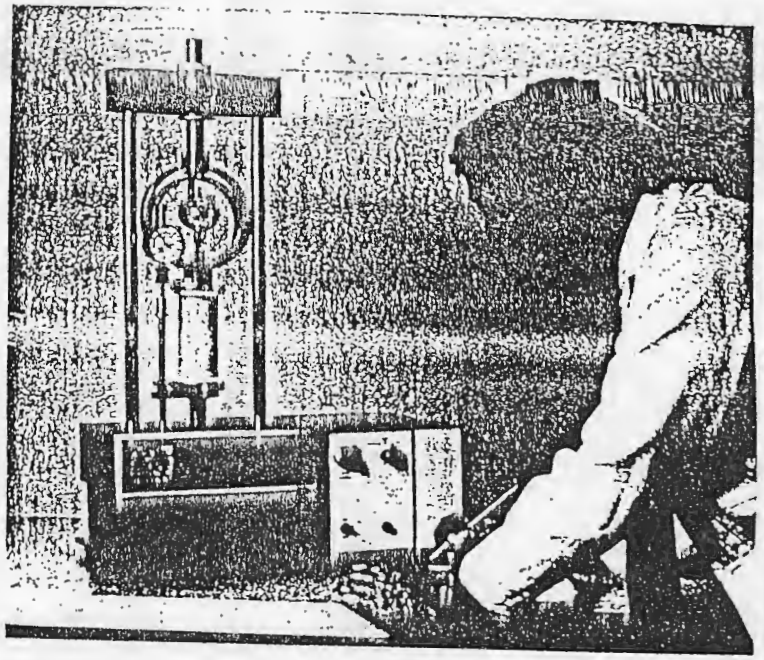

▼ **FIGURE 1.33** Unconfined compression test in progress (courtesy of Soiltest, Inc., Lake Bluff, Illinois)

The undrained cohesion, c_u, is an important parameter in the design of fou tions. For normally consolidated clay deposits (Figure 1.34), the magnitude increases almost linearly with the increase of effective overburden pressure, p. Sk ton (1957) correlated c_u with p in the form

$$\boxed{\frac{c_u}{p} = 0.11 + 0.0037(PI) \qquad \text{(normally consolidated clay)}}$$

where PI = plasticity index

The variation of c_u/p with overconsolidation ratio, $OCR = p/p_c$ (p_c = consolidation pressure) for some natural clays is shown in Figure 1.35. Based on t observations, we can say that

$$\left(\frac{c_u}{p}\right)_{\text{overconsolidated}} = 2\left(\frac{c_u}{p}\right)_{\text{normally consolidated}}$$

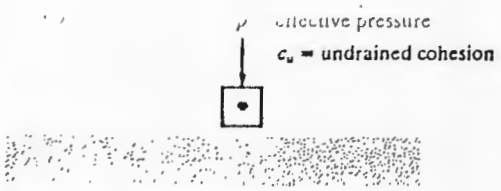

▼ **FIGURE 1.34** Clay deposit

Figure 1.36 shows the range of variation of α with *OCR* based on the experimental results depicted in Figure 1.35. For initial estimation purposes, the value of α from the average plot of Figure 1.35 may be used in Eq. (1.89).

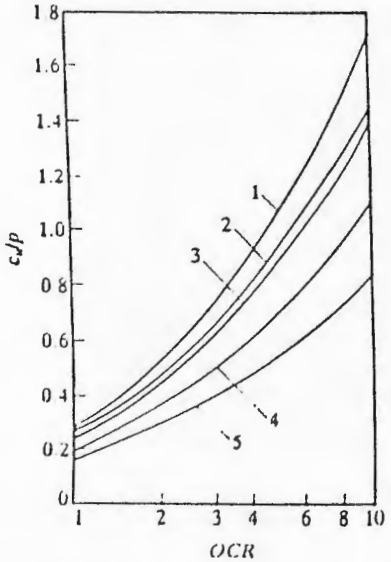

Curve	Soil	PI
1	Marine organic clay	34
2	Bangkok clay	41
3	Atchafalaya clay	75
4	Boston Blue clay	21
5	Connecticut varve	
	Clay layer	39
	Silt layer	12

▼ **FIGURE 1.35** Variation of c_u/p with *OCR* for five clay soils (after Ladd and Foott, 1974)

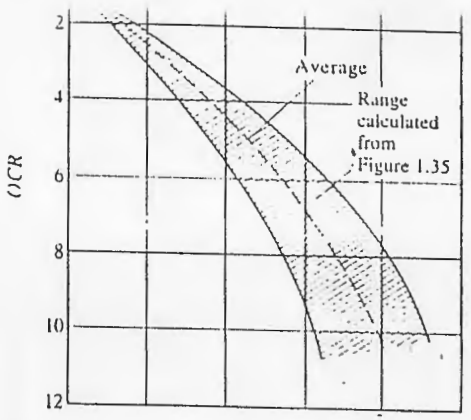

▼ **FIGURE 1.36** Variation of α with *OCR* [Eq. (1.89)] based on the results shown in Figure 1.35

▼ EXAMPLE 1.10

At a point in a saturated overconsolidated clay deposit, $p = 2300$ lb/ft². The plasticity index of the clay is 24, and the overconsolidation ratio, *OCR*, is 2.5. Estimate the undrained cohesion, c_u.

Solution

From Eq. (1.88) for normally consolidated clay,

$$\frac{c_u}{p} = 0.11 + 0.0037(PI) = 0.11 + 0.0037(24)$$

$$= 0.199$$

For *OCR* = 2.5, the value of α from Figure 1.36 is about 1.9. From Eq. (1.89)

$$\left(\frac{c_u}{p}\right)_{\text{overconsolidated}} = \alpha\left(\frac{c_u}{p}\right)_{\text{normally consolidated}}$$

$$= (1.9)(0.199) = 0.378$$

So

$$c_u = (0.378)(p) = (0.378)(2300) = 869.4 \text{ lb/ft}^2$$ ▼

1.17 SENSITIVITY

For many naturally deposited clay soils, the unconfined compression strength is much less when the soils are tested after remolding without any change in the moisture content. This property of clay soil is called *sensitivity*. The degree of sensitivity is the ratio of the unconfined compression strength in an undisturbed state to that in a remolded state, or

$$S_t = \frac{q_{u(\text{undisturbed})}}{q_{u(\text{remolded})}} \tag{1.90}$$

The sensitivity ratio of most clays ranges from about 1 to 8; however, highly flocculent marine clay deposits may have sensitivity ratios ranging from about 10 to 80. Some clays turn to viscous liquids upon remolding, and these clays are referred to as "quick" clays. The loss of strength of clay soils from remolding is caused primarily by the destruction of the clay particle structure that was developed during the original process of sedimentation.

PROBLEMS

1.1 For a natural sand, $D_{60} = 0.8$ mm, $D_{30} = 0.3$ mm, and $D_{10} = 0.15$ mm. Calculate:
- a. The uniformity coefficient
- b. The coefficient of gradation

1.2 A moist soil has a void ratio of 0.65, the moisture content of the soil is 14%, and $G_s = 2.7$. Determine:
- a. Porosity
- b. Degree of saturation (%)
- c. Dry unit weight (kN/m³)

1.3 For the soil described in Problem 1.2:
- a. What would be the saturated unit weight in kN/m³?
- b. How much water, in kN/m³, needs to be added to the soil for complete saturation?
- c. What would be the moist unit weight in kN/m³ when the degree of saturation is 70%?

1.4 The moist unit weight of a soil is 119.5 lb/ft³. For a moisture content of 12% and $G_s = 2.65$, calculate:
- a. e
- b. n
- c. S
- d. γ_d

1.5 For the soil described in Problem 1.4:
- a. What would be the saturated unit weight in lb/ft³?
- b. How much water, in lb/ft³, needs to be added to the soil for complete saturation?
- c. What would be the moist unit weight in lb/ft³ when the degree of saturation is 80%?

1.6 A saturated soil specimen has $w = 36\%$ and $\gamma_d = 85.43$ lb/ft³. Determine:
- a. Void ratio
- b. Porosity
- c. Specific gravity of soil solids
- d. Saturated unit weight (in lb/ft³)

1.7 For a soil sample, $V = 3.2$ ft³, $W = 378$ lb, $w = 12.5\%$, and $G_s = 2.67$. Calculate:
- a. e
- b. n
- c. γ
- d. γ_d
- e. S

1.8 The laboratory test results of a sand are $e_{max} = 0.91$, $e_{min} = 0.48$, and $G_s = 2.67$. What would be the dry and moist unit weights of this sand when compacted at a moisture content of 10% to a relative density of 65%?

1.9 The laboratory test results of six soils are given in the following table. Classify the soils by the AASHTO soil classification system and give the group indices.

	Sieve analysis—percent passing					
	Soil					
Sieve no.	A	B	C	D	E	F
4	92	100	100	95	100	100
10	48	60	98	90	91	82
40	28	41	82	79	80	74
200	13	33	72	64	30	55
Liquid limit	31	28	56	35	43	35
Plastic limit	26	25	31	26	29	21

1.10 Classify the soils in Problem 1.9 by using the Unified Soil Classification System.

1.11 The permeability of a sand was tested in the laboratory at a void ratio of 0.6 and was determined to be 0.14 cm/sec. Use Eq. (1.27) to estimate the coefficient of permeability of this sand at a void ratio of 0.8.

1.12 A sand has a coefficient of 0.3 cm/sec at a void ratio of 0.65. Estimate the void ratio at which its coefficient of permeability would be 0.15 cm/sec. Use Eq. (1.29).

1.13 The *in situ* coefficient of permeability of a clay is 4.2×10^{-6} cm/sec at a void ratio of 0.[illegible]. What would be the coefficient of permeability at a void ratio of 0.72? Use Eq. (1.31).

1.14 A soil profile is shown in Figure P1.14. Determine the total stress, pore water pressure, and effective stress at A, B, C, and D

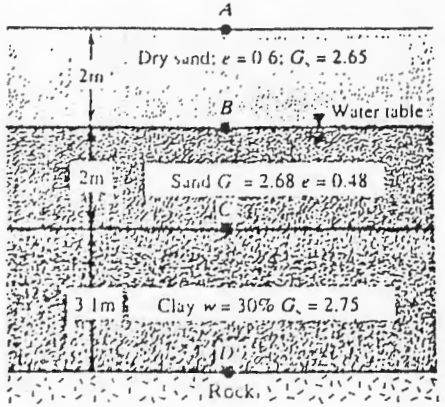

▼ FIGURE P1.14

1.15 A sandy soil ($G_s = 2.66$), in its densest and loosest states, has void ratios of 0.42 and 0.97, respectively. Estimate the range of the critical hydraulic gradient in this soil at which quicksand condition might occur.

1.16 A saturated clay deposit in the field has

Liquid limit = 61%

Plastic limit = 21%

Moisture content = 38%

Estimate the preconsolidation pressure, p_c (lb/ft²). Use Eq. (1.53).

1.17 A normally consolidated clay layer 8.53 ft thick has a void ratio of 1.3, $LL = 41$, and average effective stress on the clay layer = 1720 lb/ft². How much consolidation settlement would the clay layer undergo if the average effective stress on the clay layer is increased to 2510 lb/ft² as a result of the construction of a foundation?

1.18 Refer to Problem 1.17. Assume that the clay layer is preconsolidated, $p_c = 1980$ lb/ft², and $C_s = \frac{1}{4}C_c$. Estimate the consolidation settlement.

1.19 Refer to Figure P1.14. The clay is normally consolidated. A laboratory consolidation test on the clay gave the following results.

Pressure (kN/m²)	Void ratio
100	0.866
200	0.815

a. Calculate the average effective stress on the clay layer.
b. Determine the compression index, C_c.
c. If the average effective stress on the clay layer is increased ($p_0 + \Delta p$) to 115 kN/m, what would be the total consolidation settlement?

1.20 Refer to Problem 1.19c. For the clay soil, if $C_v = 5.6$ mm²/min, how long will it take reach half the consolidation settlement? (*Note:* The clay layer in the field is drained on o side only.)

1.21 A clay soil specimen, 1 in. thick (drained on top and bottom), was tested in the laborato For a given load increment, the time for 50% consolidation was 5 min 20 sec. How lo will it take for 50% consolidation of a similar clay layer in the field that is 8.2 ft thick a drained on one side only?

1.22 A direct shear test was conducted on a 2 in. × 2 in. specimen of dry sand, with following results.

Normal force (lb)	Shear force at failure (lb)
33	20.67
55.17	35.8
66.16	40.2

Draw a graph of shear stress at failure vs. normal stress and determine the soil fricti angle.

1.23 A consolidated-drained triaxial test on a normally consolidated clay yielded the followi results:

All around confining pressure = σ_3 = 20 lb/in.²

Added axial stress at failure = $\Delta\sigma$ = 40 lb/in.²

Determine the shear strength parameters.

1.24 Following are the results of two consolidated-drained triaxial tests on a clay.

Test I: $\sigma_3 = 82.8$ kN/m²; $\sigma_{1(\text{failure})} = 329.2$ kN/m²

Test II: $\sigma_3 = 165.6$ kN/m²; $\sigma_{1(\text{failure})} = 558.6$ kN/m²

Determine the shear strength parameters—that is, c and ϕ.

1.25 A consolidated-undrained triaxial test was conducted on a saturated normally consolidate clay. Following are the test results.

σ_3 = 13 lb/in.²

$\sigma_{1(\text{failure})}$ = 32 lb/in.²

Pore water pressure at failure = u_f = 5.5 lb/in.²

Determine c_u, ϕ_{cu}, c, and ϕ.

1.26 A normally consolidated clay soil has $\phi = 28°$ and $\phi_{cu} = 20°$. If a consolidated-undrainec test is conducted on this clay with σ_3 = 21.5 lb/in.², what would be the magnitude of th principal stress, σ_1, and the pore water pressure, u, at failure?

1.27 A saturated clay layer has

Saturated unit weight, γ_{sat} = 19.6 kN/m³

Plasticity index = 21

The water table coincides with the ground surface. If the clay is normally consolidated, estimate the magnitude of c_v (kN/m²) at a depth of 8 m from the ground surface.

1.28 Assume that the clay layer in Problem 1.27 is overconsolidated and that the OCR = 2.5. Estimate the magnitude of c_v (kN/m²) at a depth of 6.5 m below the ground surface.

REFERENCES

American Society for Testing and Materials (1992). *Annual Book of ASTM Standards*, Vol. 04.08, Philadelphia, Pa.

Azzouz, A. S., Krizek, R. J., and Corotis, R. B. (1976). "Regression Analysis of Soil Compressibility," *Soils and Foundations*, Vol. 16, No. 2, pp. 19–29.

Casagrande, A. (1936). "Determination of the Preconsolidation Load and Its Practical Significance," *Proceedings*, First International Conference on Soil Mechanics and Foundation Engineering, Cambridge, Mass., Vol. 3, pp. 60–64.

Darcy, H. (1856). *Les Fontaines Publiques de la Ville de Dijon*, Paris.

Das, B. M. (1993). *Soil Mechanics Laboratory Manual*, 3rd ed., Engineering Press, San Jose, Calif.

Hazen, A. (1930). "Water Supply," *American Civil Engineers Handbook*, Wiley, New York.

Highway Research Board (1945). *Report of the Committee on Classification of Materials for Subgrades and Granular Type Roads*, Vol. 25, pp. 375–388.

Kenney, T. C. (1959). "Discussion," *Journal of the Soil Mechanics and Foundations Division*, American Society of Civil Engineers, Vol. 85, No. SM3, pp. 67–69.

Kulhawy, F. H., and Mayne, P. W. (1990). *Manual on Estimating Soil Properties for Foundation Design*, Report EL-6800, EPRI.

Ladd, C. C., and Foott, R. (1974). "New Design Procedure for Stability of Soft Clays," *Journal of the Geotechnical Engineering Division*, American Society of Civil Engineers, Vol. 92, No. GT2, pp. 79–103.

Leroueil, S., Tavenas, F., and LeBihan, J. P. (1983). "Propriétés Caractéristiques des Argiles de l'est due Canada," *Canadian Geotechnical Journal*, Vol. 20, No. 4, pp. 681–705.

Nagaraj, T. S., and Murthy, B. R. S. (1985). "Prediction of the Preconsolidation Pressure and Recompression Index of Soils," *Geotechnical Testing Journal*, American Society for Testing and Materials, Vol. 8, No. 4, pp. 199–202.

Rendon Herrero, O. (1980). "Universal Compression Index Equation," *Journal of the Geotechnical Engineering Division*, American Society of Civil Engineers, Vol. 106, No. GT11, pp. 1178–1200.

Schmertmann, J. H. (1953). "Undisturbed Consolidation Behavior of Clay," *Transactions*, American Society of Civil Engineers, Vol. 120, p. 1201.

Sivaram, B., and Swamee, P. (1977). "A Computational Method for Consolidation Coefficient," *Soils and Foundations*, Tokyo, Japan, Vol. 17, No. 2, pp. 48–52.

Skempton, A. W. (1944). "Notes on the Compressibility of Clays," *Quarterly Journal of Geological Society*, London, Vol. C, pp. 119–135.

Skempton, A. W. (1957). "The Planning and Design of New Hong Kong Airport," *Proceedings*, The Institute of Civil Engineers, London, Vol. 7, pp. 305–307.

Stas, C. V., and Kulhawy, F. H. (1984). *Critical Evaluation of Design Methods for Foundations Under Axial Uplift and Compression Loading*, Report EL-3771, EPRI.

Tavenas, F., Jean, P., Leblond, P., and Leroueil, S. (1983). "The Permeability of Natural Soft Cla Part II: Permeability Characteristics," *Canadian Geotechnical Journal*, Vol. 20, No. 4, 645–660.

Terzaghi, K., and Peck, R. B. (1967). *Soil Mechanics in Engineering Practice*, Wiley, New York.

U.S. Department of the Navy (1971). "Design Manual—Soil Mechanics, Foundations and Ea Structures," *NAVFAC DM-7*, U.S. Government Printing Office, Washington, D.C.

U.S. Department of the Navy (1982). "Soil Mechanics," *NAVFAC DM7.1*, U.S. Government Pri ing Office, Washington, D.C.

Wood, D. M. (1983). "Index Properties and Critical State Soil Mechanics," *Proceedings*, Sym sium on Recent Developments in Laboratory and Field Tests and Analysis of Geotechni Problems, Bangkok, pp. 301–309.

Wroth, C. P., and Wood, D. M. (1978). "The Correlation of Index Properties with Some Ba Engineering Properties of Soils," *Canadian Geotechnical Journal*, Vol. 15, No. 2, pp. 1 145.

Youd, T. L. (1973). "Factors Controlling Maximum and Minimum Densities of Sands," *Spe Technical Publication No. 523*, American Society for Testing amd Materials, pp. 98–122.

CHAPTER 7

INTRODUCTION TO HYDRAULIC MODIFICATION

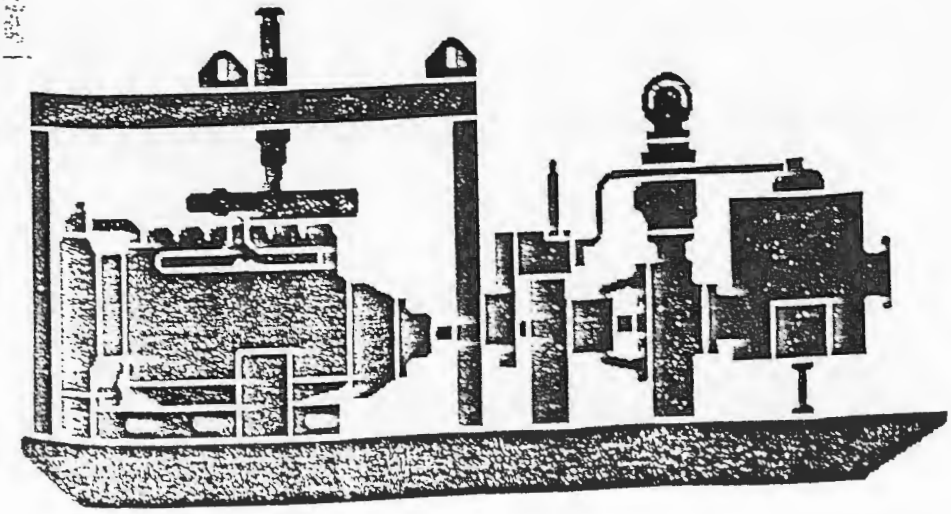

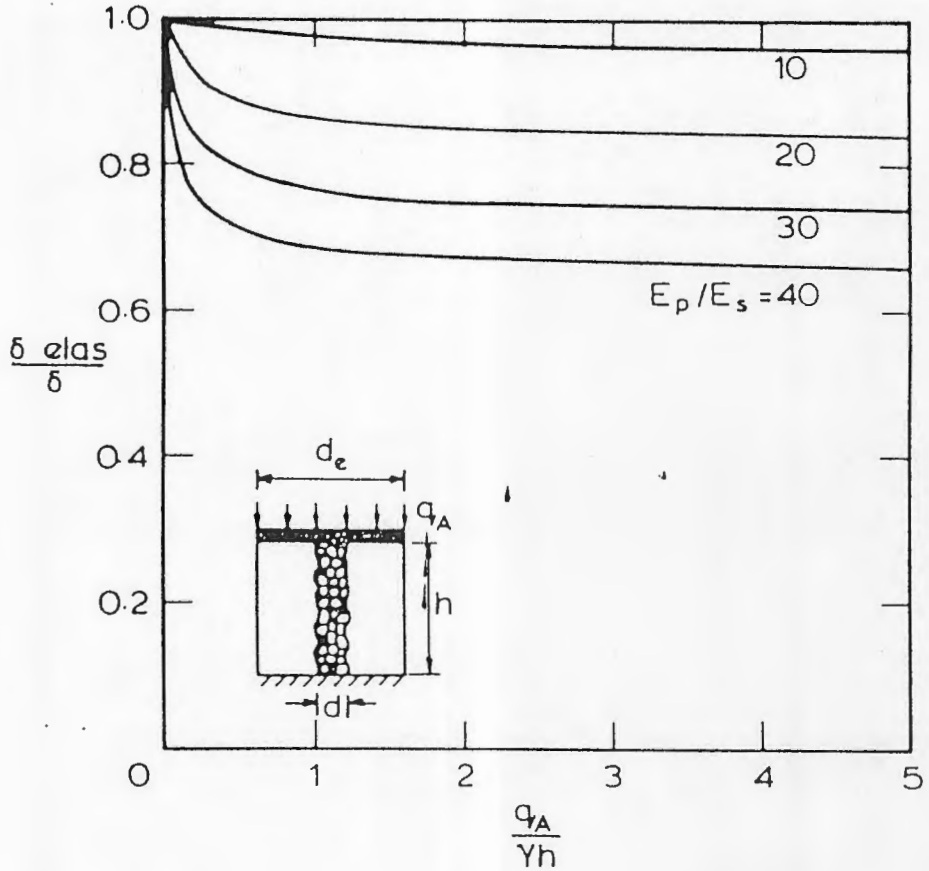

FIG.12 ELASTIC SETTLEMENT CORRECTION FACTORS ; $d_e/d = 5, \phi = 40°, \psi = 0, \nu_s = 0.4$

CH 5.14

Settlement Prediction of Rigid Raft Foundation Constructed on Treated Clay foundation

- Assumptions
  (1) The clayey soil and stone columns are elastic material.
  (2) No shear between the stone columns and clayey soil.

For Pile E_p, $\nu_p \Longrightarrow \lambda_1, G_1$

For Soil E_s, $\nu_s \Longrightarrow \lambda_2, G_2$

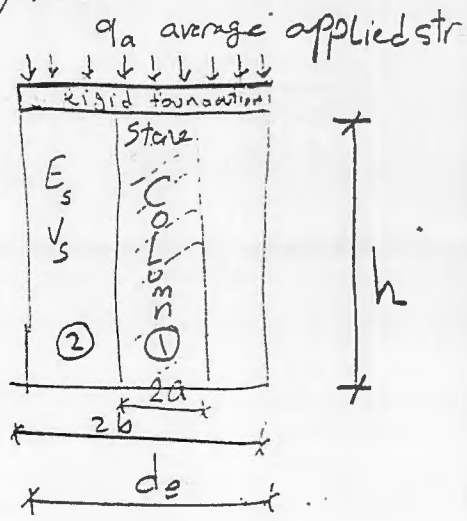

Unit Cell

Step 1 Calculate Lame parameter λ
& Shear modulus G

$$\lambda = \frac{\nu E}{(1-2\nu)(1+\nu)}, \quad G = \frac{E}{2(1+\nu)}$$

Step 2 Calculate Parameter F

$$F = \frac{(\lambda_1 - \lambda_2)(b^2 - a^2)}{2\left[a^2(\lambda_2 + G_2 - \lambda_1 - G_1) + b^2(\lambda_1 + G_1 + G_2)\right]}$$

Step 3 ε (vertical strain) and average applied stress are related as follows:

$$\frac{q_a}{A} b^2 = \Big[\underbrace{(\lambda_1 + 2G_1)}_{\text{Pile}} a^2 + \underbrace{(\lambda_2 + 2G_2)}_{\text{Soil}}(b^2 - a^2) - 2a^2(\lambda_1 - \lambda_2)F\Big]\varepsilon$$

$$\varepsilon = \frac{\Delta h}{h} = \frac{\delta_{elastic}}{h}$$

Step 4 Correct the (calculated elastic) settlement by taking into account developed yielding in the stone column.

- Estimate $\dfrac{q_A}{\gamma_{sub}\, h}$ non dimensional load level.

- Get $\dfrac{\delta_{elast}}{\delta}$ = ---- factor

$\therefore\ \delta = \dfrac{\delta_{elast}}{\text{factor}}$

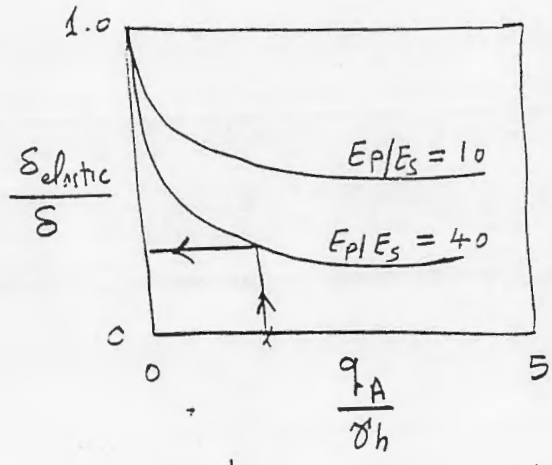

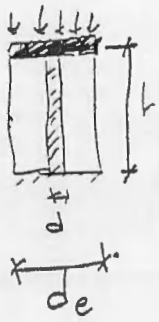

For $\dfrac{d_e}{d}$ = , ϕ = ---, ψ = ---, ν_s = 0.0

---

due to Load concentration on pile some yielding of the pile material occurs which results in increase of settlement of the system.

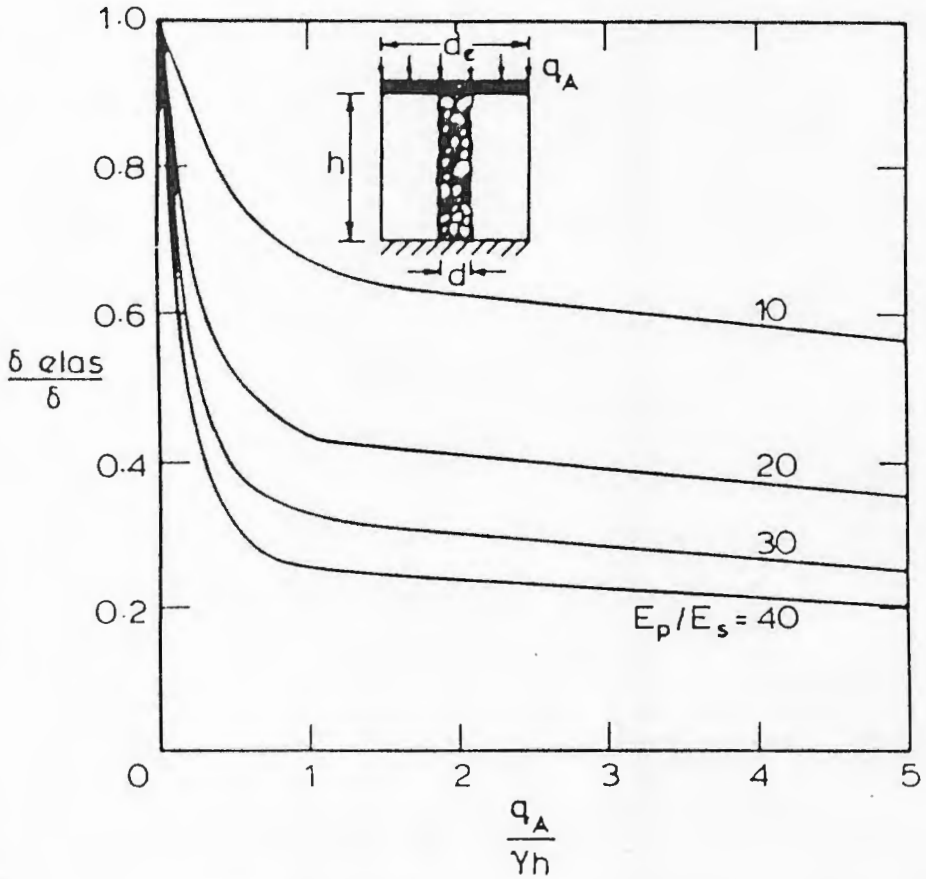

FIG 1. ELASTIC SETTLEMENT CORRECTION FACTORS ; $d_e/d = 2$, $\phi = 30°$, $\psi = 0$, $\nu_s = 0.3$

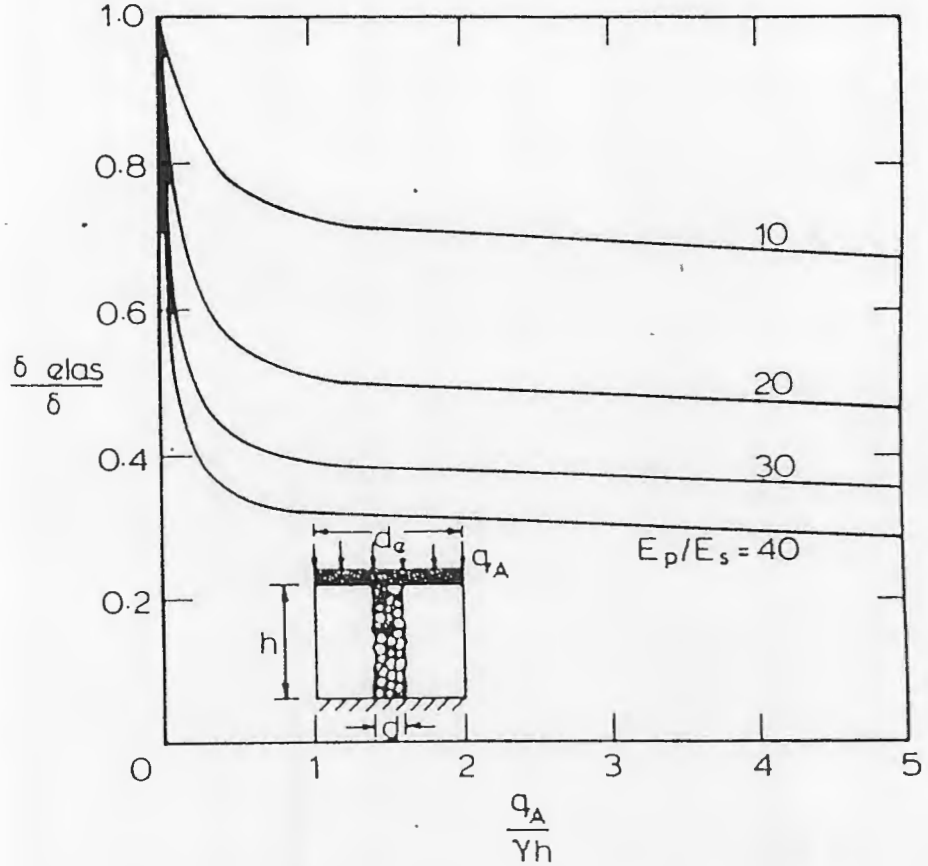

FIG 2 ELASTIC SETTLEMENT CORRECTION FACTORS, $d_e/d = 3$, $\phi = 30°$, $\psi = 0$, $\nu_s = 0.3$

Ch 5.8

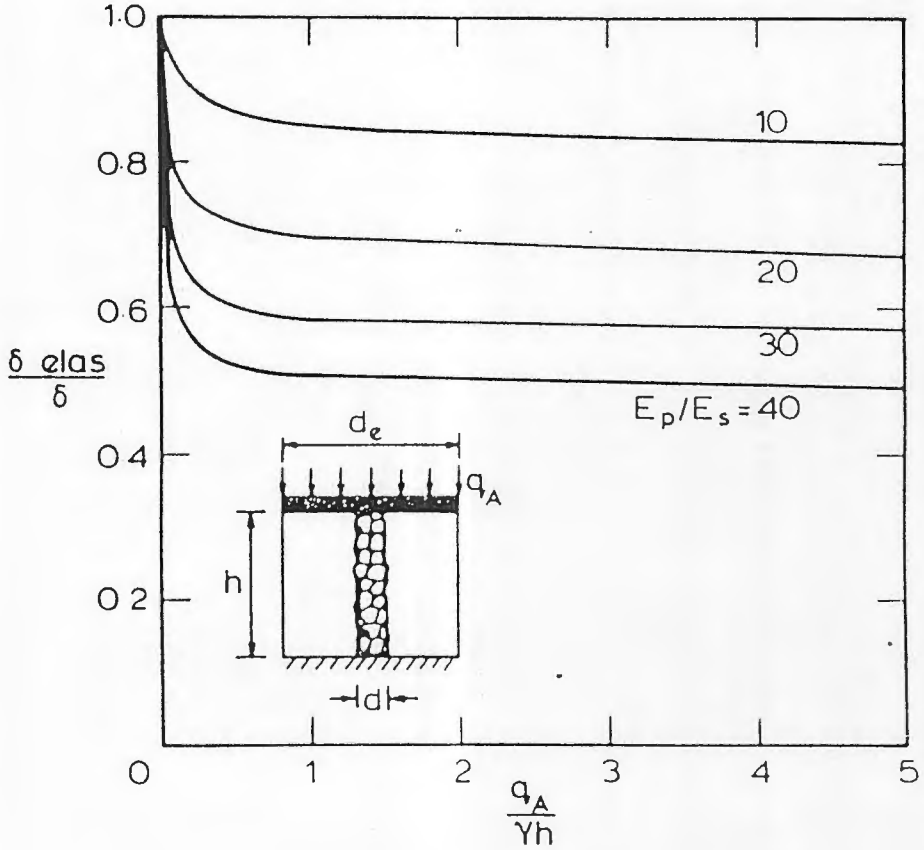

FIG 3 ELASTIC SETTLEMENT CORRECTION FACTORS, $d_e/d = 5, \phi = 30°, \psi = 0, \nu_s = 0.3$

Ch 5.9

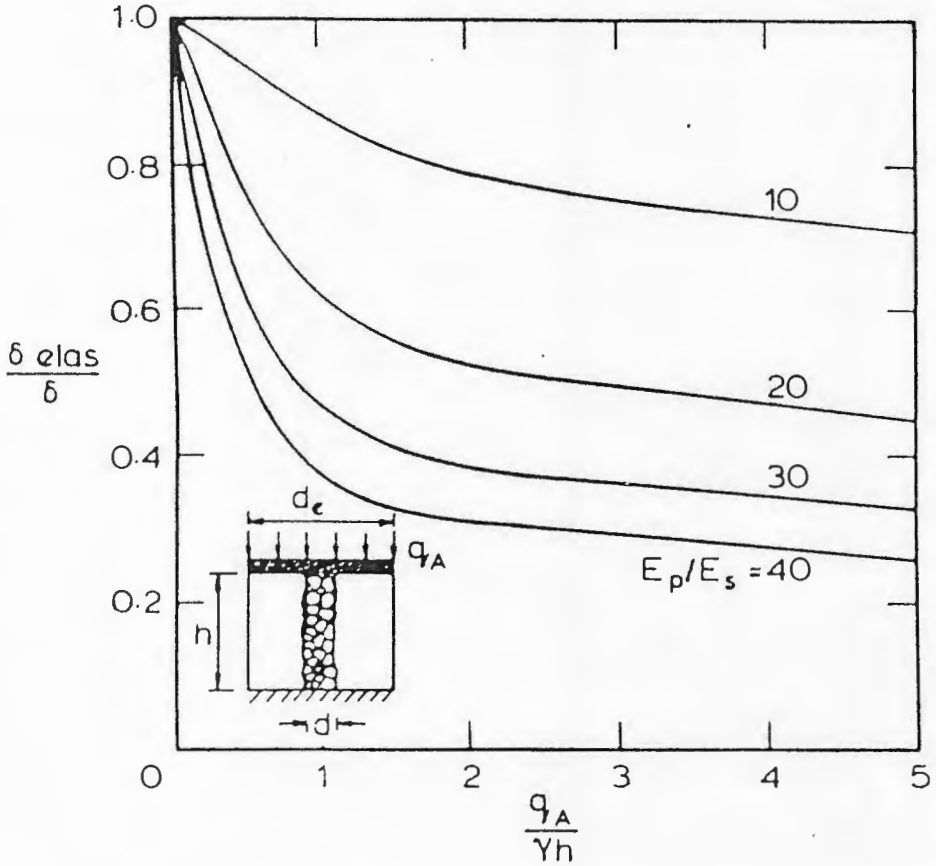

FIG 4 ELASTIC SETTLEMENT CORRECTION FACTORS, $d_e/d = 2$, $\phi = 40°$, $\psi = 0$, $\nu_s = 0.3$

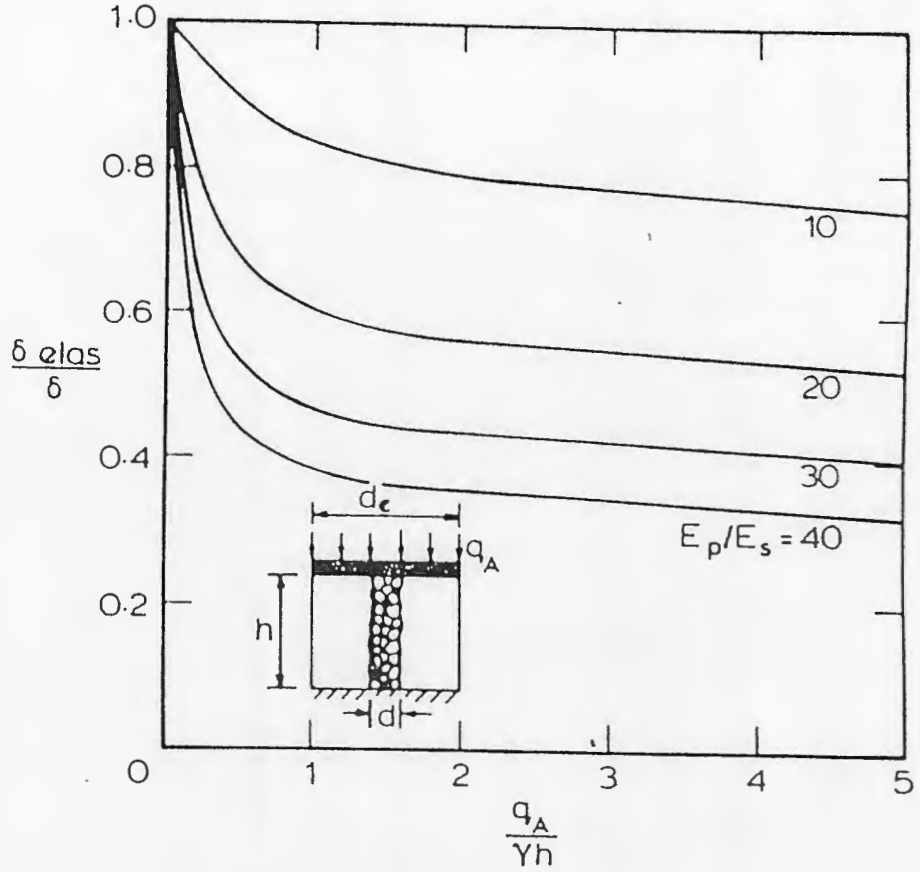

FIG 5 ELASTIC SETTLEMENT CORRECTION FACTORS; $d_e/d = 3$, $\phi = 40°$, $\psi = 0$, $\nu_s = 0.3$

Ch 5 9

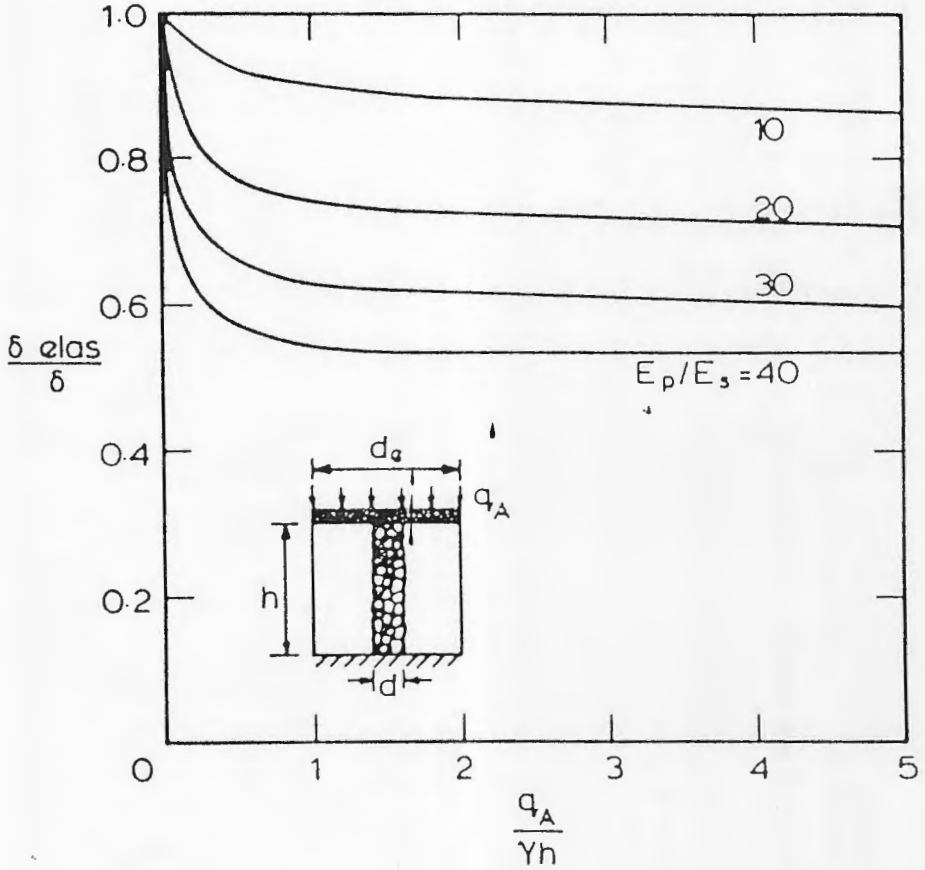

FIG 6 ELASTIC SETTLEMENT CORRECTION FACTORS, $d_a/d = 5$, $\phi = 40°$, $\psi = 0$, $\nu_s = 0.3$

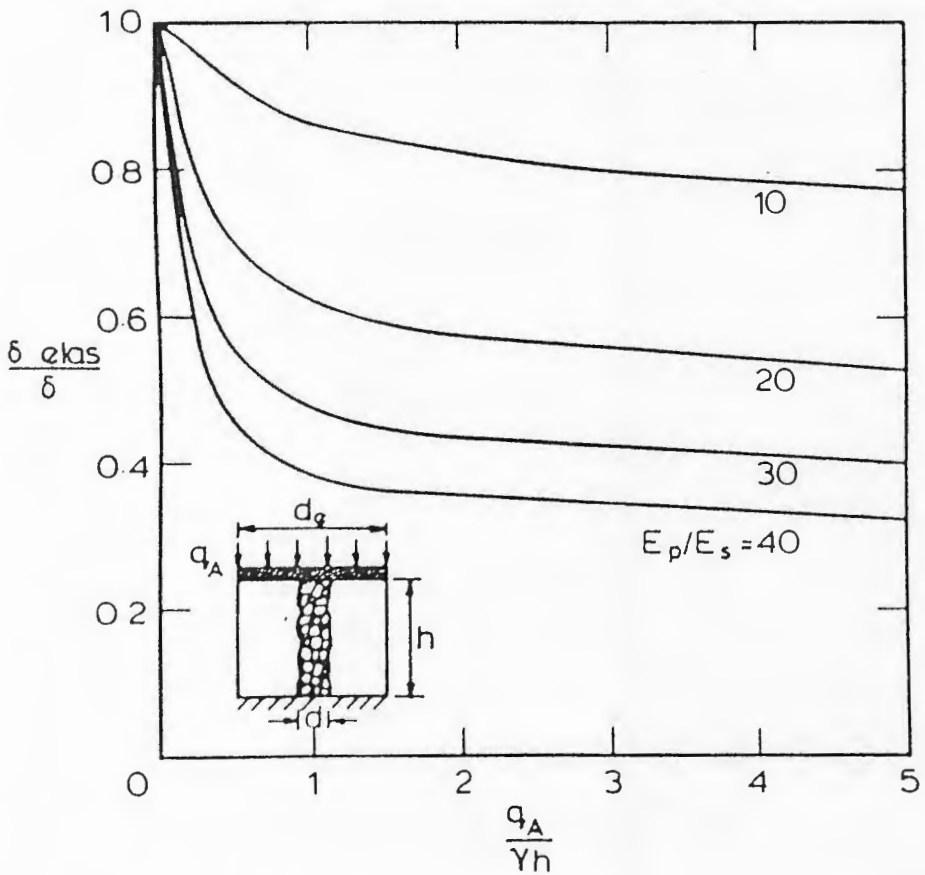

FIG 7 ELASTIC SETTLEMENT CORRECTION FACTORS, $d_e/d = 2$, $\phi = 30°$, $\psi = 0$, $\nu_s = 0.4$

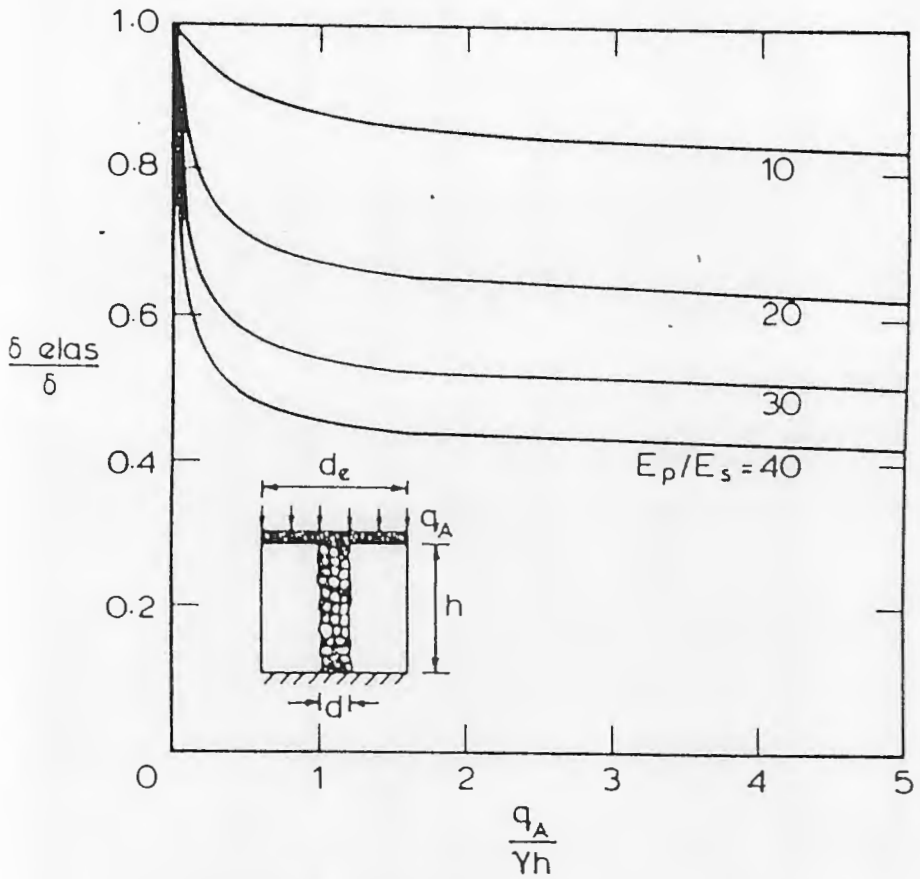

FIG. 8 ELASTIC SETTLEMENT CORRECTION FACTORS; $d_e/d = 3$, $\phi = 30°$, $\psi = 0$, $\nu_s = 0.4$

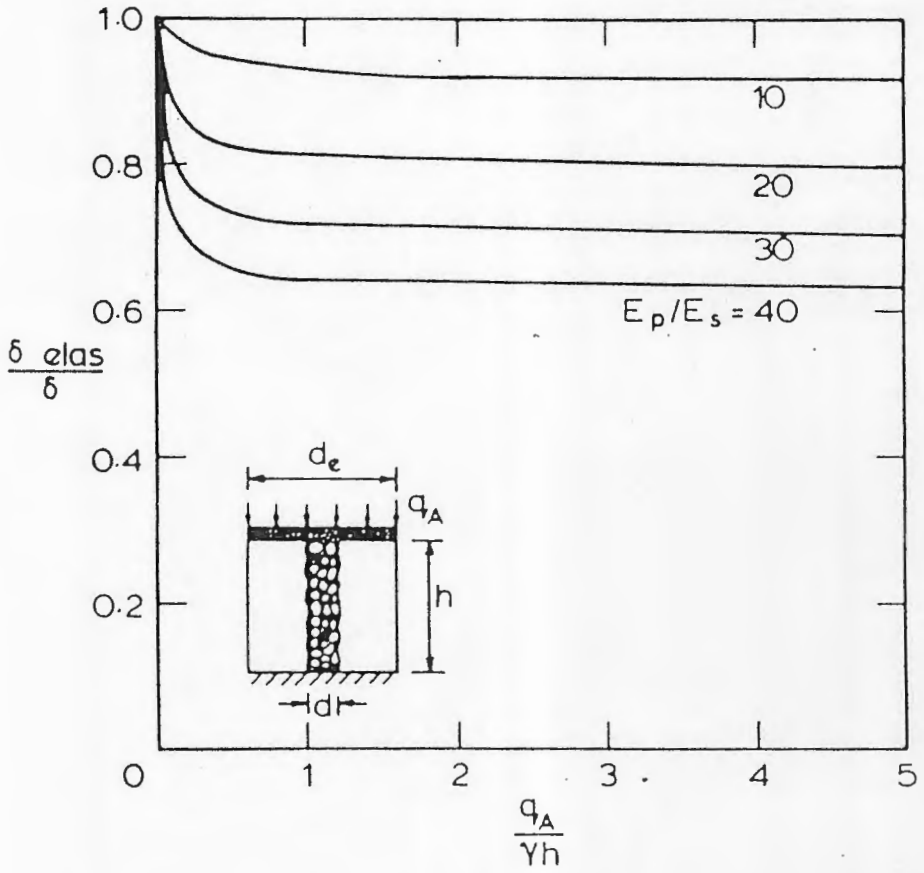

FIG 9 ELASTIC SETTLEMENT CORRECTION FACTORS; $d_e/d = 5, \phi = 30°, \psi = 0, \nu_s = 0.4$

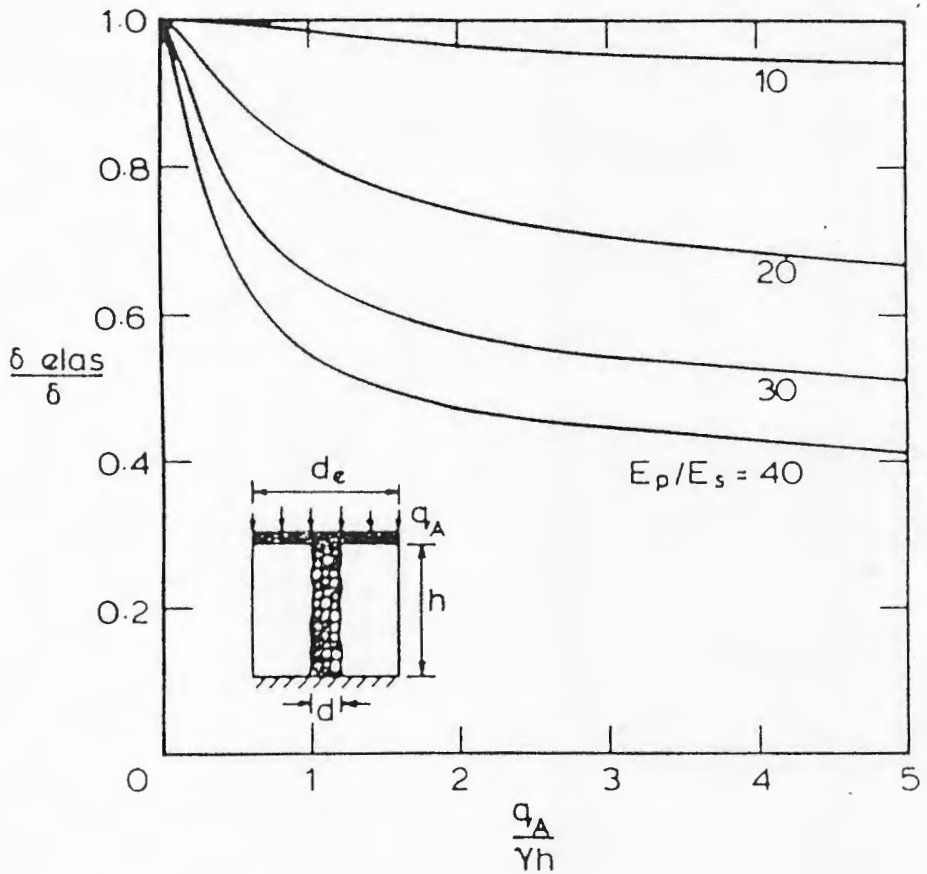

FIG 10 ELASTIC SETTLEMENT CORRECTION FACTORS, $d_e/d = 2, \phi = 40^\circ, \psi = 0, \nu_s = 0.4$

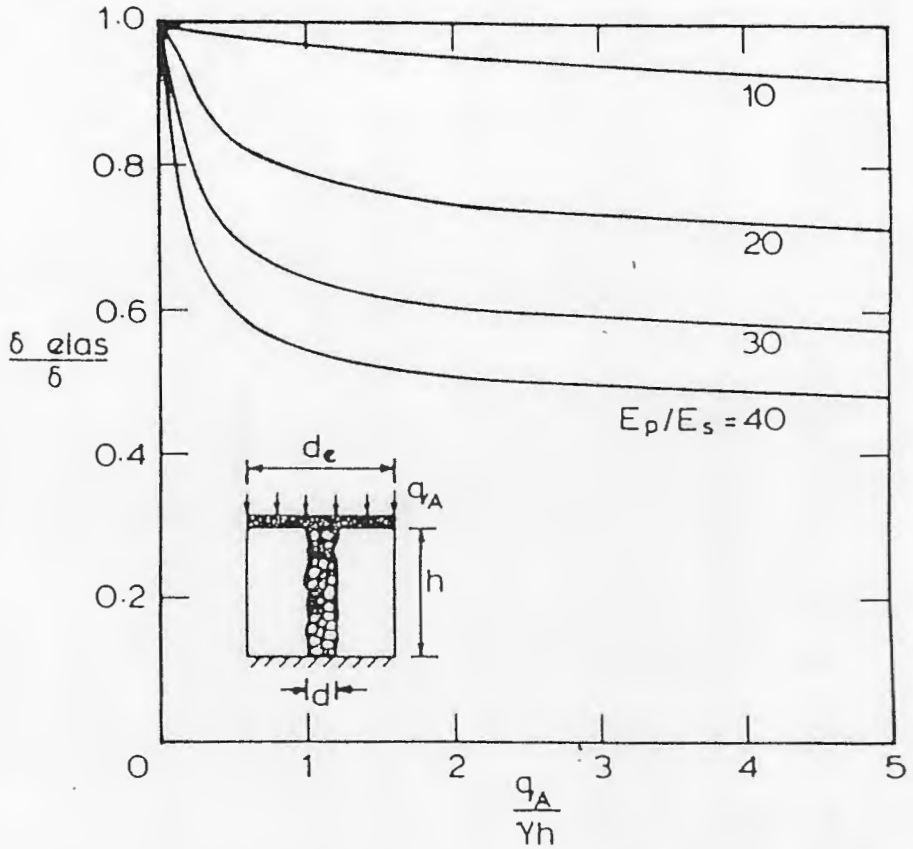

FIG. 11 ELASTIC SETTLEMENT CORRECTION FACTORS; $d_e/d = 3, \phi = 40^\circ, \psi = 0, \nu_s = 0.4$

C 45-13

5.5 Hydraulic Modification

Preloading & The use of Vertical Drains

5.5.1 Pre Compression

Usually used when highly compressible N.C. clayey soil lies at a limited depth and large consolidation settlement is expected

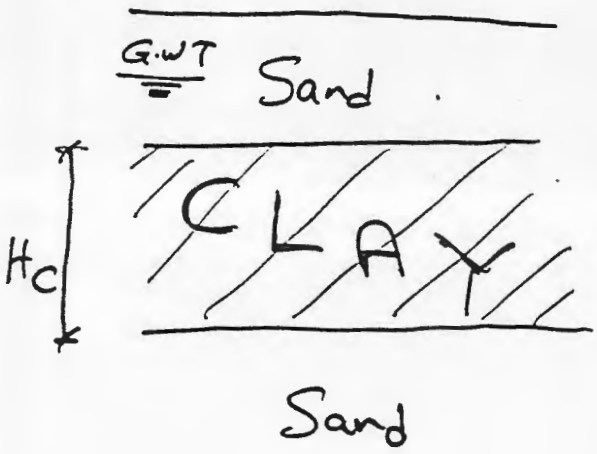

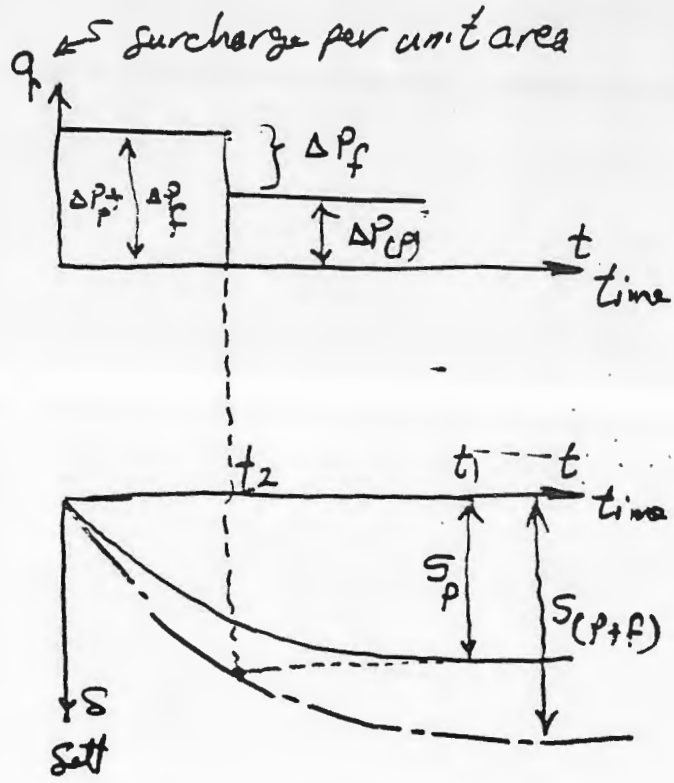

$$S_p = \frac{C_c}{1+e_0} H_c \log \frac{P_0 + \Delta P_p}{P_0} \quad \text{---------- (1)}$$

$$S_{(p+f)} = \frac{C_c}{1+e_0} H_c \log \frac{P_0 + (\Delta P_p + \Delta P_f)}{P_0} \quad \text{---------- (2)}$$

Equation for ΔP_f and t_2

Under a surcharge of $\Delta P_p + \Delta P_f \Rightarrow U$ at time t_2 is given by:

$$U = \frac{S_{(P)}}{S_{(P+f)}}$$

from Eq (1) & (2) we get

$$U = \frac{\log\left[1 + \frac{\Delta P_p}{P_o}\right]}{\log\left\{1 + \frac{\Delta P_p}{P_o}\left(1 + \frac{\Delta P_f}{\Delta P_p}\right)\right\}} \quad \text{------} \; (3)$$

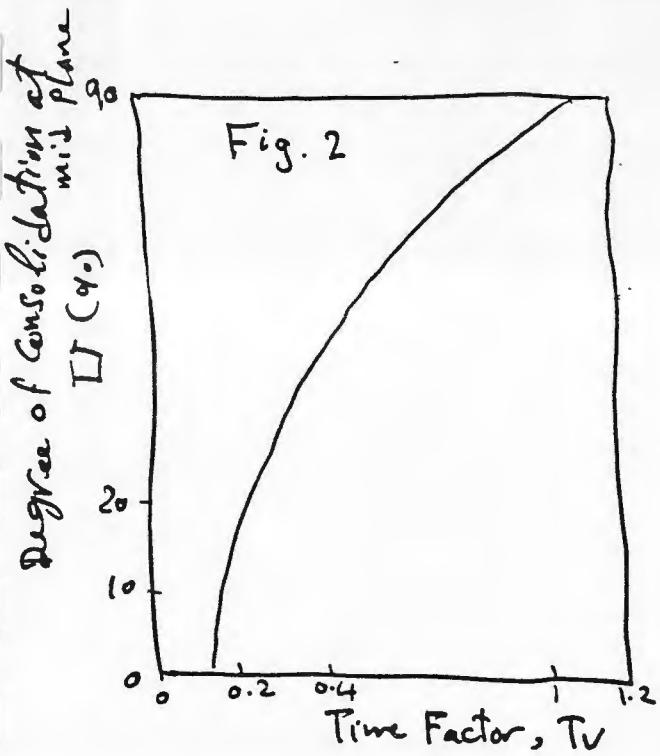

$$T_v = \frac{C_v t}{H^2}$$

$H^2 \Leftarrow$ drainage path

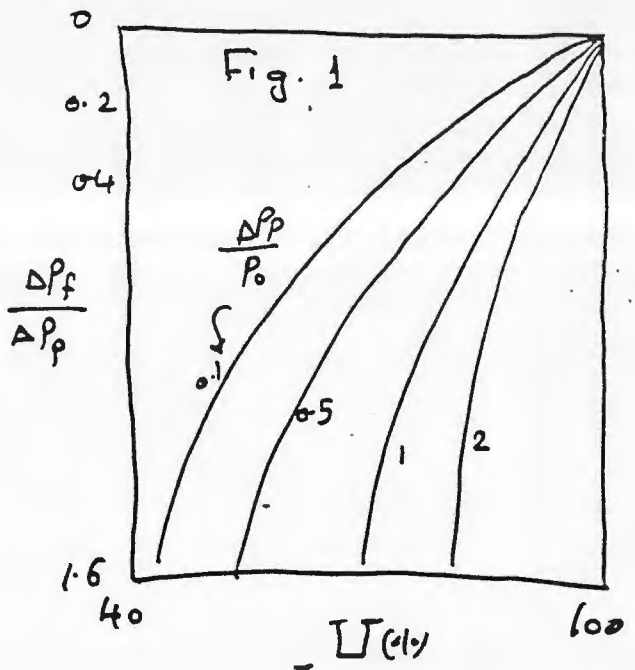

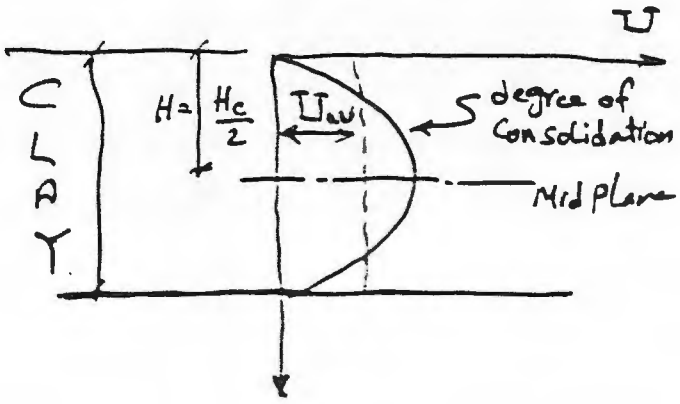

Analysis Examples

Given: ΔP_p, P_o, ΔP_f, C_v, H_{clay}

Req: t_2

Sol.: ① Calculate $\frac{\Delta P_p}{P_o}$ & $\frac{\Delta P_f}{\Delta P_p}$

② Get $\square$ from Fig. 1

③ Get T_v from Fig. 2

④ $T_v = \frac{C_v t_2}{H^2}$

Given: ΔP_p, P_o, t_2, C_v, H_{clay}

Req.: ΔP_f

Sol.: ① Calculate $T_v = \frac{C_v t_2}{H^2}$

② Get $\square$ from Fig. 2

③ From $\frac{\Delta P_p}{P_o}$ and Fig. 1 Get $\frac{\Delta P_f}{\Delta P_p}$

④ Get ΔP_f = -----

5.5.2 Sand Drains

- Sand drained are used to increase the rate of drainage (because of radial consolidation).

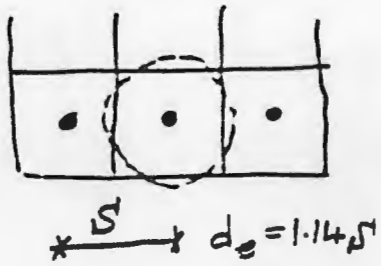

- <u>Construction</u>

- Arrangement of sand drains
  - * Square pattern.
  - * Hexagonal (triangular) pattern

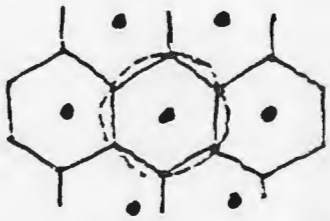

$d_e = 1.05\,S$

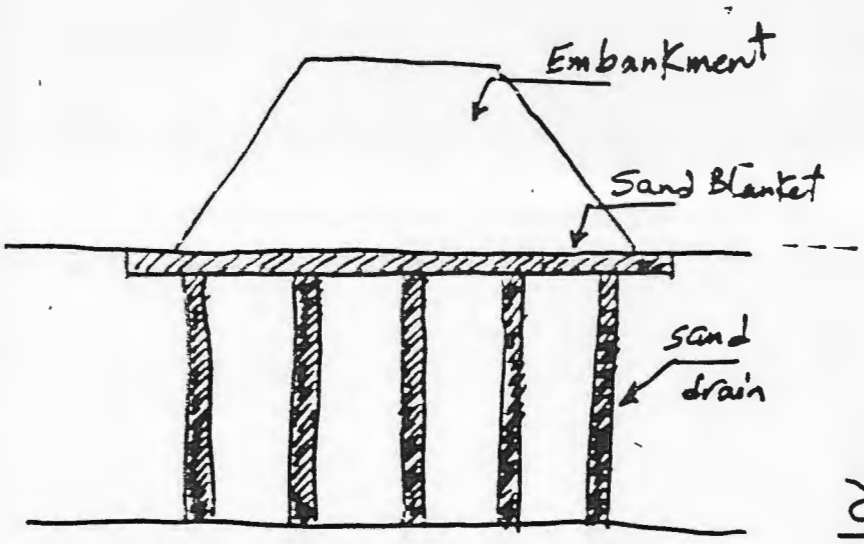

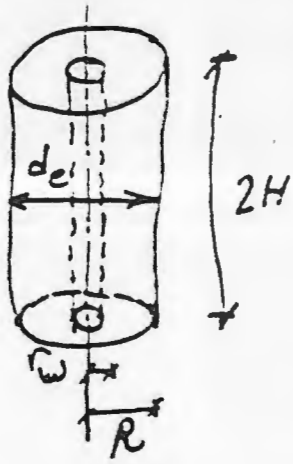

$$\frac{\partial \bar{u}}{\partial t} = C_{v_r}\left[\frac{\partial^2 \bar{u}}{\partial r^2} + \frac{1}{r}\frac{\partial \bar{u}}{\partial r}\right]$$

Theories of Sand Drains

- Free strain Case
- Equal strain Case

* Solution For Radial Flow only

$$U_r = 1 - e^{\left(\frac{-8T_r}{\alpha}\right)}$$

U_r average degree of radial consolidation

$$T_r = \frac{C_h t}{d_e^2}, \qquad \boxed{\alpha = \frac{n^2}{n^2-1}\ln n - \frac{3n^2-1}{4n^2}}$$

C_h coefficient of consolidation for radial drainage.

d_e effective diameter

t time elapsed since application of the surcharge

α is a function of $\frac{d_e}{d}$

$n = \frac{d_e}{d}$ ← equivalent diamet
← Sand drain diamete

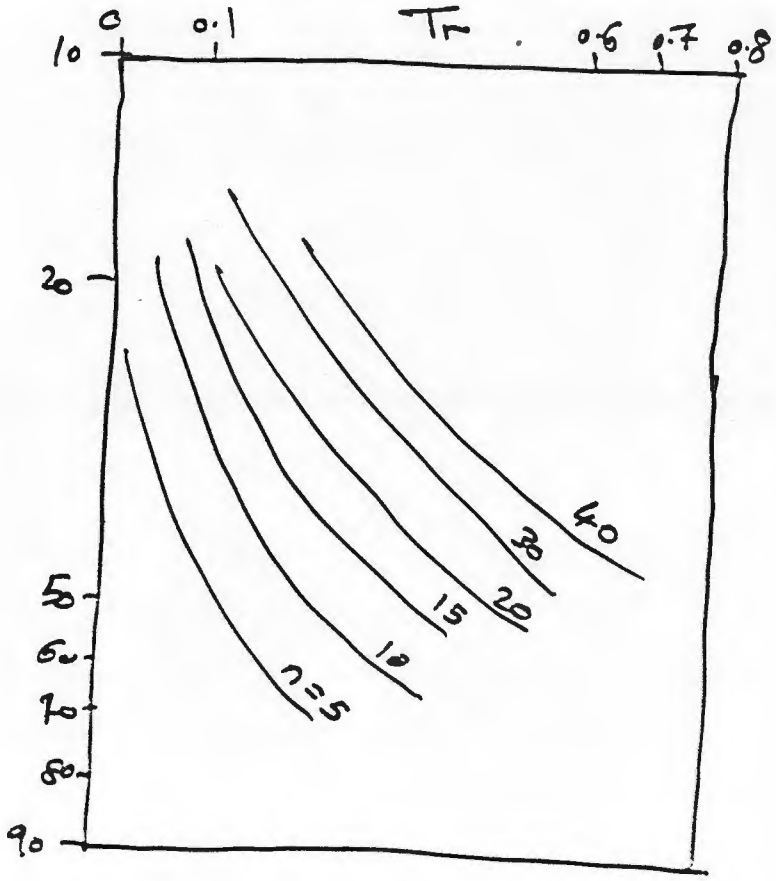

Solution for Vertical Drainage Only

time factor

$$T_v = \frac{\pi}{4}\left(\frac{U_v}{100}\right)^2 \quad \text{for } U < 60\%$$

$$= 1.78 - 0.93 \log(100 - U_v) \quad \text{for } U_v > 60$$

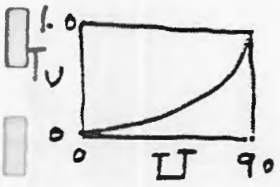

where $T_v = \dfrac{C_v t}{H^2}$

C_v — Coefficient of Consolidation for vertical drainage

H — drainage path

$$C_v = \frac{K_v}{m_v \gamma_w}$$

Average degree of Consolidation due to Vertical & Radial Drainage

Given: Surcharge $= q$
Certain duration of time t

The average degree of Consolidation due to drainage in the vertical and radial direction is:

$$U_{v,r} = 1 - \left[(1 - U_r)(1 - U_v)\right]$$

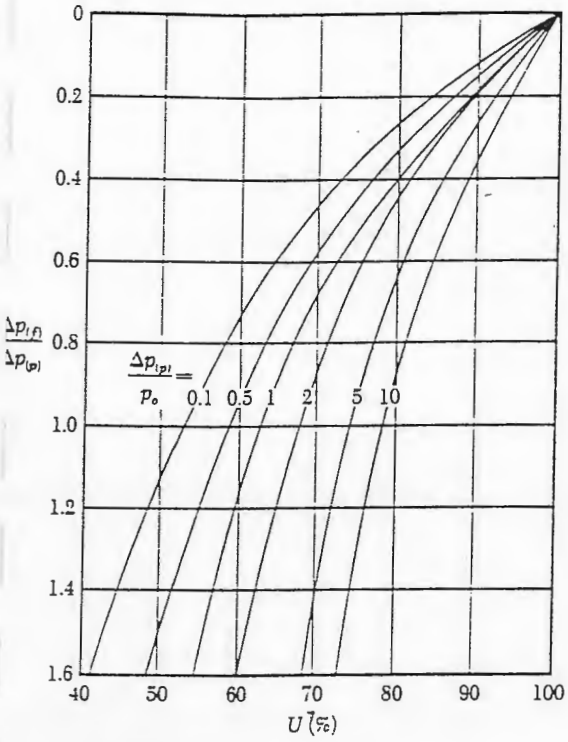

FIGURE 1 Plot of $\Delta p_{(f)}/\Delta p_{(p)}$ against U for various values of $\Delta p_{(p)}/p_o$

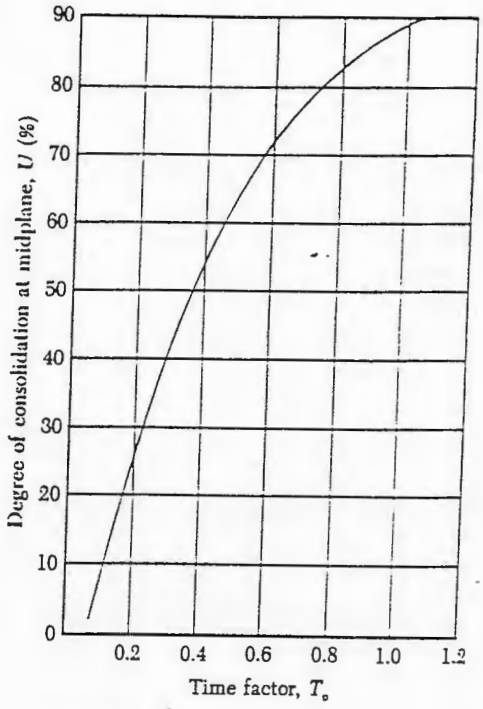

FIGURE 2 Plot of midplane degree of consolidation against T_v

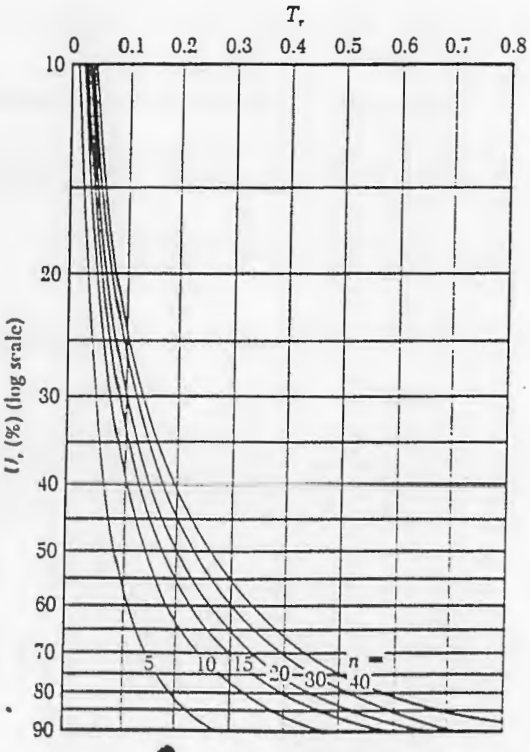

FIGURE 3 Average degree of consolidation for radial drainage only

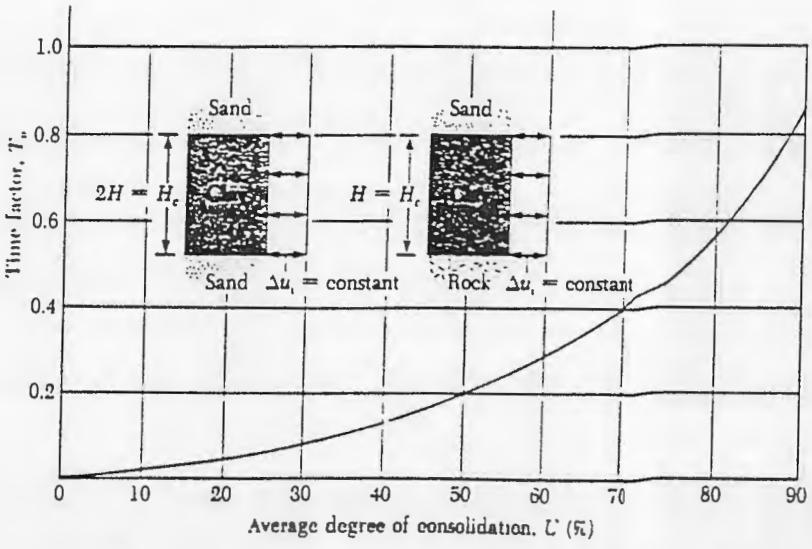

FIGURE 4 Plot of time factor against average degree of consolidation (Δu_i = constant)

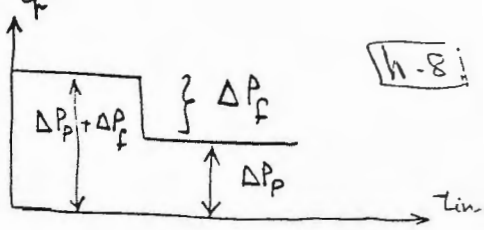

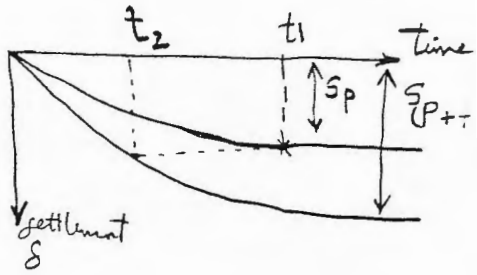

Example During the construction of a highway bridge, the average permanent load on the clay layer is expected to increase by about 115 kPa. The average effective overburden pressure at the middle of the clay layer is 210 kPa.

$H_{clay} = 6m$, $C_c = 0.28$, $e_o = 0.9$ and $C_v = 0.36 \frac{m^2}{month}$

The clay is normally consolidated. Determine:

(a) The total primary consolidation settlement of the bridge without precompression.

(b) The surcharge, ΔP_f, needed to eliminate by compression the entire primary consolidation settlement in 9 months.

(c) If sand drains are going to be used in a combination of additional surcharge, find the value of ΔP_f. For sand drains $r_w = 0.1$ $d_e = 3m$ & $C_v = C_{vr}$

Sol.:

Given: $\Delta P = 115$ kPa, $P_o = 210$ kPa } Loads

$H_{clay} = 6$ m
$C_c = 0.28$
$e_o = 0.9$
$C_v = 0.36 \frac{m^2}{month}$ } clay properties

Sand drains
$r_w = 0.1$ m
$d_e = 3$ m

Req.: (a) Priminary settlement without ΔP_f

(b) ΔP_f - value to eliminate completely the settlement due to structure load if the surcharge load will be kept for 9 month.

(c) If sand drains 0.2 m in diameter & $d_e = 3$ m will be used, what would be ΔP_f

(a) $S_{(p)} = \frac{C_c}{1+e_0} H_c \log \frac{P_0 + \Delta P_p}{P_0}$

$= \frac{0.28\,(6)}{1+0.9} \log \frac{210+115}{210} = 0.167\ m$

$= \boxed{16.7\ Cm}$

(b) $T_V = \frac{C_V t_2}{H^2} = \frac{0.36\,(9)}{3^2} = 0.36$

from Fig (2) when $T_V = 0.36 \longrightarrow U = 47\%$

$\frac{\Delta P_p}{P_0} = \frac{115}{210} = 0.548$

from Fig. (1) for $U = 47\%$ $\frac{\Delta P_p}{P_0} = 0.548 \xrightarrow{\text{Get}} \frac{\Delta P_f}{\Delta P_p} = 1.8$

$\therefore\ \Delta P_f = 1.8\,(115) = \boxed{207\ \frac{KN}{m^2}}$

(C) <u>Analysis for Vr. drainage</u>

$T_V = \frac{C_V t_2}{H^2} = \frac{0.36\,(9)}{3^2} = 0.36$

Get U from $T_V = 1.78 - 0.93 \log (100 - U_V)$ %

$\therefore\ U_V = 67\%$

<u>Analysis for Radial drainage</u>

$n = \frac{d_e}{2r_w} = \frac{3}{2 \times 0.1} = 15$

$T_r = \frac{C_{vr} t_2}{d_e^2} = \frac{0.36\,(9)}{3^2} = 0.36$

from n & T_r get $U_r = 77\%$

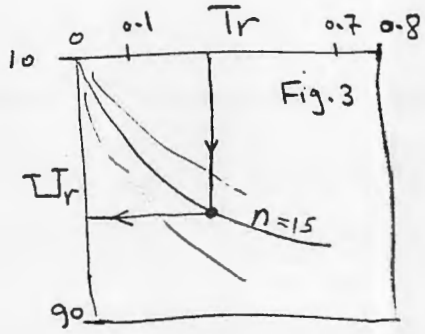

Combined flow

$U_{V,r} = 1 - [(1-U_V)(1-U_r)]$

$= 1 - [(1-0.67)(1-0.77)] = 0.924 = 92.4$

with $U_{V,r} = 92.4$ & $\frac{\Delta P_p}{P_0} = \frac{115}{210} = 0.548 \xrightarrow{\text{Fig. 1}}$ Get $\frac{\Delta P_f}{\Delta P_p} = 0.12$

$\therefore\ \Delta P_f = (115)\,0.12 = \boxed{13.8\ \frac{KN}{m^2}}$

5.6 Lime Stabiligation

* Introduction

* Surface stabiligation with lime
  Characteristics & Applications

* Lime Columns
  - Construction.
  - Characteristics.
  - Lime columns as foundations of structures.
  - Stabiligation of embankments with lime columns.
  - Treatment of expansive soil with lime columns.

GEOTECHNICAL PROPERTIES OF SOIL

1.1 INTRODUCTION

The design of foundations of structures such as buildings, bridges, and dams generally requires a knowledge of such factors as (a) the load that will be transmitted by the superstructure to the foundation system, (b) the requirements of the local building code, (c) the behavior and stress-related deformability of soils that will support the foundation system, and (d) the geological conditions of the soil under consideration. To a foundation engineer, the last two factors are extremely important because they concern soil mechanics.

The geotechnical properties of a soil—such as the grain-size distribution, plasticity, compressibility, and shear strength—can be assessed by proper laboratory testing. And, recently, emphasis has been placed on *in situ* determination of strength and deformation properties of soil, because this process avoids the sample disturbances that occur during field exploration. However, under certain circumstances, all of the needed parameters cannot be determined or are not determined because of economic or other reasons. In such cases, the engineer must make certain assumptions regarding the properties of the soil. To assess the accuracy of soil parameters—whether they were determined in the laboratory and the field or were assumed—the engineer must have a good grasp of the basic principles of soil mechanics. At the same time, he or she must realize that the natural soil deposits on which foundations are constructed are not homogeneous in most cases. Thus the engineer must have a thorough understanding of the geology of the area—that is, the origin and nature of soil stratification and also the groundwater conditions. Foundation engineering is a clever combination of soil mechanics, engineering geology, and proper judgment derived from past experience. To a certain extent, it may be called an "art."

When determining which foundation is the most economical, the engineer must consider the superstructure load, the subsoil conditions, and the desired tolerable settlement. In general, foundations of buildings and bridges may be divided into two

major categories: (1) *shallow foundations* and (2) *deep foundations*. *Spread footings*, *wall footings*, and *mat foundations* are all shallow foundations. In most shallow foundations, the *depth of embedment can be equal to or less than three to four times the width of the foundation*. *Pile* and *caisson* foundations are deep foundations. They are used when top layers have poor load-bearing capacity and when use of shallow foundations will cause considerable structural damage and/or instability. The problems relating to shallow foundations and mat foundations are considered in Chapters 3 and 4, respectively. Chapter 8 discusses pile foundations, and Chapter 9 examines drilled shafts.

This chapter serves primarily as a review of the basic geotechnical properties of soils. It includes topics such as grain-size distribution, plasticity, soil classification, effective stress, consolidation, and shear strength parameters. It is based on the assumption that you have already been exposed to these concepts in a basic soil mechanics course.

1.2 GRAIN-SIZE DISTRIBUTION

In any soil mass, the sizes of various soil grains vary greatly. To classify a soil properly, you must know its *grain-size distribution*. The grain-size distribution of *coarse-grained* soil is generally determined by means of *sieve analysis*. For a *fine-grained* soil, the grain-size distribution can be obtained by means of *hydrometer analysis*. The fundamental features of these analyses are presented in this section. For detailed descriptions, see any soil mechanics laboratory manual (for example, Das, 1993).

Sieve Analysis

A sieve analysis is conducted by taking a measured amount of dry, well-pulverized soil. The soil is passed through a stack of progressively finer sieves with a pan at the bottom. The amount of soil retained on each sieve is measured, and the cumulative percentage of soil passing through each sieve is determined. This percentage is generally referred to as *percent finer*. Table 1.1 contains a list of U.S. sieve numbers and the corresponding size of their hole openings. These sieves are commonly used for the analysis of soil for classification purposes.

The percent finer for each sieve determined by a sieve analysis is plotted on *semilogarithmic graph paper*, as shown in Figure 1.1. Note that the grain diameter, D, is plotted on the *logarithmic scale*, and the percent finer is plotted on the *arithmetic scale*.

Two parameters can be determined from the grain-size distribution curves of coarse grained soils: (1) the *uniformity coefficient* (C_u) and (2) the *coefficient of gradation, or coefficient of curvature* (C_z). These coefficients are

$$C_u = \frac{D_{60}}{D_{10}} \tag{1.1}$$

▼ **TABLE 1.1** U.S. Standard Sieve Sizes

Sieve no.	Aperture (mm)
4	4.750
6	3.350
8	2.360
10	2.000
16	1.180
20	0.850
30	0.600
40	0.425
50	0.300
60	0.250
80	0.180
100	0.150
140	0.106
170	0.088
200	0.075
270	0.053

$$C_z = \frac{D_{30}^2}{(D_{60})(D_{10})} \tag{1.}$$

where D_{10}, D_{30}, and D_{60} are the diameters corresponding to percents finer than 10, 3 and 60%, respectively

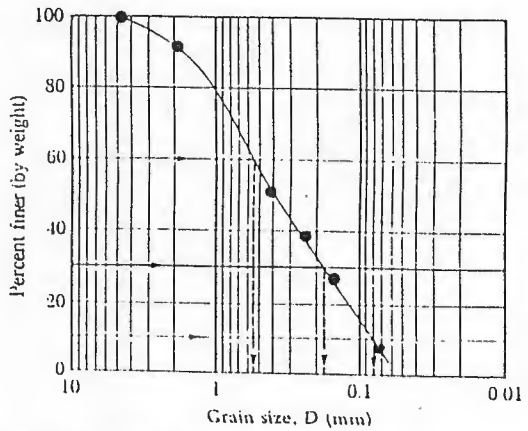

▼ **FIGURE 1.1** Grain size distribution curve of a coarse-grained soil obtained from sieve analysis

For the grain-size distribution curve shown in Figure 1.1, $D_{10} = 0.08$ mm, $D_{30} = 0.17$ mm, and $D_{60} = 0.57$ mm. Thus the values of C_u and C_z are

$$C_u = \frac{0.57}{0.08} = 7.13$$

$$C_z = \frac{0.17^2}{(0.57)(0.08)} = 0.63$$

Parameters C_u and C_z are used in the *Unified Soil Classification System*, which is described later in this chapter.

Hydrometer Analysis

Hydrometer analysis is based on the principle of sedimentation of soil particles in water. This test involves the use of 50 grams of dry, pulverized soil. A *deflocculating* agent is always added to the soil. The most common deflocculating agent used for hydrometer analysis is 125 cc of 4% solution of sodium hexametaphosphate. The soil is allowed to soak for at least 16 hours in the deflocculating agent. After the soaking period, distilled water is added, and the soil-deflocculating agent mixture is thoroughly agitated. The sample is then transferred to a 1000-ml glass cylinder. More distilled water is added to the cylinder to fill it to the 1000-ml mark, and then the mixture is again thoroughly agitated. A hydrometer is placed in the cylinder to measure—usually over a 24-hour period—the specific gravity of the soil–water suspension in the vicinity of its bulb (Figure 1.2). Hydrometers are calibrated to show the amount of soil that is still in

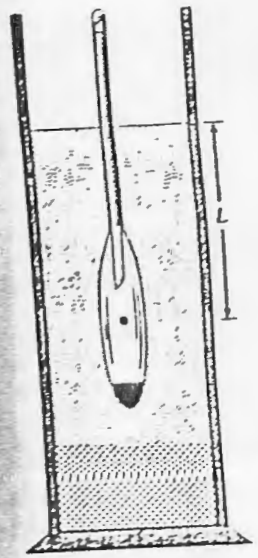

▼ FIGURE 1.2 Hydrometer analysis

suspension at any given time, t. The largest diameter of the soil particles still in suspe sion at time t can be determined by Stokes's law:

$$D = \sqrt{\frac{18\eta}{(G_s - 1)\gamma_w}}\sqrt{\frac{L}{t}} \quad (1.$$

where D = diameter of the soil particle
G_s = specific gravity of soil solids
η = viscosity of water
γ_w = unit weight of water
L = effective length (that is, length measured from the water surface in t cylinder to the center of gravity of the hydrometer; see Figure 1.2)
t = time

Soil particles having diameters larger than those calculated by Eq. (1.3) wou have settled beyond the zone of measurement. In this manner, with hydromet readings taken at various times, the soil *percent finer* than a given diameter D c be calculated, and a grain-size distribution plot can be prepared. The sieve and hydr meter techniques may be combined for a soil having both coarse-grained and fi grained soil constituents.

1.3 SIZE LIMITS FOR SOILS

Several organizations have attempted to develop the size limits for *gravel, sand, silt,* a *clay* based on the grain sizes present in soils. Table 1.2 presents the size limits reco mended by the American Association of State Highway and Transportation Offici (AASHTO) and the Unified (Corps of Engineers, Department of the Army, and Bure of Reclamation) Soil Classification systems. Table 1.2 shows that soil particles smal than 0.002 mm have been classified as *clay*. However, clays by nature are cohesive a can be rolled into a thread when moist. This property is caused by the presence of *c*

▼ TABLE 1.2 Soil-Separate Size Limits

Classification system	Grain size (mm)
Unified	Gravel: 75 mm to 4.75 mm
	Sand: 4.75 mm to 0.075 mm
	Silt and clay (fines): <0.075 mm
AASHTO	Gravel: 75 mm to 2 mm
	Sand: 2 mm to 0.05 mm
	Silt: 0.05 mm to 0.002 mm
	Clay: <0.002 mm

rinerals such as *kaolinite, illite,* and *montmorillonite.* In contrast, some minerals such s *quartz* and *feldspar* may be present in a soil in particle sizes as small as clay min-rals. But these particles will not have the cohesive property of clay minerals. Hence hey are called *clay-size particles,* not *clay particles.*

T–VOLUME RELATIONSHIPS

In nature, soils are three-phase systems consisting of solid soil particles, water, and air (or gas). To develop the *weight–volume relationships* for a soil, the three phases can be separated as shown in Figure 1.3a. Based on this separation, the volume relationships can be defined in the following manner.

Void ratio, e, is the ratio of the volume of voids to the volume of soil solids in a given soil mass, or written as

$$e = \frac{V_v}{V_s} \tag{1.4}$$

where V_v = volume of voids
V_s = volume of soil solids

Porosity, n, is the ratio of the volume of voids to the volume of the soil specimen, or

$$n = \frac{V_v}{V} \tag{1.5}$$

where V = total volume of soil

Moreover,

$$n = \frac{V_v}{V} = \frac{V_v}{V_s + V_v} = \frac{\frac{V_v}{V_s}}{\frac{V_s}{V_s} + \frac{V_v}{V_s}} = \frac{e}{1+e} \tag{1.6}$$

Degree of saturation, S, is the ratio of the volume of water in the void spaces to the volume of voids, generally expressed as a percentage, or

$$S(\%) = \frac{V_w}{V_v} \times 100 \tag{1.7}$$

where V_w = volume of water

Note that, for saturated soils, the degree of saturation is 100%.

The weight relationships are *moisture content, moist unit weight, dry unit weight,* and *saturated unit weight.* They can be defined as follows:

$$\text{Moisture content} = w(\%) = \frac{W_w}{W_s} \times 100 \tag{1.8}$$

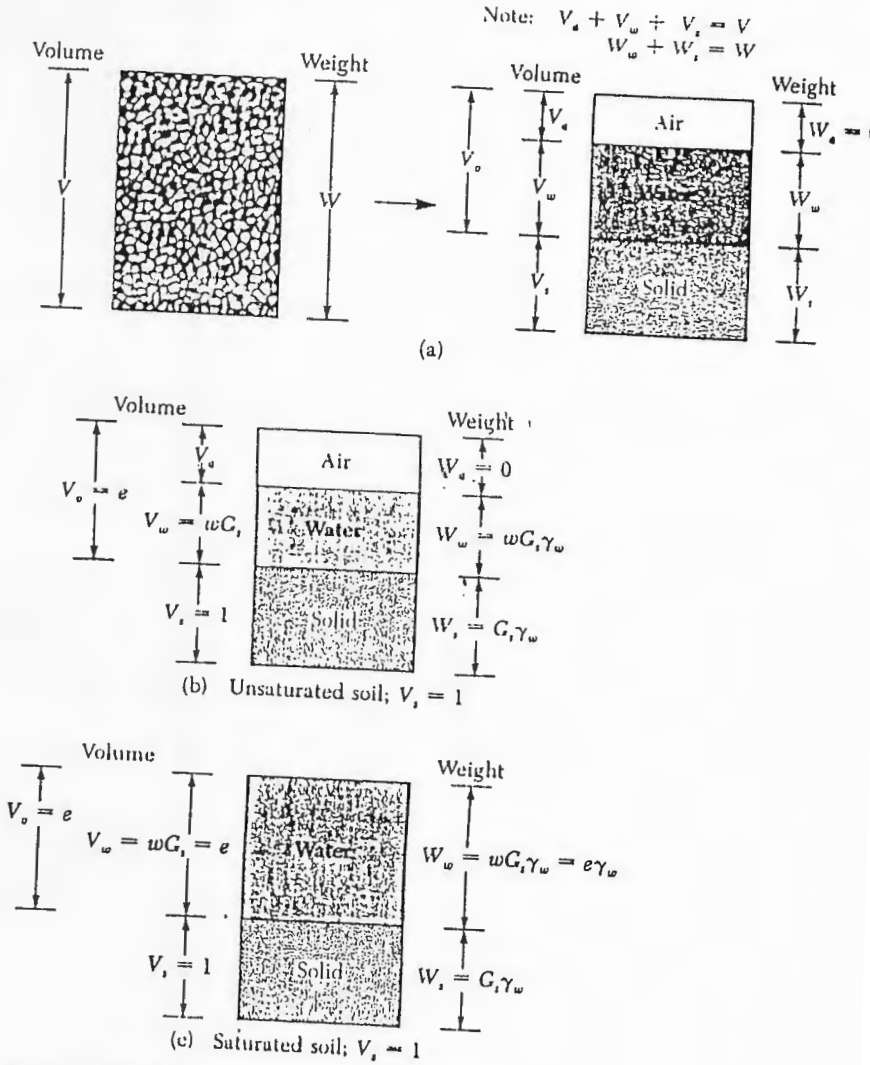

▼ **FIGURE 1.3** Weight–volume relationships

where W_s = weight of the soil solids
W_w = weight of water

$$\text{Moist unit weight} = \gamma = \frac{W}{V}$$

where W = total weight of the soil specimen = $W_s + W_w$

7.1 OBJECTIVES AND TECHNIQUES

In its most general sense, dewatering means modifying ground by lowering the water table, redirecting seepage, or simply reducing its water content. In coarse-grained soils, dewatering can be achieved by gravity drainage into sumps, ditches, and wells. In fine-grained soils, gravity drainage is slow or ineffective; for this type of ground, the process of dewatering becomes synonymous with forced consolidation (induced by preloading or electroosmosis).

Dewatering of soil (or fissured rock) in civil engineering or mining projects is carried out for one or more of the following reasons:

To provide a dry working area, such as in excavations for building foundations, dams, and tunnels

To stabilize constructed or natural slopes

To reduce lateral pressures on foundations or retaining structures

To reduce the compressibility of granular soils

To increase the bearing capacity of foundations

To improve the workability or hauling characteristics of borrow materials

To prevent liquefaction due to an upward gradient

To reduce the liquefaction potential during earthquakes

To prevent soil particle movement by groundwater (leading to piping)

To prevent surface erosion

To preveht or reduce damage due to frost heave

Every engineer dealing with soil is acutely aware of the significance of the water phase in the soil, yet each engineer's perspective may differ significantly, depending on his or her specialist background. A groundwater hydrologist may emphasize the characteristics of water flow in terms of quantities and directions. The geotechnical engineer is more aware of what benefits reducing pore water pressures has for soil strength (and the consequent increase in bearing capacity and slope stability). A road engineer's interests may extend to evaluating equilibrium moisture conditions in a subgrade. In pavement design an engineer may also be concerned with the transmission of water in vapor rather than just liquid form. However, here in our discussion of hydraulic modification of ground, we will only deal with the control and management of free water in soils and rocks.

The installation of drainage systems and wells could be considered an age-old building problem. Nevertheless, drilling and pumping technology has been improving steadily, and today construction procedures are highly efficient and may include the use of geotextiles and geomembranes.

Dewatering techniques based on traditional gravity drainage and pumping from sumps and wells are briefly introduced in this chapter, which also includes a review of fundamental soil-water relationships. The hydraulics of slots and wells is covered.

in Chap. 8; its principles underlie the design of dewatering systems for excavations and slopes (Chap. 9). Because they are relatively new but rapidly growing in importance, geosynthetics and their applications for filtration, drainage, and seepage control are treated separately in Chap. 10. The concept of preloading as a means of dewatering fine-grained soils is covered in Chap. 11; this topic is now closely associated with geosynthetics, because today vertical drains are almost exclusively made of synthetic materials. Chapter 12 recalls electroosmosis as a means of consolidating (=dewatering) fine-grained soils. This process has been known for many years but has seen relatively few practical applications. Nevertheless its potential for modifying difficult ground and improving the performance of foundation elements within it is well recognized.

Besides the traditional dewatering by gravity and the more involved preloading or electroosmosis, other geotechnical processes can be resorted to for eliminating or controlling groundwater. These include compressed air techniques in caisson construction and tunneling, and various cutoff systems (diaphragm walls, sheet piling, geomembranes). Although these methods may be important in combination with dewatering, they are considered outside the scope of ground modification in this text.

It should be pointed out that physical and chemical modification (Chap. 13–15) also affects ground water and permeability. However, because aspects other than dewatering are the dominant features of these techniques, they are treated as a separate group (Part IV).

The suitability of soils for the more traditional groundwater control techniques depends largely on their grain size distribution as illustrated in Fig. 7.1.

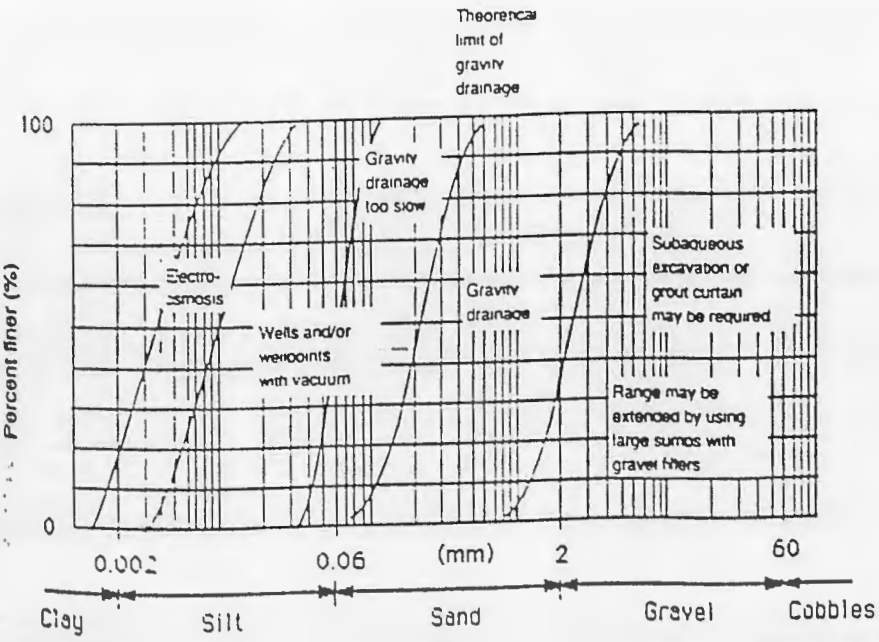

FIGURE 7.1
Dewatering methods applicable to various soils. [After Mansur and Kaufmann as found in Leonards (1962).]

7.2 TRADITIONAL DEWATERING METHODS

7.2.1 Open Sumps and Ditches

Collecting seepage water in open sumps and ditches and removing it by gravity flow or pumping is the most common and cheapest dewatering method. This technique works well in relatively shallow excavations in dense, well-graded coarse soils, in rock, and in the case of permeable soils overlying impermeable strata. It may also be considered in situations where floaters or other obstructions do not allow the sinking of wells. When used for sheeted and braced excavations, there is the danger of slumping, wall collapse or bottom instability due to an upward seepage gradient. The latter is referred to as a "quick" condition (Fig. 7.2).

Dewatering of clayey slopes may possibly be accomplished by a combination of a toe drain and gravel-filled lateral slots (Fig. 7.3). Stabilization is then effected not only by gradual dewatering but also by the supporting (reinforcing) effect of the buried gravel walls. A similar concept applies to the use of "sand piles" or "gravel columns" in foundations.

7.2.2 Gravity Flow Wells

If the water level in a borehole is lowered by steady pumping, groundwater will flow into the well under gravity until the phreatic surface, the level at which the water

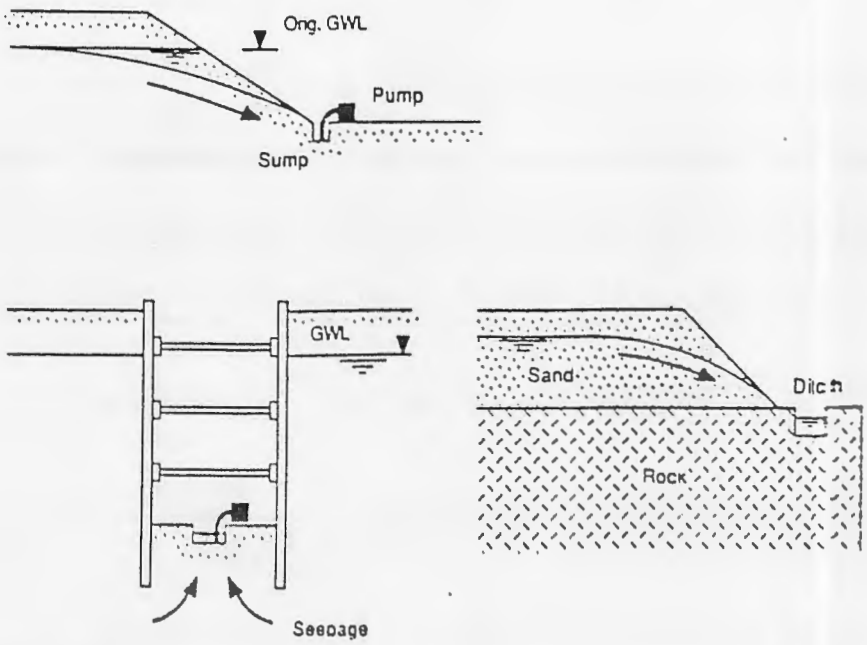

FIGURE 7.2
Dewatering by open sumps and ditches.

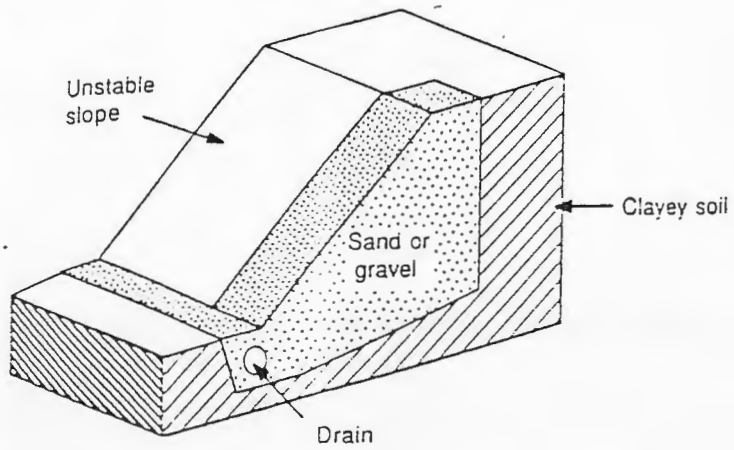

FIGURE 7.3
Lateral drainage slots.

pressure is atmospheric, has dropped to a new equilibrium position. This process can be used to lower the water level for construction purposes as illustrated in Fig. 7.4. The usual aim of dewatering is to lower the phreatic line to a level at least 0.5 m below the base of an excavation in gravel and coarse sand; in fine sands, the water level should be lowered further, preferably more than 0.7 m below the base of the excavation.

Standard bored wells involve the insertion of an inner casing (with a screen section at the bottom) into the cased borehole. After dropping appropriately graded filter material into the space between the inner and outer casing, the latter is withdrawn. Water is pumped to the surface through a riser pipe lowered into the inner casing. The casing and well screens may extend to a depth of 10 to 20 m; usual diameters are 150 to 200 mm. One-stage installations generally allow the lowering of the water level by a maximum of about 3.5 to 4 m near the center of a building excavation. Although more complicated, multistage installations are frequently used (Fig. 7.5).

The use of eductor wells, working on the Venturi principle, allows considerably deeper wells than in the standard arrangements. As demonstrated by many deep large-diameter wells in operation for municipal and industrial water supply, submersible pumps have virtually no limit as far as depth and diameter of practical wells are concerned.

A system of closely spaced single-pipe wells of small diameter with a common header pipe and a central pump installation is commonly referred to as a *well-point system*. The well points (or spears) are driven or jetted into the ground. Several patented systems are available (Fig. 7.6). Generally, after sinking the well point to the desired depth, a sand filter is formed around the point by feeding coarse sand down the hole. This is referred to as "sanding in." Water flows to the well under gravity and is drawn to the surface by the vacuum in the header main.

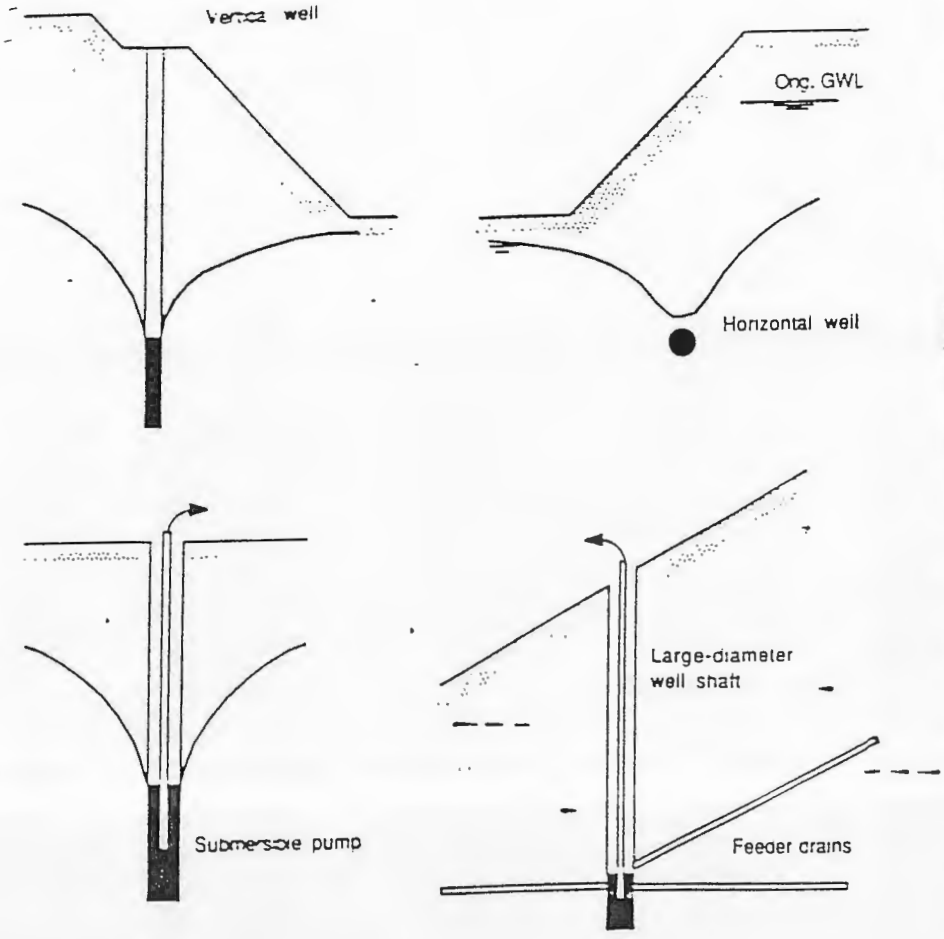

FIGURE 7.4
Well types.

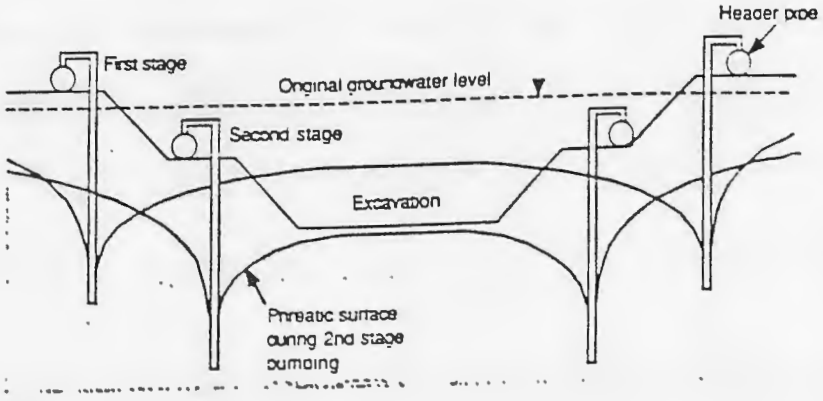

FIGURE 7.5
Multistage well-point system.

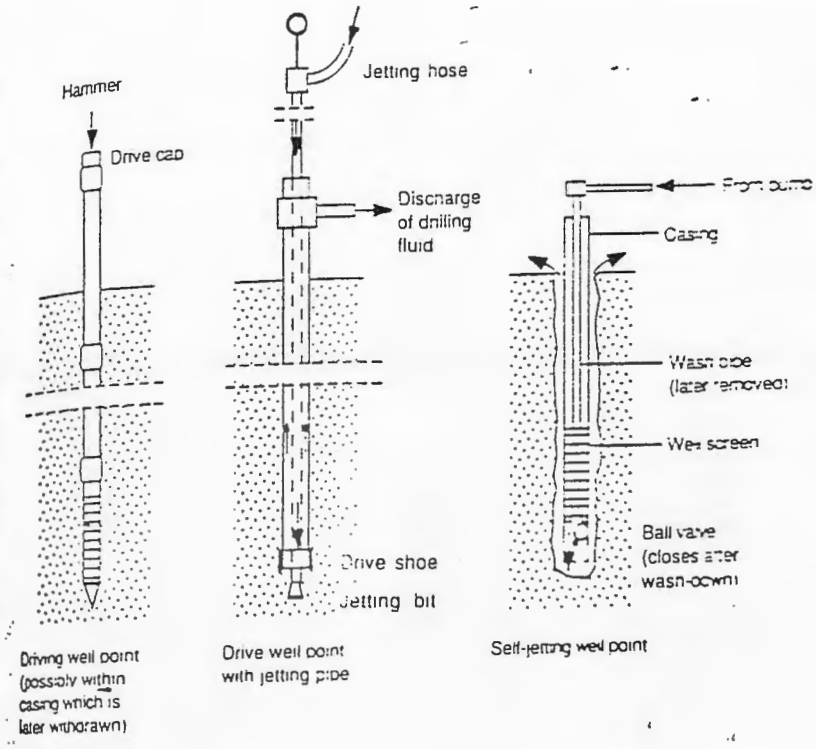

FIGURE 7.6
Types of well points.

7.2.3 Vacuum Dewatering Wells

In fine sands and silts, with permeabilities of 10^{-4} to 10^{-6} m/s, water does not flow freely under the influence of gravity, due to capillary tension. To make dewatering and stabilizing of these soils possible, a vacuum may be applied to the sealed-off filter section of the well. Seepage into the well is then increased due to the influence of the atmospheric pressure. Water inflow is generally low and wells may only require intermittent pumping out.

Vacuum action is also present in well-point systems which use a combined vacuum and centrifugal pump: the net vacuum applied at the well point is, however, only equivalent to the vacuum in the header pipe less the lift in the riser pipe. Care has to be taken that all connections in the pipe system are airtight and an effective seal is formed around the riser pipe in its upper section.

To be effective, vacuum wells have to be spaced very closely, say 1 to 2.5 m apart. The distance between rows of wells should not be more than 15 to 20 m.

Submersible pumps in combination with vacuum pumps could provide dewatering to great depth. Horizontal systems are also conceivable (Fig. 7.7).

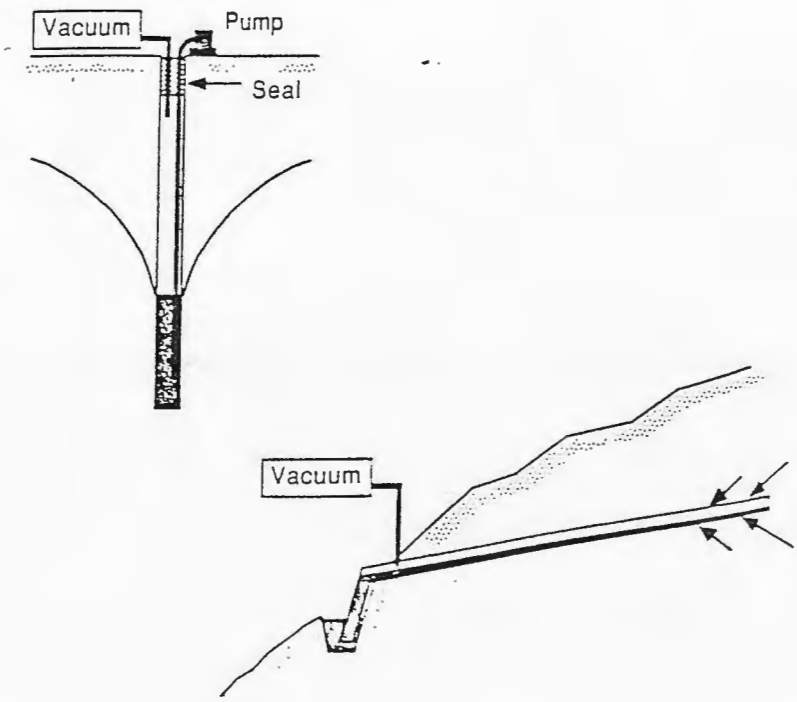

FIGURE 7.7
Vacuum dewatering wells.[1]

7.3 FUNDAMENTAL SOIL-WATER RELATIONSHIPS

This section reviews basic phase relationships, the concept of pore pressures, the principle of effective stress, and Darcy's law. These topics are usually covered in a first course on soil mechanics and are included here for those readers who wish to briefly brush up on these concepts. At the same time it attempts to form a bridge between the vocabulary familiar to the hydrologist and that commonly used by the geotechnical engineer.

7.3.1 Phase Relationships

Soil mechanics describe unfrozen soil as a multiphase material consisting of three distinct phases: solid, liquid, and gas. In most problems these phases represent soil solids, water, and air. For the definition and derivation of basic relationships between these components, an element of soil is conveniently separated into its phases as shown in Fig. 7.8.

where V = total volume
V_s = volume of soil solids
V_w = volume of water

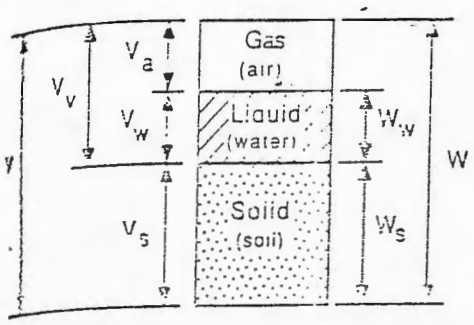

FIGURE 7.3
Soil phases—schematic representation.

V_a = volume of air
V_v = volume of voids (filled with air or water)
W = total weight
W_s = weight of soil solids
W_w = weight of water

Unit weights (kN/m^3) are defined as follows:

$$\gamma_t = \frac{W}{V} = \text{total unit weight (also referred to as bulk unit weight)}$$

$$\gamma_s = \frac{W_s}{V_s} = \text{unit weight of soil solids}$$

$$\gamma_d = \frac{W_s}{V} = \text{dry unit weight}$$

$$\gamma_w = \frac{W_w}{V_w} = \text{unit weight of water}$$

$$\gamma_b = \gamma_t - \gamma_w = \text{buoyant unit weight}$$

Specific gravities can be defined for water and soil solids, but it is the latter which is most often referred to:

$$G_s = \frac{\gamma_s}{\gamma_w} = \text{specific gravity of soil solids}$$

In this definition the unit weight of water must be measured at a temperature of 4°C. This stipulation is, however, normally not relevant, and γ_w is set equal to 9.81 kN/m^3. For most weight and volume calculations, it is recommended that γ_w = 9.81 kN/m^3 be used rather than the approximation of γ_w = 10 kN/m^3 which is usually sufficient for the computation of stresses.

For some calculations it may be preferable to work in mass units, rather than in weight units. For example, the total mass density of a soil may be expressed as

$$\rho_t = \frac{\gamma_t}{g}$$

where g is the acceleration of gravity. Preferred units are (t/m^3) and grams per milliliter; sometimes grams per cubic centimeter are used.

In soil mechanics the water content is expressed in terms of weight:

$$w = \frac{W_w}{W_s} = \text{water content (usually expressed in \%)}$$

In groundwater hydraulics, the water content may also be expressed as the ratio of volume of water over total volume.

Important volume relationships are

$$n = \frac{V_v}{V} = \text{porosity (usually expressed in \%)}$$

$$e = \frac{V_v}{V_s} = \text{void ratio}$$

$$S = \frac{V_w}{V_v} = \text{saturation (usually expressed in \%)}$$

Saturation, porosity, and water content are usually expressed in percent, while the void ratio is always a number, ranging from 0 to more than 1. A number of useful interrelationships are worth remembering:

$$G_s w = Se \tag{7.1}$$

$$n = \frac{e}{1 + e} \tag{7.2}$$

$$\gamma_t = \frac{G + Se}{1 + e}\gamma_w \tag{7.3}$$

$$\gamma_d = \frac{\gamma_t}{1 + w} \tag{7.4}$$

These expressions can be easily verified using the schematic representation of the phases of a soil element as given in Fig. 7.8, particularly if simplifying assumptions are made such as setting V_s equal to 1.

Depending on the type of deposition and stress history, soils may have a considerable range of densities, void ratios, and water contents. For typical values of the various properties of soils the reader is referred to standard soil mechanics texts. However, as a guide to the order of magnitude, the following values are reasonable assumptions for a medium dense sandy, gravelly soil:

$$G_s = 2.65$$

$$e = 0.6$$

$$n = 40\%$$

$$\gamma_d = 18\ \text{kN/m}^3$$

$w = 20\%$ (saturated)

$\gamma_t = 20$ kN/m^3 (partially saturated)

Note that these values do not exactly correspond to each other and that they are guidelines only. Densities could easily vary by $\pm 20\%$ and void ratios by $\pm 40\%$. Specific gravities of soil solids generally do not vary by more than $\pm 5\%$.

7.3.2 Geostatic Stresses and Pore Pressures

Geostatic stresses are stresses due to the soil's own weight in a deposit with a horizontal surface and where properties do not change appreciably in a horizontal direction. In this case we can relate the vertical stress σ_v on an element of soil at depth z simply to the weight of soil above that element:

$$\sigma_v = \gamma_t z \tag{7.5}$$

The determination of the horizontal stress is not straightforward. Mathematically the horizontal stress is obtained by multiplying the vertical stress with a factor K, the coefficient of lateral stress. The value of K depends on the stress history of the soil mass and the state of equilibrium it is in. For geostatic conditions, K is set equal to K_0, which is the coefficient of lateral stress at rest, meaning that the soil mass is neither undergoing compression nor expansion. The factor K defines the ratio of horizontal to vertical stresses in terms of effective stresses. The effective vertical stress is equal to the total vertical stress σ_v minus the pore water pressure u:

$$\sigma'_v = \sigma_v - u \tag{7.6}$$

The effective vertical stress in a saturated soil deposit can also be calculated directly by multiplying depth z with the buoyant unit weight of the soil. Effective horizontal stress and total horizontal stress is then obtained as follows:

$$\sigma'_h = K\sigma'_v \tag{7.7}$$

$$\sigma_h = \sigma'_h + u \tag{7.8}$$

Effective stresses are of particular relevance in stability problems. Wherever pore pressures increase without a corresponding increase in total stresses, such as might be due to seepage or external forces, the stability of a soil mass with frictional shear strength is reduced. In situations like this the benefits of dewatering can be clearly demonstrated.

The level at which the pore water pressure is atmospheric is referred to as the groundwater level, the water table, or the phreatic surface. In the geostatic condition, the pore pressure increases linearly with depth below the water table (Fig. 7.9). Following the laws of hydrostatics, the pore pressure is equal in all directions. As already indicated, external influences may create "excess" hydrostatic pressures, usually detrimental to stability.

Because of capillary forces, water may rise above the groundwater level. The capillary rise in soils may vary from 0.05 m in coarse gravel to more than 1 m in fine

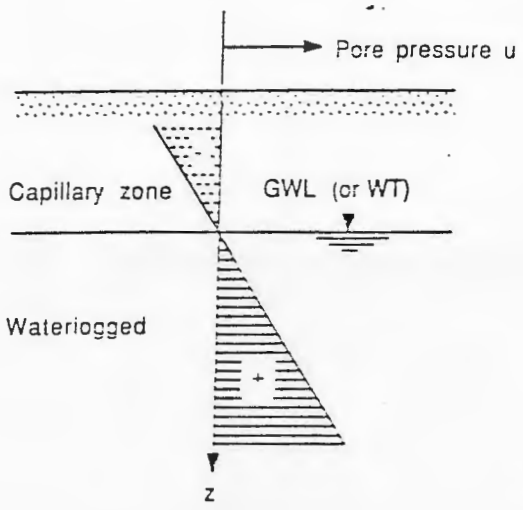

FIGURE 7.9
Pore pressure and capillary rise.

sand and to more than 3 m in silt. The pore pressure above the water table is negative. This negative pressure is referred to as tension, suction, or capillary pressure. As long as there is a continuous channel of water down to the phreatic surface, this negative pressure varies linearly with the distance from this level (Fig. 7.9). Where there is no continuity to the fully saturated zone, the magnitude of the pore water suction can be related to the water content.

The extent of the saturated zone above the water table depends on how a particular new phreatic surface evolved. The levels of saturation maintained following a fall in the groundwater level are higher than those resulting from capillary rise alone.

Depending on the type of soil and the history of water level changes, the total unit weight of soil above and below the water table may be measurably different. However, because most soils retain a significant amount of water after drainage, it is usually not appropriate to calculate stresses above the water table using dry unit weight equivalent to that of the saturated soil below.

Another aspect of importance is the conclusion that the lowering of the groundwater level will increase effective stresses below the original water table. An increase in effective stress will cause settlement of compressible strata. This is the reason why dewatering of an excavation may lead to damage of adjacent buildings. In order to avoid this problem recharging of the aquifer may be required in critical areas.

7.3.3 Drainable Pore Water

Figure 7.10 illustrates the changes which occur in the saturation of a soil when the water table is lowered from a depth z_1 to depth z_2. Because of capillary forces, the water does not drain out completely above the new water table. The ratio of the volume of water which will drain from an element of soil under gravity to its total volume is termed specific yield or phreatic storage coefficient. Typical values for coarse sands and gravels range from 0.2 to 0.3.

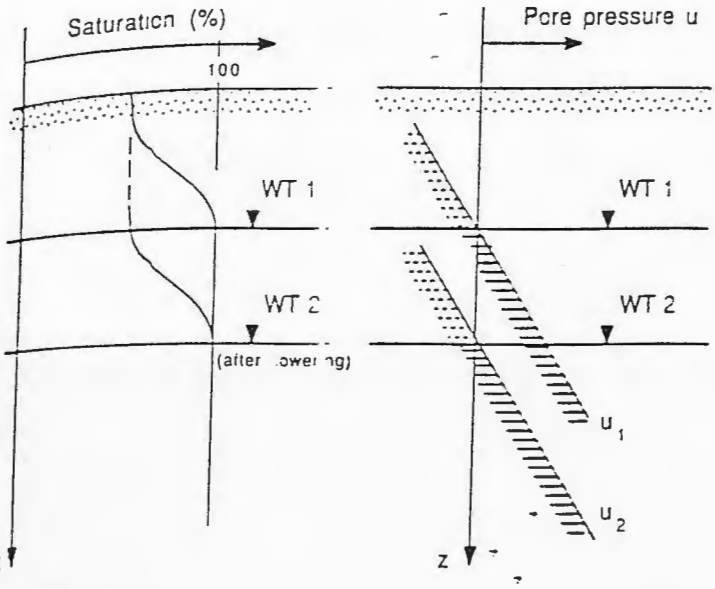

FIGURE 7.10
Saturation with changing water table.

The *specific retention* is a measure of the amount of water retained after the *specific yield* has been released. The sum of the specific yield and the specific retention must equal the porosity of the porous medium, or we can write:

$$\text{Specific retention} = \text{porosity} - \text{specific yield}$$

As pointed out earlier, a decrease in pore pressure means an increase in effective stress which leads to compression of the soil skeleton. This causes some water to be released from the soil which remains fully saturated. In soil mechanics this process is called consolidation. In groundwater hydrology the volume of water released from the soil per unit volume of aquifer per unit change in head (or water pressure) is called specific storage or *specific mass storativity*. If the specific mass storativity is multiplied by the thickness of the water-bearing layer, it becomes the *storage coefficient* (or storativity) of an aquifer.[1]

7.3.4 Darcy's Law

Figure 7.11 illustrates a simple experiment in which water is made to flow under a constant head dh through a column of sand of length dx. Darcy conducted this experiment some 130 years ago and found the following relationship:

$$Q = kiA \tag{7.9}$$

[1] The storativity of an unconfined aquifer is the same as its specific yield. For confined aquifers only the term "storativity" is used; in this case the definition of specific yield would not make sense, since the soil remains saturated. (Aquifer types are defined in Sec. 8.1.)

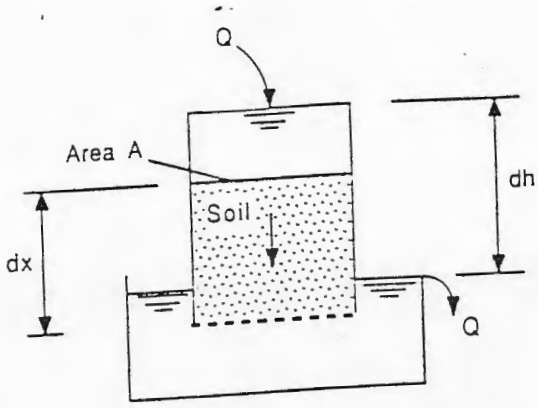

FIGURE 7.11
Darcy's experiment.

where Q = flow through area A per unit time, m^3/s
k = coefficient of permeability (or hydraulic conductivity), m/s
i = hydraulic gradient = dh/dx

Darcy's law is only valid for laminar flow. In most groundwater problems gradients are small and the motion is indeed laminar. However, this may not be the case in the vicinity of pumped wells or for water flow in very fine soils such as clays.

In the traditional soil mechanics literature, the coefficient of permeability is quoted in units of centimeters per second. Hydrologists may use all kinds of other units, such as meters per day. In these notes either centimeters per second or meters per second will be used. Typical values are:

Coarse gravel	$k = 10$ cm/s
Fine gravel	$k = 1$ cm/s
Coarse sand	$k = 10^{-1}$ cm/s
Sandy gravel	$k = 10^{-2}$ cm/s
Fine sand	$k = 10^{-3}$ cm/s
Silty sand	$k = 10^{-5}$ cm/s
Clay	$k < 10^{-7}$ cm/s

These values are meant as a guide only. The coefficient of permeability of a particular soil can easily vary by a factor of 100 if the soil is deposited or compacted at different densities. The determination of k in the field and laboratory will be discussed in Sec. 9.1.1.

The coefficient of permeability k depends on the density of the fluid and its viscosity ν. The desire to have a permeability value which is independent of the fluid properties has led to the definition of the intrinsic permeability which is only related to the properties of the porous medium. With

k_i = intrinsic permeability m^2
η = dynamic viscosity t/m/s
ρ = mass density t/m^3

g = acceleration of gravity $\quad m/s^2$

υ = kinematic viscosity $\quad m^2/s$

The intrinsic permeability is calculated as follows:

$$k_i = k\frac{\eta}{\rho g} = k\frac{\upsilon}{g} \quad m^2 \tag{7.10}$$

This term is not commonly used in soil engineering but does find application in the study of pollutant flow in the ground.

In groundwater hydrology, flow through an aquifer is often expressed per unit width. The cross-sectional area A of an aquifer can be expressed as the product of aquifer height h and width b. Darcy's equation then becomes

$$Q = kihb = hkib = Tib \quad m^3/s \tag{7.11}$$

where T = transmissivity (s^{-1}) = kb.

The transmissivity term has proved useful in describing the in-plane permeability of geotextiles (Sec. 10.2).

PROBLEMS

Prefixes indicate problem type: C = calculations, B = brief answer, M = multiple choice.

Section 7.1 (Objectives and Techniques)

B7.1. Name four methods of controlling groundwater.
(a) _____
(b) _____
(c) _____
(d) _____

B7.2. Name two geotechnical processes which could be used to eliminate or control groundwater but do *not* necessarily result in a reduction of the amount of free pore water present in the soil.
(a) _____
(b) _____

B7.3. Name four reasons for dewatering soil or rock.
(a) _____
(b) _____
(c) _____
(d) _____

M7.4. The following method of ground modification generally results in a reduction of the amount of free water present in the soil (by water draining out of the soil or chemically combining with other molecules):
(a) Compaction
(b) Use of geomembranes
(c) Electroosmosis
(d) Soil freezing

M7.5. Lowering the groundwater level may cause
(*a*) Liquefaction.
(*b*) Settlement.
(*c*) A decrease in bearing capacity.
(*d*) Decreased effective stresses in the soil mass.

M7.6. The suitability of various groundwater lowering techniques depends significantly on
(*a*) The bearing capacity of the soil.
(*b*) The grain size distribution.
(*c*) The cohesiveness of the soil.
(*d*) The physicochemical properties of the soil.

M7.7. Dewatering of soil may
(*a*) Cause swelling.
(*b*) Reduce liquefaction potential.
(*c*) Reduce bearing capacity.
(*d*) Reduce effective unit weight.

M7.8. The *most* suitable soil for dewatering by gravity wells or slots is
(*a*) Gravel.
(*b*) Sand.
(*c*) Silt.
(*d*) Clay.

Section 7.2 (Traditional Dewatering Methods)

M7.9. Vacuum wells
(*a*) Are the same as eductor wells.
(*b*) May make dewatering in fine sands and silts possible.
(*c*) Always need submerged pumps.
(*d*) Are gravity wells using vacuum pumps.

M7.10. Vacuum wells, rather than gravity wells, may be needed for
(*a*) Coarse gravel.
(*b*) Fine gravel.
(*c*) Coarse to medium sands.
(*d*) Fine sands and silts.

B7.11. Name three types of wells which are different in hydraulic action.
(*a*) _____
(*b*) _____
(*c*) _____

Section 7.3 (Fundamental Soil-Water Relationships)

C7.12. A soil has a water content of 45.2% when fully saturated (below the groundwater level). The specific gravity of the soil solids is 2.65.

Total unit weight γ_t = _____ kN/m³
Total density ρ_t = _____ g/cm³
Void ratio e = _____
Porosity n = _____ %

Now assume that the groundwater level drops and some water drains out of the soil, reducing w to 40%. If no compression of the soil mass occurs, the new values are:

Total density ρ_t = _____ t/m³
Total unit weight γ_t = _____ kN/m³
Saturation S = _____ %

C7.13. A saturated soil has a water content of 26%. The total saturated density is 2 t/m³. Determine

Dry density γ_d = _____ t/m³
Submerged density or buoyant density ρ_b = _____ t/m³
Specific gravity of soil solids G_s = _____

M7.14. A soil contains 80 g of soil solids and 20 g of water. The volume of the soil solids is 30 mL. The total volume of the soil is 60 mL. Correspondingly,
(*a*) The water content is 20%.
(*b*) The void ratio is 0.5.
(*c*) The total density is 1.66 t/m³.
(*d*) The saturation is 13.3%.

M7.15. If the total stress in a saturated soil is 100 kPa and the effective stress is 60 kPa, the implied pore pressure is
(*a*) 0 kPa.
(*b*) 40 kPa.
(*c*) 60 kPa.
(*d*) 100 kPa.

M7.16. Lowering the groundwater level in a soil mass may cause settlement because it
(*a*) Decreases the weight of the soil.
(*b*) Causes downward seepage pressure.
(*c*) Increases effective vertical stresses in the soil.
(*d*) Makes the soil softer.

M7.17. In groundwater hydrology, the volume of water released from a unit volume of saturated soil per unit change in head (or pore water pressure) is called
(*a*) Specific storage.
(*b*) Storage coefficient.
(*c*) Conductivity.
(*d*) Permeability.

M7.18. Above the phreatic surface
(*a*) A soil is completely dry.
(*b*) A soil is always saturated.
(*c*) Pore pressures are positive (higher than air pressure).
(*d*) Pore pressures are negative (less than air pressure).

M7.19. A permeability of 10^{-3} cm/s (10^{-5} m/s) is typical for a
(*a*) Fine gravel.
(*b*) Coarse sand.
(*c*) Fine sand.
(*d*) Silty clay.

B7.20. The following notation is used to describe an element of soil: total volume = V, volume of soil solids = V_s, volume of water = V_w, weight of soil solids = W_s, and weight of water = W_w. Using these designations define:

(*a*) Water content = _____ .
(*b*) Porosity = _____ .
(*c*) Void ratio = _____ .
(*d*) Saturation = _____ .

B7.21. A sample of wet fly ash (G_s = 2.0) has a volume of 150 mL and weighs 240 g. After being dried in an oven, the sample weighs 200 grams. Determine
(*a*) Water content w = _____%.
(*b*) Dry density ρ_d = _____ t/m^3.
(*c*) Saturation S = _____ %.
(*d*) Void ratio e = _____ .

B7.22. Define *one only* of the following terms:
(*a*) Specific yield (or phreatic storage coefficient)
(*b*) Specific retention
(*c*) Specific storage (or specific mass storativity)

B7.23. Darcy's law expressed in Q, k, i, and A reads:

_____ = _____

where k = _____ in units of _____ .
i = _____ in units of _____ .
A = _____ in units of _____ .
Q = _____ in units of _____ .

CHAPTER

8

HYDRAULICS OF SLOTS AND WELLS

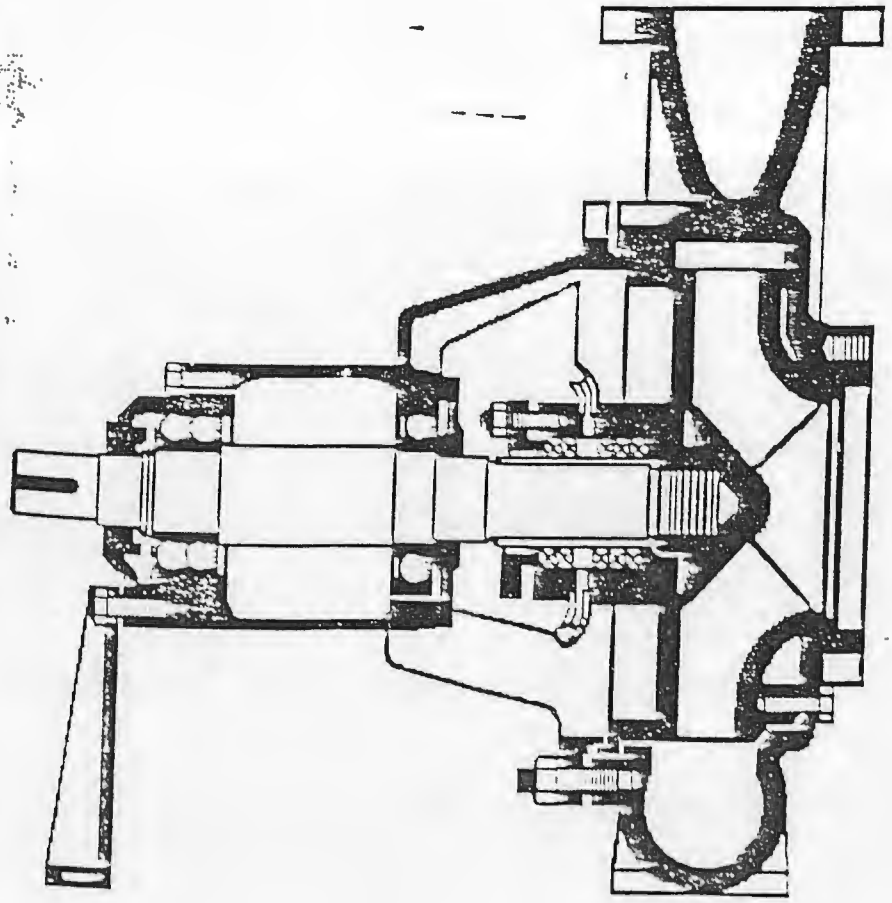

8.1 AQUIFER TYPES

A permeable soil or rock formation which stores or transmits significant amounts of water is called an *aquifer*. If it is fully saturated and confined by impervious layers at its upper and lower boundaries, it is referred to as an *artesian aquifer*. If a permeable layer is only partially filled with water, it is described as an *unconfined aquifer* (Fig. 8.1). In nature, semiconfined (or leaky) acquifers and semiunconfined aquifers may occur [for definitions see textbooks on groundwater hydrology, e.g., Hazel (1975)].

When sinking a bore, several water-bearing layers may be encountered, and therefore more than one groundwater level may be identified, possibly including temporary or permanent perched groundwater. A perched aquifer is an unconfined aquifer separated from an underlying body of groundwater by an unsaturated zone.

For the analysis of the most basic problems in the flow of water to drainage slots and wells, an aquifer is idealized to have horizontal boundaries, to consist of homogeneous and isotropic porous material, and to have infinite extent. The simplest solutions are derived for the case where the slot or well fully penetrates the aquifer. In terms of hydraulic theory, Darcy's law is assumed to be valid, and simplifying assumptions are made with respect to the hydraulic gradient.

8.2 DUPUIT-THIEM APPROXIMATION

According to the Dupuit-Thiem approximation, the hydraulic gradient below any point of the drawdown curve is assumed to be equal to the slope of the drawdown curve at that point.

Figure 8.2 shows what sometimes is referred to as a perfect slot or well with gravity flow. It fully penetrates a homogeneous and isotropic horizontal water-bearing stratum overlying impermeable soil or rock. The water flow is unconfined. Feeding the system is a line source (for the case of a drainage slot) or a circular source (for the case of a well) at a distance L. Of basic interest to the engineer is the determination of the pump discharge required and the equation of the drawdown curve for steady-

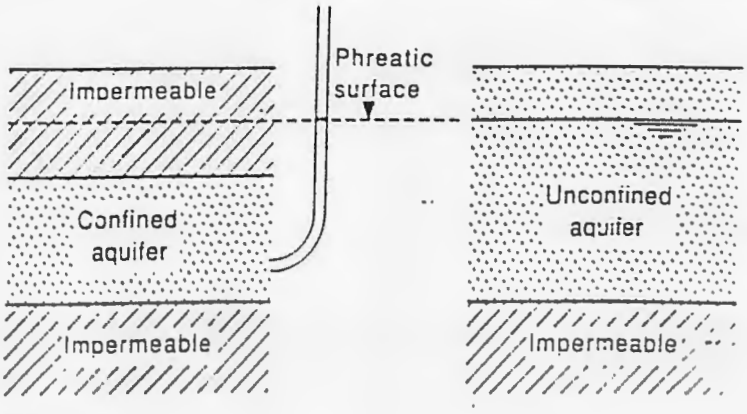

FIGURE 8.1
Aquifer types.

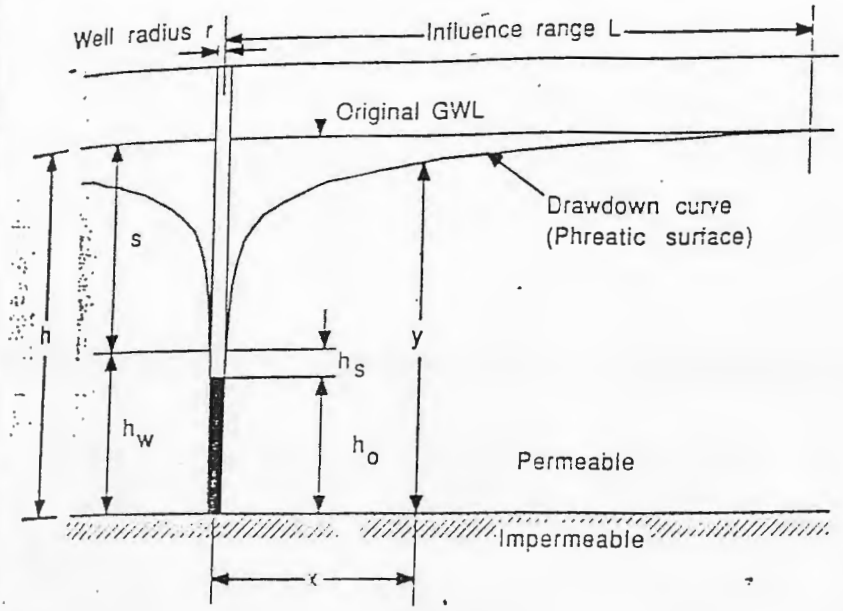

FIGURE 8.2
Perfect slot or well with gravity flow.

state seepage conditions. Their derivation makes use of Darcy's law and the Dupuit-Thiem approximation.

For a perfect slot we first find the discharge quantity q per unit length as [from Eq. (7.9)]

$$q = kiA \qquad \text{where } A = y \text{ (unit slice)}$$

$$= k\frac{dy}{dx}y$$

Now the variables are separated and both sides of the equation are integrated:

$$\int_{h_w}^{h} y\,dy = \frac{q}{k}\int_0^L dx$$

$$\frac{h^2 - h_w^2}{2} = \frac{qL}{k}$$

Solving for q (flow from one side), we find

$$q = \frac{(h^2 - h_w^2)k}{2L} \tag{8.1}$$

The total flow from both sides is equal to $2q$.

For the equation of the drawdown curve we can derive

$$h^2 - y^2 = \frac{L - x}{L}(h^2 - h_w^2) \tag{8.2}$$

Similarly, for a perfect well we can find the discharge quantity

$$Q = \frac{\pi k(h^2 - h_w^2)}{\ln (L/r)} \tag{8.3}$$

The phreatic surface (or cone of depression) is defined by

$$y^2 - h_w^2 = \frac{Q \ln (x/r)}{\pi k} \tag{8.4}$$

For the determination of the seepage quantities it is generally safe to use h_0 (see Fig. 8.2) instead of h_w in the formula, as this will result in a conservative design of the pump capacity.

8.3 FREE DISCHARGE HEIGHT

The water level in a slot or well is generally below the point of entrance of the phreatic line (or drawdown curve), resulting in vertical drainage over the so-called free discharge height

$$h_s = h_w - h_0 \tag{8.5}$$

The free discharge height depends on the drawdown in the well (or slot). The steeper the phreatic line near the well, the more significant h_s is. For rough calculations the existence of a free discharge height may be ignored.

Formulas for estimating h_s are of an empirical nature and are usually based on model tests, results of which appear to vary considerably. For slots, the distance h_s may be determined using diagrams proposed by Chapman (1956). The diagram shown in Fig. 8.3 is recommended for gravity flow to a fully penetrating slot. For wells, Kezdi (1969) gives a formula attributed to Ollos (elsewhere credited to Ehrenberger):

$$h_s = \frac{C(h - h_0)^2}{h} \tag{8.6}$$

Ollos proposed a value of $C = 0.5$. Herth and Arndts (1973) give no less than six other formulas for estimating the free discharge height in wells. Some are reproduced in App. 8B.

The ratio $(h - h_w)/(h - h_0)$ is also called the well efficiency, usually expressed in percent. It increases if the well screen has insufficient openings or is too short, if the surrounding filter zone restricts the flow, or if construction of the well contaminates the adjacent soil with fines (as sometimes happens with drilling fluids). Inefficient wells mean higher costs of pumping.

8.4 INFLUENCE RANGE

For drainage slots the influence range L should be known with reasonable accuracy, since the discharge quantity is indirectly proportional to it [Eq. (8.1)]. In the well formula [Eq. (8.3)] L (also called the radius of influence) appears in a logarithmic

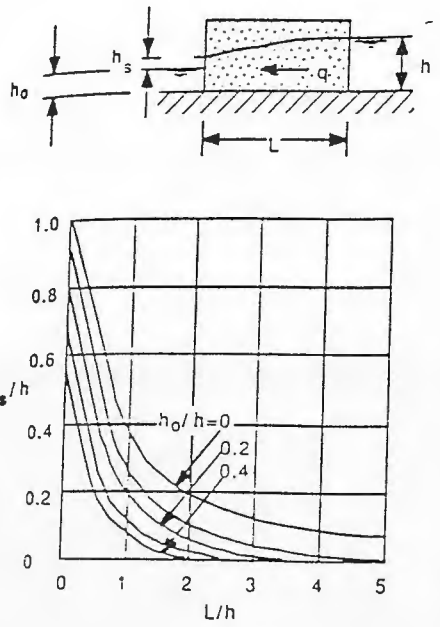

FIGURE 8.3
Free discharge surface for slots. [*Chapman (1956).*]

term, and a good assessment of the coefficient of permeability k is much more important than the value of the influence range.

Strictly speaking, pumping from an aquifer will only produce a steady-state condition of groundwater flow if the aquifer is continually recharged from somewhere. If an open watercourse or reservoir is near the dewatering point, the distance to that source will represent the distance L in the discharge formula for slots. Special formulas for wells, e.g., near a line source, are given in Apps. 8B and 8C. If no recharge occurs, the influence range will continually increase with time, although at a decreasing rate. For this nonsteady state of flow for an ordinary perfect well, Kozeny (1953) quotes a time-dependent expression for L as follows:

$$L = 1.5\,\frac{\sqrt{hkt}}{n} \tag{8.7}$$

The term n represents the porosity of the soil.

In most cases it is sufficiently accurate to obtain an approximate value for L according to an empirical formula proposed by Sichardt (1928):

$$\begin{aligned} L &= C(h - h_w)\sqrt{k} \\ &= Cs\sqrt{k} \end{aligned} \tag{8.8}$$

For s in meters and k in meters per second, the value of the constant is

$$C = \begin{cases} 3000 \text{ for wells (Sichardt)} \\ 1500 \text{ to } 2000 \text{ (U.S. Corps of Engineers) for single-line well points} \end{cases}$$

The latter values given by Mansur and Kaufmann are quoted in Leonards (1962).

According to Kezdi and Marko (1969) the following values may serve as a guide for unconfined aquifers:

Coarse gravel and cobbles	$L = 500$ m
Coarse gravel	$L = 100$ to 150 m
Medium gravel	$L = 50$ m
Sand	$L = 33$ m
Fine sand	$L = 5$ to 10 m

8.5 FORCHHEIMER EQUATION FOR MULTIWELL INSTALLATIONS

Forchheimer (1930) derived a formula for the discharge from a system of perfect gravity flow wells of equal length and capacity.

Consider a point P in a field of wells as shown in Fig. 8.4. If only well number 1 is active, the water level y at P can be derived from the equation

$$Q_1 = \frac{\pi k(h^2 - y^2)}{\ln L - \ln x_1} \tag{8.9}$$

A similar equation can be written for the situation where only well number 2 is operating, and so on. For the simultaneous pumping from n equivalent wells, Forchheimer found that the total discharge quantity is equal to

$$Q = \frac{\pi k(h^2 - y^2)}{\ln L - (1/n) \ln x_1 x_2 \cdots x_n} \tag{8.10}$$

In deriving this formula it is assumed that the aquifer is thin relative to its horizontal expansion and that the rules of potential theory apply.

For a circular arrangement of wells (Fig. 8.5), the water level y at the center of the excavation can readily be calculated from a simplified version of Eq. (8.10) as follows:

$$Q = \frac{\pi k(h^2 - y^2)}{\ln L - \ln a} \tag{8.11}$$

The water level h_0 of an individual well in the circular group can be computed from Eq. (8.10) with x_1 equal to the well radius and $x_2 \cdots x_n$ the distance from well number 1 to all the other wells (Fig. 8.6).

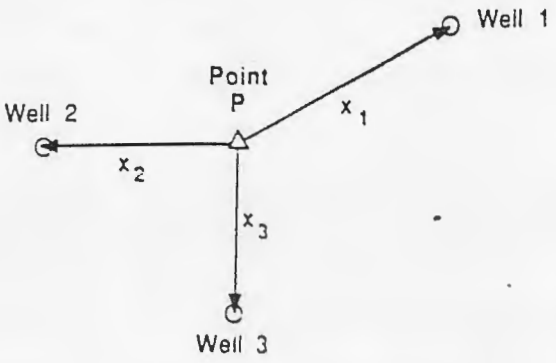

FIGURE 8.4
Multiple wells—notation.

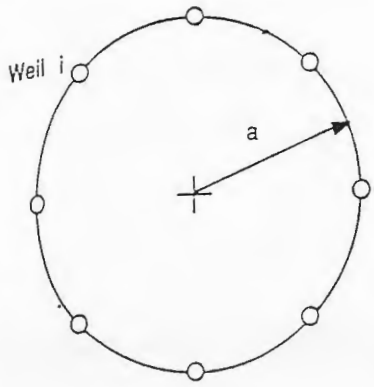

FIGURE 8.5
Circular arrangement of wells.

8.6 IMPERFECT WELLS AND OTHER CASES

Partially penetrating (imperfect) wells occur more often in practice than fully penetrating wells. According to Schröder (1966) practical rules suggest that the discharge quantity Q calculated for a perfect well is to be increased by 10 to 30% for $t = 0$ to $t > 2h$, respectively (Fig. 8.7). When the discharge from imperfect wells is estimated, the fact that vertical permeability of natural deposits is often more than 10 times smaller than horizontal permeability should also be considered. Soil layers below the well tip may therefore only contribute relatively little water. Another factor which may reduce the inflow of water from below a well is the fact that well points and sumps often only allow side entry, rather than side and bottom entry of water.

Artesian wells (Fig. 8.8) and slots have been analyzed for perfect and imperfect conditions by Kozeny, Muskat, and others, as quoted by Mansur and Kaufmann in Leonards (1962). Further references are given by Schröder (1966).

An approximate evaluation of the discharge from vacuum wells was developed by Széchy (1959).

In dewatering projects encountering inhomogeneous, nonisotropic soil deposits with uncertain recharge patterns, and where irregularly shaped excavations are needed, there is still a considerable amount of engineering judgment required in order to design

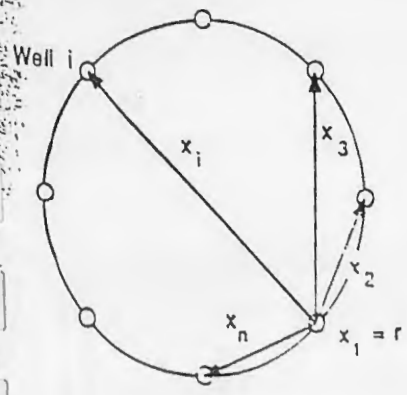

FIGURE 8.6
Water level in individual well—notation.

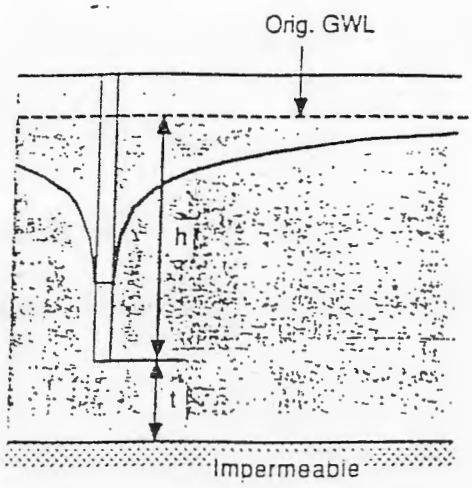

FIGURE 8.7
Partially penetrating well.

a satisfactory and economical well system, unless an extensive field testing program is undertaken.

Discharge formulas for the most common arrangements of slots and wells with gravity flow are given in Apps. 8A, 8B, and 8C for slots, single wells, and multiple wells, respectively.

8.7 DEVELOPMENT OF DRAWDOWN WITH TIME

In most dewatering projects, the major design decisions, such as the determination of the number of wells and the pump capacity required, can be made assuming a steady-state flow condition and using a constant influence range L as estimated by Sichardt's

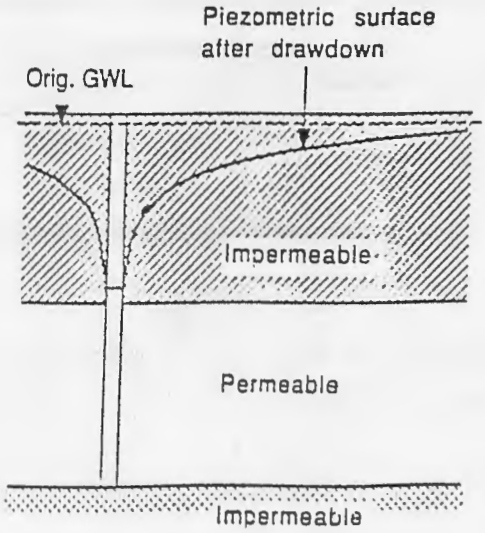

FIGURE 8.8
Artesian well

empirical formula. However, if the construction schedule is tight and relatively slow draining soils are involved, it may be important to assess how long the pumps have to be operated before it is safe to commence excavating. Extra pump capacity may be required for the initial period of dewatering. The Theis formula, particularly as modified by Jacobs, provides a practical solution to this problem.

8.7.1 Theis Formula

Theis (1935) developed a nonequilibrium well formula for gravity flow to a single well, making the following assumptions:

- *"Perfect" well conditions exist.* The well fully penetrates a homogeneous, isotropic horizontal aquifer overlying an impermeable stratum.
- *The Dupuit-Thiem approximation holds.* The hydraulic gradient below any point of the drawdown curve is assumed to be equal to the slope of the drawdown curve at that point.
- *There is no recharge of the aquifer*
- *Water flows out of the pores of the soil as quickly as the drawdown of the phreatic surface occurs.*
- *The drawdown* s *is small relative to the aquifer thickness* h *so that* h − s *is approximately equal to* h. This is equivalent to assuming an artesian aquifer of thickness $h = m$.

The derivation starts with equating the water flow through a cylindrical area around the well at a distance x to the volume of water removed from the soil beyond x due to lowering of the phreatic surface (Fig. 8.9). The formula is usually written as

$$s = \frac{Q}{4\pi km} W(u) \tag{8.12}$$

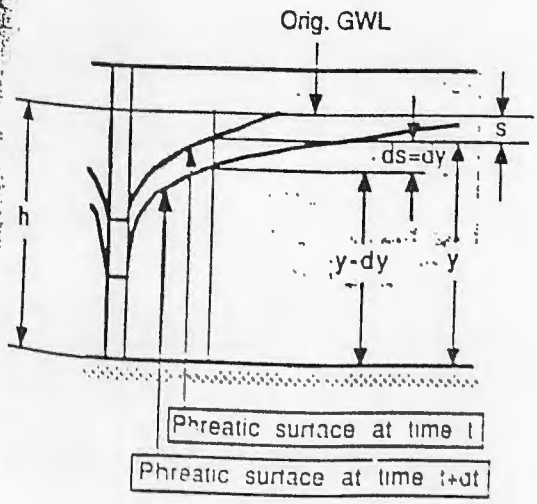

FIGURE 8.9
Lowering of phreatic surface with time.

The function $W(u)$ is the so-called well function, defined by

$$W(u) = -0.5772 - \ln u + u - \frac{u^2}{2 \times 2!} + \frac{u^3}{3 \times 3!} - \frac{u^4}{4 \times 4!} \pm \cdots \tag{8.13}$$

The variable u is given by

$$u = \frac{x^2 S}{4tkm}$$

The product of the coefficient of permeability k (also called the hydraulic conductivity) and the thickness of the aquifer m is referred to as the *transmissivity* of the aquifer. The term S represents the storage coefficient (or storativity, specific yield) of the water-bearing layer (see Sec. 7.3.3). For an unconfined aquifer it is equal to the ratio of the volume of drainable water over the total volume of the soil. Numerically the storativity must be equal to or less than the soil porosity, which, in soil mechanics, is designated with the letter n and defined as the volume of voids to the total volume of an element of soil. For confined aquifers, which remain saturated during pumping, S may be as low as 10^{-5}; for unconfined aquifers, it ranges from 0.01 to 0.3.

The function $W(u)$ is tabulated in most handbooks on hydrology and groundwater, e.g., in the book *Groundwater and Wells* [Driscoll (1986, 2d ed.)].

Figure 8.10*a* gives a numerical example of the drawdown developed at various distances from the well with time. If plotted on semilog paper, the drawdown curves plot as straight lines (Fig. 8.10*b*), except perhaps very close to their well or at distances approaching the influence range. A similar picture is obtained if the drawdown at specific locations is plotted versus log (time) (Fig. 8.11).

8.7.2 Modification by Jacob (1940)

If pumping time t is sufficiently large, the value u is small. For $u < 0.05$ the well function may be approximated by

$$\begin{aligned} W(u) &= -0.577 - \ln u \\ &= \ln \frac{2.25}{4u} \\ &= \ln \frac{2.25kmt}{x^2 S} \end{aligned} \tag{8.14}$$

The drawdown as a function of time then becomes

$$s = \frac{Q}{4\pi km} \ln \frac{2.25kmt}{x^2 S} \tag{8.15}$$

This function plots as a straight line on a semilog scale taking either time t or distance x as a variable as a function of time. Figure 8.12 compares the result determined according to the Theis formula with Jacob's approximation.

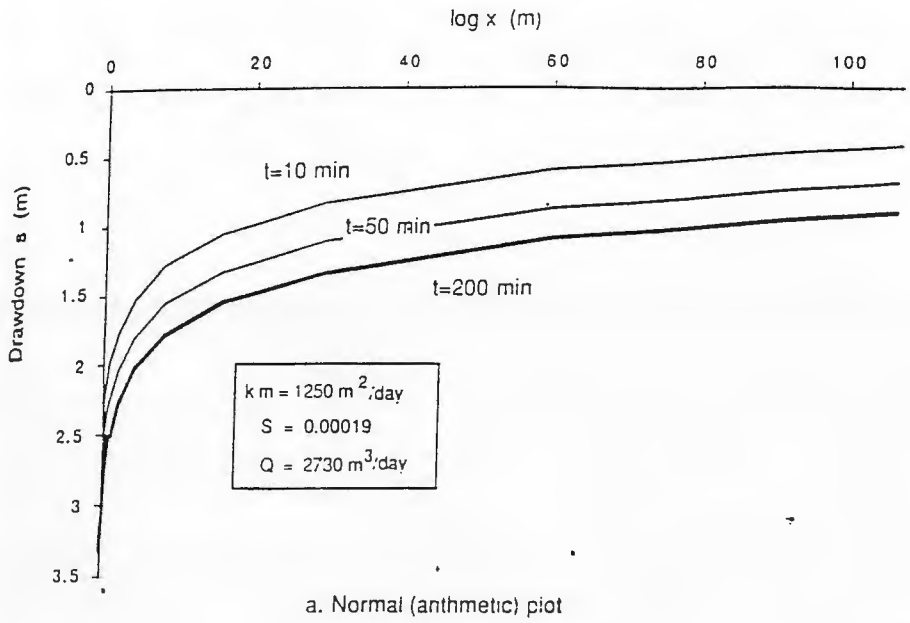

a. Normal (anthmetic) plot

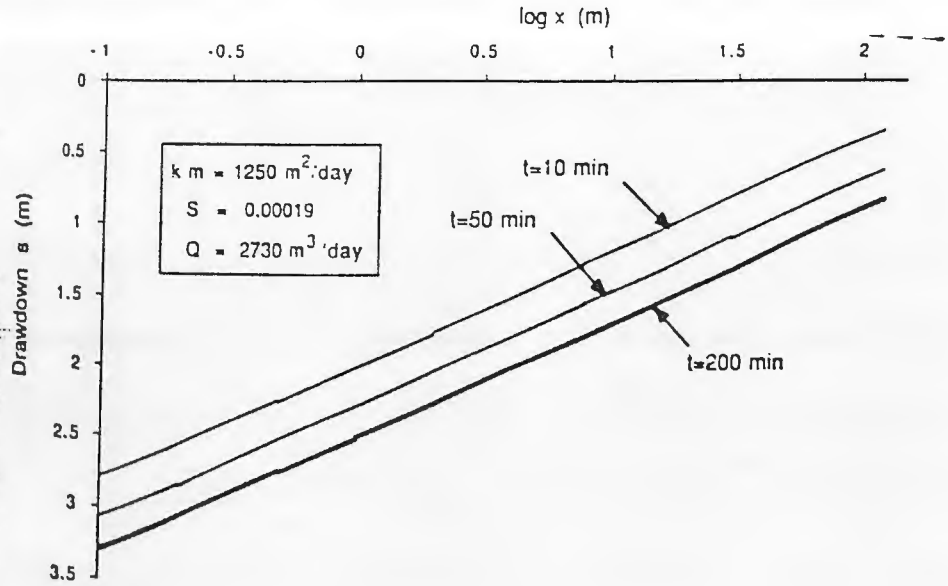

b. Log-normal plot

FIGURE 8.10
Drawdown at various time intervals.

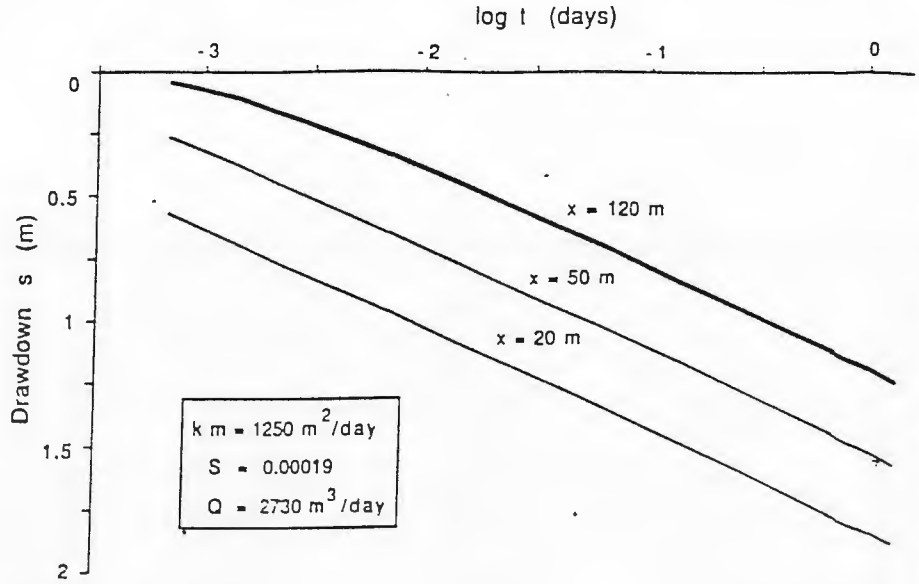

FIGURE 8.11
Drawdown at specific locations.

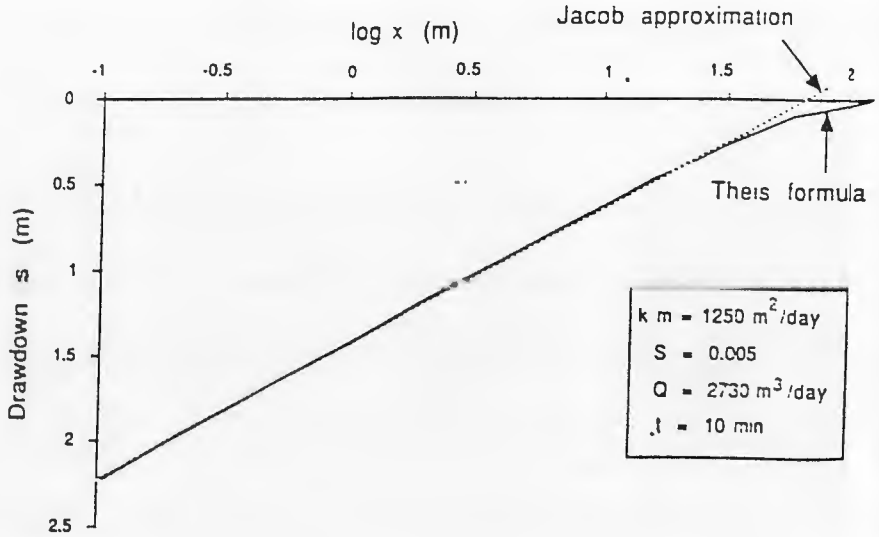

FIGURE 8.12
Drawdown according to the Theis formula and Jacob's approximation.

8.7.3 Extension to Unconfined Flow

To extend Jacob's formula from artesian to unconfined flow, we set $m = h$ and make use of the analogy

$$\underset{\text{artesian}}{2ms} = \underset{\text{unconfined}}{h^2 - y^2} \qquad (8.10)$$

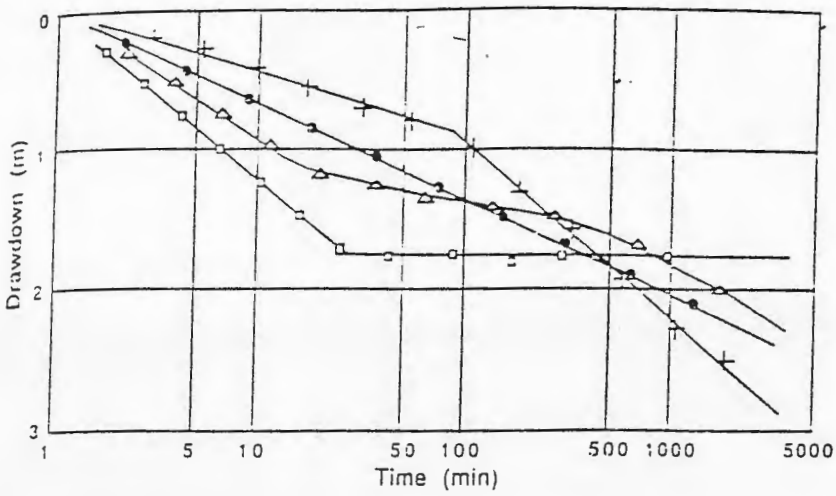

- • Ideal curve
- ▫ Recharge of aquifer occurs within influence range
- + Impervious boundary encountered
- △ Transient influence evident (other wells, tides, fluctuating recharge)

FIGURE 8.13
Time-drawdown curves encountered in the field.

which holds for fully penetrating wells. We then find

$$s = \frac{h^2 - y^2}{2h} \tag{8.17}$$

and

$$\frac{h^2 - y^2}{2h} = \frac{Q}{4\pi kh} \ln \frac{2.25kht}{x^2 S} \tag{8.18}$$

8.7.4 Interpretation of Time-Drawdown Measurements

As discussed at the beginning of Sec. 8.7.1, Theis had to make a number of simplifying assumptions in order to arrive at a time-drawdown relationship. It would be rare that all these assumptions are met fully in natural geologic and hydrologic conditions. Driscoll (1986) as well as Powers and Burnett (1986) give good discussions of the effect of nonideal conditions on the results of field pumping tests. Figure 8.13 illustrates some of these cases.

8.7.4.1 DETERMINATION OF PERMEABILITY. Equation (8.15) can be used to determine the permeability k (or transmissivity $= km$) of an aquifer from time-drawdown measurements in a single observation hole, if the plot is a straight line on semilog paper, as is theoretically expected for ideal conditions. If s_1 and s_2 are the drawdowns observed at times t_1 and t_2, we can write

$$s_2 - s_1 = \frac{Q}{4\pi km} \ln \frac{t_2}{t_1} \tag{8.19}$$

and

$$km = \frac{Q}{4\pi(s_2 - s_1)} \ln \frac{t_2}{t_1} \tag{8.20}$$

8.7.4.2 DETERMINATION OF STORATIVITY. If the time-drawdown line on the semilog plot is extended to zero drawdown, the corresponding time t_0 easily yields the storativity S. If $s = 0$, it follows that the value of the argument of ln in Eq. (8.15) must be equal to 1:

$$1 = \ln \frac{2.25kmt_0}{x^2S} \tag{8.21}$$

or

$$S = \frac{2.25\ kmt_0}{x^2} \tag{8.22}$$

8.7.4.3 INTERPRETATION OF THE INFLUENCE RANGE. A value for the influence range can be calculated from Jacob's approximation by setting $s = 0$ and solving for x. We then obtain

$$L = \sqrt{\frac{2.25kmt}{S}} = 1.5\sqrt{\frac{kmt}{S}} \tag{8.23}$$

This is the same expression Kozeny (1953) gives when referring to work published in the 1930s.

Sichardt's empirical estimate of the influence range L can therefore be viewed as being associated with the development of drawdown of an unrecharged aquifer at a particular point in time. Since most natural aquifers are recharged, either underground or through rainfall, Sichardt's formula still proves to be a useful approximation.

PROBLEMS

Prefixes indicate problem type: C = calculations, M = multiple choice, B = brief answer.

Calculations

C8.1. Determine the discharge quantity q for a 100-m-long slot assuming "perfect" conditions and a free discharge height according to Chapman. The following data is given:

$$k = 2 \times 10^{-6}\ \text{m/s}$$

$$h = 4\ \text{m}$$

$$h_0 = 0.4\ \text{m}$$

C8.2. Wells are located at the corner of a square of width 8 m. The aquifer is 12 m thick. The water level in the center has to be lowered by 4 m. Determine the pump rate required. The coefficient of permeability is 0.003 m/s, and the well radius is 0.3 m. Assume h_0 equals 7.6 m for the estimate of the influence range.

C8.3. Two wells are 22.5 m apart. From each well, 25 L/s are pumped. The water level in the wells is 8.87 m above the base of the aquifer, which is 15 m thick. The well radius is 0.3 m. Estimate the permeability of the soil. Use Sichardt's formula to estimate the influence range, assuming an initial value of k = 0.0005 m/s. Iterate to find a more accurate value.

C8.4. Three wells are equidistant from each other. For the following data calculate the water level in the center of the triangle and in a well:

$$h = 15 \text{ m}$$

$$\text{Distance between wells} = 19.5 \text{ m}$$

$$r = 0.2 \text{ m}$$

$$Q = 47 \text{ L/s}$$

$$k = 0.0005 \text{ m/s}$$

C8.5. Two wells are spaced 10 m apart in an unconfined aquifer with a thickness of 5 m. The radius of the wells is 0.2 m, and the coefficient of permeability is 0.0004 m/s. If each well yields 0.5 L/s after steady-state conditions are reached, what is the drawdown at a point 4 m away from one well and 6 m away from the other well?

C8.6. Water is pumped from a 20-m-thick confined aquifer at a rate of 2000 m^3/day from a single well. In an observation hole at a distance of 70 m from the well, the drawdown after 10 min of pumping was 0.66 m; after 1000 min, it was 1.92 m. Calculate the coefficient of permeability (m/day) and the storativity.

C8.7. A circular excavation (diameter = 60 m) is to be made in an unconfined aquifer which is 12 m thick and underlain by an impermeable layer. The total amount of water pumped is 0.2 m^3/s. The soil has a permeability of 10^{-4} m/s, and the porosity is 0.3. Determine the time required to draw down the level at the center of the excavation by 3 m. Use the Jacob formula.

Multiple Choice

M8.8. Discharge quantities from wells are directly proportional to the
- (a) Diameter of the well.
- (b) Permeability of the soil.
- (c) Soil grain size.
- (d) Pump capacity.

M8.9. The Dupuit-Thiem approximation
- (a) Is used in the derivation of a simple formula for the estimation of the influence range.
- (b) Says that the gradient of the water flowing toward the well is the same at equal distances from the well regardless of the depth.
- (c) Is used to derive Darcy's law.
- (d) Allows us to estimate the free discharge height.

M8.10. With respect to the level at which the phreatic surface intersects the well perimeter, the water level in the well itself is
(*a*) Always higher.
(*b*) Exactly the same regardless of pumping rate and soil type.
(*c*) About the same or lower.
(*d*) Higher or lower depending on soil type.

M8.11. According to Sichardt, the influence range is *not* related to the
(*a*) Drawdown in the well.
(*b*) Configuration of wells.
(*c*) Soil permeability.
(*d*) Well radius.

M8.12. Kozeny's formula for the influence range L is
(*a*) $\sqrt{hk}/n$.
(*b*) $h5\sqrt{kt}/n$.
(*c*) $1.5\sqrt{hkt}/n$.
(*d*) $mr^2/2$.

M8.13. In dewatering projects, the number of wells and the pump capacity required is estimated by assuming that
(*a*) Soil behaves as water.
(*b*) Steady flow conditions exist.
(*c*) Nonsteady flow conditions exist.
(*d*) There is no recharge of the aquifer.

M8.14. For natural sedimentary soil deposits we often find that vertical and horizontal permeabilities compare as follows:
(*a*) $k_v > 10k_h$.
(*b*) $k_h > 10k_v$.
(*c*) $k_v = k_h$.
(*d*) $k_v > 100\ k_h$.

M8.15. The equation most frequently used to assess drawdown with time for gravity flow toward a well
(*a*) Was proposed by Sichardt.
(*b*) Was proposed by Forchheimer.
(*c*) Makes use of the well function.
(*d*) Assumes the aquifer is continuously recharged.

M8.16. Theis developed a formula for gravity flow to a single well for
(*a*) Nonequilibrium conditions.
(*b*) Equilibrium conditions.
(*c*) Nonisotropic soil.
(*d*) Continuous recharge conditions.

Brief Answer

B8.17. Figure P8.1 shows a perfect well with gravity flow. Name the items that are labeled a, b, c, and d.

a = _____
b = _____
c = _____
d = _____

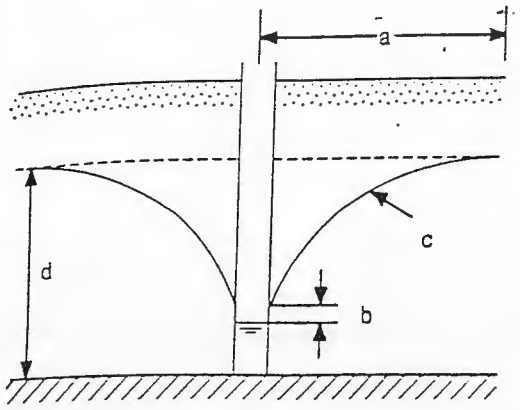

FIGURE P.8.1

B8.18. In the derivation of the equation of the drawdown curve for a slot or well, we make an approximation first proposed by Dupuit and Thiem. This means we assume _____ .

B8.19. Deriving a discharge formula for a "perfect" well or slot means we assume that four ideal or simplified conditions hold. List them.

(a) _____

(b) _____

(c) _____

(d) _____

B8.20. The designations h_s, h_w, and h_0 refer to water levels in and around the borehole. Define these terms and their interrelationship:

(a) h_s is the _____ .

(b) h_w is the _____ .

(c) h_0 is the _____ .

(d) h_s = _____ .

B8.21. Identify the following formulas which are associated with the names of Darcy, Sichardt, Forchheimer, and Kozeny.

$$Q = \frac{\pi k(h^2 - y^2)}{\ln L - (1/n) \ln x_1 x_2 \cdots x_n}$$ _____

$$Q = kiA$$ _____

$$Q = \frac{2\pi r h_0 \sqrt{k}}{15}$$ _____

$$Q = \frac{1.5\sqrt{hkt}}{n}$$ _____

B8.22. Theis developed a formula for the development of drawdown with time. List two of the simplifying assumptions he made.

(a) _____

(b) _____

APPENDIX 8A

DRAINAGE SLOT FORMULAS

8A1 FULLY PENETRATING ("PERFECT") SLOTS

8A1.1 Unconfined Gravity Flow

For designations see Fig. A8.1.

The variable q = flow per unit length of slot.

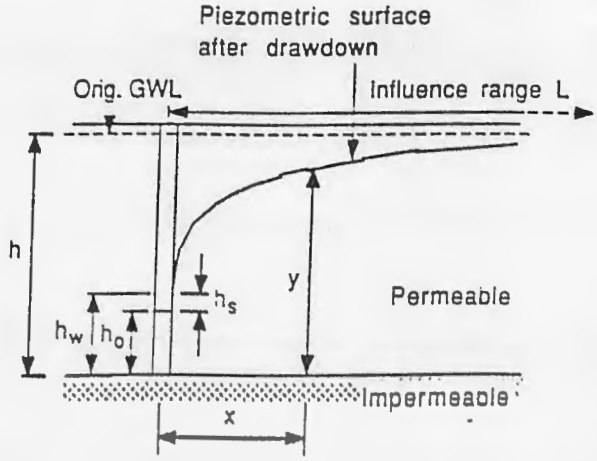

FIGURE A8.1

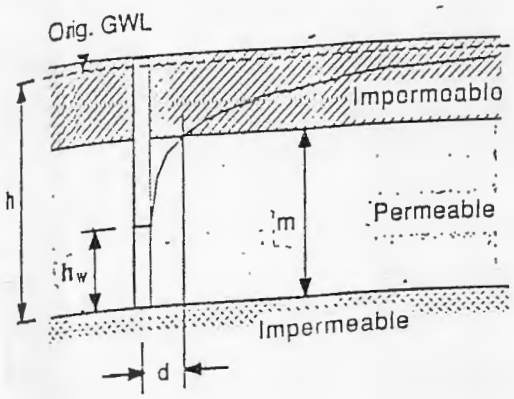

FIGURE A8.2

$$q = \frac{(h^2 - h_w^2)k}{2L} \tag{A8.1}$$

$$h^2 - y^2 = \frac{L - x}{L}(h^2 - h_w^2) \tag{A8.2}$$

The free discharge height h_s may be estimated according to Chapman (1957) from data given in Fig. 8.3.

8A1.2 Artesian Flow

For designations see Fig. A8.2.

For full artesian flow ($d = 0$, or $h_w \geq m$):

$$q = \frac{(h - h_w)km}{L} \tag{A8.3}$$

$$h - y = \frac{q(L - x)}{km} \tag{A8.4}$$

For partial artesian flow ($h_w < m$):

$$q = \frac{k[2m(h - m) + m^2 - h_w^2]}{2L} \tag{A8.5}$$

$$d = \frac{L(m^2 - h_w^2)}{2m(h - m) + m^2 - h_w^2} \tag{A8.6}$$

8A2 PARTIALLY PENETRATING SLOTS

8A2.1 Unconfined Flow, Single Slot

See Fig. A8.3.

$$q = \left[0.73 + \frac{0.27(T - t_0)}{T}\right]\frac{k}{2L}(T^2 - t_0^2) \tag{A8.7}$$

provided $L, T > 3$ [after Chapman (1957), as quoted in Leonards (1962)].

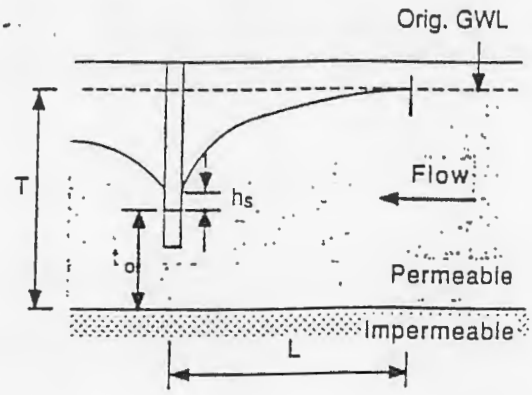

FIGURE A8.3

8A2.2 Unconfined Flow, Double Slot

See Fig. A8.4.

Residual head

$$t_d = t_0 \left[\frac{C_1 C_2}{L} (T - t_0) + 1 \right] \tag{A8.8}$$

$$(C_1 C_2)_{max} \approx 1.48$$

Factors C_1 and C_2 are from Figs. A8.5 and A8.6.

8A2.3 Artesian Flow, Single Line Source

See Fig. A8.7.

$$q = \frac{km(T - t_0)}{L + e} \tag{A8.9}$$

$$t_d = \frac{e(T - t_0)}{L + e} + t_0 \tag{A8.10}$$

Given L, m, and m_1, the distance e can be calculated from data presented in Fig. A8.8 [after Barron, as quoted by Mansur and Kaufman in Leonards (1962)].

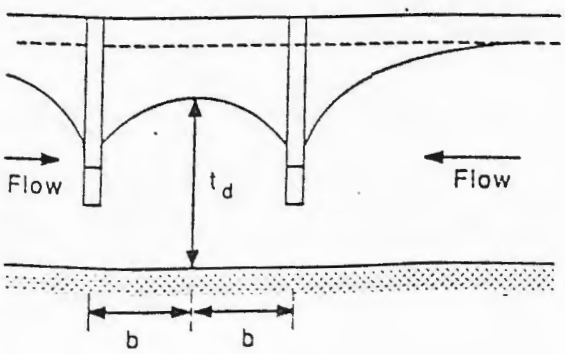

FIGURE A8.4

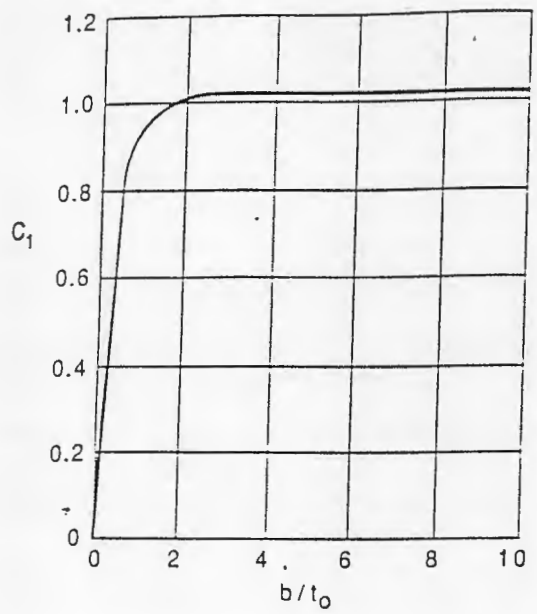

FIGURE A8.5
[*After Chapman, (1956).*]

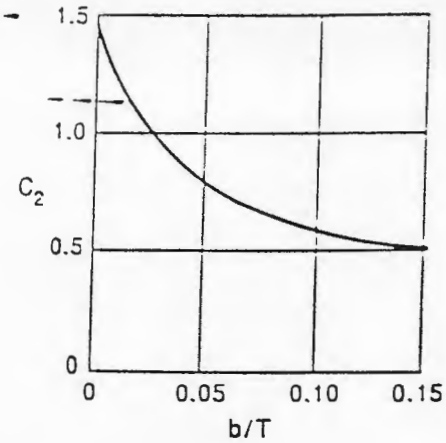

FIGURE A8.6
[*After Chapman, (1956).*]

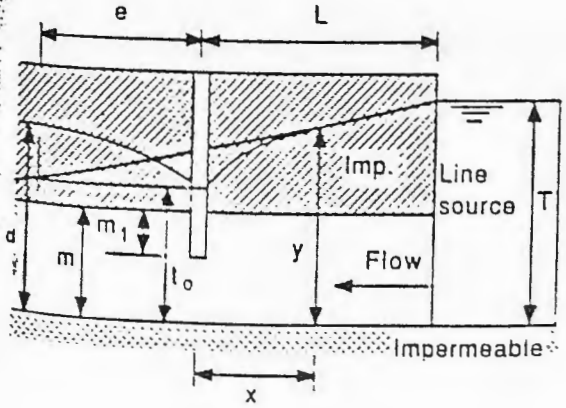

FIGURE A8.7

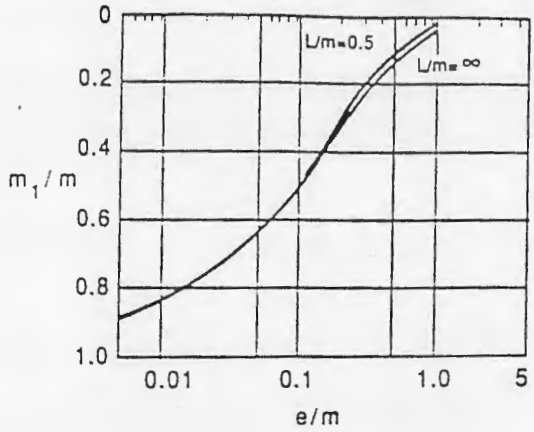

FIGURE A8.8
[After Barron, as quoted by Mansur and Kaufman in Leonards (1962).]

8A2.4 Artesian Flow, Double Line Source

Total flow

$$q_t = \frac{2km(T - t_0)}{L + \lambda m} \tag{A8.11}$$

$$y = t_0 + (T - t_0)\frac{x + \lambda m}{L + \lambda m} \tag{A8.12}$$

The factor λ is obtained from Fig. A8.9.

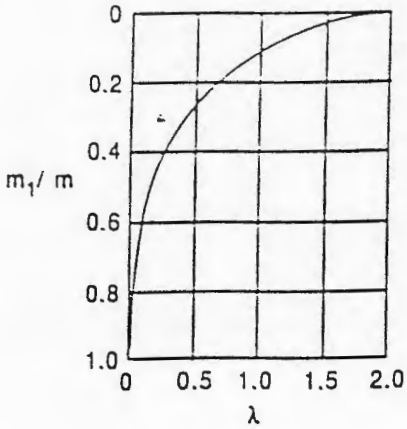

FIGURE A8.9

APPENDIX 8B

SINGLE-WELL FORMULAS

8B1 SINGLE WELL, CIRCULAR SOURCE

8B1.1 Fully Penetrating Wells

8B1.1.1 PERFECT WELL (UNCONFINED GRAVITY FLOW). For designations see Fig. B8.1.

$$Q = \frac{\pi k(h^2 - h_w^2)}{\ln (L/r)} \tag{B8.1}$$

$$y^2 - h_w^2 = \frac{Q}{\pi k} \ln (x/r) \tag{B8.2}$$

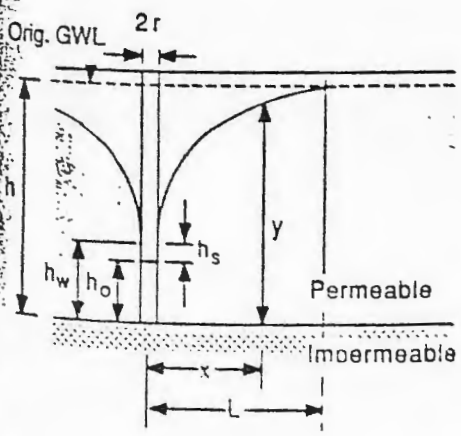

FIGURE B8.1

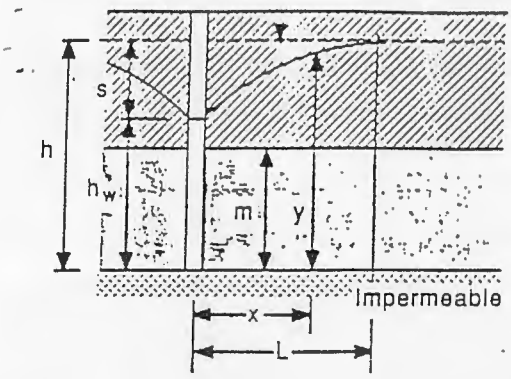

FIGURE B8.2

Note: A wide variety of formulas has been proposed for estimating the free discharge height h_s. The following expressions were presented by Herth and Arndts (1973):

$$h_s = \begin{cases} 0.5(h - h_0) & \text{(Boulton)} \quad \text{(B8.3)} \\ \dfrac{(h - h_0)^2}{2h} & \text{(Ehrenberger)} \quad \text{(B8.4)} \\ (h - h_0)\, e^{(-\alpha/\pi)} & \text{(Juhász)} \quad \text{(B8.5)} \end{cases}$$

where $\alpha = \dfrac{\sqrt{k}}{15} \dfrac{2r\pi h_0}{Q}$.

8B1.1.2 ARTESIAN WELL. See Fig. B8.2.

$$Q = \frac{2\pi kms}{\ln (L/r)} \quad \text{(B8.6)}$$

$$y - h_w = \frac{Q}{2\pi km} \ln (x/r) \quad \text{(B8.7)}$$

8B1.2 Partially Penetrating Wells

8B1.2.1 UNCONFINED GRAVITY FLOW. See Fig. B8.3.

$$Q = \frac{\pi k[T^2 - (h_w + t)^2]\alpha}{\ln (L/r)} \quad \text{(B8.8)}$$

where

$$\alpha = \sqrt{\frac{h}{T}} \sqrt{\frac{2T - h}{T}} \quad \text{(B8.9)}$$

Or, after Breitenöder [as quoted by Herth and Arndts (1973)]:

$$Q = \frac{\pi k(h^2 - h_w^2)}{\ln (L/r)} \epsilon \quad \text{(B8.10)}$$

where ϵ is obtained from Fig. B8.4.

8B.1.2.2 ARTESIAN FLOW. See Fig. B8.5.

$$Q = \frac{2\pi k(T - t_0)}{\ln (L/r)} \mu \quad \text{(B8.11)}$$

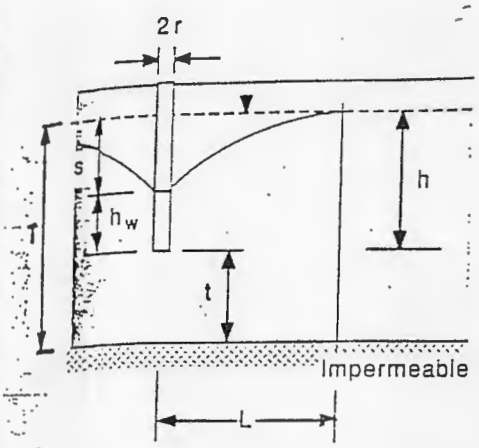

FIGURE B8.3

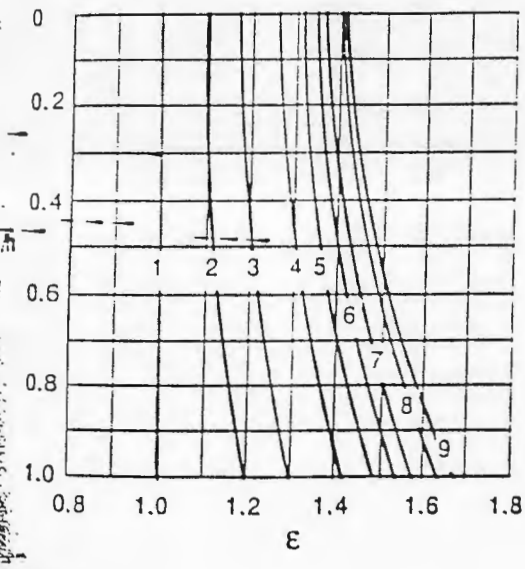

Curve no.	h/T
1	1.0
2	0.95
3	0.9
4	0.8
5	0.7
6	0.6
7	0.5
8	0.25
9	0

FIGURE B8.4

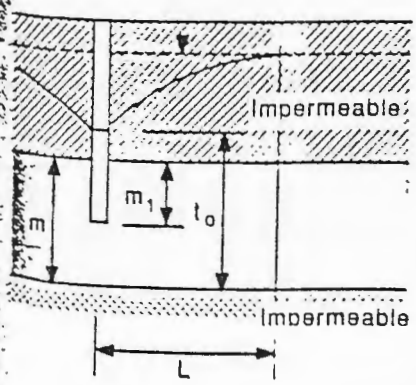

FIGURE B8.5

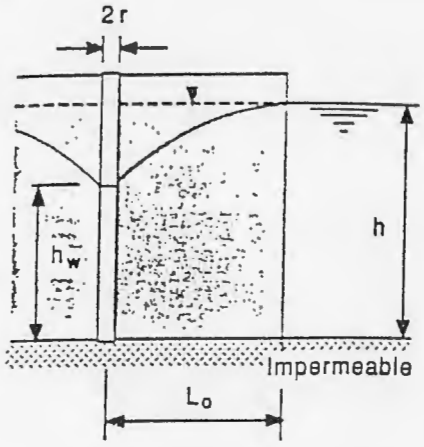

FIGURE B8.6

where $\mu = 1 + 7 \sqrt{\frac{r}{2m}} \sqrt{\frac{m}{m_1}} \cos \frac{\pi m_1}{2m}$.

8B2 SINGLE WELL, LINE SOURCE

8B2.1 Unconfined Gravity Flow

For designations see Fig. B8.6.

$$Q = \frac{\pi k(h^2 - h_w^2)}{\ln (2L_0/r)} \tag{B8.12}$$

Note: This formula was derived using the method of image wells. If $2L_0 > L$, use $2L_0 = L$.

8B2.2 Artesian Flow

See Fig. B8.7.

$$Q = \frac{2\pi kms}{\ln (2L_0/r)} \tag{B8.13}$$

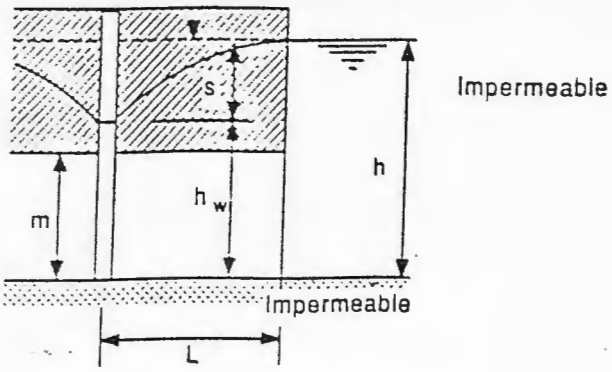

FIGURE B8.7

APPENDIX 8C

MULTIPLE-WELL FORMULAS (UNCONFINED GRAVITY FLOW)

8C1 MULTIPLE WELLS. CIRCULAR SOURCE

8C1.1 General Case

For designations see Fig. C8.1.

For well (i) only:

$$h^2 - y_i^2 = \frac{Q_i}{\pi k} \ln \frac{L}{x_i} \qquad \text{(C8.1)}$$

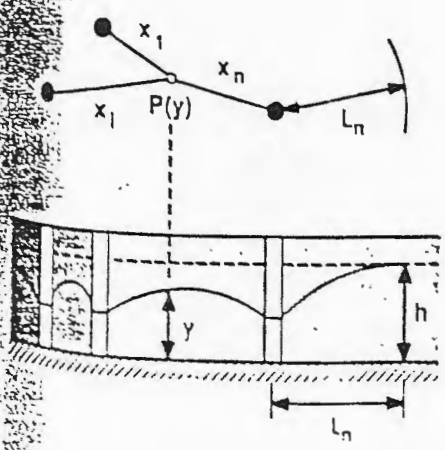

FIGURE C8.1

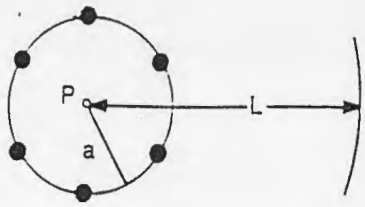

FIGURE C8.2

For n wells:

$$h^2 - y^2 = \sum_{i=1}^{n} \frac{Q_i}{k} \ln \frac{L_i}{x_i} \tag{C8.2}$$

$$Q = \sum_{i=1}^{n} Q_i \tag{C8.3}$$

Note: For artesian flow formula, replace $h^2 - y^2$ by $2ms$ as for single-well cases.

8C1.2 Circular Arrangement of Wells

See Fig. C8.2.

For n wells at distance a from point P:

$$h^2 - y^2 = \frac{Q}{\pi k} \ln \frac{L}{a} \tag{C8.4}$$

8C1.3 Rectangular Arrangement of Wells

See Fig. C8.3.

For preliminary design, replace the rectangular area by the equivalent circular-area with radius a calculated as follows:

$$a = \sqrt{\frac{wl}{\pi}} \tag{C8.5}$$

8C2 MULTIPLE WELLS, LINE SOURCE

8C2.1 General Case

For designations see Fig. C8.4.

For well (i) only:

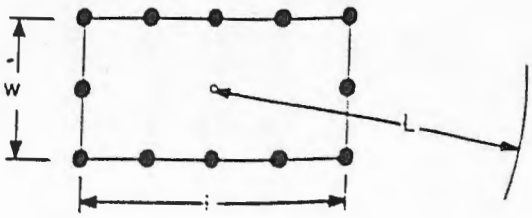

FIGURE C8.3

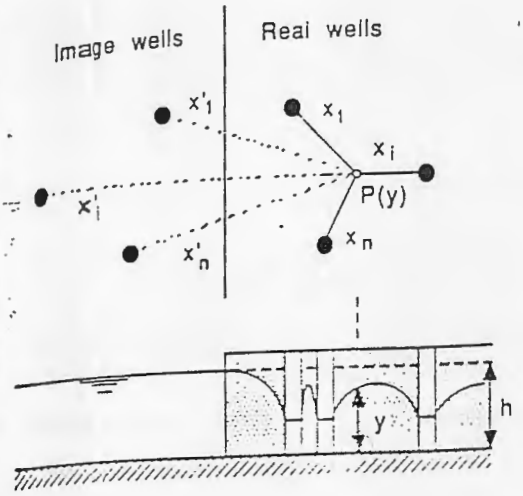

FIGURE C8.4

$$h^2 - y_i^2 = \frac{Q_i}{\pi k} \ln \frac{x_i'}{x_i} \tag{C8.6}$$

For n wells:

$$h^2 - y^2 = \sum_{i=1}^{n} \frac{Q_i}{k} \ln x_i'/x_i \tag{C8.7}$$

If $x_i' > L$, use $x_i = L$.

CHAPTER

9

DESIGN OF DEWATERING SYSTEMS (EXCAVATIONS AND SLOPES)

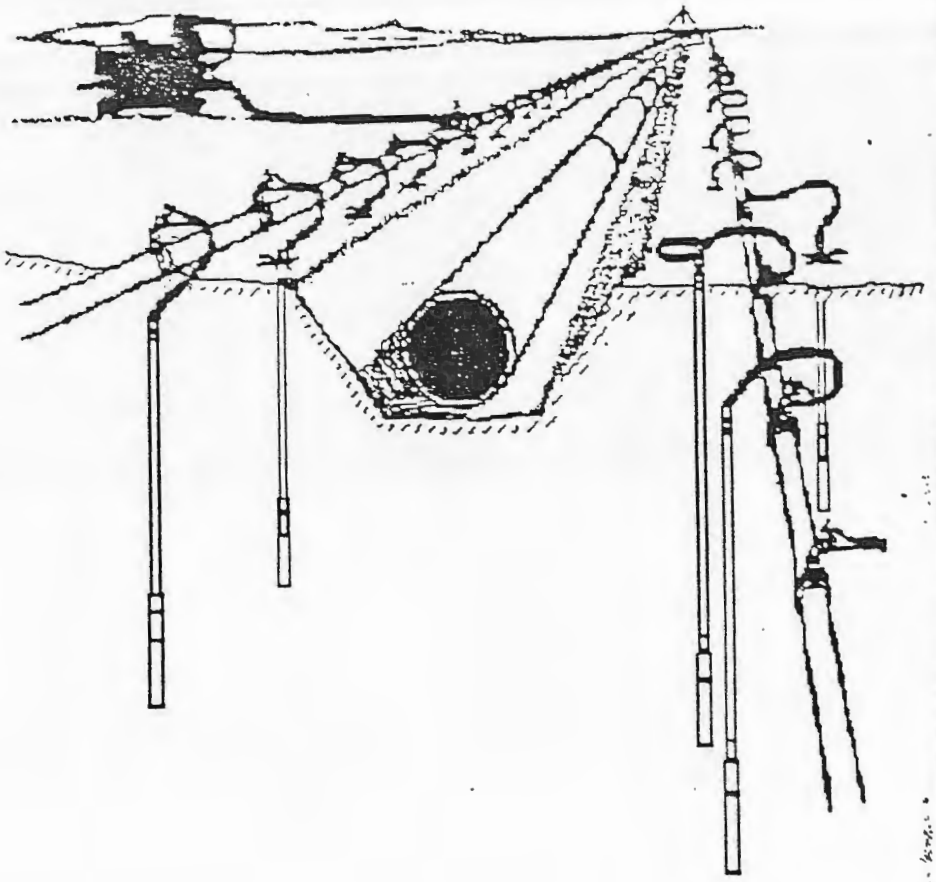

9.1 GROUND AND WELL DETERMINANTS

9.1.1 Determination of Ground Permeability

The discharge quantity from a well or slot is directly proportional to the coefficient of permeability k. For sands and gravels, the soils most suitable for dewatering by wells and open drainage systems, k may vary from 0.0001 to 0.01 m/s. A reliable estimate of k is therefore of great importance in the planning of well systems and in the prediction of the required pump capacity.

The soil properties which significantly affect the permeability are [Lambe and Whitman (1969)]:

1. Particle size
2. Void ratio
3. Mineral composition
4. Fabric (soil structure)
5. Degree of saturation

For a cohesionless soil, the void ratio is likely to be the most important determinant of its permeability; mineral composition and the fabric component of the soil structure are more important for fine-grained soils than for sands and gravels.

Because it is very difficult to obtain representative undisturbed samples of cohesionless soils, standard laboratory constant or falling-head tests may not give permeability coefficients which are sufficiently reliable for design purposes. For this reason and because of the variability of natural soil deposits, field tests are highly recommended. However, if only a disturbed sample of soil is available, recourse may be taken to an empirical relationship between grain size distribution and permeability.

9.1.1.1 ESTIMATING k FROM PARTICLE SIZE. Many textbooks quote a formula attributed to Hazen (1892) who experimented with filter sands:

$$k = 100D_{10}^2 \quad \text{cm/s} \tag{9.1}$$

where D_{10} is the diameter in centimeters corresponding to 10% passing, as read from a grain-size-distribution curve determined from a sieve analysis.

More generally the formula is written as

$$k = CD_{10}^2 \quad \text{cm/s} \tag{9.2}$$

The constant C has been found to vary with the uniformity coefficient C_u. According to Beyer [as quoted by Schröder (1966)], C is related to C_u as follows:

$C_u = D_{60}/D_{10}$	C
1–1.9	110
2–2.9	100
3–4.9	90
5–9.9	80
10–19.9	70
> 20	60

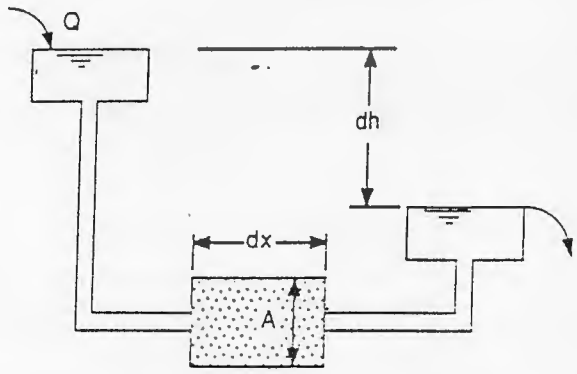

FIGURE 9.1
Constant head test.

Powers and Burnett (1986) [also see Powers (1981)] have published charts originally produced by Prugh (1959) which give the permeability as a function of D_{50} and the uniformity coefficient for either a loose, medium, or dense state of the granular soil. These correlations are said to be reliable, provided the samples tested are representative and there is no excessive stratification present.

9.1.1.2 LABORATORY PERMEABILITY TESTS. In the constant head test (Fig. 9.1) water flows from an upper reservoir through a cylindrical soil sample of length dx and cross-sectional area A to a lower reservoir. For a given difference dh in water level between the constant head reservoirs, the flow of water Q is measured. The coefficient of permeability k is calculated directly from Darcy's law [Eq. (7.9)]:

$$k = \frac{Q}{A}\frac{dx}{dh} \tag{9.3}$$

In the falling head test (Fig. 9.2) water drains from a standpipe through the soil specimen into a constant-level reservoir. At time t_1 the head of water in the standpipe

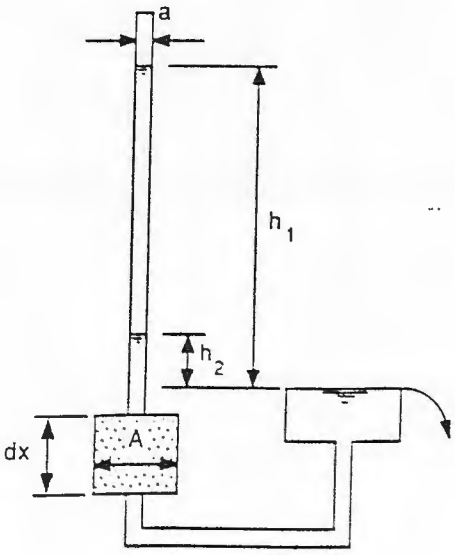

FIGURE 9.2
Falling head test.

is observed as h_1; at time t_2 it has fallen to h_2. If the cross-sectional area of the standpipe is a and that of the dx-long specimen is A, the coefficient of permeability is found to be

$$k = \frac{a\,dx}{A(t_2 - t_1)} \ln \frac{h_1}{h_2} \tag{9.4}$$

It is important to keep an account of density and saturation of the specimens tested.

9.1.1.3 FIELD PERMEABILITY TESTS. Although it seems most desirable to determine k in situ, the interpretation of field test results is not always easy because of soil disturbance, clogging of screens and filters, anisotropic conditions, and other difficulties.

Pumping test with observation holes. The most reliable field test requires the installation of a full-size pumping well plus at least two additional boreholes where the piezometric level can be observed. For steady-state conditions, the equation of the drawdown curve [Eq. (8.4)] is written in terms of the water levels y_1 and y_2 in the observation holes which are at distances x_1 and x_2 from the well. For unconfined flow the coefficient of permeability can then be calculated from

$$k = \frac{Q \ln (x_2/x_1)}{\pi(y_2^2 - y_1^2)} \tag{9.5}$$

For a confined (artesian) aquifer of thickness m the expression for k is

$$k = \frac{Q \ln (x_2/x_1)}{2\pi m(h_2 - h_1)} \tag{9.6}$$

The determination of k from measurements of the development of drawdown with time at a steady pump rate was discussed in Sec. 8.7.4.

Single-borehole tests. Formulas for single-borehole tests for a variety of geometric, soil, and water level configurations can be found in the "Design Manual" (U.S. Navy, 1962) and in Lambe and Whitman (1969) referring to Hvorslev (1949). These tests are either carried out by observing the equilibrium water level in the well for a specific pumping rate (in or out) or by recording the change in water level in the well with time after pumping has ceased (rising or falling head test).

9.1.2 Filter Criteria and Design of Well Screens.

In open drainage situations (Fig. 7.2) it is desirable that water does not exit on the slopes, in order to prevent slumping. This may be achieved by constructing a sloping filter as shown in Fig. 9.3. Cedergren (1960) provides design charts that give the desired k(filter)/k(soil) ratio as a function of the slope S and the geometry of the filter zone.

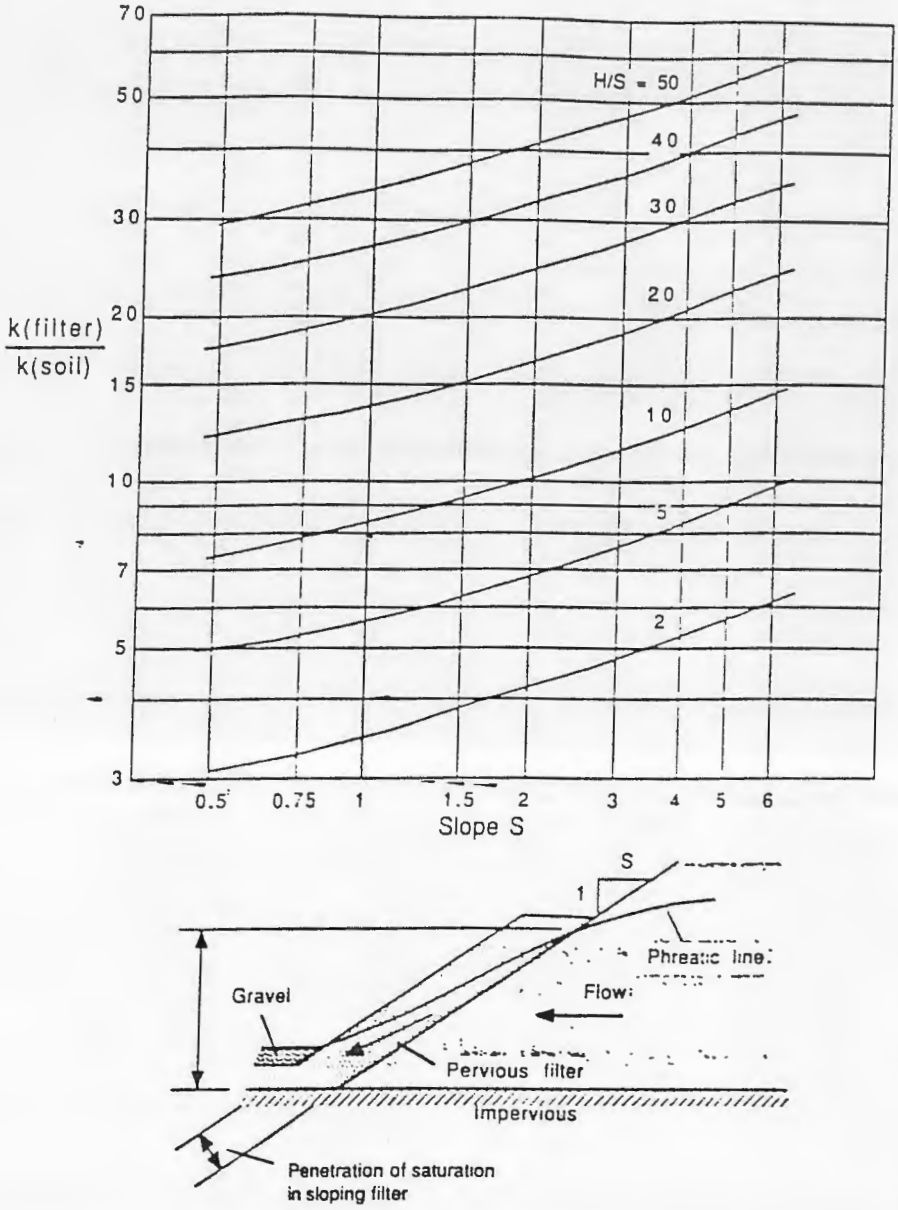

FIGURE 9.3
Sloping filter design. [*Cedergren (1967)*.]

The traditional way of preventing the migration of fine soil particles into gravel-filled drainage ditches and screened sumps is to construct one or several filter layers, usually consisting of sand with a grain size chosen according to filter criteria such as recommended by the U.S. Corps of Engineers [Eqs. (11.11), (11.12), and (11.13)]. These criteria ensure adequate flow through the filter zone, prevention of piping, and sufficient uniformity of the material. The criteria are expressed in terms of the grain size indicators D_{15}, D_{50}, and D_{85} of both the soil to be protected and the filter material.

Indicators D_{15}, D_{50}, and D_{85} represent the diameters corresponding to 15, 50, and 85% passing on a grain-size-distribution curve.

It is becoming more common to fully or partially replace granular filters by geotextiles, introduced in Chap. 11. Filter action, particularly as related to geotextiles, is discussed further in Sec. 11.2.3.

Temporary wells may consist only of perforated casing surrounded by a sand or gravel pack, chosen according to proper filter criteria. More permanent installations are likely to be fitted with commercial well screens, which have considerable advantages compared with makeshift slotted and perforated pipes. They are usually made of corrosion-resistant metal, provide continuous uninterrupted inflow over a maximum percentage of open area, have V-shaped slot openings that widen inwardly to prevent clogging, and are built strong enough to resist stresses during and after installation. A properly chosen well screen will give the well a maximum specific capacity, measured in liters per second per meter of drawdown.

9.1.3 Individual Well Capacity

The preliminary design of a dewatering system usually starts with a determination of the total quantity of water to be pumped for a circular excavation with an area equal to the one to be dewatered. In order to be able to estimate the required number of wells of a given size, knowledge of the capacity of an individual well is required. For an individual well of radius r, the discharge quantity is calculated according to

$$Q_i = 2\pi r h_w k i_e \tag{9.7}$$

where h_w can be set equal to h_0 if the free discharge height is ignored and i_e is the average entry gradient. According to empirical findings by Sichardt, the entry gradient should not exceed

$$i_{emax} = \frac{1}{15\sqrt{k}} \tag{9.8}$$

(where k is entered in meters per second), otherwise turbulence, high head losses, and filter instability may result. This rule is recommended for well spacings larger than about 15 well diameters. The capacity of an individual well is therefore limited to

$$Q_{imax} = 2\pi r h_0 \frac{\sqrt{k}}{15} \tag{9.9}$$

with r and h_0 in meters, k in meters per second, and Q in cubic meters per second. Note that both expressions [Eqs. (9.8) and (9.9)] are empirical rules and are not dimensionally consistent.

If Q_{imax} is plotted as a function of h_0, a straight line results as shown in Fig. 9.4. This figure also shows Q_i calculated according to Eq. (8.3) which reads (neglecting the free discharge height):

$$Q_i = \frac{\pi k(h^2 - h_0^2)}{\ln (L/r)} \tag{9.10}$$

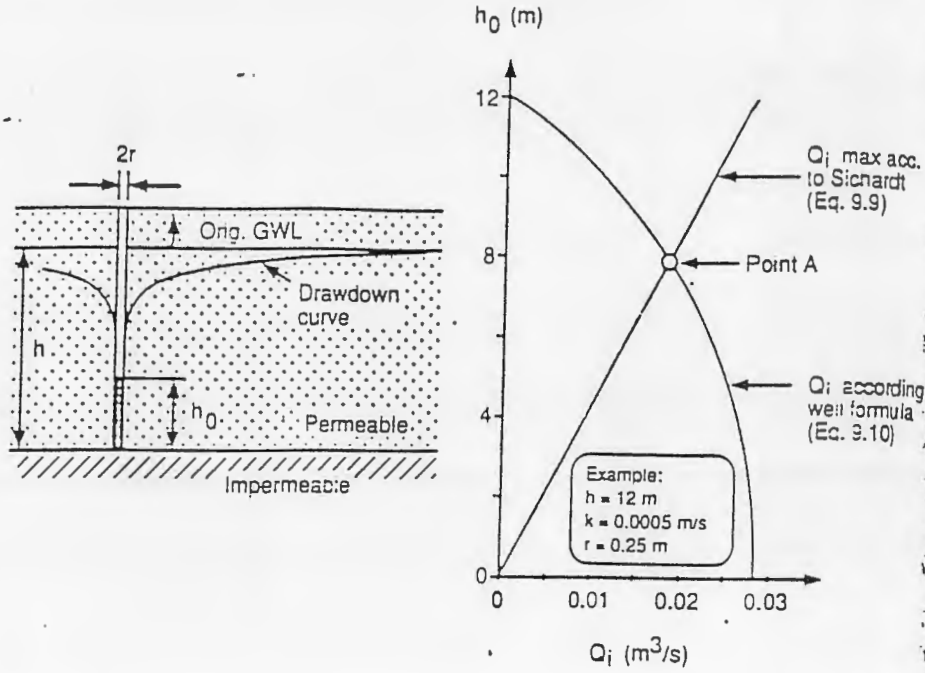

FIGURE 9.4
Well capacity.

In Fig. 9.4 this function is represented by a parabola. The point A corresponds to a desirable minimum water level in the well h_{0min} and an optimum discharge Q_{opt}, representing the individual well capacity. If Q is increased further, the maximum feasible entry gradient according to Sichardt is exceeded and the well may be pumped dry.

9.1.4 Well Diameter, Depth, and Spacing

It is of interest to note some of the guidelines published by various authors with respect to the preliminary layout of a well system. It should however be remembered that many of these design rules may have originated from engineers involved in the development of groundwater for municipal or industrial water supply, rather than for temporary dewatering projects. In addition, the technology of drilling and pumping undergoes continuous development. Nevertheless, in particular geographic areas or specific geological formations, successful traditional guidelines and techniques may be maintained.

As mentioned earlier, shallow installations using surface pumps allow a maximum suction head of about 8 m; well screens may extend the installation to a total depth of 10 to 12 m. Schröder (1966) quotes as a rule that the distance between adjacent wells should not be less than 3 to 4 m for 150-mm-diameter wells and not less than 5 to 6 m for 300- to 350-mm-diameter wells; otherwise an uneconomical system of too many wells with only marginally increased total discharge may result.

However, in well-point installations, where emphasis is on easy and quick temporary installation of reusable components, spacing is often much closer. Design charts presented by Mansur and Kaufmann (1962) consider spacings as low as 0.2 m for gravels and 1.5 m for fine sands.

For individually developed deep wells, the diameter and depth chosen will depend on the type of submersible pump to be used.

9.2 DEWATERING OF EXCAVATIONS

9.2.1 Standard Design Approach

The aims of the calculations are to determine the required pump rate and the number of wells needed in order to lower the water level by a specified amount below the base of the excavation. Calculations proceed in four steps.

Step 1: Obtain a rough guess of the total quantity of water to be pumped. We replace the actual excavation with a circular one of equal area and use an equation analogous to Eq. (8.11):

$$Q_{tot} = \frac{\pi k(h^2 - y^2)}{\ln (L/a)} \tag{9.11}$$

The values of h, y, and k are determined by the dimensions of the aquifer, the required drawdown, and the soil type. The a is the radius of the substitute circular excavation. If the actual excavation is rectangular with a length X and width Y, then

$$a = \sqrt{\frac{XY}{\pi}} \tag{9.12}$$

The L can be estimated using Eq. (8.8), but this requires an initial assumption for h_0. The assumed h_0 is checked in step 3, and the calculation is repeated if necessary.

Step 2: Estimate the number of wells needed (n). For a given well radius and the assumed wetted filter length h_0 the maximum yield of one well is calculated according to Eq. (9.9). We then find

$$n = \frac{Q_{tot}}{Q_{max}} \tag{9.13}$$

Step 3: Check original guess of h_0. Use the following version of Eq. (8.10), still referring to the circular excavation (Fig. 8.6).

$$Q_{tot} = \frac{\pi k(h^2 - h_0^2)}{\ln L - (1/n) \ln (x_1 x_2 \cdots x_n)} \tag{9.14}$$

Solving this equation for h_0, results in a new, improved value for h_0. Using this value, a new L and new Q's are computed. Steps 1 to 3 are repeated until h_0 assumed is sufficiently close to h_0 calculated in step 3.

Step 4: Return to the original excavation. Distribute the n wells around its parimeter. It is then necessary to check the water level at critical points below the excavation in order to verify whether the design requirements are satisfied. For example, the water level at the center and near the corners of the excavation should be calculated. This is done using Eq. (8.10). If the water level is too high, the pumping rate Q_{tot} has to be increased. This, in turn, will result in a reduced h_0 and an entry gradient which may be in excess of that recommended by Sichardt or, in the extreme, dry wells. If this is the case, the number of wells should also be increased and all calculations repeated until a satisfactory solution is found.

Increasing the number of wells but keeping Q_{tot} is unlikely to significantly lower the phreatic surface further, although a more even drawdown may be beneficial in critical areas.

It should be noted that because of inherent deficiencies in this method, h_0 calculated using Eq. (9.14) for individual wells around a noncircular excavation will not be a constant. To use an average value, where necessary in the calculations, appears to be a reasonable compromise.

9.2.2 Modification by Herth and Arndts

Herth and Arndts (1973) maintained that the standard approach as described in the preceding section leads to an overestimation of h_0. This is because the flow to an individual well within a group of wells located around an excavation is not equal from all directions. In particular, the flow from within the excavation area toward the wells is less than from outside the excavation. In addition, the free discharge height is not considered.

They proposed that the following modified formula be used:

$$h_0 = \sqrt{y^2 - \frac{fQ_i \ln (b/r)}{\pi k}} \tag{9.15}$$

The terms b, y, r, and h_0 are defined in Fig. 9.5.

The recommended values for the correction factor f are

$$f = \begin{cases} 1.5 & \text{for large well spacings,} \\ 2 & \text{for small well spacings } (b < 5\pi r) \end{cases}$$

The justification of the latter is that for wells closely spaced around an excavation, water flows into the wells only from one side. Thus, to calculate h_0, it is assumed that there is a $2Q_i$ flow to the well. This results in a reduced value of h_0 which should be compared with the minimum allowable h_0 calculated using Sichardt's formula [Eq. (9.9)]:

$$h_0 = \frac{15Q_{imax}}{2pr\sqrt{k}} \tag{9.16}$$

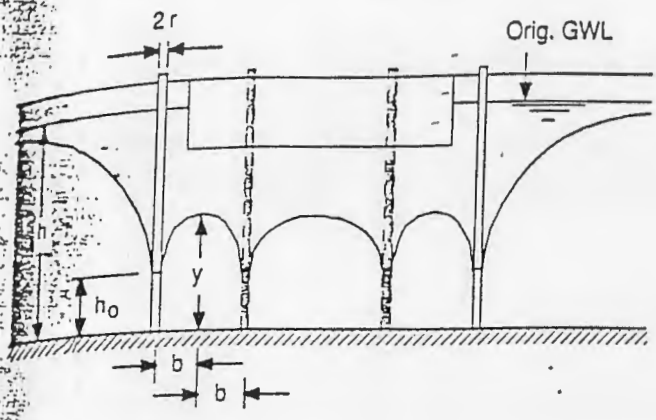

FIGURE 9.5
Multiwell system. [*Herth and Arnáts (1973).*]

9.2.3 Pipelines and Pumping Plant

The velocity in suction pipes (or header pipes) with 200- to 400-mm diameters is usually kept below 1.5 to 2 m/s in order to keep friction losses within reasonable limits. Pressure lines (discharge lines) are dimensioned for velocities between 2 to 3 m/s.

The pump capacity required can be calculated using the following formula:

$$N = \frac{Qh\gamma_w}{\eta} \tag{9.17}$$

where η is the efficiency of the system, with friction losses in the pipes also being taken into account. Usually the value η is between 0.3 and 0.5.

Assuming an efficiency $\eta = 0.3$ and setting $\gamma_w = 10$ kN/m^3 (or 10 N/L) the formula simplifies to

$$N = \frac{Qh}{40} \quad \text{kW} \tag{9.18}$$

for Q in liters per second and h in meters.

The total discharge, total head, and suction lift required are the principal parameters affecting the choice of a pump. Self-priming centrifugal pumps are most common, but the water pumped has to be relatively clean. Pneumatic pumps and diaphragm pumps are able to move limited amounts of silt and sand without excessive wear. Rotary displacement pumps are used if the water pumped from sumps and wells contains more sediment. Submersible pumps are usually of the centrifugal type with one or more impellers on a vertical shaft driven by a motor.

Standby pump capacity should be available in case of breakdown or interrupted power supply or in case unexpected geological features result in increased flow into the dewatering system.

9.2.4 Settlement of Adjacent Structures and Other Side Effects

Lowering of the groundwater table increases effective stresses in a soil deposit, causes consolidation, and results in settlement of the structures supported by it. It may also cause negative skin friction on pile foundations.

A rough estimate of settlement can be made using the one-dimensional settlement formula:

$$\text{Settlement} = \frac{H}{1 + e} C_c \log \frac{\sigma'_{vo} + \Delta\sigma}{\sigma'_{vo}} \tag{9.19}$$

The H is the thickness of the consolidating soil layer, which has an initial void ratio e and a compressive index C_c. The initial average effective vertical stress in this layer is designated σ'_{vo}, and the stress increase caused by lowering the water table is $\Delta\sigma$. For a reduction in the groundwater level by Δh, the stress increase may be approximated by

$$\Delta\sigma = \Delta h \gamma_w \tag{9.20}$$

if the total unit weight of the soil does not change markedly because of dewatering.

The compressive index C_c is determined in a consolidation test or, less reliably, is estimated from empirical relationships, such as $C_c = 0.009[\text{liquid limit (\%)} - 10]$. Depending on the stress history of the consolidating layer, the recompression index (often designated C_R) may give more realistic settlement values than C_c.

If the above formula indicates measurable settlement, this by itself will not necessarily mean impairment of adjacent buildings. If the consolidating layer is thick and highly impermeable, the rate of settlement may be so slow that temporary dewatering of an overlying aquifer has little effect. Also, the differential settlement experienced by a structure may be relatively small, with no effect on its function. Much will depend on the nature of the structure and the service it provides: A corrugated, ironclad, steel-framed warehouse is less susceptible to differential movement than a multistory brick building.

If settlement is likely to damage structures adjacent to the dewatered excavation, it may be possible to either provide a *cutoff* (sheet pile, slurry wall, grouted or frozen ground) or to artificially *recharge* the water-bearing layer in their vicinity in order to maintain the original groundwater level (Fig. 9.6). The cost associated with these preventative measures could, however, be more than the cost of underpinning, grouting, or repairing the affected buildings.

It should also be noted that recharging an aquifer may be more problematic than dewatering it, because

There may be practical limitations to the head of water which can be built up in the recharge well.

The ground could appear less permeable because the pumped water is contaminated with fines and clogs the walls of the recharge wells or trenches.

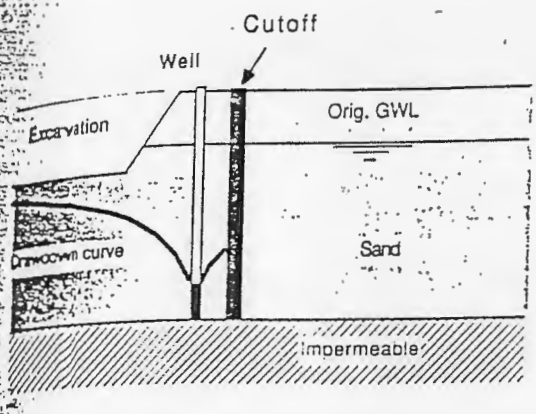

a. Cutoff

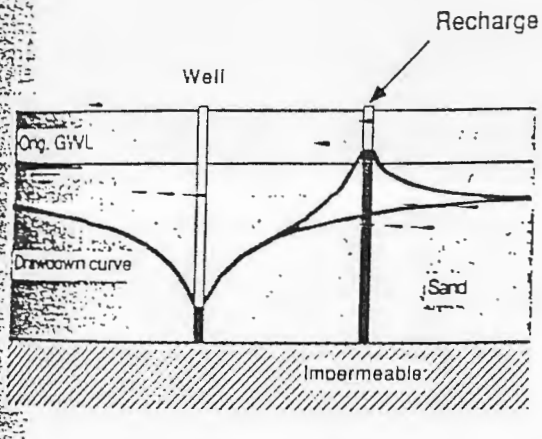

b. Artificial recharge

FIGURE 9.6
Preventing unwanted side effects of dewatering by cutoff or recharge.

The aquifer soil could be significantly less permeable than originally measured, if it is unsaturated prior to recharge.

Recharging the aquifer may reduce total settlements but also may increase differential settlements.

Besides settlement, other "unwanted side effects" [Powers (1985)] of dewatering may include the following:

Effect on nearby water supply wells

Saltwater intrusion in coastal areas (or spread of underground pollutants in industrial areas)

Degradation of old, untreated timber piles when they are exposed to air
Harmful effect on vegetation
Activation of sinkholes

Proper consideration of the possible negative effects of dewatering is necessary in order to prevent unexpected construction and legal costs.

9.2.5 Performance Evaluation

The location of the drawdown curve is easily monitored by simple piezometers. The discharge quantity can be measured by V-notch weirs or from the flow into calibrated containers. It can also be estimated by measuring the characteristics of the exit parabola of the water jet, as illustrated in Fig. 9.7, using the expression

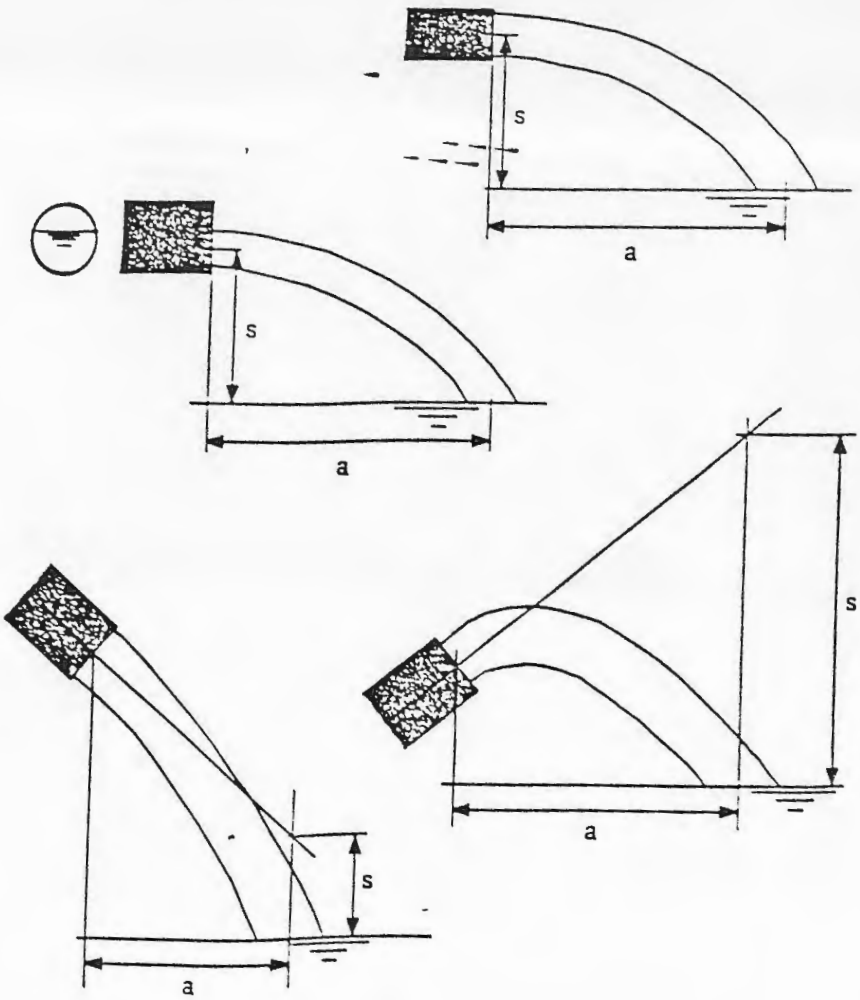

FIGURE 9.7
Estimating discharge quantities based on exit parabola. [*Schroder (1966).*]

$$Q = 2.22F_a \frac{a}{\sqrt{s}} \tag{9.21}$$

Distances a and s in meters are as defined in Fig. 9.7. The F is the cross-sectional area of the pipe in square meters, and F_a is the cross-sectional area of the water jet at the exit point in square meters, in the case where the pipe is partially full.

Performance evaluation allows the design parameters to be checked, and the procedures to be modified during construction of multistage installations, in order to reduce costs or improve efficiency.

9.3 DRAINAGE OF SLOPES

9.3.1 Effect of Water on Slope Stability

The presence of static or flowing water in a soil or rock mass may decrease its slope stability for the following reasons:

- It reduces the shear resistance of the material by increasing its water content and/or by producing higher pore pressures.
- It increases the total weight of the material.
- It may cause seepage forces in the direction of the slope movement.
- It may cause erosion and/or piping.
- It may change the physicochemical characteristics of the soil. (This could be the case when fresh water seeps through soils originally deposited in saltwater.)
- It increases the susceptibility to liquefaction during an earthquake.

Some of these effects are difficult to assess numerically, particularly in the absence of a comprehensive field and laboratory testing program. However, the effect of reducing pore pressures on the safety factor of a slope in frictional material can be clearly shown using conventional methods of slope stability analysis.

9.3.2 Methods of Stabilizing Slopes

If a civil engineering structure is to be located in a potentially unstable area or if cutting into an existing slope endangers its stability, a variety of preventative and corrective measures can be taken.

Drainage is the most common and generally applicable method. It takes the form of surface drainage (open ditches, sloping filters, sealing of the surface) and subdrainage (vertical and horizontal drains, tunnels, stone filled trenches, etc.) as described in Chap. 7.

Drainage alone may however not be sufficient to stabilize the slope, and additional measures may have to be taken. These could include:

- Altering the geometry of the slope, i.e., flattening the slope, benching, removal of material at the head, or placing fill at the toe of the slope

- Structural reinforcement of the soil mass using retaining walls, piling, or anchors
- Improving the soil or rock properties by grouting or using other geotechnical processes

In exceptional cases, blasting may improve the stability of a slope, not only by changing the geometry but also by making jointed bedrock more permeable, thus facilitating drainage. Furthermore, blasting could result in additional consolidation and improved strength, e.g., before a road cut is constructed.

9.3.3 Analysis of Stability

There are many different methods of slope stability analysis available to the engineer. They may be categorized according to the assumptions made for the following:

- Failure geometry
- Failure law
- Type of strength or deformation parameters
- Numerical technique used

Here, in order to illustrate the effect of water on slope stability, the infinite slope analysis and the Swedish method of slices, which is based on a circular failure surface, are introduced. Both rely on the Mohr-Coulomb failure law. As it suits the evaluation of the long-term stability of the slope, the analysis is usually carried out in terms of effective stresses. If large strains and slow movement are typical for a particular stability problem, residual rather than peak shear strength should be used.

9.3.3.1 INFINITE SLOPE ANALYSIS. The infinite slope analysis is applied to problems where the likely failure plane lies parallel to the surface. This may be due to particular geological circumstances, the pattern of weathering, or because of the way the soil or rock mass was deposited or dumped. The factor of safety of an infinite slope (Fig. 9.8) is expressed as

$$F = \frac{\tau_a}{\tau_m} = \frac{\text{available shear strength}}{\text{mobilized shear strength}} \tag{9.22}$$

The available shear strength refers to the maximum possible shear stress in the potential failure plane. The mobilized shear strength is equal to the actual shear stress required for equilibrium.

For a soil of unit weight γ and with effective strength parameters c' and ϕ', we obtain for the general case

$$F = \frac{c' + (z\gamma \cos^2 \beta - u) \tan \phi'}{z\gamma \cos \beta \sin \beta} \tag{9.23}$$

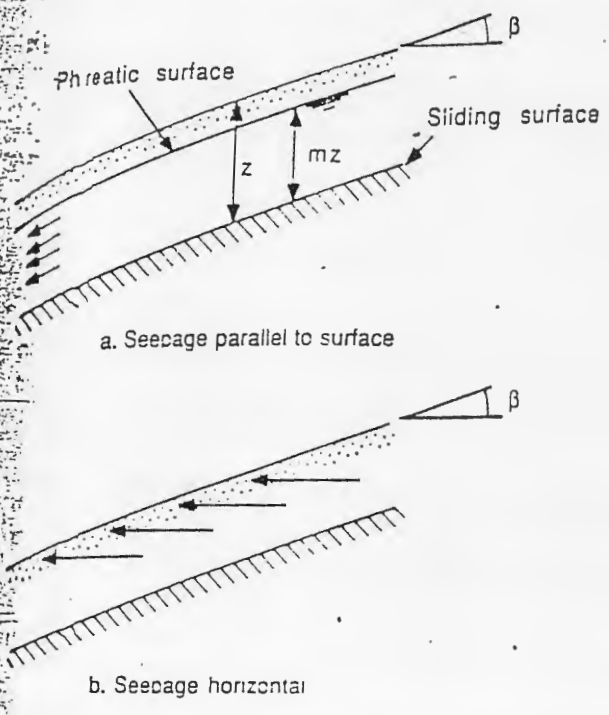

FIGURE 9.8
Infinite slope analysis.

In the special case of $c' = 0$ and $m = 1$ (water table at the surface), we obtain for seepage parallel to the slope, with γ_w representing the unit weight of water:

$$u = mz\gamma_w \cos^2 \beta \tag{9.24}$$

$$F = \left(1 - \frac{\gamma_w}{\gamma}\right) \frac{\tan \phi'}{\tan \beta} \tag{9.25}$$

$$\approx \frac{\tan \phi'}{2 \tan \beta}$$

If there is no water present above the failure surface ($m = 0$), the safety factor is approximately

$$F \approx \frac{\tan \phi'}{\tan \beta} \tag{9.26}$$

For the case of horizontal seepage

$$u = z\gamma_w \tag{9.27}$$

$$F = \left(1 - \frac{\gamma_w}{\gamma \cos^2 \beta}\right) \frac{\tan \phi'}{\tan \beta} \tag{9.28}$$

As an example, take $c' = 0$, $\phi' = 35°$, and assume $\gamma_w/\gamma = 0.5$; the slope angle equivalent to a factor of safety of $F = 1$ then is as follows:

No water present	$\beta = 35°$
Seepage parallel surface	$\beta = 20°$
Seepage horizontal	$\beta = 17.5°$

The effect of water on the stability of a frictional material is clearly evident. The analysis of a purely cohesive soil would show that a decrease in pore pressures does not increase the stability unless an increase in the value of cohesion (e.g., due to consolidation) or a reduction in the overall weight of the sliding soil mass is relied upon.

9.3.3.2 SWEDISH METHOD OF SLICES. A circular failure surface is assumed as shown in Fig. 9.9. The safety factor is expressed in terms of moments about the center of the failure circle:

$$F = \frac{M_R}{M_D} = \frac{\text{resisting moment}}{\text{driving moment}} \tag{9.29}$$

Using designations as in Fig. 9.9, the safety factor is calculated as

$$F = \frac{c'L + \tan\phi' \sum_{i=1}^{n} (W_i \cos\alpha_i - U_i)}{\sum_{i=1}^{n} W_i \sin\alpha_i}$$

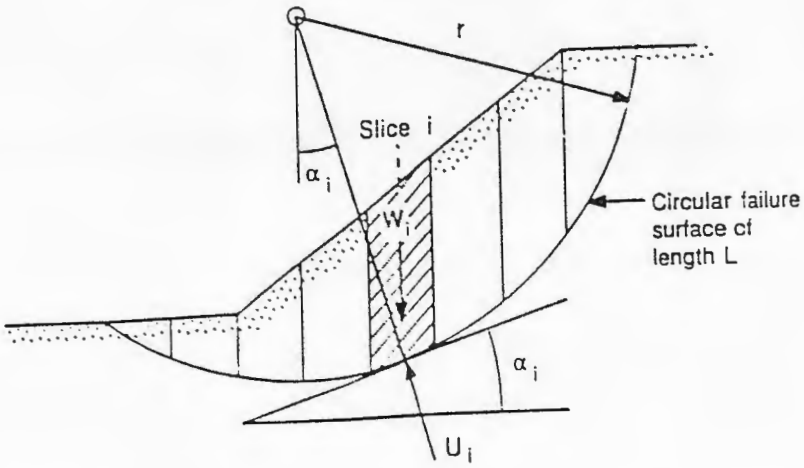

FIGURE 9.9
Swedish slip circle method of stability analysis.

where W_i is the weight of slice i and $\bar{U}_i$ is the resultant of the pore pressure acting normal to the failure arc on slice i.

The force U_i is proportional to the height of the phreatic line above the failure arc if hydrostatic conditions are assumed. The frictional resistance along the failure arc is thus greatly reduced if the water level within a sliding soil mass is increased. Provided the effective angle of internal friction is at least 10 to 20°, analysis shows a significant effect on the safety factor of a slope, even in cohesive frictional, rather than purely frictional, material.

In theory, for a purely cohesive soil, we see no improvement of stability by the relief of pore pressures alone. It should however be remembered that even highly plastic clays can have effective friction angles in excess of 0°, say 10 to 20°, as determined in a consolidated, undrained triaxial test with pore pressure measurements. Even without considering friction, drainage of cohesive soils can be seen to be beneficial for stability if the long-term reduction in water content leads to increased strength and a reduction in the total weight acting on the failure plane.

9.3.4 Design Approach

The approach to designing a drainage system for slope stabilization is basically the same as for a well system, except that topography generally allows dewatering without pumping.

As for wells, drains must be designed

- To have adequate discharge capacity
- To satisfy filter criteria

The effect of various spacings could be analyzed by drawing flow nets for idealized conditions. However, in most cases geological details such as the location of permeable layers and faults in the bedrock have an overwhelming influence on the effectiveness of the drainage system. Practical rules suggest a spacing of horizontal drains of 3 to 8 m in clayey soils and 8 to 15 m in more permeable material. Usually several drill holes are fanned out from one location in order to increase the probability of intersecting all major permeable strata and rock joints. Borehole information should be compiled so as to allow a three-dimensional assessment of the geological structure. The length of the drains depends on the particular site conditions and the location of the likely slip planes. Horizontal drains with lengths of more than 100 m have been installed as part of slope-stabilizing programs.

Vertical drains may be used in combination with a horizontal drainage system in order to intersect water-bearing layers separated by horizontal seams of impermeable clayey soil.

When attempting to stabilize an active landslide, the engineer must remember that the moving soil mass may damage the drainage system. The type of drains and their location will have to be selected accordingly; considerable maintenance work may be required in the early stages of the work.

9.3.5 Performance Evaluation

The effectiveness of the drainage system can be checked by installing piezometers and measuring the flow from the drains. Records of water levels and discharge quantities should be kept and possibly correlated with rainfall data.

Vertical and horizontal movements of the unstable soil or rock mass should be monitored by surveying surface markers and, where appropriate, borehole installations. Using a borehole inclinometer may allow identification of the actual slip surface or zone of shear failure.

9.4 CASE STUDIES

9.4.1 Dewatering of a Pumping Station Site at Cronulla, New South Wales

The Cronulla Sewage Pumping Station is located at the edge of Woolooware Bay in an area characterized by swampy, marshy conditions. The Metropolitan Water, Sewarage & Drainage Board started construction in 1974. The station started operating in 1980.

The excavation covered an area of approximately 60 by 60 m. The deeper of the two final rings of wells reached a depth of 10 m below ground level.

The excavation was accomplished in three stages. The first stage consisted of a U-shaped layout of 150 well points, spaced 1.5 m apart and reaching a depth of 6 m. The riser pipes of 50-mm diameter were connected to a 200-mm header pipe. Three pumps were in action, each serving 50 well points. This installation was only used to initiate the excavation: it was dismantled after the next two lines of well points commenced operating. It took 5 days to lower the groundwater level to about elevation (El.) 13 m.

The second and third stages of dewatering are illustrated in Figs. 9.10 and 9.11, respectively. The contractor, Sykes Pumps Australian Pty., Ltd., used perforated plastic well points covered with cheesecloth as filter material. Lowering the water

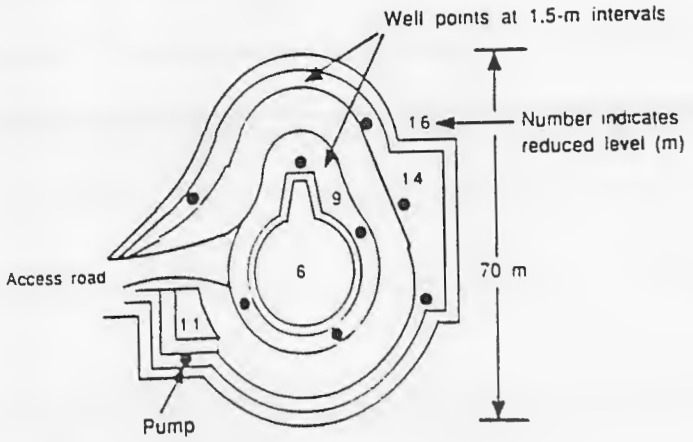

FIGURE 9.10
Layout of well points and pumps around pumping station at Cronulla.

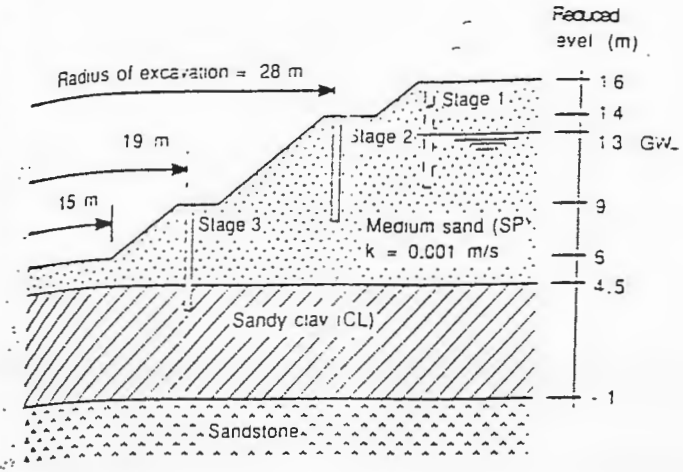

FIGURE 9.11
Schematic cross section showing levels of upper and lower well points at pumping station site at Cronulla (stages 2 and 3 of the dewatering program).

table to El. 6 m took 4 weeks, with all wells operating. After this period, every second well point was disconnected in order to prevent excess air being sucked by the vacuum-assisted centrifugal pumps; this measure increased the efficiency of the system. Five pumps were used during normal operations, when the pumping rate was on the order of 23 to 25 L/min per well point.

Dewatering was kept up for a period of about 6 months. In an attempt to prevent excessive surface erosion due to rain, embankments were treated with concrete spray or bituminous emulsions. The latter was generally considered to be the more economical of the two techniques.

9.4.2 Stabilizing Embankment at Newport, New South Wales

A major road embankment near Newport, approximately 20 m high with a slope of 35° (1.5:1), had already shown movement for several months before heavy rainfalls and a 6-m-deep cut near the toe brought about a semirotational failure, resulting in damage to the footpath and the closing of one lane of traffic. A typical cross section is shown in Fig. 9.12.

From November, 1973, to February, 1974, the subsidence at the top of the embankment reached a total of 3 m, at a rate of as much as 300 mm per week.

A geological investigation showed that there were major joint systems and several faults in the area. Water was thought to permeate through the jointed sandstone and travel along the more impermeable horizontal shale layers into the failure zone. It was decided that some 30 horizontal drains over a 100-m section of the fill should be drilled in order to reduce the pore water pressure along possible slip planes. It was estimated that reducing pore pressures in the wet contact zone above bedrock could increase the safety factor by more than 20%.

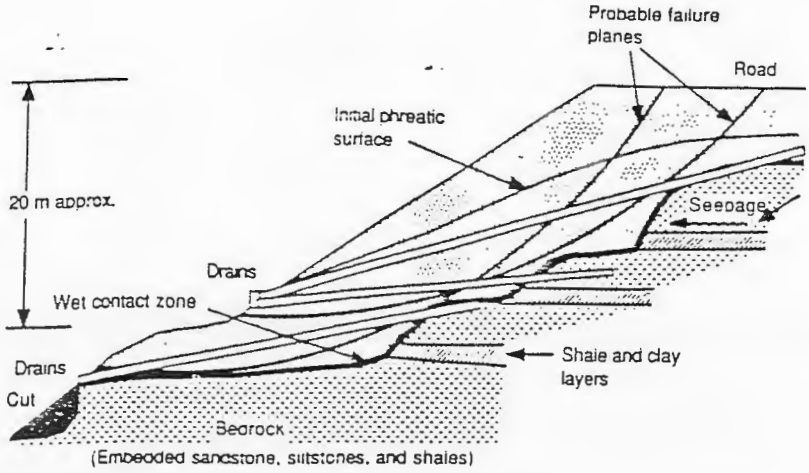

FIGURE 9.12
Embankment at Newport.

Because of the low permeability of the material in the wet contact zone, a complete relief of pore pressures did not occur. Although the rate of movement decreased so as to allow repair of the pavement, further works were thought to be necessary in order to increase the safety factor to an acceptable level. Measures considered included the building of retaining walls, placing fill at the toe of the embankment, and installing further drains.

9.4.3 Dewatering of the Morwell Open-Cut Coal Mine

This project, located in the Latrobe valley, Victoria, is described in a pamphlet by James Hardie & Co. (1973) as follows (refer to Figs. 9.13 and 9.14):

> The Morwell open cut development commenced in the early 1950's when overburden removal began. The first coal was excavated in 1960.

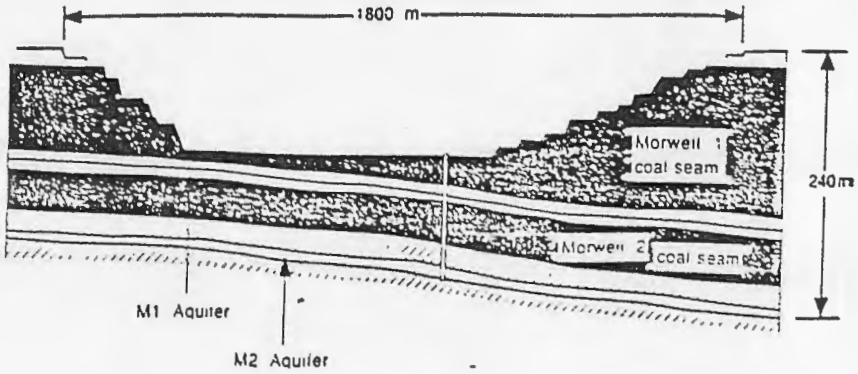

FIGURE 9.13
Morwell open cut. Diagrammatic north-south cross section.

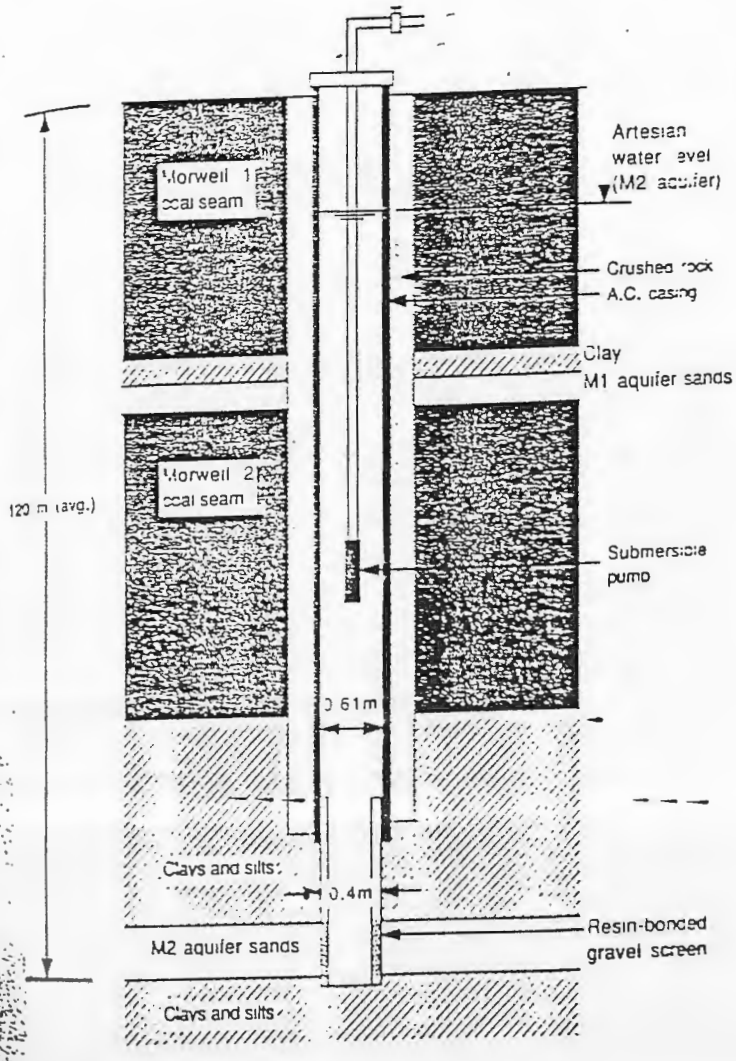

FIGURE 9.14
Diagrammatic sketch of a production bore.

The diagrammatic north-south cross-section shows the two major coal seams and the M1 and M2 aquifers, which consists of generally flat lying sand beds which underlie the coal seams.

The two aquifers contain artesian water, the original pressure levels being at the top of the M1 coal seam, immediately below the overburden.

As excavation proceeds, the weight of the coal seam is reduced and less pressure is available to equalize the pressure exerted by the artesian water. This excess pressure in the aquifers must be relieved to prevent it bursting through the now thinner coal layer above, possibly flooding the open cut and causing instability of the batters of the open cuts.

Bore pumping first commenced in 1960 from bores drilled around the perimeter of the open cut. The majority of subsequent bores were located within the open cut itself, and during the period 1961–65 the water pressures were lowered by free-flowing bores, one of which initially produced 130,000 gallons (~500,000 liters) per hour. As the

excavation deepened the free artesian flows reduced, and by 1965 it became necessary to introduce pumping bores to maintain stability.

A great number of bores have been drilled through the coal seam into the aquifers. The locations are determined by the requirement to lower pressures most at the deepest area of the open cut.

Continued excavation caused the pressures of the deeper M2 aquifer to have greater influence on the stability of the open cut, and it became necessary to include this sand layer in the bore pumping programme. This required additional and larger capacity bores and pumps to handle the flow.

Eighteen bores are in operation in the Morwell open cut (as of September, 1973). Six are located in the upper sand aquifer, from which 3000 gallons per minute are pumped. 12,000 gallons (≈45,000 liters) per minute are pumped from the 12 bores located in the lower aquifer.

At that date the average depth of bore to the upper aquifer was 150 ft (=45 m), and to the lower aquifer 400 ft (=120m).

9.4.4 Dewatering of the Lochiel Trial Pit

This case study illustrates the trial use of vacuum-assisted pumped wells for the dewatering of a proposed open-cut mine development. The following information was obtained mainly through personal communication [O'Brien (1987)] and from a paper presented by Sullivan and Burman (1986).

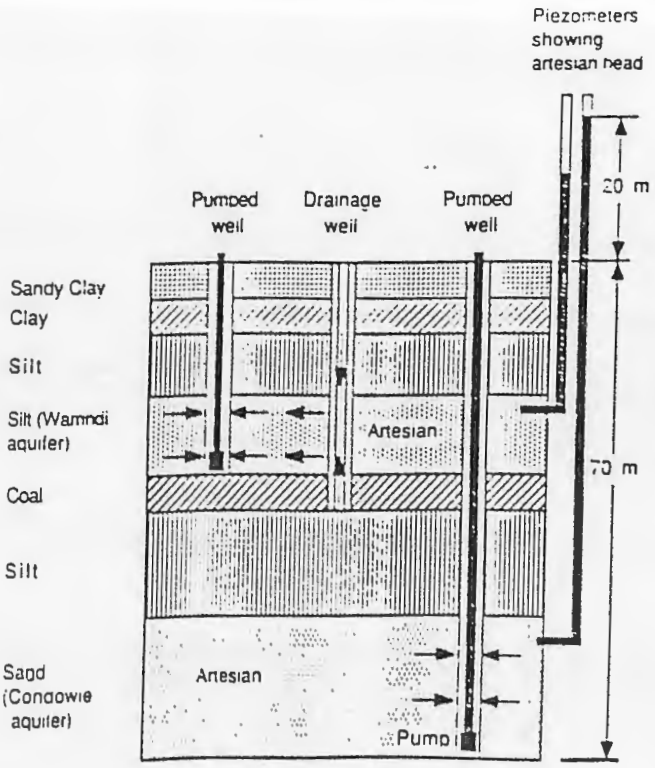

FIGURE 9.15
Lochiel coal deposit: Typical profile.

The Lochiel soft brown coal deposit, 130 km north of Adelaide, was discovered in 1982 and has since been investigated as a source of fuel for power generation in the late 1990s by the Electricity Trust of South Australia. The coal seams are embedded in fine silt and clay material. A typical profile shows 20 to 60 m of overburden above the coal zone, which is up to 20 m thick and can be divided into three main seams.

Immediately below the coal is a silt layer, which overlies fine to medium sand. A simplified profile is shown in Fig. 9.15 which also identifies the main water-bearing layers: the Warrindi aquifer and the Condowie aquifer. Additional minor aquifers may occur elsewhere in the profile. The groundwater was under artesian pressure with a hydraulic head up to 20 m above ground level. The aquifers consisted of coarse silt to medium sand and had permeabilities on the order of 10^{-5} to 10^{-4} m/s.

Open-cut mining of the Lochiel deposit obviously needs dewatering of the aquifers in order to ensure the stability of steep pit walls and a dry working area. Because of the complex geological and hydrogeological conditions a trial excavation was carried out. The trial pit was 100 m square and 29 m deep, with side slopes ranging from 45 to 60°. A 300-m-long ramp provided access to the bottom.

Eight wells were installed to pump from the Warrindi aquifer: two of these went down to the Condowie aquifer. Because of the relatively low permeability of some of the aquifers, the wells were fitted with airtight collars (Fig. 9.16) so that a vacuum

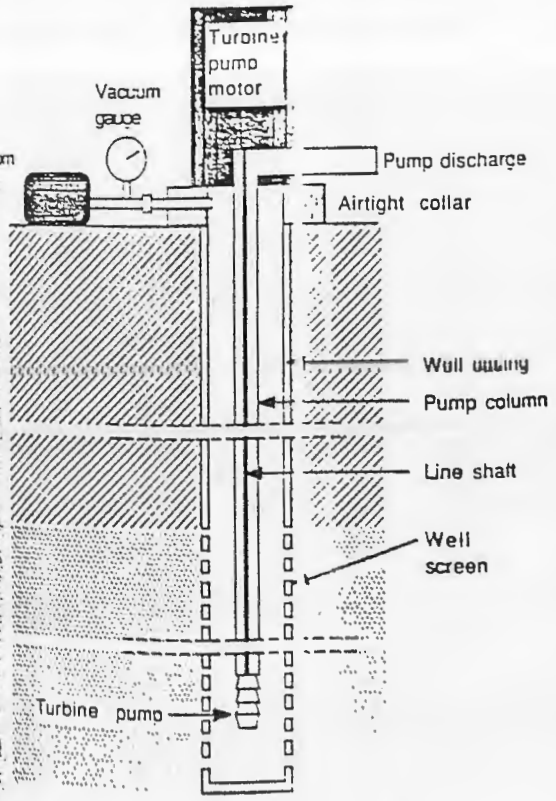

FIGURE 9.16
Lochiel trial pit: Vacuum-assisted pumped well.

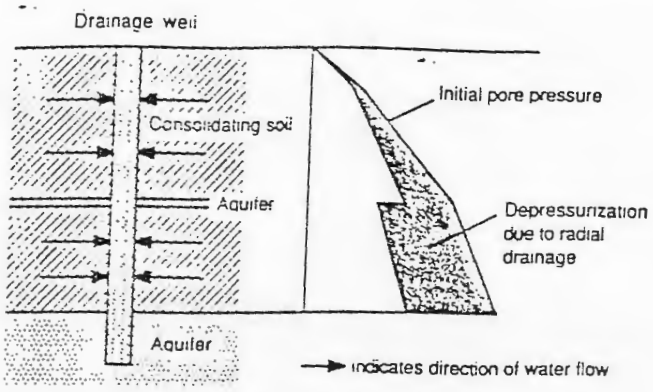

a. Depressurization by horizontal radial drainage

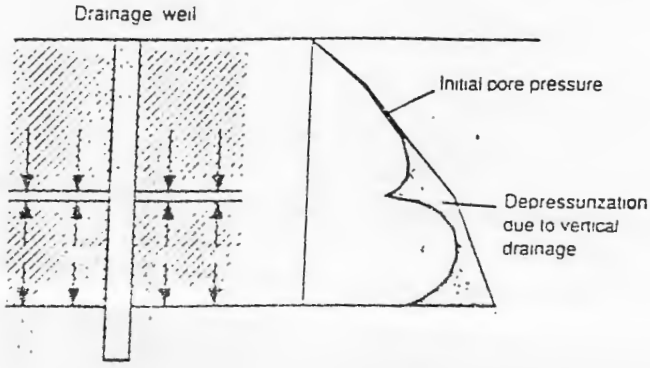

b. Depressurization by vertical drainage

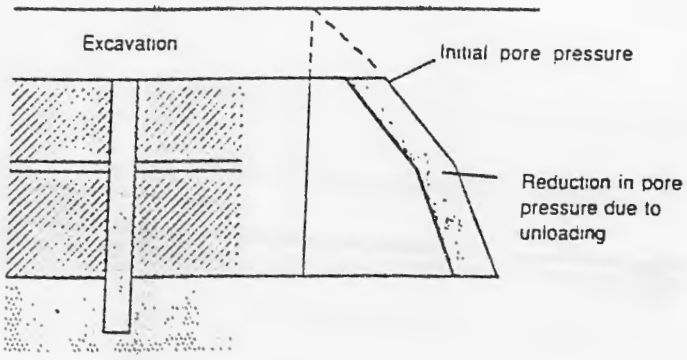

c. Pore pressure reduction due to removal of overburden

FIGURE 9.17
Pore pressure reduction by drainage and unloading. [*Adapted from Sullivan and Burman (1986).*]

could be applied. Within 20 min a vacuum of −90 kPa was established, raising the water level in the well by 9 m. The pump rate was then increased by opening the control valve until the water level in the well fell to within 6 m of the pump. After considerable adjustment, the stable flow rate from all wells increased by 40 to 50%.

In addition to the pumped wells, some 20 sand-filled drainage wells (600-mm diameter) were installed (Fig. 9.16). They intercepted minor aquifers and made ho

izontal drainage possible, accelerating the consolidation of the finer-grained water-bearing layers. Water could then drain vertically downward or upward into the Warrindi aquifer, from where it was pumped to the surface.

Extensive instrumentation allowed detailed performance evaluation. The following were installed: 224 piezometers, 6 extensometers, 38 slip indicators, 10 slope inclinometers, 12 slope alarms (to warn personnel of impending slope failures), 30 surface settlement gauges, 40 survey stations, and other instruments measuring pump flow rate, vacuum pressure, and pump water levels.

The application of a vacuum to the wells was considered very successful and economical. In one particular fine-grained layer, the piezometric fall in 1 day of vacuum-assisted pumping was equal to the fall recorded over the previous 6 weeks.

The effect of dewatering was analyzed by Sullivan and Burman (1986) based on the following mechanisms, illustrated in Fig. 9.17:

a. Depressurization (lowering the pore pressure) due to horizontal drainage into the wells (horizontal consolidation)
b. Depressurization due to vertical drainage of the finer-grained layers into the more permeable aquifers (vertical consolidation)
c. Pore pressure reduction associated with unloading (change in vertical stress due to the excavation process)

The pore pressures determined for the various stages of depressurization could then be used in the stability analysis of the high walls of the planned open-pit mine. This assisted in the choice of the most economical mining method (e.g., dragline or bucketwheel excavators).

PROBLEMS

Prefixes indicate problem type: C = calculations, M = multiple choice, B = brief answer.

Calculations

C9.1. The coefficient of permeability of an 11-m-thick unconfined aquifer is to be determined by a pump-out test performed using two observation holes, 5 and 10 m from the well. For steady-state conditions at a pumping rate of 25.8 L/s the water levels in the observation holes were 3.1 and 2.4 m below the original groundwater level, respectively. Calculate the coefficient of permeability.

C9.2. Draw a diagram of h_0 versus Q for a perfect well based on the discharge formula [Eq. (9.10)] and Sichardt's formula [Eq. (9.9)] which is based on a maximum entry gradient. Calculate a new influence range for each h_0 value. Based on the diagram obtained, determine the well capacity. The well radius is 0.25 m, the aquifer has a thickness of 12 m, and the soil permeability is 0.0005 m/s.

C9.3. Wells spaced around the perimeter of a 36-m-wide circular excavation must lower the water level by a minimum of 5 m below the existing groundwater level. The unconfined water-bearing layer is 12 m thick and is located above an impermeable stratum. Other data available are

CHAPTER

2

INTRODUCTION TO MECHANICAL MODIFICATION

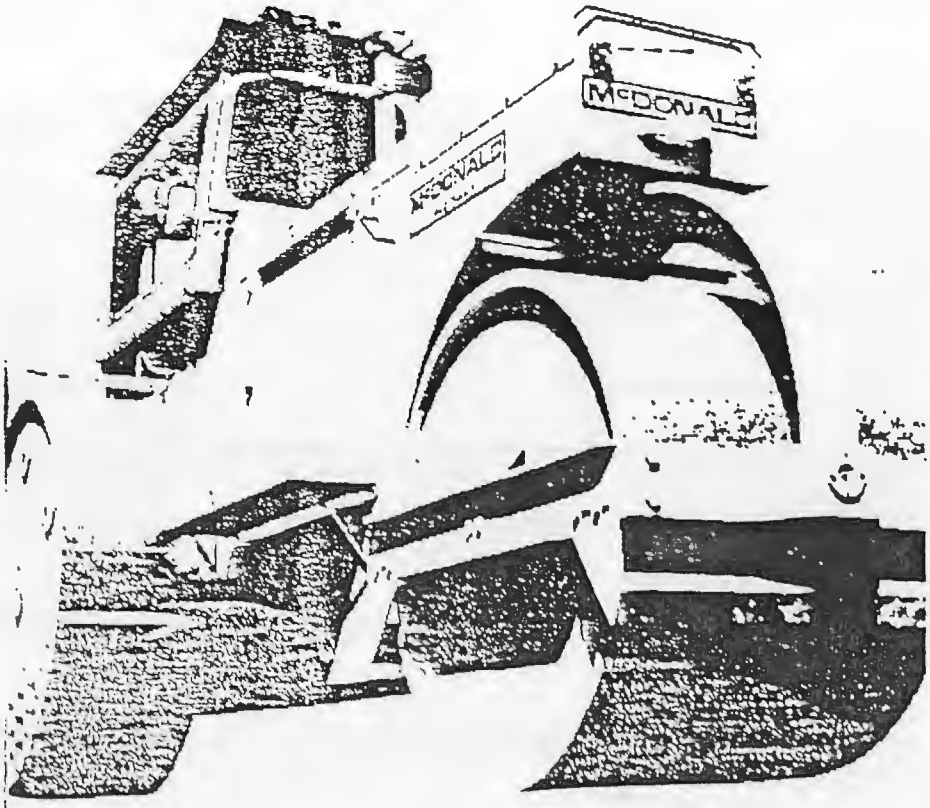

2.1 TERMINOLOGY AND AIMS OF MECHANICAL MODIFICATION

2.1.1 Terminology

Mechanical ground modification refers to soil densification by external forces. In most practical applications mechanical modification is synonymous with compaction. In its classic sense, *compaction* means densification of an unsaturated soil by a reduction in the volume of voids filled with air, while the volume of solids and the water content remain essentially the same. Compaction implies that soil particles are packed closer together by the application of sudden heavy loads or dynamic forces; crushing of some of the soil grains or rock particles may assist this densification.

The above definition of compaction holds true for most surface compaction methods but must be extended for deep compaction techniques. The latter may also involve saturated soils, water jetting, and partial replenishment of the in situ soil but are nevertheless included here under mechanical modification.

The geotechnical engineer makes a clear distinction between the processes of compaction and those of stabilization and consolidation.

For the nonspecialist, *stabilization* may refer generally to an increase in strength or a reduction in the deformation of a soil mass. When used in road engineering and soil mechanics, it usually implies soil improvement by physicochemical reactions caused by additives or induced by environmental changes.

Consolidation is a process where the volume of a soil mass is reduced by the expulsion of water. As modeled by the classic consolidation theory, it involves stress transfer from the water to the solid phase. It is usually achieved by the long-term application of static loads or electric forces to saturated soils. Consolidation may also be induced or accelerated by temporary liquefaction caused by impact forces or vibration—thus the term "dynamic consolidation" in relation to heavy tamping, a deep compaction technique (see Sec. 2.2.3.2).

2.1.2 Compaction Purpose and Strategies

The major aims of compacting soil are to

1. Increase shear strength
2. Reduce compressibility
3. Reduce permeability
4. Reduce liquefaction potential
5. Control swelling and shrinking
6. Prolong durability

It could be added that properly managed engineered compaction may reduce the variability of engineering soil properties in a natural deposit or a human-constructed fill.

Compaction is the most commonly used method of ground modification. Significant early advances in the knowledge of compaction principles were made in the

st quarter of this century by engineers building roads for increasingly bigger traffic numbers and wheel loads. Later, in the 1930s, the construction of large earth dams, whose failure would have catastrophic consequences, forced the adoption of a scientific approach to compaction. Today, compaction is of equal importance in highway, airfield, and marine construction; in the preparation of foundation soils; and in the backfill behind abutments, walls, and in trenches.

Improvement of engineering properties by densification is possible for natural soils as well as for soils stabilized with chemicals such as lime and cement. The principles and techniques of compaction also have relevance for other soil-related construction materials, such as asphalt surfacing and concrete.

In soil engineering, strategies developed for optimizing the densification process may include some or all of the following steps.

1. In the case of human-constructed fills, specify placement conditions (water content, density, depth of layers, etc.).
2. Select appropriate equipment (roller, vibro-compactor, tamping) and method of operation (number of passes, patterns of tamping, etc.).
3. Set up adequate control procedures (type and number of tests, statistical evaluation, etc.).

To achieve efficient compaction requires knowledge of the available equipment, the principles of compaction, the properties of compacted soils, and control procedures.

2.2 METHODS OF COMPACTION

2.2.1 Laboratory Procedures

The aim of laboratory compaction tests is to simulate field compaction procedures. Their results should aid in the optimization and control of placement conditions. The most common type of test is the standard compaction test, in which a steel rammer is dropped on loose soil placed in a mold. It employs dynamic compaction as against kneading or static compaction.

2.2.1.1 DYNAMIC COMPACTION. The standard compaction (or Proctor) test is described in the Australian standard AS 1289.E1.1-1977; equivalent procedures are described in other national standards [American Society for Testing and Materials (ASTM), American Society for State Highway and Transportation Officials (AASHTO), British Standard (BS), Australian Standard (AS), etc.]. The test is carried out on that portion of the soil which passes the 19-millimeter (mm) sieve. Five or more samples are prepared at different moisture contents and allowed to cure. Every sample is compacted in three layers, each receiving 25 blows with a 2.7-kilogram (kg) rammer dropping 300 mm. The diameter of the flat rammer head is approximately half the diameter of the mold.

In the modified compaction (or Proctor) test (AS 1289.E2.1) the compactive effort is increased so that the densities achieved are closer to those obtained by the very heavy compaction equipment as employed in airport and road engineering. The

TABLE 2.1
Compaction apparatus and procedures

Detail	Standard compaction	Modified compaction
Mold volume, cm^3	1000	1000
diameter, mm	105	105
height, mm	115.5	115.5
Rammer diam., mm	50	50
drop, mm	300	450
mass, kg	2.7	4.9
Number of layers	3	5
Blows per layer	25	25
Energy input, kJ/m^3*	596	2703

*Kilojoules per cubic meter.

rammer that is used weighs more and is dropped from a greater height than in standard compaction, and five, rather than three, layers are subjected to 25 blows. Details of both tests are given in Table 2.1.

In order to obtain consistent results, care has to be taken that sample preparation and test procedures meet the appropriate standard. An automatic compaction apparatus may be used provided that essential dimensions are adhered to. Small variations in cylinder size, number of blows, etc., will not cause significant error provided that the total energy expended per cubic meter of compacted soil remains the same. In some cases it may be desirable to use an extra large mold so that particles larger than 19 mm can be included in the laboratory test. Results from such tests should not normally be expected to correspond exactly to those obtained in the standard mold.

Compaction test results are plotted in terms of dry density versus moisture content on a diagram as shown in Fig. 2.1. The dry density γ_{dry} is calculated from the total (or wet) density γ_{tot} as follows:

$$\gamma_{dry} = \frac{\gamma_{tot}}{1 + w} \tag{2.1}$$

where w represents the moisture content (or water content). The density γ may be expressed in mass units [metric tons per cubic meter (t/m^3) or grams per milliliter (g/mL)] or force units [kilonewtons per cubic meter (kN/m^3)]. Some engineers prefer the symbol ρ instead γ if mass units are used.

It is highly recommended that a compaction curve be accompanied by the zero-air-void (ZAV) curve. This facilitates the drawing of the compaction curve and assists in identifying erroneous results. The ZAV curve represents dry densities corresponding to a saturation $S = 100\%$ at given water contents and for a particular specific gravity G_s of the soil solids. With γ_w designating the unit weight of water, points of the ZAV curve can be calculated from

$$\gamma_{dry} = \frac{G_s\gamma_w}{1 + wG_s/S} = \frac{G_s\gamma_w}{1 + e} \tag{2.2}$$

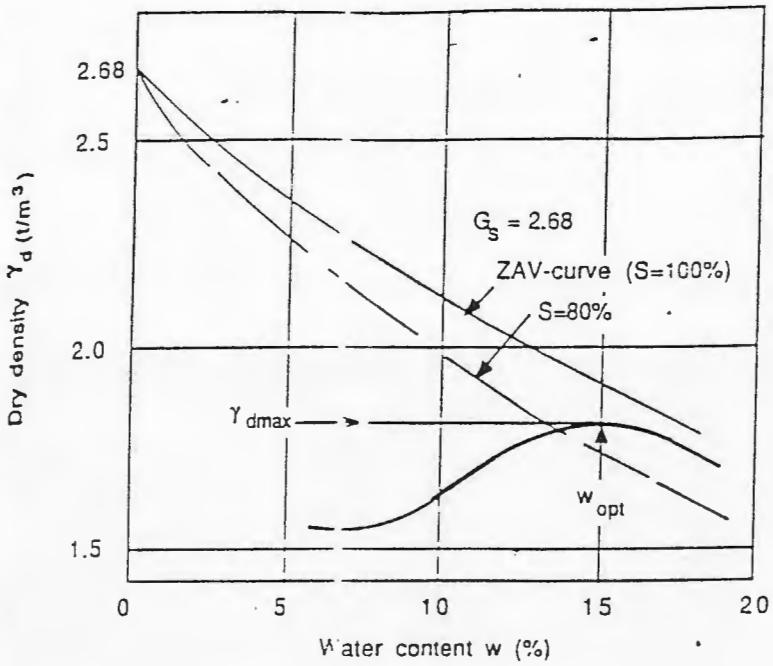

FIGURE 2.1
Dry density versus moisture content.

where e is the void ratio. A line similar to the ZAV curve but representing, e.g., 80% saturation could be drawn; this information would help in estimating the degree of saturation of the compacted soil specimen.

Most soils, in particular cohesive soils, show a distinct peak in dry density, probably in the range of 80 to 90% saturation. This peak is called the *maximum dry density* (MDD) γ_{dmax}, and the corresponding water content is the *optimum moisture content* (OMC) w_{opt}. This means that given a certain compactive effort, maximum dry density (and, correspondingly, high shear strength and low compressibility) is only achieved if the soil is at its optimum moisture content.

For certain types of soil, the concept of a single optimum moisture content may not be applicable, nor relevant. For example, highly permeable granular soils may densify best if completely dry or completely saturated. With organic soils, such as peat, the dry density may simply decrease with increasing moisture content and not even be significantly affected by the compactive effort.

2.2.1.2 KNEADING COMPACTION. The California Division of Highways employs kneading compaction for the preparation of specimens used in the stabilometer test. The samples are placed in molds, about 102 mm in diameter and 127 mm high and are compacted by being kneaded 100 times at 2413 kilopascals (kPa). It is said that the soil structure created by this type of compaction closely resembles that obtained with compaction equipment typically used for fine-grained soils in the field, such as sheepsfoot and tamping rollers.

In the Miniature Harvard Compaction Test, a 25.3-mm-diameter specimen is produced by tamping with a calibrated spring-loaded piston, which is small in relation to the mold. Each time the piston is forced down onto the soil, it tends to cause shear failure which is characteristic in kneading compaction and not unlike what happens in the application of sheepsfoot roller. The Miniature Harvard Compaction Test is no longer a recommended standard by ASTM, but it is still widely used for research purposes because it allows a large number of specimens to be produced in a short time, with only a small amount of material used. Because of its miniature size, the mold is only suitable for fine-grained soils.

2.2.1.3 STATIC COMPACTION. Specimens of prescribed density can be made by compressing a known amount of soil into a calibrated cylindrical mold placed in a universal-type testing machine. The compressive force is steadily increased until the desired density is reached. This type of compaction is described as static compaction or *odometric compression* (an *odometer* is a one-dimensional consolidation apparatus). It is known to create a soil particle orientation which may differ to that obtained by other methods of compaction, but it can be most useful for research purposes, particularly in the evaluation of stabilizing additives. It should, however, be remembered that the compactive effort in the field cannot be changed as readily as during laboratory static compaction.

2.2.1.4 LABORATORY COMPACTION USING STRESS PATH SIMULATION. If stresses in a soil mass under the influence of specific compaction machinery are known, an attempt can be made to reproduce these stresses in the laboratory in order to predict the densities which are going to be obtained in the field for particular placement conditions. There is no generally valid stress-strain law available for soils, but under certain conditions, linear elastic theory provides reasonable values for the stresses generated, and these can serve as a guide to laboratory simulation.

As an example, linear elastic theory, or more specifically the Boussinesq theory, is said to yield good results for the compaction stresses generated beneath a rubber-tired roller, particularly in a firm cohesive soil. Elastic solutions are also available for the effect of a rigid wheel. Even vibratory compaction stresses have been analyzed using linear stress-strain theory.

Fry (1980) illustrated the in situ stress path below a roller and how it is approximated in conventional laboratory tests (Fig. 2.2). He concluded that the odometric stress path does not give a good representation of what happens below a roller. One result quoted by him shows that in order to achieve 100% γ_{dmax} (standard Proctor test) for a highly plastic clay at a water content 4% below optimum, a single application of a compressive stress of around σ_1 = 1000 kPa was required. In the same proceedings, Biarez (1980) gave evidence that an all-around triaxial stress of only say 400 kPa may achieve the same density.

Fry (1980) feels that a repeated triaxial test (σ_3 = constant) is suitable to simulate roller compaction in clay. For cohesionless soils, repeated compression-extension triaxial tests are thought to be more representative of field compaction. These tests induce a rotation of the principal axes. If a repeated compression-extension

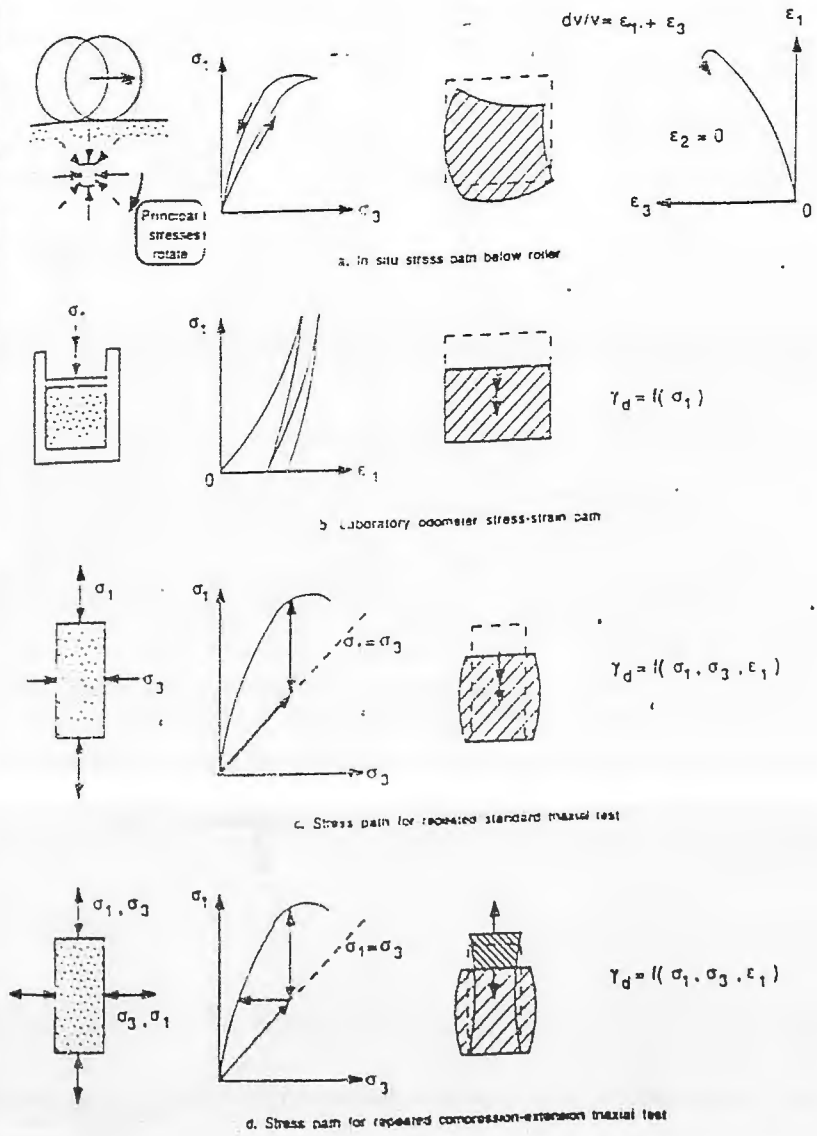

FIGURE 2.2
Stress paths below roller and in laboratory tests. [*Adapted from Fry (1980).*]

test is performed so as to induce repeated shear in a clay soil, this process comes close to the concept of kneading compaction.

2.2.2 Shallow Surface Compaction

Compaction by surface equipment is achieved by static pressure and/or dynamic pressure caused by impact or vibration.

There is a long history in the development of surface compaction machinery resulting in a wide variety of equipment, differing in size, shape, and mode of operation. Records from the last century show rollers pulled by horses and oxen and

later by steam engines. The first sheepsfoot rollers appeared in the United States around 1905. Organizations such as the Bureau of Reclamation and the Corps of Engineers in the United States contributed greatly to advances in compaction from the 1930s onward. At the same time, vibratory compaction of soils came into use in Germany.

2.2.2.1 STATIC ROLLERS

Smooth steel rollers and pneumatic-tired rollers. Traditional steel rollers are relatively slow compared to newer types of equipment. They exert high static pressures which makes them most suitable for granular soils. On clays they may help in bridging uneven surfaces. However, if a soil is relatively soft, they may have a plowing effect without causing significant compaction; in addition, traction is likely to be poor.

Rubber-tired and pneumatic-tired rollers compact by the static weight of the ballast and the kneading action of the tires. The compactive effort depends on

1. Gross weight
2. Wheel diameter
3. Wheel load
4. Tire width and size
5. Inflation pressure

The working speed of pneumatic rollers seems to have little influence on their efficiency; it is generally chosen around 6 kilometers per hour (km/h). These rollers work on most types of soil. It should be remembered that a high gross weight alone does not guarantee good compaction.

Sheepsfoot rollers. Sheepsfoot and tamping or padfoot rollers are distinguished by "feet" protruding from the cylindrical steel shell of the roller. The term "tamping," or "padfoot," roller generally refers to equipment with relatively large "footprints" (illustrated as type 4 in Fig. 2.3). Examples of the different shapes of feet employed are shown in Fig. 2.4. Generally, the wetter and softer the soil, the larger the contact area (footprint) required for optimum compaction. Sheepsfoot rollers have proved more suitable for cohesive soils than other rollers. They exert high pressures on the soil, first compacting lower layers and then gradually working to the surface as the soil underneath gains in strength. When the soil yields no further, the sheepsfoot roller is said to "walk out" of the lift ("Compaction Data Handbook"). Blending of the material is assisted by the sheepsfoot action. Moisture control is made easier because of the pockmarked surface during compaction. Steel rollers may be used to level off areas worked by sheepsfoot or rubber-tired rollers.

Grid rollers. Grid rollers have drums covered or consisting of a heavy steel grid. This creates high contact pressures while preventing excessive shear deformation responsible for the plastic wave ahead of the roll. Grid rollers are suitable for compacting

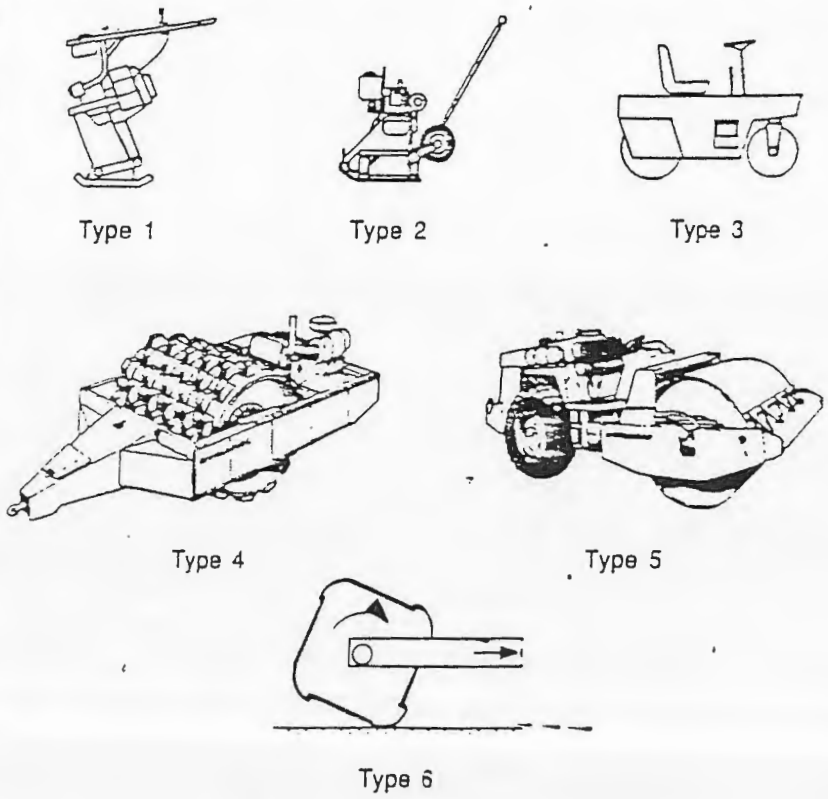

FIGURE 2.3
Vibratory and impact compactors for shallow compaction (refers to Table 2.2).

weathered rock, such as sandstone, by breaking and rearranging gravel and cobble-size particles. Clayey soils, however, may clog the grid and make it ineffective. A relatively high operating speed assists in the breakdown of material, while a lower speed enhances the densification effect.

2.2.2.2 IMPACT AND VIBRATORY EQUIPMENT. Table 2.2 summarizes typical characteristics of vibratory equipment commonly used for surface compaction today. The equipment discussed is illustrated in Fig. 2.3.

Tampers, rammers, and plate compactors. Vibrating *tampers* or *rammers* and vibrating *plate compactors* are used in confined areas such as on backfill in trenches, around pipes, and behind retaining walls and bridge abutments. Rammers may have a stroke length of 30 to 70 mm and therefore mainly work on the impact principle. Plate compactors have a smaller amplitude of vibration and, for the same weight, would be less efficient at depth for most soils. By changing the position of the rotating weights, the compacting force can be adjusted and the plate compactor can be made to move forward or backward.

TABLE 2.2
Typical characteristics of impact and vibratory equipment for shallow compaction*

Type no. and name	Typical characteristics				
	Mass, t	Max. working speed, km/h	Vibrating frequency, Hz	Depth of lift, m	Number of passes
1. Vibrating rammer	0.3–0.1	—	7–10	0.2–0.4	2–4
2. Light vibrating plate	0.06–0.8	1	10–80	0.15–0.5	2–4
3. Light vibrating roller	0.6–2	2–4	25–70	0.3–0.5	4–6
4. Heavy towed vibrating roller	6–15	8–10	25–30	0.3–1.5	4–6
5. Heavy self-propelled vibrating roller	6–15	6–13	25–40	0.3–1.5	4–6
6. Impact roller	7	10–14	—	0.5–3	Up to 30

*See Fig. 2.3 for illustrations.

Vibrating rollers. Lightweight vibratory rollers have little impact effect; the vibrational amplitude is on the order of 1 or 2 mm. In order to achieve the same depth effect as rammers and vibrating plates, they have to be considerably heavier.

The heavy vibrating drums of towed or self-propelled vibratory rollers are isolated from the frame by rubber shock absorbers. The mass given in Table 2.2 includes the frame and drum. Vibrations are caused by rotating weights. As stated by Forssblad (1977), the compactive effort of vibrating rollers is primarily dependent on

1. Static weight
2. Frequency and amplitude
3. Roller speed
4. Ratio between frame mass and drum mass
5. Drum diameter

The centrifugal force is a function of the moment of the eccentric weight (mr) and the frequency n:

$$\text{Centrifugal force} = mr4\pi^2n^2 \tag{2.3}$$

where m is the weight and r is the eccentricity. The actual instantaneous force exerted on the ground will also depend on the properties of the soil and its support.

Impact rollers. Impact rollers consist of a noncircular mass which is towed along the ground. As its center rises and falls, its mass exerts a high impact force causing compaction of the soil. Clifford (1980) described a new type of impact roller developed

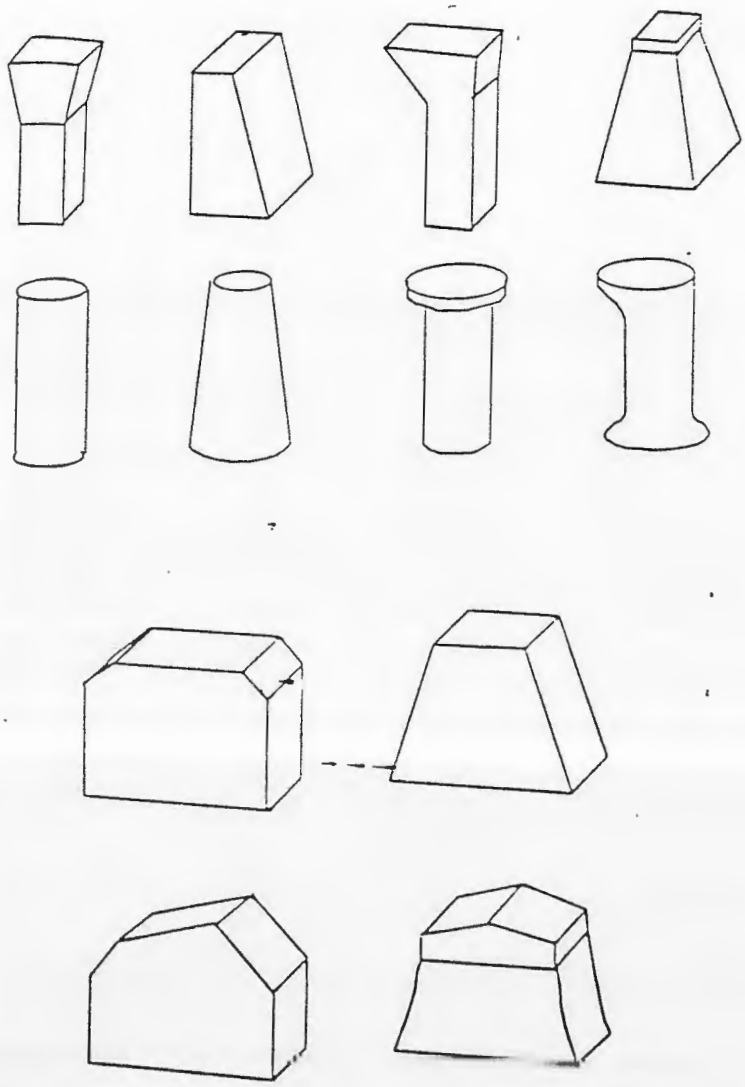

FIGURE 2.4
Sheepsfoot and padfoot shapes. [*After Poesch and Ikes (1975).*]

in South Africa. It consists of a 1.5-m-thick "square" roller with rounded edges. It was found suitable for natural ground and fill. Because the impact roller leaves an uneven surface, it is recommended for subgrades and earth fills rather than for surfacing works.

2.2.2.3 OPERATIONAL ASPECTS OF SHALLOW COMPACTION

Operating frequency. The frequency of vibration of heavy vibratory rollers is usually between 25 and 30 cycles per second (Hz); however, the compactive effort does not appear to vary significantly in the range of 25 to 50 Hz. According to Forssblad (1977), with respect to vibrating rollers, a combination of a large amplitude and a frequency just over the resonance frequency (say 25 Hz) normally results in a better

compaction and depth effect than the combination of high frequency and small amplitude.

Carrying out cyclic shear strain tests on sand in the laboratory, Youd (1972) found a similar result. He concluded that not frequency but shear strain amplitude was the dominant factor causing compaction.

Number of passes. A minimum of 4 to 6 passes are normally required for the economical use of vibratory rollers (compare Table 2.2). An exception may apply to saturated sands, where the compaction at depth seems to continue to improve with an increasing number of passes, such as up to 15 to 20. For static rollers and rollers equipped with sheepsfoot or padfoot drums, the minimum number of passes recommended is usually in the range of 4 to 8.

Figure 2.5 shows the typical relationship between the number of passes of a roller and the density obtained. Most-effective compaction is said to be achieved in the range up to the number of passes associated with the point of maximum curvature.

A high number of passes may lead to increased crushing of particles at the interface between the compactor and the soil. This could lead to undesirable stratification of the fill, e.g., by creating preferred shear planes (lack of bonding between adjacent layers) or affecting the overall permeability. Minimizing the number of passes may therefore have technical as well as economic advantages.

Depth of layers. The layer depth which can be satisfactorily compacted is indirectly proportional to the pressure required to effectively compact the soil. This in turn is a function of the type of soil. According to Forssblad (1977, 1981), a vertical stress of 50 to 100 kPa is sufficient for vibratory compaction of sand. Clay requires considerably more pressure: 400 to 700 kPa. In sand, the motion of soil particles induced by vibration reduces internal friction, which aids in the rearrangement of the sand grains under the influence of shear strains. This is not likely to happen in clays; therefore, higher compressive and shear stresses are needed for densification. Figure 2.6 illustrates the depth effect of different types of compactors; superimposed is an indication of the stress range required for effective compaction of sands and clays.

Compaction at freezing temperatures. Because they are so strongly bonded, frozen soils are difficult to compact effectively. If winter compaction is unavoidable, Forssblad (1981) recommends the following strategies:

1. Use dry coarse materials for construction, such as crushed rock or coarse gravel.
2. If fill can be obtained in the borrow area in an unfrozen state, place and compact it without delay, exposing the least possible surface area to freezing. This is helped by using relatively thick lifts and careful planning of construction stages. It should be realized that at −10°C gravel may freeze to a depth of 50 mm within two hours.
3. Recompact and regrade the surface during the following summer, after the entire fill has thawed. Where it was impossible to avoid frozen fill being placed, large settlement may be evident.

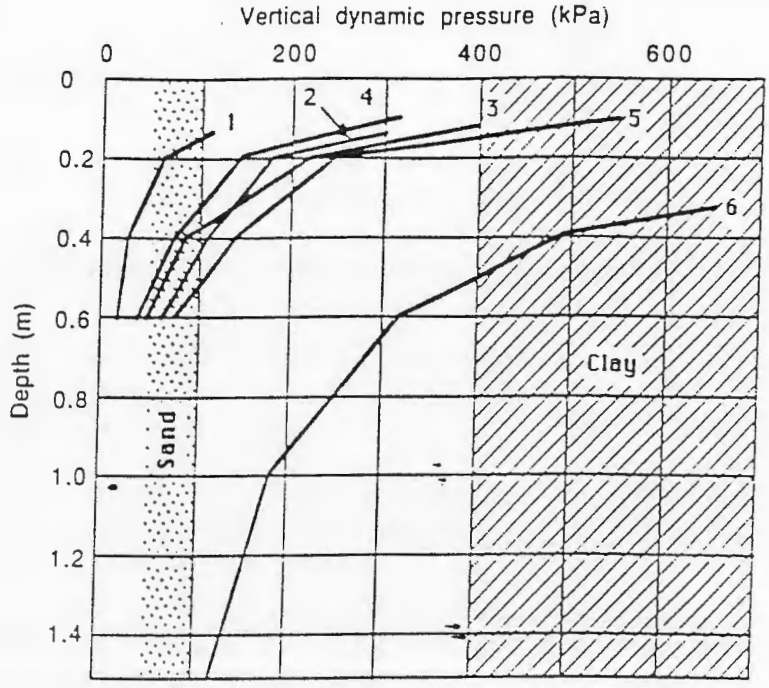

Notes:

Pressure range recommended for sands

Pressure range recommended for clays

Pressure measurements relate to the following equipment:

1	Vibrating plate compactor	135 kg
2	Vibrating plate compactor	400 kg
3	Vibrating tamper	60 kg
4	Vibrating roller	1,400 kg
5	Vibrating roller	3,300 kg
6	Vibrating roller	13,000 kg

FIGURE 2.6
Dynamic pressures at various depths during compaction. [*Forssblad (1977, 1981)*.]

well demonstrated in laboratory compaction tests (see Fig. 2.1). This also applies to lime-stabilized soils. Just like cohesive soils, the latter can be compacted efficiently using padfoot or sheepsfoot rollers. The properties of soils modified with lime and other admixtures are further discussed in Chap. 13.

Basic principles of compaction have also been established for manufactured materials such as asphalt, macadams and "rolled" concrete, and special applications such as treating railway ballast. For further information in these areas, the reader is referred to the specialist literature on pavement materials and railway engineering.

Applicability and production rate. A guide to the applicability of different types of compaction equipment is given in Table 2.3. It identifies the most- and least-suitable

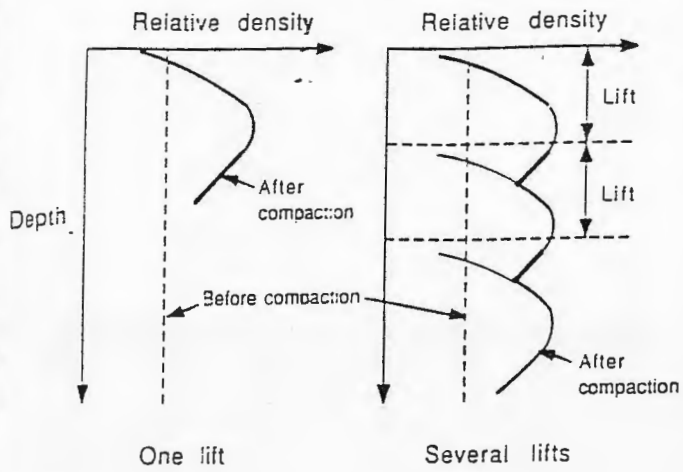

FIGURE 2.7
Density in sand before and after compaction (one or more lifts).

TABLE 2.3
Applicability of compaction equipment

Equipment	Most-suitable soils	Typical applications	Least-suitable soils
Smooth wheel rollers, static or vibrating	Well-graded sand-gravel mixtures, crushed rock, asphalt	Running surface, base courses, subgrades for roads and runways	Uniform sands
Rubber-tired rollers	Coarse-grained soils with some fines	Road and airfield subgrade and base course proof-rolling	Coarse uniform cohesionless soils, and rock
Grid rollers	Weathered rock, well-graded coarse soils	Subgrade, subbase	Clays, silty clays, uniformly graded materials
Sheepsfoot rollers:			
Static	Fine-grained soils with more than 20% fines	Dams, embankments, subgrades for airfields, highways	Clean coarse-grained soils, soils with cobbles, stones
Vibrating	As above, but also sand-gravel mixtures	Subgrade layers	
Vibrating plate (light)	Coarse-grained soils, 4 to 8% fines	Small patches	Cohesive soils
Tampers, rammers	All types	Difficult-access areas	
Impact rollers	Wide range of moist and saturated soils	Subgrade earthworks (except surface)	Dry, cohesionless soils

soils and typical applications. Any compaction will, of course, always be better than no compaction.

Knowing the production rate (or compaction capacity) assists in the selection of the most economical compaction equipment. The production rate is calculated as follows:

$$P = \frac{Best}{n} 1000 \tag{2.4}$$

where P = production rate, m^3/h
B = drum width, m
e = efficiency
s = rolling speed, km/h
t = layer thickness, m
n = number of passes

The efficiency factor, equal to 0.75 to 0.85, allows for overlap between adjacent passes and the time required to change direction, stop, and start.

2.2.3 Deep Compaction Techniques

Densification of deep soil deposits is achieved by the following techniques:

Precompression. A site is preloaded by means of a surcharge or by lowering the groundwater level, causing the ground to consolidate. After restoring original stress levels, future structures built on this site will settle less than those on the untreated ground.

This technique is usually reserved for cohesive soils. Consolidation of these soils is a long-term process, unless the existing longest drainage paths are shortened by the installation of sand columns, paper wicks, or geocomposite drains. Because the success of precompression is essentially dependent on the hydraulic parameters of the soil, precompression is considered a method of hydraulic modification of the soil in this text (see Chap. 11).

Explosion. Explosives are detonated on the surface or, more likely, in an array of boreholes, causing a loose soil structure to collapse which leads to a denser arrangement of the particles. The final density may not be achieved immediately, as the dissipation of excess pore pressures generated may take some time.

Heavy tamping. A large mass is dropped onto the ground surface, causing compaction and possibly long-term consolidation, thus the term "dynamic consolidation."

Vibration. Densification is achieved by a vibrating probe or pile, possibly aided by water jets or pressurized air and the addition of granular material, possibly with added cementing agents.

Compaction grouting. "Zero-slump" mortar is injected into the ground under high pressure, displacing and compacting the surrounding soil. This technique is discussed in Chap. 14.

Vibration is most suitable for free-draining cohesionless soils. Impact loading by explosion and heavy tamping is also suitable for less-pervious silty sands; it may even find application for clayey silts and sands. Precompression may be the only technique feasible for clayey soil and is likely to be less economical than other methods for permeable soils.

The following sections give a brief introduction to compaction by explosion, heavy tamping, and vibro-compaction. Reference is made to some of the field evaluation methods, such as penetration testing, which are discussed in greater detail in either Chap. 4 or 5.

2.2.3.1 EXPLOSION. Explosives can be employed to modify sands, loose rock, and special soils such as loess, which is characterized by relatively high porosity and a distinct soil skeleton.

Explosion of charges on the ground surface or in deep boreholes causes shear stresses in the soil which break down the soil structure, resulting in a reorientation of soil particles and subsequent volumetric compression. In saturated soils temporary high pore pressures are set up, causing liquefaction. These excess semidynamic pore pressures (in excess of hydrostatic pressures) are essential for effective densification ensuing from subsequent consolidation. Installation of vertical drains may assist the explosion-induced consolidation process.

Care must be taken that structures adjacent to the blasting site are not affected and that no large-scale slip or similar shear failure is induced.

Excess pore pressure and settlement due to explosion are related to the ratio

$$N_h = \frac{W^{1/3}}{R} \tag{2.5}$$

where N_h = Hopkinson's number
W = weight of explosives, equivalent kilograms of TNT
R = radial distance from point of explosion, m.

If N_h is less than the range of 0.09 to 0.15, little or no liquefaction is said to occur [Barendsen and Kok (1983)]. This relationship can be used to estimate a "safe" distance from the explosion.

According to Barendsen and Kok (1983), the ratio of excess pore pressure Δu over the effective overburden pressure σ', as well as the ratio of surface settlement Δh to the height h of the soil layer affected by the explosion, are both related to N_h. Experience with sandy soils in the Netherlands suggested the following relationships obtained from a statistical analysis of field results:

$$\frac{\Delta u}{\sigma'} = 1.65 + 0.65 \ln N_h \tag{2.6}$$

and

$$\frac{\Delta h}{h} = 2.73 + 0.9 \ln N_h \tag{2.7}$$

where N_h is calculated using units of kilograms for W and meters for R.

Barendsen and Kok state that for optimum densification, a ratio

$$\frac{\Delta u}{\sigma'} > 0.8 \tag{2.8}$$

is required. For lower ratios, only partial liquefaction may occur, resulting in lower compaction efficiency.

In a typical application in the Netherlands, a charge equivalent to 10 kg of TNT was used in each of the 15-m-deep holes, spaced 16 m apart, resulting in the use of about 100 g of TNT per 1 m^3 of soil.

Dembicki and Kisielowa (1983) describe the compaction of a deposit of sand and silt with thick layers of organic material in Gdansk harbor using explosives. The use of 0.125 kg of explosives per cubic meter of soil decreased the volume of sand by 6% and that of the organic mud by 4% over a total depth of 18 m. The density index (relative density) of the sand increased from 0.35 to over 0.8. The deposit was observed to consolidate for 2 months after the blasting work was completed.

Ivanov (1980) gave details of 12 USSR projects involving consolidation of saturated soils by explosives. A considerable variety of conditions were encountered, indicated by the amount of explosives used, which ranged from 8 to 220 g/m^3. A typical application may have involved a 5-m-thick soil layer, densified by 7 kg of TNT located 3 m down each borehole (spaced 7 m apart), resulting in 0.3 m surface settlement. These figures are given only as a guide to the order of magnitude of the determinants involved. It is obvious that judicious placement and timing of the charges coupled with performance measurements (piezometer readings, penetration tests, etc.) can lead to significant economies on a large project.

2.2.3.2 HEAVY TAMPING AND DYNAMIC CONSOLIDATION. Heavy tamping and dynamic consolidation, also called "dynamic compaction," refer to the compaction method where a heavy weight is dropped onto the ground surface from a great height. The term "dynamic consolidation" was introduced by Menard and usually refers to very heavy equipment with characteristics such as

Tamper mass	Up to 170 t
Fall	Up to 22 m
Compaction effect	To 40 m depth
Spacing	To 14 m

The use of a smaller mass falling from a lower height, say 12 t dropping 12 m, is normally just called heavy tamping, rather than dynamic consolidation; typically, the drops would be spaced 2 to 3 m apart, causing compaction to about 6 m. However, it would seem appropriate to let "heavy tamping" describe the construction "technique" and reserve the term "dynamic consolidation" for explaining the geotechnical "process" which may accompany heavy tamping. Dynamic consolidation could then be defined as the process of densification of a saturated or nearly saturated soil caused by sudden loading, involving shear deformation, temporarily high pore pressures (possibly liquefaction), and subsequent consolidation.

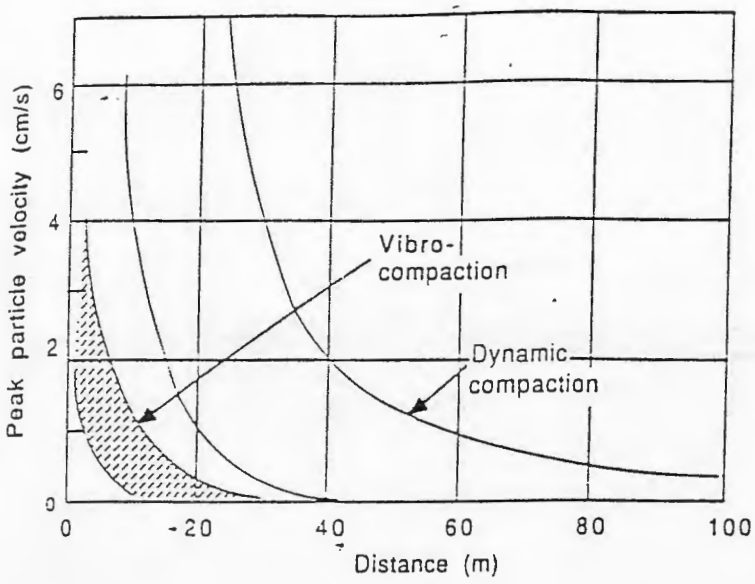

FIGURE 2.9
Comparison of general vibration levels induced by vibro-compaction and heavy tamping (or dynamic compaction). [*Dobson and Slocombe (1982)*.]

load-carrying capacity on the order of 100 to 400 kN. This "bottom-feed" method is increasingly being preferred to other vibro-replacement techniques.

Vibro-compaction and vibro-replacement are illustrated in Fig. 2.10. Vibro-compaction is most successful in loose sandy soils, typically with an original SPT value of 5 to 10 near the surface and is not applicable to clays. Depending on the spacing, relative densities of up to 85% can be achieved (Fig. 2.11). In contrast, vibro-replacement is most effective in cohesive soils with an undrained shear strength in the range of 20 to 60 kPa.

The firm of GKN Hayward Baker (1986) summarized the relative effectiveness of vibro-compaction and vibro-replacement as follows:

Type of soil	Vibro-compaction	Vibro-replacement
Sands	Excellent	Not applicable
Silty sands*	Good	Excellent
Silts	Poor	Good
Clays	Not applicable	Good
Mine spoils	Good	Excellent
Dumped fill	Depends on nature of fill	Good
Garbage	Not applicable	Not applicable

*Say less than 20% fines (comment added by the author).

Vibro-compaction is considerably less hazardous from a personnel and structural safety point of view. The magnitude of vibrations felt on or adjacent to the site are significantly less than are experienced with heavy tamping, as illustrated in Fig. 2.9.

Heavy tamping may also assist in establishing better drainage in a soil layer, thus speeding up the process of consolidation due to the soils own weight or added surcharge. Field observations after heavy tamping show that pore pressures in excess of hydrostatic pressures may exist for hours or days in sand and silty soils and for longer times in clays.

Heavy tamping has also proved effective for the rehabilitation of waste disposal areas by densifying highly variable, loosely dumped material, possibly containing large voids. Rubbish tips can thus be made into storage areas, playing fields, etc., with less problems due to long-term settlements.

A simple rule of thumb suggests that the depth D, in meters, to which heavy tamping is effective can be estimated conservatively by

$$D = 0.5\sqrt{WH} \tag{2.9}$$

where W is the mass of the falling weight in metric tons and H is the height of fall in meters. According to Mayne et al. (1984) the degree of soil improvement peaks at a "critical depth" which is roughly one half of the maximum depth of influence D. A typical set of test results before and after heavy tamping is presented in Fig. 5.17, as part of an introduction to the control of deep compaction with penetrometers and pressuremeters.

Dynamic consolidation can be combined with a static surcharge and assisted by vertical drains. It can also be used to form sand or gravel pillars in soft soil by punching sections of granular fill placed on the surface into the ground.

An example of a time-settlement record of static (fill) and dynamic loading is shown in Fig. 2.8. The vertical steps in the curve are due to repeated passes of a super-heavy tamper.

As for other deep compaction techniques, the ground improvement achieved is most commonly checked by static or dynamic penetrometers, pressuremeters, dila-

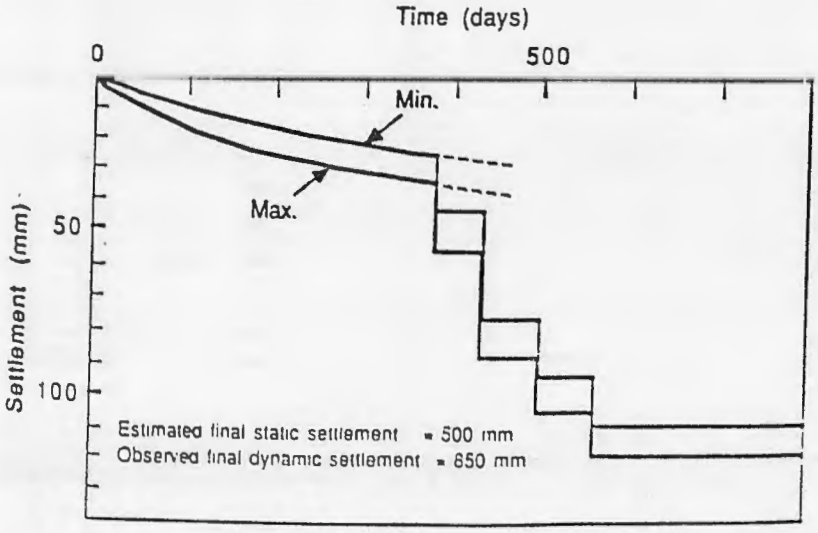

FIGURE 2.8
Time settlement record for precompression combined with dynamic consolidation. [Gambin (1983).]

tometers, or other methods as discussed in Chap. 5. Although the plate load test (Sec. 5.1.5) is more likely to be called on for the control of surface compaction, it is sometimes undertaken for evaluating the effect of heavy tamping, particularly where the job objective is an improvement of the bearing capacity of footings. Since the stress induced by a loaded plate is only significant to a depth equal to about 1½ times its width, the test must be carried out in a trench or large-diameter borehole in order to yield a result which is representative for soil conditions below a large footing.

Significant vibrations are generated during heavy tamping, and this may represent a serious limitation in the applicability of this method of ground modification. Dobson and Slocombe (1982) recorded peak particle velocities on several sites, and their findings, which suggest clearances of at least 30 m, are presented in Fig. 2.9. Additional hazards reported were flying fragments or lumps of soil, so, for safety reasons, a clearance of at least 60 m is preferred.

2.2.3.3 VIBRO-COMPACTION AND VIBRO-REPLACEMENT. Depth vibrators have been used in construction since the 1930s. Some consist of vibrators attached to the top of steel sections which are lowered into the ground. Other types transmit the vibrations from the bottom end of extension tubes lowered into the ground. In standard vibration systems, the dominant direction of vibration is vertical. *Vibro-flotation* is a term coined for systems where the vibrating unit is inserted to the desired depth and vibrated horizontally.

Typical machine characteristics may be as follows [adapted from Jebe and Bartels (1983)]:

Motor output	35 to 120 kilowatts (kW)
Speed	1800 to 3000 revolutions per minute (r/min) (30 to 50 Hz)
Centrifugal force	160 to 220 kN
Amplitude	4 to 16 mm
Depth of penetration	To 35 m
Total depth per day	200 to 500 m

The rate of penetration depends on the soil type, the weight of the vibrating system, and the vibration parameters. It is usually aided by water jets or compressed air. A typical depth vibrator would be 3 to 5 m long, with a mass of 2 t. Loose sand responds best to vibration at depth; as it densifies, a crater forms at the surface which is backfilled with sand or sand and gravel. A 2- to 4-m-diameter column of densified cohesionless soil is thus formed in the ground, increasing the ground's bearing capacity and reducing its compressibility.

Vibro-replacement is a method applied to cohesive ground. The vibrator creates a cylindrical cavity in the ground which is filled with coarse-grained material, such as gravel and crushed rock, that in turn is compacted by vibration. Rather than a solid probe, a hollow tube may be vibrated into the ground with the aid of pressurized water or air. As it is withdrawn, crushed stone or coarse gravel is fed through the tube and compacted. The end result is a column of dense sand and/or gravel with a

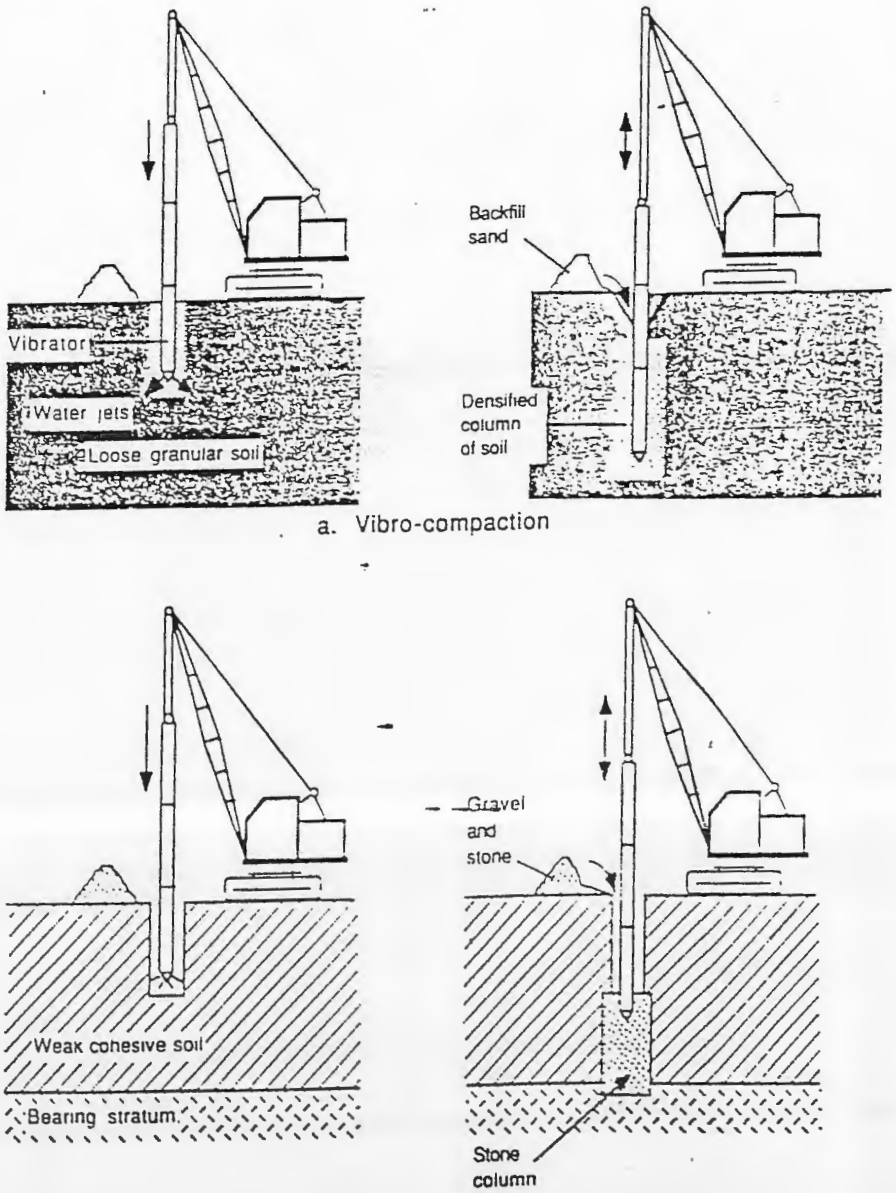

FIGURE 2.10
Vibro-compaction and vibro-replacement.

Vibro-replacement with the addition of stabilizing agents is more appropriately classified as compaction grouting. Such construction methods include *mortared stone columns*, formed by injecting mortar into a stone column, and *concrete vibro-columns*, created by pumping concrete into ground cavities created by a vibrator.

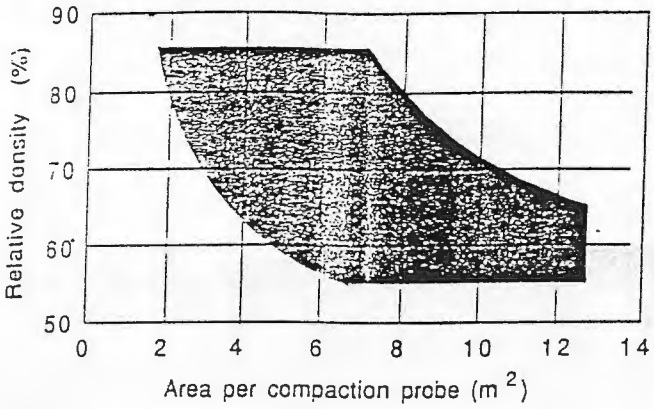

FIGURE 2.11
Envelope for spacing of vibro-centers in clean granular soils. *(Courtesy GKN Keller.)*

2.2.4 Hydromechanical Compaction

Water can assist deposition as well as compaction of cohesionless silts, sand-gravel mixtures, and rock fill.

2.2.4.1 HYDRAULIC FILL. The hydraulic fill method is applicable to predominantly sandy soils. The fill material is pumped through pipelines onto the construction site and is discharged with immediate drainage or fed into a pool at the core of the embankment being formed. Without additional compaction, relative densities of only 50 to 60% are obtained.

The hydraulic fill method is no longer used for major dams because of the danger of liquefaction failures, but it finds application in building minor embankments, flood levees, and fly-ash and mine-waste disposal structures. Turnbull and Mansur (1973) investigated a number of hydraulic fill projects completed in the period from about 1940 to 1970 and concluded that a well-controlled hydraulic fill should satisfy the following requirements:

1. The true water table must be below the surface of the fill so that there is a downward drainage at all times.
2. Material must not be bulldozed into low places without subsequent sluicing; otherwise even lower densities will result.
3. A uniform flow must be maintained over the fill surface by use of bulldozers and shear boards to direct the flow of water.
4. Deposition into pools of water must be prevented in order to eliminate the accumulation of fines and low densities.

Relative densities above 50 or 60% can only be reached if additional surface or deep compaction methods are employed.

2.2.4.2 DRY FILL WITH SUBSEQUENT SPRAYING OR FLOODING. Saturatio free-draining coarse fill materials can assist densification, particularly in combina with vibratory equipment. Through a reduction in capillary tension and increased p pressures during vibration, the frictional resistance against particle rearrangemen reduced. Fines cannot accumulate at the surface but are washed into the larger vo of the fill material, and segregation is counteracted.

According to Striegler and Werner (1973) emphasis is on the addition of la quantities of water rather than on high pressure. They quote the following exampl

150 l/m^3	Göschenerälp Dam (Switzerland)
250 l/m^3	Quoich Dam (U.S.A.)
500 l/m^3	Lewis-Smith Dam (U.S.A.) and Sance Dam (Czechoslovak Social Republic)

2.2.4.3 COMPACTION OF ROCK FILL WITH WATER JETS. Construction of roc fill dams and embankments with conventional surface compaction is rarely done lifts exceeding 2.5 m. Using water jets for compaction allows placement of up to 6 m (!) of rock in one operation [Striegler and Werner (1973)], with correspondin economic advantages.

The types of pumps used deliver a 50- to 70-mm water jet at up to about 80- kPa pressure and at a rate of up to 150 liters per second (L/s). Several water jets may be in action at the same time, aimed at the material being dumped, and normally oriented in the down-the-slope direction. The amount of water used is on the order of 2 to 4 m^3 per 1 m^3 of rock fill.

Good results have been achieved with the kind of material whose fines do not fill the larger voids completely. In that situation it has been observed that sharp edges of boulders and cobble-size particles are broken off by impact forces during placement, resulting in a denser fill. This process may be aided by the water addition, partly because it may reduce the strength of the rock itself.

One of the disadvantages of high fills compacted with water jets is that segregation can occur, causing a predominance of large rock pieces at the bottom of the fill and a relatively high percentage of smaller particles in the upper layers. Compaction in small lifts by surface rollers, if at all feasible, is likely to result in higher overall densities than hydromechanical compaction of high fills, particularly where segregation occurs.

PROBLEMS

Prefixes indicate problem type: C = calculations, M = multiple choice, D = discussion.

Calculations

C2.1. The following measurements were taken in a laboratory water content determination:

Mass of wet soil − container = 120 g
Mass of dry soil − container = 100 g
Mass of container = 20 g

What is the water content of this soil?

C2.2. The total (or wet) unit weight of a compacted well-graded gravel is 22 kN/m^3. The water content is 10%. Calculate

(*a*) The dry unit weight.

(*b*) The saturation, using γ_w = 9.81 kN/m^3 and G_s = 2.65.

(*c*) The error involved if the saturation is computed using γ_w = 10 kN/m^3.

C2.3. Calculate points on a ZAV curve for a specific gravity of soil solids of 2.7 and water contents of 10, 15, 20, 25, 30, and 35%. In addition, calculate the dry density for the same conditions but with a saturation of 80%.

C2.4. Standard compaction of a highly plastic tropical black clay (liquid limit = 55%, plasticity index = 30) at various water contents produced the following dry densities:

w (%) =	16.0	18.5	22.0	23.5	25.0	27.5	31.0
γ_{dry} (kN/m^3) =	1.47	1.50	1.54	1.54	1.50	1.45	1.41

The specific gravity of the soil solids is 2.71.

(*a*) Plot the ZAV curve for the appropriate water content and density range. (Choose the scales so that the ZAV curve is inclined at approximately 45°.)

(*b*) Plot the results and draw the compaction curve.

(*c*) Determine the optimum moisture content, maximum dry density, and corresponding saturation.

C2.5. Calculate the production rate (m^3/h) for a roller with the following characteristics:

Drum width	= 2.14 m
Efficiency	= 80%
Speed	= 8 km/h
Layer thickness	= 0.6 m
Number of passes	= 6

C2.6. A 5-m-deep deposit of sand and silt containing organic layers is to be compacted using explosives placed in boreholes located 8 m apart on a square grid. It is intended to create pore pressures which are at least equal to 80% of the effective overburden pressure. Estimate how many kilograms of TNT have to be distributed in each borehole in order to achieve this degree of liquefaction? How much is that per cubic meter of compacted soil? Refer to the experiences by Barendsen and Kok in the Netherlands.

C2.7. Estimate the "safe" distance from an underground explosion of 10 kg of TNT, beyond which little or no soil liquefaction is likely to occur.

C2.8. To what depth is heavy tamping effective for

(*a*) A 10-t mass dropping 10 m?

(*b*) A 170-t mass dropping 22 m?

C2.9. If a structure adjacent to a site is in danger of being damaged by a peak particle velocity in excess of 2 cm/s in the ground, what is the minimum safe distance for heavy tamping?

C2.10. What is a typical range of plan area (m^2) densified by one application of a vibrocompactor, if a relative density of 80% is to be achieved in clean granular soil?

C2.11. Speculate on the usefulness of elephants as soil compactors, given the following information:

Soil type: Sandy clay

Standard Proctor test results: γ_{dmax} = 1.87 t/m^3, w_{opt} = 14.5%

Elephant: weight = 2000 kg, foot print = 175 cm^2 (three legs on the ground while walking)

From Figure 8.28b, for $\phi = 35°$, $K_u = 1.9$. Similarly, from Figure 8.28c, for a relative density = 60%, $(\delta/\phi) \approx 0.97$. So, $\delta = (0.97)(35) = 33.95°$. Substituting these values into Eq. (8.76)

$$T_{un} = \left(\frac{1}{2}\right)(4 \times 0.305)(16.8)(3.87)^2(1.9)\tan(33.95)$$
$$+ (4 \times 0.305)(16.8)(3.87)(1.9)\tan(33.95)(12 - 3.87)$$
$$= 1021.2 \text{ kN}$$

8.11 Laterally Loaded Vertical Piles

Granular Soils

A general solution for determination of moments and displacements of a vertical pile subjected to lateral load and moment at the ground surface has been given by Matlock and Reese (1960). Consider a pile of length L subjected to a lateral force Q_g and a moment M_g at the ground surface (that is, at $z = 0$), as shown in Figure 8.29a. Figure 8.29b shows the general nature of the deflected shape of the pile and the soil resistance caused by the applied load and the moment.

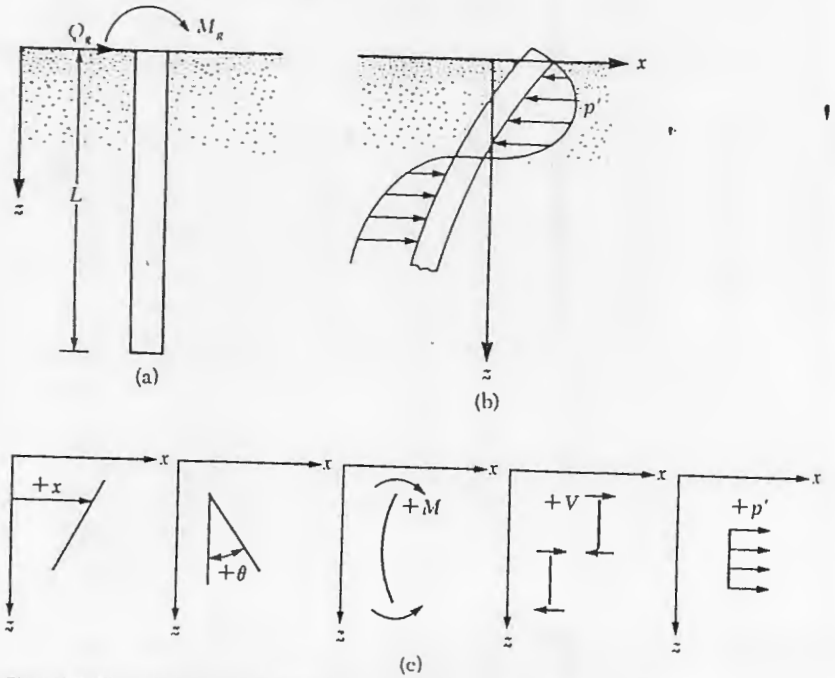

Figure 8.29 (a) Laterally loaded pile; (b) soil resistance on pile caused by lateral load; (c) sign conventions for displacement, slope, moment, shear, and soil reaction

According to a simpler Winkler's model, an elastic medium (which is soil in this case) can be replaced by a series of infinitely close independent elastic springs. With this assumption, one can write that

$$k = \frac{p' \text{ (kN/m)}}{x \text{ (m)}} \tag{8.77}$$

where k = modulus of subgrade reaction
p' = pressure on soil
x = deflection

The subgrade modulus for granular soils at a depth z can be defined as

$$k_z = n_h z \tag{8.78}$$

where n_h = constant of modulus of horizontal subgrade reaction

Referring to Figure 8.29b and using the theory of beams on an elastic foundation, one can write

$$E_p I_p \frac{d^4x}{dz^4} = p' \tag{8.79}$$

where E_p = Young's modulus of the pile material
I_p = moment of inertia of the pile section

Based on Winkler's model

$$p' = -kx \tag{8.80}$$

The sign in the preceding equation is negative because the soil reaction is in the opposite direction to the pile deflection.

Combining Eqs. (8.79) and (8.80)

$$E_p I_p \frac{d^4x}{dz^4} + kx = 0 \tag{8.81}$$

Solution of the preceding equation results in the following expressions:

Pile deflection at any depth $[x_z(z)]$:

$$\boxed{x_z(z) = A_x \frac{Q_g T^3}{E_p I_p} + B_x \frac{M_g T^2}{E_p I_p}} \tag{8.82}$$

Slope of pile at any depth $[\theta_z(z)]$:

$$\boxed{\theta_z(z) = A_\theta \frac{Q_g T^2}{E_p I_p} + B_\theta \frac{M_g T}{E_p I_p}} \tag{8.83}$$

Moment of pile at any depth $[M_z(z)]$:

$$M_z(z) = A_m Q_g T + B_m M_g \tag{8.84}$$

Shear force on pile at any depth $[V_z(z)]$:

$$V_z(z) = A_v Q_g + B_v \frac{M_g}{T} \tag{8.85}$$

Soil reaction at any depth $[p'_z(z)]$:

$$p'_z(z) = A_{p'} \frac{Q_g}{T} + B_{p'} \frac{M_g}{T^2} \tag{8.86}$$

where A_x, B_x, A_θ, B_θ, A_m, B_m, A_v, B_v, $A_{p'}$, and $B_{p'}$ are coefficients and

T = characteristic length of the soil-pile system

$$= \sqrt[5]{\frac{E_p I_p}{n_h}} \tag{8.87}$$

n_h has been defined in Eq. (8.78).

When the pile length, $L \geq 5T$, it is considered to be a *long pile*. For $L \leq 2T$, the pile is considered to be a *rigid pile*. Table 8.12 gives the values

Table 8.12 Coefficients for Long Piles. $k_z = n_h z$

Z	A_x	A_θ	A_m	A_v	A_p	B_x	B_θ	B_m	B_v	B_p
0.0	2.435	−1.623	0.000	1.000	0.000	1.623	−1.750	1.000	0.000	0.000
0.1	2.273	−1.618	0.100	0.989	−0.227	1.453	−1.650	1.000	−0.007	−0.145
0.2	2.112	−1.603	0.198	0.956	−0.422	1.293	−1.550	0.999	−0.028	−0.259
0.3	1.952	−1.578	0.291	0.906	−0.586	1.143	−1.450	0.994	−0.058	−0.343
0.4	1.796	−1.545	0.379	0.840	−0.718	1.003	−1.351	0.987	−0.095	−0.401
0.5	1.644	−1.503	0.459	0.764	−0.822	0.873	−1.253	0.976	−0.137	−0.436
0.6	1.496	−1.454	0.532	0.677	−0.897	0.752	−1.156	0.960	−0.181	−0.451
0.7	1.353	−1.397	0.595	0.585	−0.947	0.642	−1.061	0.939	−0.226	−0.449
0.8	1.216	−1.335	0.649	0.489	−0.973	0.540	−0.968	0.914	−0.270	−0.432
0.9	1.086	−1.268	0.693	0.392	−0.977	0.448	−0.878	0.885	−0.312	−0.403
1.0	0.962	−1.197	0.727	0.295	−0.962	0.364	−0.792	0.852	−0.350	−0.364
1.2	0.738	−1.047	0.767	0.109	−0.885	0.223	−0.629	0.775	−0.414	−0.268
1.4	0.544	−0.893	0.772	−0.056	−0.761	0.112	−0.482	0.688	−0.456	−0.157
1.6	0.381	−0.741	0.746	−0.193	−0.609	0.029	−0.354	0.594	−0.477	−0.047
1.8	0.247	−0.596	0.696	−0.298	−0.445	−0.030	−0.245	0.498	−0.476	0.054
2.0	0.142	−0.464	0.628	−0.371	−0.283	−0.070	−0.155	0.404	−0.456	0.140
3.0	−0.075	−0.040	0.225	−0.349	0.226	−0.089	0.057	0.059	−0.213	0.268
4.0	−0.050	0.052	0.000	−0.106	0.201	−0.028	0.049	−0.042	0.017	0.112
5.0	−0.009	0.025	−0.033	0.015	0.046	0.000	−0.011	−0.026	0.029	−0.002

of the coefficients for long piles ($L/T \geq 5$) in Eqs. (8.82) to (8.86). Note that, in the first column of Table 8.12, Z is the nondimensional depth, or

$$Z = \frac{z}{T} \tag{8.88}$$

The positive sign conventions for $x_z(z)$, $\theta_z(z)$, $M_z(z)$, $V_z(z)$, and $p'_z(z)$ assumed in the derivations in Table 8.12 are shown in Figure 8.29c. Also, Figure 8.30 shows the variation of A_x, B_x, A_m, and B_m for various values of $L/T = Z_{max}$. These figures indicate that when L/T is greater than about 5, the coefficients do not change. This is true of long piles only.

To calculate the characteristic length T for the pile, one needs to assume a proper value of n_h. Some representative values of n_h are given in Table 8.13.

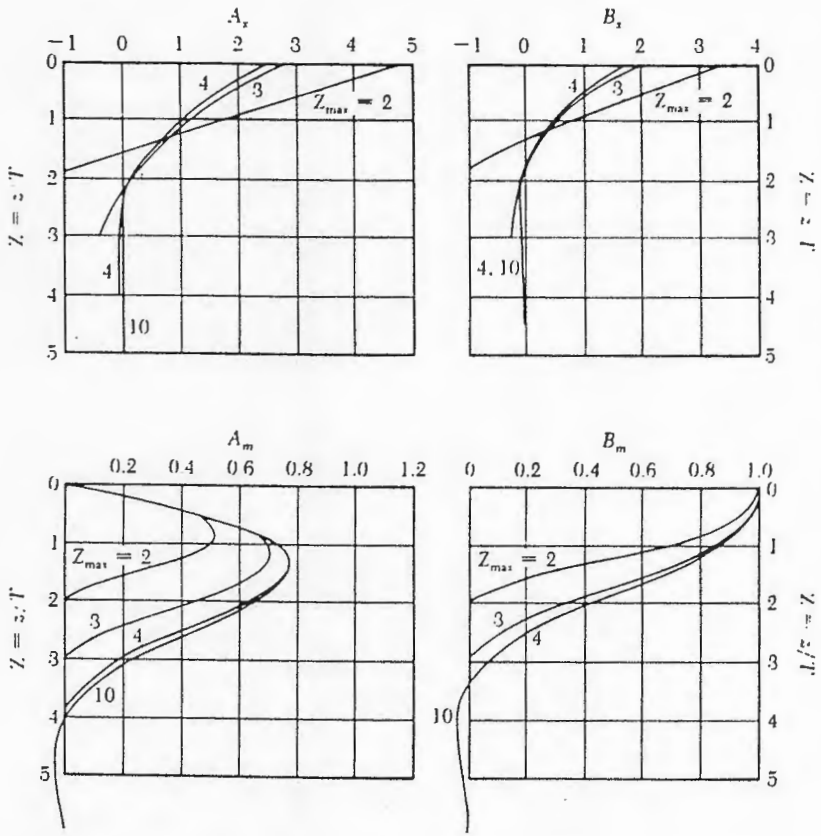

Figure 8.30 Variation of A_x, B_x, A_m, and B_m with Z (after Matlock and Reese, 1960)

Table 8.13 Representative Values of n_h

Soil type	n_h (kN/m³)
Dry or moist sand	Loose: 1800–2200 Medium: 5500–7000 Dense: 15000–18000
Submerged sand	Loose: 1000–1400 Medium: 3500–4500 Dense: 9000–12000

Note: 1 kN/m³ = 6.36 lb/ft³

Cohesive Soils

Solutions similar to those given in Eqs. (8.82)–(8.86) have been given by Davisson and Gill (1963) for the case of piles embedded in clay. According to these solutions

$$\boxed{x_z(z) = A'_x \frac{Q_g R^3}{E_p I_p} + B'_x \frac{M_g R^2}{E_p I_p}} \tag{8.89}$$

and

$$\boxed{M_z(z) = A'_m Q_g R + B'_m M_g} \tag{8.90}$$

where A'_x, B'_x, A'_m, and B'_m are coefficients and

$$R = \sqrt[4]{\frac{E_p I_p}{k}} \tag{8.91}$$

The values of the A and B coefficients are given in Figure 8.31. Note that, in this figure,

$$Z = \frac{z}{R} \tag{8.92}$$

and

$$Z_{max} = \frac{L}{R} \tag{8.93}$$

To use Eqs. (8.89) and (8.90), one must know the magnitude of the characteristic length, R. This can be calculated from Eq. (8.91) provided the coefficient of the subgrade reaction is known. For sands, the coefficient of

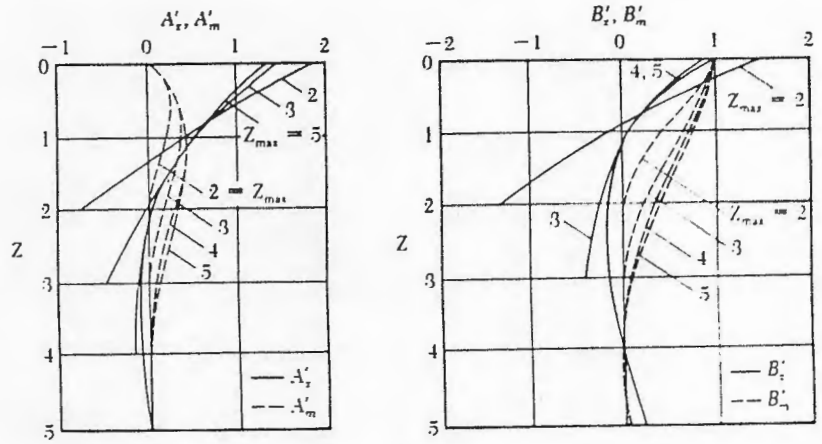

Figure 8.31 Variation of A'_x, B'_x, A'_m, and B'_m with Z (after Davisson and Gill, 1963)

subgrade reaction was given by Eq. (8.78), which showed a linear variation with depth. However, in cohesive soils, the subgrade reaction can be assumed to be approximately constant with depth. Vesic (1961) has proposed the following equation to estimate the value of k:

$$k = 0.65 \sqrt[12]{\frac{E_s D^4}{E_p I_p}} \frac{E_s}{1 - \mu_s^2} \tag{8.94}$$

where E_s = Young's modulus of soil
D = pile width (or diameter)
μ_s = Poisson's ratio of the soil

The Young's modulus of clay, E_s, can be obtained from laboratory consolidation of the soil as

$$E_s = \frac{3(1 - \mu_s)}{m_v} \tag{8.95}$$

where m_v = volume coefficient of compressibility—see Chapter 1

$$m_v = \frac{\Delta e}{\Delta p(1 + e_{av})}$$

The value of μ_s can be assumed to vary between 0.3–0.4.

Example 8.17

Consider a steel H-pile (HP 250 × 0.834) 25 m long embedded fully in a granular soil. Assume that n_h = 12,000 kN/m³. The allowable displacement at the top of the

pile is 8 mm. Determine the allowable lateral load, Q_g. Assume that M_g is equal to zero.

Solution

From Table 8.1a, for an HP 250 × 0.834 pile,

$$I_p = 123 \times 10^{-6}\ \text{m}^4 \quad \text{(about the strong axis)}$$

$$E_p = 207 \times 10^6\ \text{kN/m}^2$$

From Eq. (8.87)

$$T = \sqrt[5]{\frac{E_p I_p}{n_h}} = \sqrt[5]{\frac{(207 \times 10^6)(123 \times 10^{-6})}{12{,}000}} = 1.16\ \text{m}$$

$L/T = 25/1.16 = 21.55 > 5$. So, this is a long pile. Because $M_g = 0$, Eq. (8.82) takes the form

$$x_z(z) = A_x \frac{Q_g T^3}{E_p I_p}$$

So

$$Q_g = \frac{x_z(z) E_p I_p}{A_x T^3}$$

Given: $x_z(z = 0) = 8$ mm $= 0.008$ m. At $z = 0$, $A_x = 2.435$ (Table 8.12). So,

$$Q_g = \frac{(0.008)(207 \times 10^6)(123 \times 10^{-6})}{(2.435)(1.16^3)} = 53.59\ \text{kN}$$

The preceding value of $Q_g = 53.59$ kN has been determined based on the *limiting displacement condition only*. However, the value of Q_g based on the *moment capacity* of the pile also needs to be determined. For that, referring to Eq. (8.84) (with $M_g = 0$),

$$M_z(z) = A_m Q_g T$$

According to Table 8.12, the maximum value of A_m at any depth is equal to 0.772. The maximum allowable moment that the pile can carry is equal to

$$M_{z(\max)} = \sigma_{all} \frac{I_p}{\frac{d_1}{2}}$$

Let $\sigma_{all} = 125{,}000$ kN/m². From Table 8.1a, $I_p = 123 \times 10^{-6}$ m⁴ and $d_1 = 0.254$ m. So

$$\frac{I_p}{\left(\frac{d_1}{2}\right)} = \frac{123 \times 10^{-6}}{\left(\frac{0.254}{2}\right)} = 968.5 \times 10^{-6}\ \text{m}^3$$

Now

$$Q_g = \frac{M_{z(\max)}}{A_m T} = \frac{(968.5 \times 10^{-6})(125{,}000)}{(0.772)(1.16)} = 135.2\ \text{kN}$$

This value of $Q_g = 135.2$ kN is greater than 53.59 kN. So the deflection criteria apply. Hence, $Q_g = 53.59$ kN.

This is only the first approximation. The validity of the assumption of $n_h = 12{,}000$ kN/m³ may now be checked using $Q_g = 53.59$ kN. ≡

8.12 Pile-Driving Formulas

To develop the desired load-carrying capacity, a point bearing pile must sufficiently penetrate the dense soil layer or have sufficient contact with a layer of rock. This requirement cannot always be satisfied by driving a pile to a predetermined depth, because soil profiles vary. For that reason, several equations have been developed to calculate the ultimate capacity of a pile during driving. These dynamic equations are widely used in the field to determine if the pile has reached satisfactory bearing value at the predetermined depth. One of the earliest of these dynamic equations—commonly referred to as the *Engineering News Record (ENR) formula*—is derived on the basis of the work-energy theory. This means that

energy imparted by the hammer per blow =

(pile resistance) × (penetration per hammer blow)

According to the ENR formula, the pile resistance is the ultimate load Q_u and can be expressed as

$$\boxed{Q_u = \frac{W_R h}{S + C}} \tag{8.96}$$

where W_R = weight of the ram (for example, see Table 8.6)
h = height of fall of the ram
S = penetration of pile per hammer blow
C = a constant

The pile penetration, S, is usually based on the average value obtained from the last few driving blows. In the equation's original form, the following values of C were recommended:

For drop hammers:

$C = 1$ in. (if the units of S and h are in inches)

For steam hammers:

$C = 0.1$ in. (if the units of S and h are in inches)

Also, a factor of safety, $FS = 6$, was recommended to estimate the allowable pile capacity. Note that, for single- and double-acting hammers, the term $W_R h$ can be replaced by EH_E (where E = hammer efficiency and H_E = rated